IMPLICATION OF METASTASIS SUPPRESSOR GENE, KISS-1 AND ITS RECEPTOR KISS-1R IN COLORECTAL CANCER, MOLECULAR AND CELLULAR MECHANISMS

by

Ke Ji

Metastasis & Angiogenesis Research Group
Cardiff University School of Medicine
Cardiff

March 2013

Thesis submitted to Cardiff University for the degree of Doctor of Medicine (MD)

D**EDICATION**

I would like to dedicate this work to my family especially my parents. I would not be where I am today without them

Acknowledgements

I would like to thank my supervisors Professor Wen G. Jiang and Professor Malcolm D. Mason for their guidance and support throughout my two years of study. I enjoyed being a part of the Metastasis and Angiogenesis Research Group and it was the perfect place to get my MD. I would especially like to thank Dr Lin Ye for his kindness, time and help during the last one and half years. I am also grateful to Dr Andrew Sanders, Miss Ariel, Miss Sioned Owen, Miss Hoi Weeks, Dr Tracey Martin, Dr Jane Lane and Mrs Fiona Ruge for their friendship and support over the years. I am grateful to Drs Leigh Mansel Davies, Anne-Marie Toms and Rachel Hargest for t heir contribution in sample collection and clinical followups

Summary

Kiss-1 and its receptor (Kiss-1R) are suggested as a novel pair of metastasis suppressors for several human solid tumours. However, the role of Kiss-1 and Kiss-1R in colorectal cancer remains largely unknown. Therefore, the aim of this study was to investigate the role and signal transduction of Kiss-1 and its receptor in colorectal cancer.

Colorectal cancer cell lines (HT115, HRT18, RKO and Caco-2) were screened for the mRNA expression levels of Kiss-1 and Kiss-1R. Sublines of cancer cells with differential expression of Kiss-1 and Kiss-1R were created, using ribozyme transgenes to knock down the expression of Kiss-1 and Kiss-1R, respectively. The stabilized transfected cells were used to study the influence of Kiss-1 and Kiss-1R on the function of colorectal cancer cells using by in vitro function assays (growth, adhesion, wounding and invasion assays) and ECIS assay. The influence of Kiss-1 on tumour growth was also tested using an *in vivo* tumour model. To further explore the receptor activation and signalling pathways downstream of Kiss-1, Kisspeptin-10 was also used in HT115 Kiss-1 knockdown cells. Phosphorylation of Kiss-1 and the effect of Kiss-1 on MMP-9 and MMP-2 were detected using immunoprecipitation and zymography, respectively. The study also investigated Kiss-1 and Kiss-1R expression and their correlation to the clinical outcome in human colorectal cancer, using real-time PCR and immunohistochemistry.

Kiss-1 and Kiss-1R played a suppressive role in the invasion and migration of colorectal cancer cells, in that knocking down both Kiss-1 resulted in increased cell-matrix invasion and cellular migration as demonstrated by a series of cell models. Exogenous Kiss-1 (Kisspeptin-10) decreased cellular migration of colorectal cancer cells and required ERK signalling as shown during the ECIS based analyses. The inhibitory influence of Kiss-1 on the motility of cancer cells was via the reduction of MMP-9, shown by zymography. In the *in vivo* tumour model, tumour growth rate of Kiss-1 knockdown colorectal cancer cells was significantly faster than the control cells. In human colorectal cancer tissues, levels of message expression of Kiss-1 had a negative correlation with Dukes staging, TNM staging, tumour size and lymph node involvement. Kiss-1R expression was significantly decreased in tumour tissues compared with adjacent normal tissues. The present study has demonstrated that Kiss-1 and Kiss-1R play a pivotal tumour suppressor role in colorectal cancer. The inhibitory effect on cancer cells involves the regulation of MMPs and the ERK signaling pathway. The molecule pair is candidate prognostic indicator in patients with colorectal cancer.

Contents

List of Figures

Chapter 1

Chapter 2

Chapter 3

Chapter 4

Chapter 5

Chapter 6

Chapter 7

List of Tables

Chapter 6

Publications

Full papers:

- Ji K, Ye L, Sun PH, Hargest R, Mason M and Jiang WG. Kiss1 suppresses invasion and migration of colorectal cancer cells and the involvement of ERK-MMP9 pathway, submitted.

- Ji K, Ye L, Mason M and Jiang WG. A negative regulator of cell motility, Kiss1 and its receptor Kiss1R in cancer metastasis (review), accepted by International Journal of Molecular Medicine.

- Frewer NC, Ye L, Sun PH, Ji K, Hargest R, Jiang WG. Potential implication of IL-24 in lymphangiogenesis of human breast cancer. International Journal of Molecular Medicine, in press,2013

- Ji K, Ye J, Toms AM, Hargest R, Martin TA, Ruge F, Ji JF, Jiang WG. Signal-induced proliferation-associated gene 1 (SIPA1), a RapGTPase-activating protein is increased in colorectal cancer and has diverse effects on functions of colorectal cancer cells. Cancer Genomics and Proteomics, 2012, 9(5), 321-327

- Jiang WG, Ye L, Ren H, Anna , Topley N, Mason MD. Tumour-endothelial and tumour-mesothelial interactions investigated by ECIS. Cancer Metastasis Biology andTreatment (ECIS in cancer metastasis), 2012, 17, DOI 10.1007/978-94-007-4927-6_9

- Ye L, Ji K, Frewer N, Jiang WG. Cellular impact of YangzhengXiaoji on the adhesion and cellular migration of human cancer cells and the potential underlying signalling pathways. Anticancer Research, 2012, 32(7), 2537-2543

- Ye L, Ji K, Ji JF, Hargest R, Jiang WG. Application of Electric Cell-Substrate Impedance Sensing in evaluation of traditional medicine on the cellular functions of gastric and colorecctal cancer cells Cancer Metastasis Biology andTreatment (ECIS in cancer metastasis), 2012, 17, DOI 10.1007/978-94-007-4927-6_10

Abstracts and conference presentations

Ji K, Ye L, Jiang WG.Increased expression of SIPA1 in colorectal cancer. September 2012. Chinese Conference on Oncology, Beijing, China.

Abbreviations

5FU: 5- fluorouacil
ABI: Applied biosystems
APC: Adenomatous polyposis coli
APS: ammonium persulphate
ASK1: apoptosis signal-regulating kinase 1
ATF-2: activating transcription factor 2
BSA: bovine serum albumin
CDKs: cyclin-dependent kinases
CEA: Carcino-embryonic antigen
Co-SMADs: co-operating SMADs
CRC: Colorectal cancer
CT: Computed tomography
DAB: Diaminobenzidine
DEPC: Diethyl Pryoncarbonate
DMEM: Dulbecco's Modified Eagle's medium
DMSO: Dimethylsulphoxide
ECACC: European collection of animal cell culture
ECM: extracellular matrix
ERK: extracellular signal-regulated kinase
ESCC: Oesophageal squamous cell carcinoma
FAK: focal adhesion kinase
FAP: Familial Adenomatous Polyposis
FBS: foetal bovine serum
GAPDH: glyceraldehyde 3-phosphate dehydrogenase
GDFs: growth and differentiation factors
GnRH: Gonadotropin-Releasing Hormone
GnT-V:a substrate of N-Acetylglucosaminyltransferase V
GRB2: Growth Factor Receptor-bound protein 2
GSTM1: glutathione S-transferase Mu 1
GSK-3β: glycogen synthase kinase-3β
GTN: Gestational trophoblastneoplasia
hCG: Human chorionic gonadotrophi
HCC: Hepatocellular carcinoma
HMGA2: High mobility group protein HMGI-C 2
HNPCC: Hereditary nonpolyposis colorectal cancer

IP: Immunoprecipitation
IQGAP1:RasGTPase-activating-like protein IQGAP1
I-SMADs: inhibitory SMADs
Kiss-1R: Kiss-1 receptor
Kisspeptin-IR: Kisspeptin-immunoreactive
LB: Liquid broth
MAPK: mitogen-activated protein kinase
MEK: MAPK/ERK kinase
MK2: MAPK-activated kinase 2; also known as MAPK2
MMP: matrix metalloproteinase
MR: Magnetic Resonance
PCR: Polymerase chain reaction
PLCβ: Phospholipase Cβ
RT-PCR: Reverse Transcription- Polymerase Chain Reaction
SCC: squamous cell carcinoma
SDS-PAGE: Sodium Dodecyl Sulphate Polyacrylamide Gel Electrophoresis
SFK: Src family kinase
Src: Sarcoma
TC: Threshold cycl
TCCs: Transitional cell carcinomas
TP: Thymidine phosphorylase
TNM: Tumor, Node, Metastasis Classification
TXNIP: Thioredoxin interacting protein

Chapter 1

General Introduction

1.1 Colorectal cancer

1.1.1 Introduction

Colorectal cancer (CRC) is the second most commonly diagnosed cancer [1] and is a major cause for mortality and morbidity globally. Worldwide, colorectal cancer is the fourth and third most common cancer in men and women respectively [2]. There are approximately 142, 000 new diagnoses and 50,000 deaths reported annually in the United States, [3-4]. In Australia, 1 in 17 men and 1 in 26 women will be diagnosed with colorectal cancer within their lifetime [5]. In the UK, colorectal cancer accounts for about 13% of all new cancer cases and in 2009, more than 41,000 new cases were diagnosed [6].

1.1.2 Epidemiology and risk factors

Incidence and Mortality

Nearly 1,200,000 new colorectal cancer cases are believed to occur globally, annually, and accounting for approximately 10% of all cancers, and resulting in 609,000deaths. In addition, around 40,700 people in the UK were diagnosed with colorectal cancer and there were approximate 15,800 deaths from colorectal cancer in the UK[7]. In 2010 it was estimated that there were 141,570 new cases of colorectal cancer and

51,370 deaths, accounting for nearly 10% of deaths from cancer in the United States [3]. Of these cases, there is a 0.5% to 2.0% probability of invasive colorectal cancer, 1.0% to 1.6% probability of carcinoma *in situ*, 7% to 10% probability of a large (1 cm or larger) adenoma, and 25% to 40% chance of an adenoma of any size in unscreened individuals age 50 years or older [8].

Increasing age is more strongly associated with colorectal cancer incidence than any other demographic factor. Consequently, the incidence of colorectal cancer increases dramatically above the age of 45 to 50 years for both men and women. In most countries, age-standardized incidence rates are lower for women than for men. Interestingly, colorectal cancer incidence has been steadily decreasing in the United States and Canada; whilst incidence in Asia is markedly increasing (Japan, Korea and China) [7]. Between 2002 and 2006, the age-standardized rate per 100,000 people was 59.0 for men and 43.6 for women in the United States for all ethnic groups combined[3]. It has been observed that there has been a reduction in both age-standardized colorectal cancer incidence and mortality in the United States over the past 10 years. It may benefit from the advance diagnosis and early screening measures.

Geographic Variation

In general, higher incidence and mortality of colorectal cancer are more commonly seen in the developed Western nations [7, 9]. On the other hand, the incidence rate in

Alaskan Natives exceeds 70 per 100,000 [10]. This is in clear contrast to rates in Gambia and Algeria which are less than 2 per 100,000 [9]. The aforementioned decrease in colorectal cancer incidence in the United States may be due to the advanced application of colonoscopy with polypectomy, although alterations in lifestyle factors (e.g. dietary change and smoking cessation) and the utilization of chemoprevention have also been suggested as the potential reasons [11].

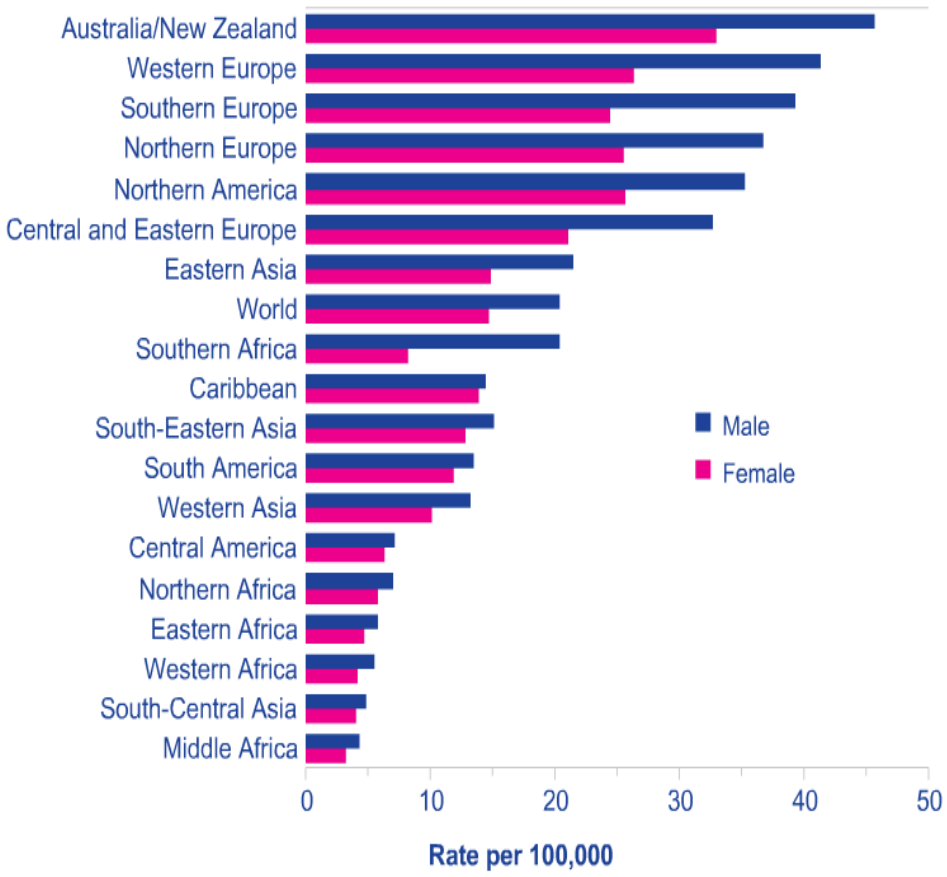

Figure 1.1. Demographic difference in the incidence of colorectal cancer worldwide [6] (http://www.cancerresearchuk.org/cancer-info/cancerstats/types/bowel/incidence/uk-bowel-cancer-incidence-statistics)

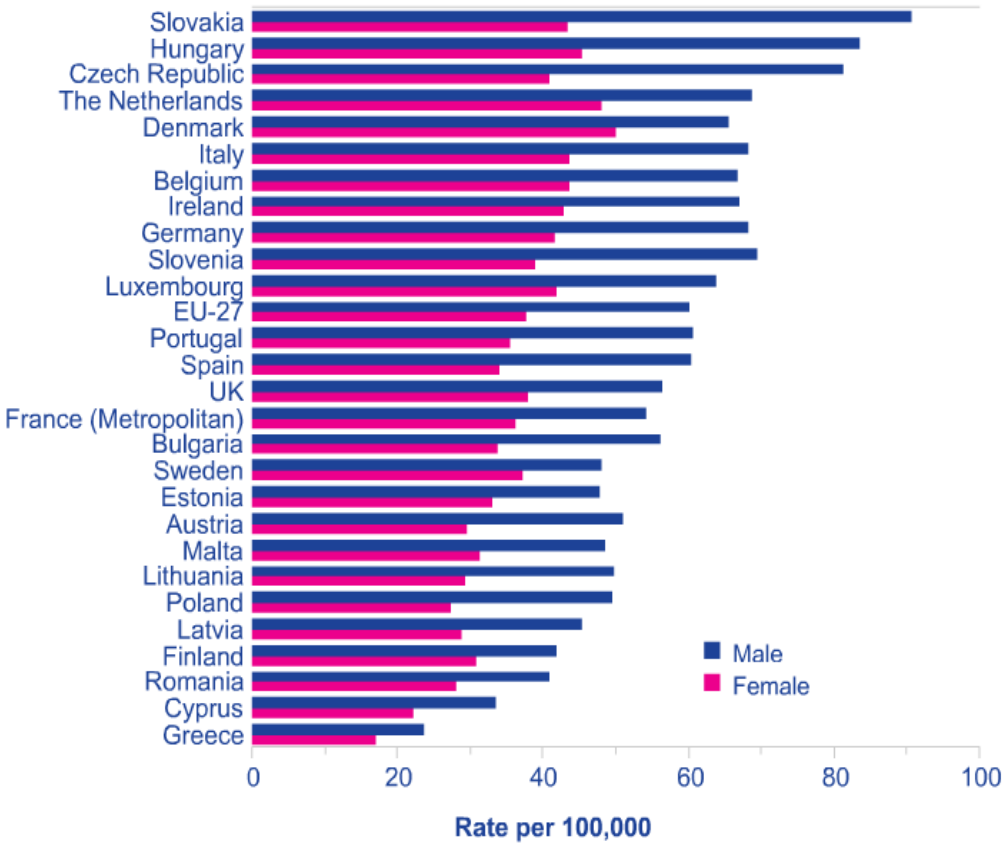

Figure 1.2. Demographic difference in the incidence of colorectal cancer in European countries [6] (http://www.cancerresearchuk.org/cancer-info/cancerstats/types/bowel/incidence/uk-bowel-cancer-incidence-statistics)

Socioeconomic Factors

Generally speaking, rates of cancer incidence and mortality are higher in economically advantaged countries. This may be related to dietary factors (such as the consumption of a high fat, high sugar, high red meat or low-fibre diet), lack of physical activity and increasing incidence of obesity.

1.1.3 Family history of colorectal cancer

Hereditary Nonpolyposis Colorectal Cancer

Hereditary nonpolyposis colorectal cancer (HNPCC), also known as Lynch Syndrome, is a genetic condition predisposing to colorectal cancer and accounts for about 3% of all colorectal cancers. It is associated with the development of up to 100 colonic polyps, usually in the right colon [12]. The most common HNPCC subtypes are type I and type II. HNPCC type I is distinguished by an increased rate of progression to colorectal cancer in polyps which may lead to the onset of colorectal cancer by the age of 40 years. HNPCC type II is associated with the development of extra colonic tumours, which originate in the skin, bile duct, liver, stomach, small intestine, renal pelvis, bladder, ureter or urethra, uterus or ovary, and pancreas. The lifetime risk of colorectal cancer in HNPCC is 80%, with a 40% increase in the risk of endometrial cancer and a less than 10% increase in the risk of developing all other cancers [13]. The modified Amsterdam criteria classification of HNPCC is shown in Table 1.1 below. The modified Amsterdam criteria classification of HNPCC is shown in Table 1.1 below.

Familial Adenomatous Polyposis

Familial Adenomatous Polyposis (FAP) accounts for 1% of colorectal cancer. The key feature of FAP is the presence of thousands of colonic polyps which usually increase with age. There is a predisposition to colorectal cancer in patients when they are in their 50s or 60s [14].Surgical treatment is preferred at an early stage as most patients with FAP develop colorectal cancer if the colon is not removed as a prophylactic procedure. Other clinical manifestations of FAP include incipient congenital hypertrophy of the retinal pigment epithelium, mandibular osteomas, supernumerary teeth, epidermal cysts, adrenal cortical adenomas and desmoid tumours in addition to and malignant conditions such as thyroid tumours, a 5% to 10% risk of duodenal adenocarcinoma and brain tumours

Table 1.1 Amsterdam criteria classification of HNPCC

Amsterdam I Criteria
>or equal to three relatives with colorectal cancer
>or equal to one case in a first degree relative
>or equal to two successive generations should be affected
>or equal to one tumour should be diagnosed before the age of 50 years
FAP should be excluded
Tumors should be confirmed with histology
Amsterdam II Criteria
>or equal to three relatives with HNPCC-associated cancer (colorectal, endometrial, small bowel, ureter, or renal pelvis) or with an HNPCC associated cancer
>or equal to two successive generations should be affected
>or equal to one case before age 50
FAP should be excluded
Tumors should be confirmed with histology
Bethesda Criteria (diagnosis of HNPCC is made if any of the following criteria are fulfilled)
Cancer in families that meet Amsterdam criteria
Two HNPCC-related cancers, including colorectal or extracolonic
Patients with colorectal cancer has first degree relative with colorectal cancer or HNPCC related cancer; one of the cancers diagnosed before age 45, and the adenoma diagnosed before age 40
Colorectal cancer or endometrial cancer before age 45
Right-sided undifferentiated (solid or cribiform) colorectal cancer on histopathology before age 45
Signet-ring cell type colorectal cancer before age 45
Colonic adenomas before age 40

Dr Frank Gaillard *et al*. Radiopaedia.org/articles/Amsterdam-criteria-for-HNPCC

1.1.4 Anatomy of the Colon

Sections of the colon

Defined as the lower segment of intestine from the ileocecal valve to the anus, the large bowel is approximately 150 cm in length. It is divided into three segments defined by different morphology and location (extraperitoneal and retroperitoneal location): the caecum, the colon (the ascending colon, the transverse colon, the descending colon and the sigmoid colon), and the rectum. The large intestine, which can be distinguished from the small intestine by its increased diameter, has a muscular wall. The muscular wall includes taenia coli, haustra coli and appendices epiploicae. The taenia coli consists of three longitudinal muscles along the longitudinal axis of the colon starting near the base of the appendix and ending in the ends of sigmoid colon. The length of taenia coli is 30cm shorter than the bowel it is attached to, and the enlarged pouch formed by the shrinkage of colonic wall is called haustracoli. Appendices epiploicae are accumulations of subserosal fat tissue along the external surface of the colon.

The right colon is made up of the caecum (with appendix) and ascending colon. It is anterior to the right kidney and the duodenum.

Blood supply to the colon

The vascular supply to the caecum and ascending colon arises from branches of the superior mesenteric artery (SMA), which divides into the inferior pancreaticoduodenal artery, the middle colic artery, the right colic artery and the ileocolic artery. The middle colic artery immediately forms two large arcades in the transverse mesocolon, which connects with the SMA and ileocolic arterial branches. The ileocolic artery splits towards a right colic artery to the upper ascending colon, which starts with the right border of the superior mesenteric artery and forms two branches at the caecum (the colic branch and the ileal branch). The colic branch forms an anastomosis with descending branches from the right colic artery. The ileal branch forms branches to the distal small bowel and caecum and anastomoses with the ends of superior mesenteric artery. The right colon is a retroperitoneal structure.

The transverse colon is supplied by branches of the middle colic artery. It is the first portion of the colon considered to be intraperitoneal, and its length is around 20cm to 50cm. Its boundaries are defined from the hepatic flexure on the right to the splenic flexure on the left. Both of these points are fixed by the transverse mesocolon. The length of transverse mesocolon fixed both hepatic flexure and splenic flexure is shorter than the rest of the transverse colon section, hence the shape of transverse colon is described as arched prolapsed. The hepatic flexure abuts the gallbladder fossa, while the splenic flexure lies anterior to the tail of the pancreas.

The descending colon is defined as the segment of colon from the splenic flexure to the sigmoid colon, where the colon becomes a retroperitoneal structure and its length is about 25-30cm. The vascular supply of descending colon is supplied by the inferior

mesenteric artery (IMA). The IMA arises from the aorta and ends at the upper part of rectum. It gives off the left colic artery and three to four sigmoidal arteries, which supply the intraperitoneal sigmoid colon. The arterial arcade between the ileocecum and the trial of sigmoid flexure, which belongs to the part of vessels anastomose between mesenteric artery and its adjacent branches is known as the marginal artery of Drummond. The arcade, which effectively connects the left and right circulations, is defined as the arc of Riolan.

Venous and lymphatic drainage of the colon

The venous and lymphatic drainage of the colon parallels the arterial supply, and all three vessels (superior mesenteric vein, inferior mesenteric vein and splenic vein) course and divide within the colonic mesocolon, which belong to the hepatic portal system. The mesocolon therefore contains the regional lymph nodes for the segment of colon it supplies and drains. The different lymphatic channels pass from the submucosa to the intramuscular and subserosal plexus of the bowel to the first tier of lymph nodes lying adjacent to the large intestine and known as epicolic nodes [15].Paracolic nodes lie on the marginal vessels along the mesenteric side of the colon and are frequently involved in metastases. Intermediate nodes are found along the major arterial branches of the SMA and IMA in the mesocolon. The principal nodes are found around the origin of these vessels from the aorta, and they drain into retroperitoneal nodes. The drainage of the superior and inferior mesenteric veins, which drain the ascending, transverse, descending, and sigmoid colon, is via the portal vein. The rectum is drained by rectal tributaries to the vena cava.

The extent of resection of the colon is defined by the vascular supply and by the lymph nodes belonging to the mesentery [16-17]. Therefore, the whole bowel supplied by related vascular should be resected thereby ensuring that all related lymph nodes from the root of the mesentery vascular are removed.

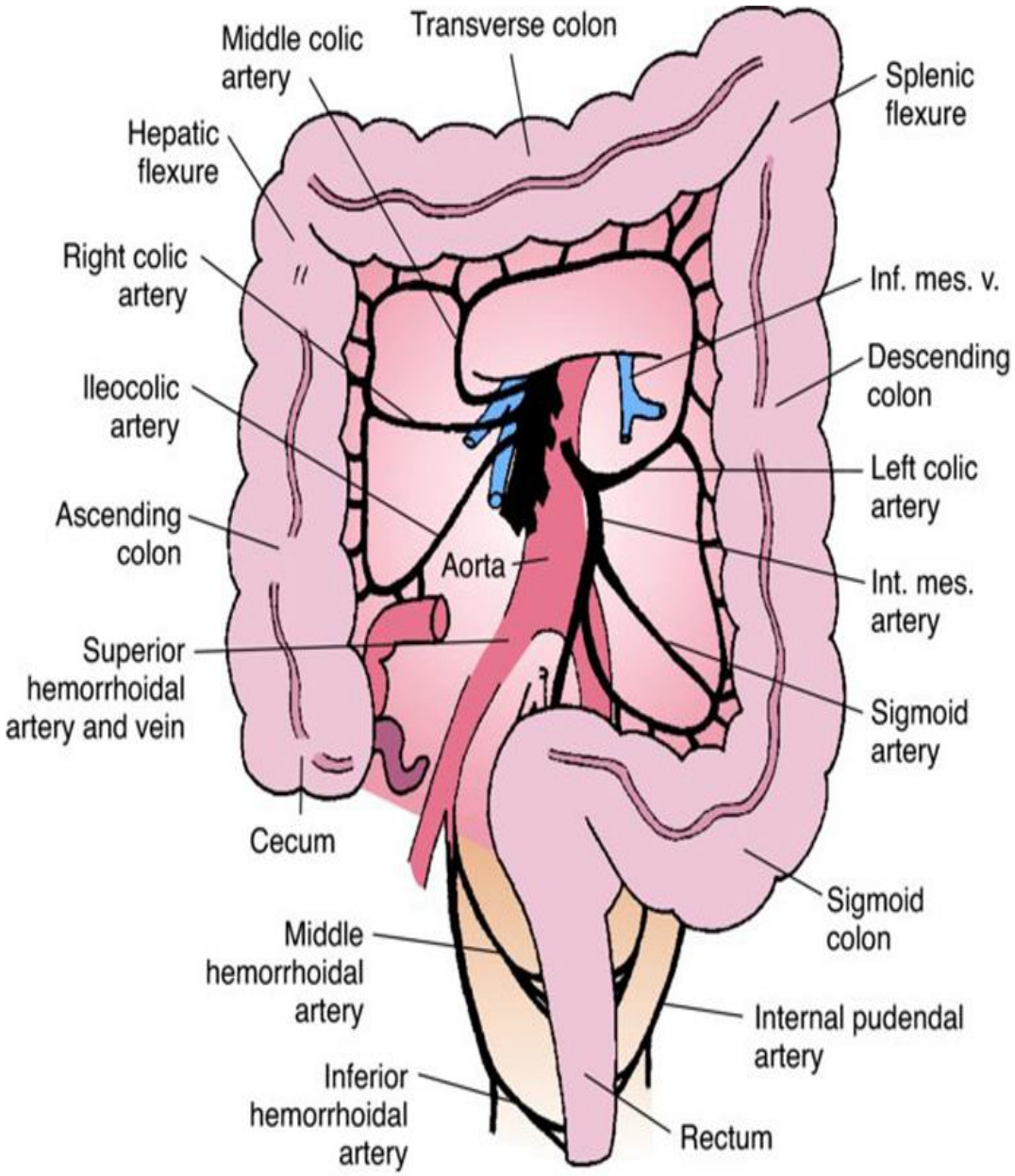

Figure 1.3. The anatomy of the colon with the vascular supply
Source: DeVita VT, Lawrence TS, Rosenberg SA: *DeVita, Hellman, and Rosenberg's Cancer: Principles & Practice of Oncology, 9th Edition*, 2011. By Lippincott Williams &Wikins.

Anatomy of the rectum

In the upper portion of the rectum there are changes both in the musculature of the large bowel and in the relationship to the peritoneal covering. In the lower portion of the rectum, the mucosal changes occur at roughly the same location as the anal sphincter. The lower rectum is the area approximately from 3 to 6 cm from the anal verge. The midrectum goes from 5 to 6, to 8 to 10 cm, and the upper rectum extends approximately from 8 to 10, to 12 to 15 cm from the anal verge, although the retroperitoneal portion of the large bowel often reaches its upper limit approximately 12 cm from the anal verge. In some patients, especially elderly women, the peritonealised portion of the large bowel can be located much lower than these definitions. The determination of the location of the boundary between rectum and sigmoid colon is important in defining adjuvant therapy, with the rectum usually being operationally defined as that area of the large bowel that is at least partially retroperitoneal.

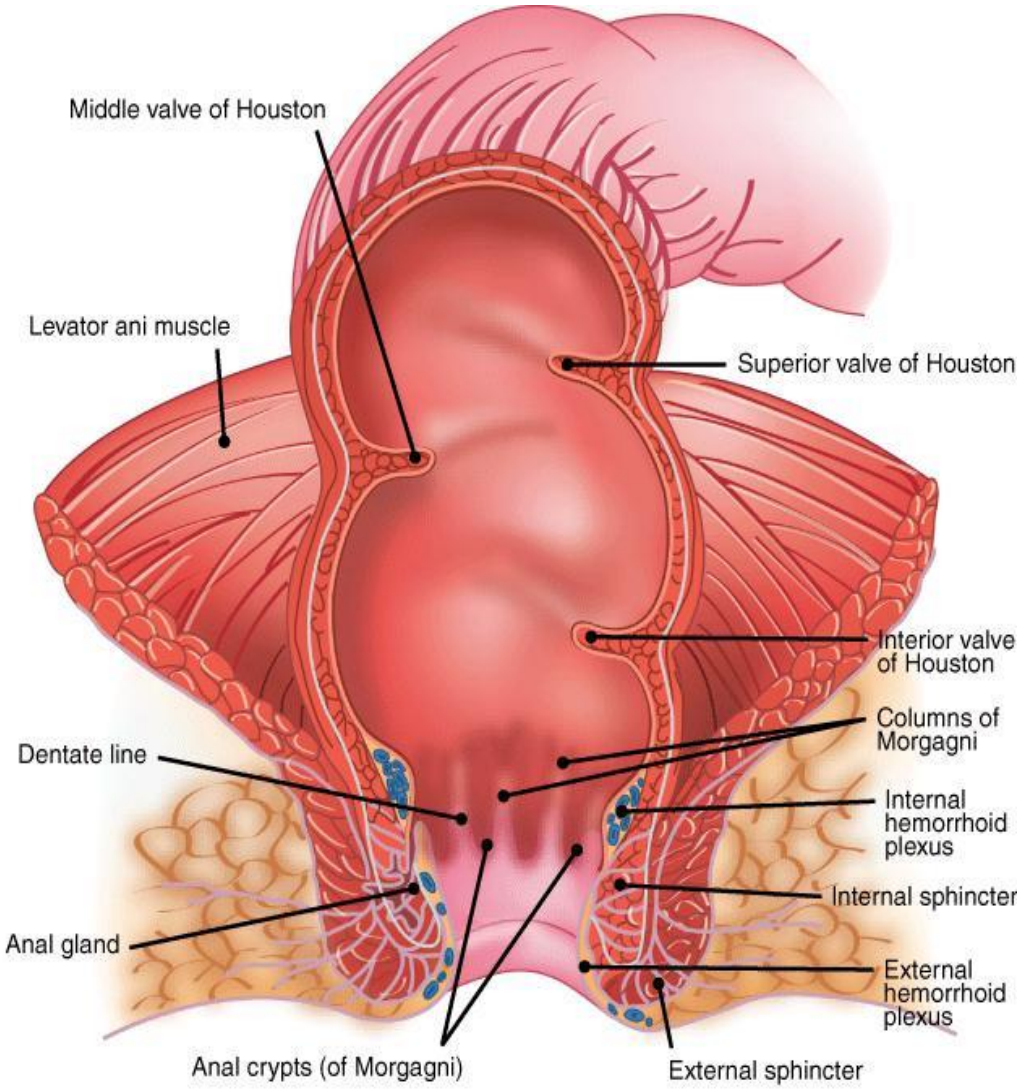

Figure 1.4. Rectal anatomy.Source: Shrieve DC, Loeffler JS: Human Radiation Injury. 2011. By Lippincott Williams &Wikins.

1.1.5 Staging and Prognosis of Colorectal cancer

The Dukes classification and its modifications

In 1932 Cuthbert E. Dukes, who was a Scottish pathologist working predominantly on a classification scheme for rectal cancer at St. Mark's hospital, developed the classification system that has borne his name after investigating more than 2,000 samples of colorectal cancer resections. The system and the several modifications made to it by Dukes and others, realized the important role played by lymphatic metastasis and tumourous local invasion in the progression of colorectal cancer. This classification supplies a modern pathological foundation for predicting the prognosis of patients with colorectal cancer. In 1936 Dukes had modified the C stage on the basis of the different levels of para-rectal lymphatic spread from superior rectal artery to inferior mesenteric artery. What is more, an adaptation further divided stages B and C in 1954 by the Americans Astler and Coller (Table 1.2).

Tumor, Nodeand Metastasis Classification

In 1954, Pierre Denoix proposed the Tumor, Node and Metastasis Classification (TNM) based on local invasion and lymphatic metastasis. Based on the AJCC Cancer Staging Manual, the 7th edition of TNM staging system had been modified in 2010. This classification system for colorectal cancer is now the only classification system that is accepted [18]. The TNM system classifies colorectal tumours based on three categories. "T" (tumour) denotes the degree of invasion of the bowel wall, "N" (node) denotes the degree of lymphatic node involvement, and "M" (Metastasis) denotes the degree of metastasis. TNM classification reasonably describes and records the

anatomic extent of cancer (Table 1.3). Anatomic stage/ prognostic groups (TNM and Duke classifications) is described in Table 1.4.

Table 1.2. Modified Dukes classification of colorectal cancer

Stage	**Feature**
A	Limited to mucosa
B1	Extending into muscularis propria but not penetrating through it; nodes not involved
B2	Penetrating through muscularis propria; nodes not involved
C1	Extending into muscularis propria but not penetrating through it. Nodes involved
C2	Penetrating through muscularis propria. Nodes involved
D	Distant metastatic spread

Astler VB, Coller FA: The prognostic significance of direct extension of carcinoma of the colon and rectum. Ann Surg 139:846, 1954

Table 1.3.TNM classification of colorectal cancer

Category	**Staging**
T stage	Tx: primary tumourcannot be valued T0: no signs of tumour Tis: tumour*in situ* T1: tumour invades submucosa T2: tumour invades muscularispropria T3: tumour invades subserosa or beyond (without other organs) T4a: tumour penetrates to the surface od the visceral peritoneum T4b: tumour directly invades or is adherent to other organs or structures
N stage	Nx: lymph nodes cannot be valued N0: tumour cells absent from regional lymph nodes N1: 1 to 3 lymph nodes close to the bowel contain cancer cells N2: there are cancer cells in more than 3 lymph nodes that are further than 3cm away from the main tumour in the bowel or there are cancer cells in lymph nodes connected to the main blood vessels around the bowel N2a: metastasis in 4-6 regional lymph nodes N2b: metastasis in 7 or more regional lymph nodes
M stage	Mx: distant metastasis cannot be evaluated M0: no distant metastasis M1: metastasis to distant organs (beyond regional lymph nodes) M1a: metastasis confined to one organ or site (e.g. liver, lung, ovary, nonregional node) M1b: metastases in more than one organ/ site or the peritoneum

Source: www.cancerstaging.org/staging/index.html

Table 1.4. Anatomic stage/ Prognostic groups

Stage	T	N	M	Duke[1]
0	Tis	N0	M0	-
Ⅰ	T1	N0	M0	A
	T2	N0	M0	A
ⅡA	T3	N0	M0	B
ⅡB	T4a	N0	M0	B
ⅡC	T4b	N0	M0	B
ⅢA	T1-T2	N1/N1c	M0	C
	T1	N2a	M0	C
ⅢB	T3-T4a	N1/N1c	M0	C
	T2-T3	N2a	M0	C
	T1-T2	N2b	M0	C
ⅢC	T4a	N2a	M0	C
	T3-T4a	N2b	M0	C
	T4b	N1-N2	M0	C
ⅣA	Any T	Any N	M1a	-
ⅣB	Any T	Any N	M1b	-

1: Duke B is a composite of better (T3 N0 M0) and Worse (T4 N0 M0) prognostic groups, as is Dukes C (any TN1 M0 and Any T N2 M0).
Source: www.cancerstaging.org/staging/index.html

1.1.6 Diagnosis of Colorectal Cancer

Although diagnosis of colorectal cancer is no longer a significant challenge due to modern technologies, early diagnosis remains a challenge.

Specific symptoms are too insidious to be detected at early-stage colorectal cancer. On average 60% of patients with colorectal cancer, do not have a definite diagnosis until 6 months after the appearance of symptoms. The main reason for this delay in diagnosis is arguably the lack of specific symptoms of colorectal cancer. Abdominal mass, change in bowel habit and abdominal pain are the most common symptoms of colorectal cancer, yet these symptoms are also commonly seen in functional gastrointestinal disorders and inflammatory bowel diseases.

Symptoms associated with colorectal cancer include change in bowel habit hematochezia, abdominal pain, abdominal mass, lower gastrointestinal bleeding, weight loss, change in appetite and anaemia. Bowel obstructive symptoms area particularly alarming sign and are seen in about 8%-29% of patients with colorectal cancer and usually indicate a well progressed tumour [19]. However, other symptoms other than obstructive symptoms do not necessarily correlation with a particular stage of disease [20]. In 1974 Welch reported the correlation between clinical symptoms and tumour location (Table 1.5). There are not any obvious symptoms at the earlier stage of rectal cancer, especially cancer *in situ* located in mucous layer. Unexplained blood and mucus in stool, altered bowel habit and urethral stimulation symptoms caused by prostate invasion by rectal cancer are classified as the symptoms associated with rectal cancer.

Table 1.5. The correlation between clinical symptoms and tumour location

	Hemoproctia (%)	**Change in bowel habit (%)**	**Abdominal Pain (%)**	**Obstruction (%)**
Right colon	20	24.7	44.7	7.9
Transverse colon	21.1	23.2	40.1	16.2
Descending colon	27.6	26.3	35.5	23.7
Sigmoid colon	43.1	39.7	26.6	15.1
Rectum	60	50.8	19.2	6.9
	Weight loss (%)	**Abdominal Mass (%)**	**Anemia (%)**	**Other (%)**
Right colon	19.4	6.3	13.8	17.4
Transverse colon	18.3	3.5	8.4	7.7
Descending colon	11.8	1.3	3.9	6.6
Sigmoid colon	12.8	1.7	2.3	6.6
Rectum	17.7	1.7	0	69

A palpable mass, melena (right-sided colon cancers), bright blood per rectum (usually left-sided colon cancers or rectal cancer) or abdominal tenderness may be detected by physical examination. Digital rectal examination is an essential part of the physical examination. Obstructions caused by colon cancer, which results in abdominal distention and constipation is usually in the sigmoid or left colon. In contrast, the symptoms of right-sided colon cancers are possibly more insidious most of the time. Adenopathy, hepatomegaly, jaundice, or even pulmonary signs (dry cough, haemoptysis and thoracalgia) may be present with metastatic disease. Complications of colorectal cancer include intestinal perforation, acute gastrointestinal bleeding, acute obstruction, and functional impairment secondary to distant metastases.

1.1.7 Screening for Colorectal Cancer

Evaluation should include complete history, family history, physical examination, and laboratory tests, colonoscopy, and pan-body computed tomography (CT) scan [21]. Upon completion of the diagnosis and staging (endoscopic ultrasound should be an integral part of staging of rectal cancer), incorporation of expertise from medical, radiation, and surgical oncologists is required to formulate and implement a treatment plan.

Laboratory examination

Routine blood analysis may detect iron-deficiency anemia, electrolyte derangements, and liver function abnormalities. Carcino-embryonic antigen (CEA) is one of the most helpful tumour markers that is monitored post-operatively to detect recurrence disease and may herald liver metastases [22]. Despite this, CEA is hardly a useful tool in early detection of colorectal cancer, and CEA rises may also occur due to tumours of non-colonic origin and non-cancer conditions. The normal level of CEA is also a challenging issue, due to different standards adopted by different laboratories in different countries. Based on the observation of sensitivity and specificity valued by different standard, Youden's index and predicted value demonstrated the highest value when the concentration of CEA was 5ng/ml (Table 1.6) (Zhang *et al*. 1993).

With the advance of molecular biological techniques, attention has been drawn to stool-based tools and new blood-based tests. Technologies now exist to extract genomic DNA or protein from stool and assay for evidence of genetic alterations [23]. Large-scale validation studies are in progress. One particularly attractive pathway for

stool-based diagnostics would be able to stratify patients as high, moderate, or low risk for colorectal cancer and thus influence modality and frequency of screening. In a complementary fashion, functional genomics are being applied to pair-wise comparisons of normal colon and colorectal cancers. This may allow screening of the entire human genome of nearly 30,000 genes and discovery of those genes, known and novel, that may be up-regulated or down-regulated and possibly linked to detection, prognosis, and therapy.

Table 1.6. Evaluation of level of CEA (ng/ml)

CEA (ng/ml)	Sensitivity	Specificity	Positive predictive value	Negative predictive value	Youden's index
>3	73	62	57	77	0.35
>5	59	84	72	75	0.43
>10	45	96	89	72	0.41
>15	36	99	96	69	0.35

(http://mall.cnki.net/magazine/Article/ZHWK405.017.htm)

Colonoscopy

The best approaches for screening will take into consideration multiple factors including benefit to risk ratio, speed, sensitivity, specificity, cost-effectiveness and other social and economic factors. To this end, colonoscopy is currently most likely to offer the most effective approach when one considers all of these factors [24].

A patient at an average-risk of having colorectal cancer is defined as a man or woman above the age of 50, without personal or family history of adenomatous polyps or colorectal cancer and absence of any occult or acute GI bleeding.

Optical colonoscopy is currently thought to be the most sensitive method for screening. The use of a colonofibroscope is suggested as a vital development of colorectal cancer diagnosis [25]. Advantages of using optical colonoscopy include direct visualization, polyp resection (although limited by the size and anatomic location of the polyps) and to obtain biopsies. The morbidity of colon cancer can decrease by approximately 76%-90% after the colorectal carcinoma resection by colonoscopy [26]. As with other examination method, optical colonoscopy has its associated side effects, such as bowel perforation, Flexible sigmoidoscopy typically allows visualization of the rectum, sigmoid colon, and descending colon up to the splenic flexure without the requirement of conscious sedation and hemodynamic monitoring but is limited in its reach compared with the colonoscopy.

Barium enema

Flexible sigmoidoscopy should not be considered as a single screening measure but requires coupling with barium enema. Barium enema allows visualization of the entire colon, and affords advantages of ease of preparation, lack of conscious sedation and haemodynamic monitoring, and ability to visualize polyps and masses. However, an obvious disadvantage is its sensitivity in which small polyps may be missed.

Other examinations

New noninvasive technologies are evolving, although most of the new methods are still under investigation. These new technologies, for example ultrasonic examination, CT scan and Magnetic Resonance (MR)-colonography, may provide some initial data demonstrating efficacy. The advantage of CT scans is that the test allows imaging of adjacent mucosa and metastasis with lymph nodes or distant organs, hence it benefits the clinical staging. According to the CT staging criteria of EC suggested by Moss *et al* in 1981, the accuracy of staging on CT was 85.7% (Table 1.7) [27]. CT virtual colonoscopy, which is specially applied by the diagnosis of prominent colorectal lesions (>5cm) is a new CT assisted diagnostic technique [28-30]. A recent study has shown that the finding from CT virtual colonoscopy is consistent with optical colonoscopy, although large-scale population studies are still needed [31].

Table 1.7.CT staging by Moss *et al* [27].

Stage	
Ⅰ	The thickness of bowel wall is normal (approximate 5cm), polypoid disease shows protrusions toward cavities.
Ⅱ	Local bowel wall is thickening; adjacent tissues have been invaded; no distant metastasis
Ⅲ	Local bowel wall is thickening; adjacent tissues have been invaded with involvement of local lymph nodes; no distant metastasis
Ⅳ	Distant metastasis (e.g. liver, lung, distant lymph nodes)

1.1.8 Pathology of Colorectal cancer

Colorectal cancer derived from the mucosa, namely adenocarcinomas, account for more than 90% of colorectal tumours [32]. Other histological types include squamous cell carcinoma, carcinoid, leiomyosarcoma, and lymphoma. Most grading systems classify adenocarcinoma into well, moderately or poorly differentiated tumours. Large bowel tumours may invade from mucosa through the entire bowel wall and beyond. Lymphatic metastasis which involves lymphatic vessels and lymph nodes are common. Haematogenous spread to the lung and liver are the most frequently seen distant metastases from colorectal cancer. There is little propensity for colon cancer to spread longitudinally within the bowel wall, in contrast to esophageal or gastric cancers. In 2000, colorectal cancer had been designated as a malignant epithelial tumour in colon or rectum and the malignancy is defined as observation of tumour penetrating the lamina muscularis into the submucosa [33]. The WHO histology classification of colorectal cancer is shown in Table 1.8

1.1.9 Therapy of colorectal cancer

Surgery

As the primary treatment of patients with colonic tumours, surgery with curative intent is possible in around 75% of patients [34]. Surgery of primary colorectal cancer is on the basis of the anatomy and mechanisms by which this disease spreads. Colorectal adenocarcinomas may grow rapidly and invade into the lymphatics of the submucosa and bowel wall. For the assurance of the curative resection, sufficient lengths of bowel need to be resected distal and proximal to the tumour. One approach of lymphatic metastasis is to extend through the serosa into mesenteric lymphatics at the root of the mesentery, and removal of the main lymphatic drainage system of the mesentery must be operated. Right hemicolectomy, transverse colectomy, left hemicolectomy and sigmoid resection are the usual procedure in colonic surgery, whilst those in rectal surgery include Dixon-operation, Parks-operation and Bacon-operation. All the operations must be performed by adherence to surgical oncologic principles (la principe aseptique, to avoid subsidiary-injury, minimal invasion, radical resection and non-neoplasia surgical operation) without major sacrifice of bowel function.

Table 1.8.WHO histology classification of colorectal cancer[33]

Epithelial tumour
Adenoma
Villiform adenoma
Tubulose adenoma
Tubulovillous adenoma
Serrated adenoma
carcinoma
Adenocarcinoma
Mucinous adenocarcinoma
Signet-ring cell carcinoma
Small cell carcinoma
Epidermoid carcinoma
Adenosquamous carcinoma
Medullary carcinoma
Undifferentiated carcinoma
Carcinoid
EC cell, secreted serotonin carcinoma
L cell, secreted glucagon peptide and PP/PYY carcinoma
Anaplastic carcinoma
Non-epithelial tumour
Lipoma
Leiomyoma
Gastrointestinal stromal tumour
Leiomyosarcoma
Hemangiosarcoma
Kaposi sarcoma
Malignant melanoma
Malignant lymphoma
MALT marginal zone Bcelllymphom
Mantle cell lymphoma
Diffuse large B-cell lymphoma
Secondary tumour
Polyp
Hyperplastic polyp
Peutz-Jeghers
Juvenile peutz-Jeghers

Chemotherapy

Moertel *et al*. reported that the addition of 5- fluorouacil (5FU) and leucovorin improved survival rates of patients with resected colorectal carcinoma [35]. What is more, as an oral 5-FU prodrug, Capecitabine has showed similar overall and disease free survival rates with 5-FU in patients with resected colorectal cancer[36]. More recently, Oxaliplatin has been investigated as one of the adjuvant therapy of resected colorectal cancer. By contrast with 5-FU/ leucovorin, the improved disease-free survival was demonstrated in patients treated with Oxaliplatin [37].New standard chemotherapeutic regimens may be established based on 5FU/leucovorin/Oxaliplatin through the investigation of these data above.

Radiotherapy

Although surgery is commonly suggested as the main therapy of colorectal cancer, local recurrence and distant metastasis was the main cause of treatment failure after the resection of colorectal cancer [38]. In addition, the local invasion and disease progression occur at the advanced diseases [39]. Hence, adjuvant therapy was necessary to adopt in the therapy of resected colorectal cancer. Colorectal cancer, especially rectum cancer, was radiosensitive and controlled locally by the adjuvant radiotherapy, even if the profit of survival has been not verified completely after the radiotherapy [40].

Gene Therapy

Several aspects of colorectal cancer make the disease a reasonable potential target for gene therapy approaches [41]. Because colorectal cancer may progress within a confined space, such as the peritoneal cavity, or within a solitary organ, such as the liver, regional administration of a gene vector may be practical. Multiple trials of different gene therapy approaches, including virus directed enzyme pro-drug therapy, immunogenic manipulation, gene correction, and viral therapy, have all been initiated. These approaches are still at testing stages, and the therapeutic benefits from gene therapy in colorectal cancer have yet to be confirmed in clinical trials.

1.1.10 Molecular Predictive Markers

With the availability of a number of active agents, the ability to prospectively select a particular drug or drug combination that would have a likelihood of increasing efficacy or a likelihood of decreasing toxicity would be clinically useful. This method is highly desirable, but does not as yet exist. The past decade has seen some intensive research looking for potential markers.

For example, one particular avenue of investigation is to elucidate markers of resistance to fluorouracil, based on knowledge of its metabolic pathways. Recent studies have indicated that high levels of either TS, DPD, [42] or thymidine phosphorylase (TP) in a tumour sample as measured by RT-PCR, may predict failure rate in response to an infusional 5-FU regimen [43-45]. These observations are intriguing but presently insufficient to exclude the use of 5-FU in a particular patient

Large-scale prospective trials are highly desirable before being applied to routine practice. There is, at the present time, no role for the use of these markers in standard practice. Others have investigated genomic analysis as an indicator of response or toxicity [46-47]. Although these approaches appear promising, they are yet to be validated and should not be considered as part of standard care.

The following are some biomarkers extensively investigated in human colorectal cancer.

1.1.11 Tumor suppressor genes in colorectal cancer

The accumulation of intracellular gene mutation results in neoplastic transformation. Normal or abnormal phenotype of a cell is dependent on cell genotype and/or intracellular epigenetic alternation. Gene mutations, which include oncogene (e.g. *K-ras, C-myc* and *src*), tumour suppressor gene and DNA mismatch repair gene, are the basis of cancerization [48-50].

Tumour suppressor gene maintains cell stability by regulating cell proliferation and differentiation. Therefore, uncontrollable cell proliferation and the formation of tumour may be a result of inactivated tumour suppressor genes caused by somatic mutation or heredity. The *APC* (*Adenomatous polyposis coli)* [51] located at chromosome 5q.22.2 and P53 gene located at chromosome 17p are the most thoroughly investigated tumour suppressor genes in colorectal cancer.

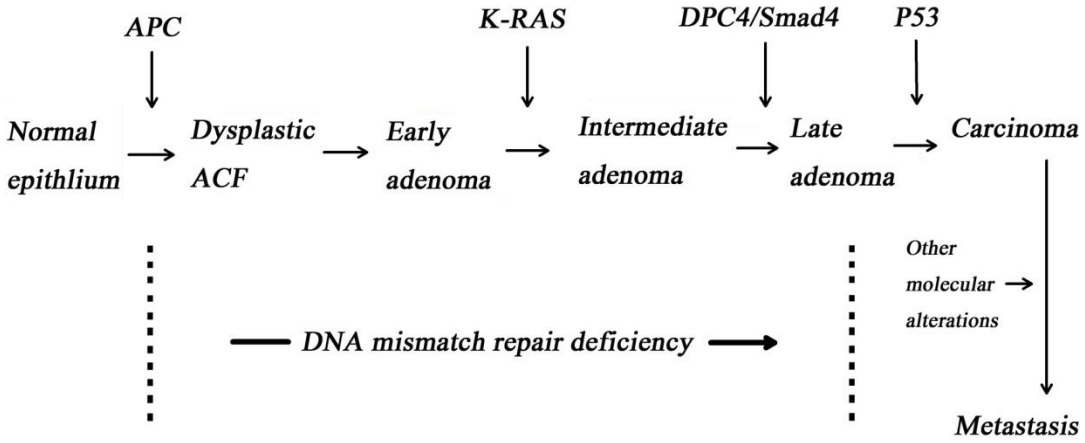

Figure 1.5. Flow chart demonstrates these gene mutations are consistent with the order of cancer progression (from adenoma to carcinoma). 1988. By Bert Vogelstein.

APC (Adenomatous Polyposis Coli) Tumour Suppressor gene

The APC protein, coded by the *APC* gene, controls many cellular functions of intestinal cells (e.g. proliferation, differentiation, migration and polarity)[52]. Many cases of colorectal cancer have been discovered primarily by loss or mutation of adenomatous polyposis coli [51]. APC was suggested as a negative regulator of Wnt signaling in tumour suppression [52]. A destruction complex is formed by APC with Axin and two kinases (casein kinase 1, CK1 and glycogen syntase kinase 3β, GSK3β) in the absence of Wnt signaling, which can phosphorylate the transcriptional co-activator β-catenin, thereby, to make β-catenin to be degraded proteasomally [53]. When the Wnt signalling is active, Wnt proteins will activate its receptor, Frizzled and subsequently dishevelled proteins, which prevent the phosphorylation of CK1 and GSK3β. This subsequently inhibits the formation of destruction protein and leads to stablisation of β–catenin protein. As a consequence, β–catenin protein is accumulated in the cytosol. The excess β–catenin protein subsequently translocates to the nucleus where it binds to the transcription factor TCF4 in the nucleus and activates target genes (e.g. c-myc and cyclin D1) [53]. Hence, the stabilised β-catenin caused by the mutation in APC protein triggers the downstream events of Wnt signaling. Consistent with this model, an abundance of mutation in the *APC* gene has been detected in adenoma formation in transgenic mice and has correlation with 7% of sporadic colon cancer [54-56].

p53 Tumour Suppressor

p53, or P53, TRP53, BCC7, is one of the best charaterised tumour suppressor genes. The *p53* gene is localised in chromosome 17p13.1 and encodes the p53 protein, a transcription factor that is involved in the regulation of cell cycle, apoptosis, cellular senescence (McBride et al 1985, Benchinol et al 1985, Rowley 1986). Abnormalities of the *p53* gene, transcript and protein expression have been widely reported in human cancers including colorectal cancer.

Allelic loss of chromosome 17p is observed in three of four colorectal carcinomas but fewer than 10% of adenomatous polyps [57]. The remaining *p53* allele is inactivated in most tumours with 17p loss of heterozygosity [58], most often at codons 175, 245, 248, 273, or 282 [59]. LOH of 17p and mutations in *p53* thus appear to arise during the transition from adenoma to carcinoma, perhaps facilitating progression. When faced with stress from DNA damage, hypoxia, reduced nutrient access, and aneuploidy, cells with intact *p53* function undergo cell cycle arrest and apoptosis. The loss of *p53* may allow cells to overcome such barriers to tumour growth and progression.

Another protein complex that may have tumour and tumour metastasis suppressing functions is Kiss-1 and Kiss-1 receptor.

1.2 Kiss-1 and Kiss-1 receptor

Discovered by Danny Welch in Pennsylvania in 1994 (Welch *et al* 1994), Kiss-1 (also known as metastin and kisspeptin-1) is a protein demonstrated to have some hallmarks of a tumour suppressor in some tumour types.

1.2.1 Regulation of Kiss-1:

Lee and colleagues (Lee et al 1996) introduced the full length of chromosome 6 into the human metastatic melanoma cell line C8161 using a microcell-mediated transferring technique and then found the introduction of chromosome 6 suppressed metastasis without impacting tumourigenicity and tumour invasion [60]. Two years later, the human Kiss-1 gene was isolated and identified from the melanoma cells by Lee *et al* [61-62].The premature coding products of the *Kiss-1* gene is a protein with 145-amino-acids. The protein is subsequently cleaved into a family of Kisspeptins, including Kisspeptin-10, Kisspeptin-13, Kisspeptin-14, Kisspeptin-54 respectively [48, 63-64]. Coincidently, the *Kiss-1*gene mapped to chromosome 1q32, which was identified as a human melanoma metastasis suppressor gene through the analysis of subtractive hybridization in highly metastatic cell lines as compared with non-metastatic cell lines [60]. These early findings suggested that there was a

regulatory gene existing on chromosome 6, which regulates the expression of *Kiss-1* gene. Subsequent research revealed that the regulatory region of Kiss-1 was in a locus of a 40-cM region between 6q16.3 and q23 of chromosome 6 [65]. Complementary studies of 51 melanoma patients by Shirasaki and co-workers showed that a loss of 6q16.3- q23 was observed in 14 melanoma patients (51%), which had significant correlation (p=0.03) with a loss of Kiss-1 expression (44%) [66]. In addition, Goldberg *et al*. found the high expression of thioredoxin interacting protein (TXNIP, also known as vitamin D up-regulated protein 1, thioredoxin binding protein 2 or VDUP1) in non-metastatic melanomas, which was mapped to chromosome 1q and also expressed in the neo6/C8161 melanoma cell line [67]. In the subsequent studies, the author detected ascended TXNIP expression inhibited metastasis of melanoma cells via an up-regulation of Kiss-1. Moreover, PCR karyotyping revealed that the expression of both Kiss-1 and TXNIP were up-regulated in the cells transfected with CRSP3 (vitamin D receptor interacting protein) which was mapped to chromosome 6 and led to a suppression of metastasis [67]. Meanwhile, decreased Kiss-1 expression and increased metastasis were evident to correlate with a loss of CRSP3 [67]. These findings indicate that CRSP3 mapped to chromosome 6 is an upstream regulator of TXNIP, which subsequently regulates the expression of Kiss-1. In other words, a loss of CRSP3 expression, which is caused by structural abnormality of chromosome 6 impairs the appropriate expression of Kiss-1 and TXNIP.

1.2.2 Kiss-1 receptor: Discovery and structure:

Kiss-1 receptor (Kiss-1R), also known as G-protein coupled receptor 54 (GPR54), HOT7T175, AXOR12, Metastin receptor, was first discovered and cloned from rat brain in 1999 [68]. In humans it maps to chromosome 19p13.3, contains 5 exons and 4 introns and encodes 398 amino acids (75 kDa) and shares 81% protein homology with the preceding cloned rat orthologue [64, 69].

Tissue distribution of Kiss-1 and its receptor are often concordant. For example, both Kiss-1 and Kiss-1R are both highly expressed in placenta tissues [48, 61, 69]. Moreover, both Kiss-1 and its receptor are widely distributed throughout the central nervous system [69]. High levels of Kiss-1R have been observed in cerebral vortex, cerebellum, thalamus and pons-medulla [69]. In contrast, its cognate ligand precursor, Kiss-1, is highly expressed in hypothalamus and pituitary [64]. In addition to placenta, the expression of Kiss-1R is also high in pancreas, whilst it is expressed at low levels in adipose tissue, lymph nodes, peripheral blood lymphocytes, pituitary gland and spleen [48, 69].

1.2.3 Kiss-1, Kiss-1 receptor and downstream pathways:

Concrete mechanism(s) by which Kiss-1 suppresses tumour metastasis are yet to be established. However, a few signal transduction pathways have been indicated as the key downstream events of Kiss-1/Kiss-1R complex.

Calcium coblization through Gq activation

Intracellular Ca+ was increased significantly in the cells transfected with Kiss-1 receptor followed with treatment of Kiss-1 or Kisspeptins, such as B16-BL6 melanoma [48], CHO-K1 [64], HEK293 [69]. Hence, the mobilization of calcium in cells, which treated with Kiss-1, manifested the important role of Kiss-1 receptor. Kiss-1Ris likely coupled to G-proteins of the Gαq/11 subfamily rather than to the Gi or Gs subfamily [69]. Through Gα q/11–mediated signaling pathway, phospholipase Cβ (PLCβ) is activated which consequently generates two kinds of second messengers in cells (Inositol triphosphate 3 and Diacylglycerol), leading to intracellular Ca^{+} release and protein kinase C activation, respectively [70]. In the meantime, increased intracellular Ca^{+} markedly suppresses tumour metastasis and induces differentiation and apoptosis in human cancer cells [70]. In addition, the capacity of colony formation of a breast cancer cell (MDA-MB-435) on hard agar medium is negatively correlated with the expression of Kiss-1 [71].

Matrix metalloproteinases (MMPs)

MMPs can degrade extracellular matrix and play dominating roles in the process of tumour metastasis. MMP-9, known as the most important protease related with tumour metastasis and is capable of degrading the primary structure of extracellular matrix and basement membrane (collagen, laminin, fibronectin), thereby promotes the tumour metastasis [72]. Yan *et al*. have shown that there was a marked reduction of *in vitro* invasion through Matrigel®-coated porous filters by HT-1080 cells which had reduced transcription and activity of MMP-9 following the overexpression of Kiss-1 [73]. This reduction is credited in part to the diminished P65 and P50 NF-KB proteins which interact with the promoter of MMP [70]. Consequently, the reduced synthesis of MMP-9 brings about certain inhibitory effects on the mobility and invasion of cancer cells [48, 70]. In addition, activated focal adhesion kinase (FAK) and paxillin, which play a crucial role in the process of formation of focal adhesion, exhibit certain links with Kiss-1 and its receptor [74]. In ARO thyroid cancer cells transfected with Kiss-1R Kiss-1 treatment elicited strong and sustained phosphorylation of ERK1/2, at the same time as weak phosphorylation of p38 or pAKT [74]. A similar concentration-dependent release of arachidonic acid caused by Kisspeptin-10 was seen in CHO-K1/MR cells, in which Kisspeptin-10 strongly inhibited cell proliferation [64]. Activated ERK1/2 can significantly induce the formation of stress fibre, focal adhesion and activated RHO, via the phosphorylation of FAK and paxillin [48, 74].

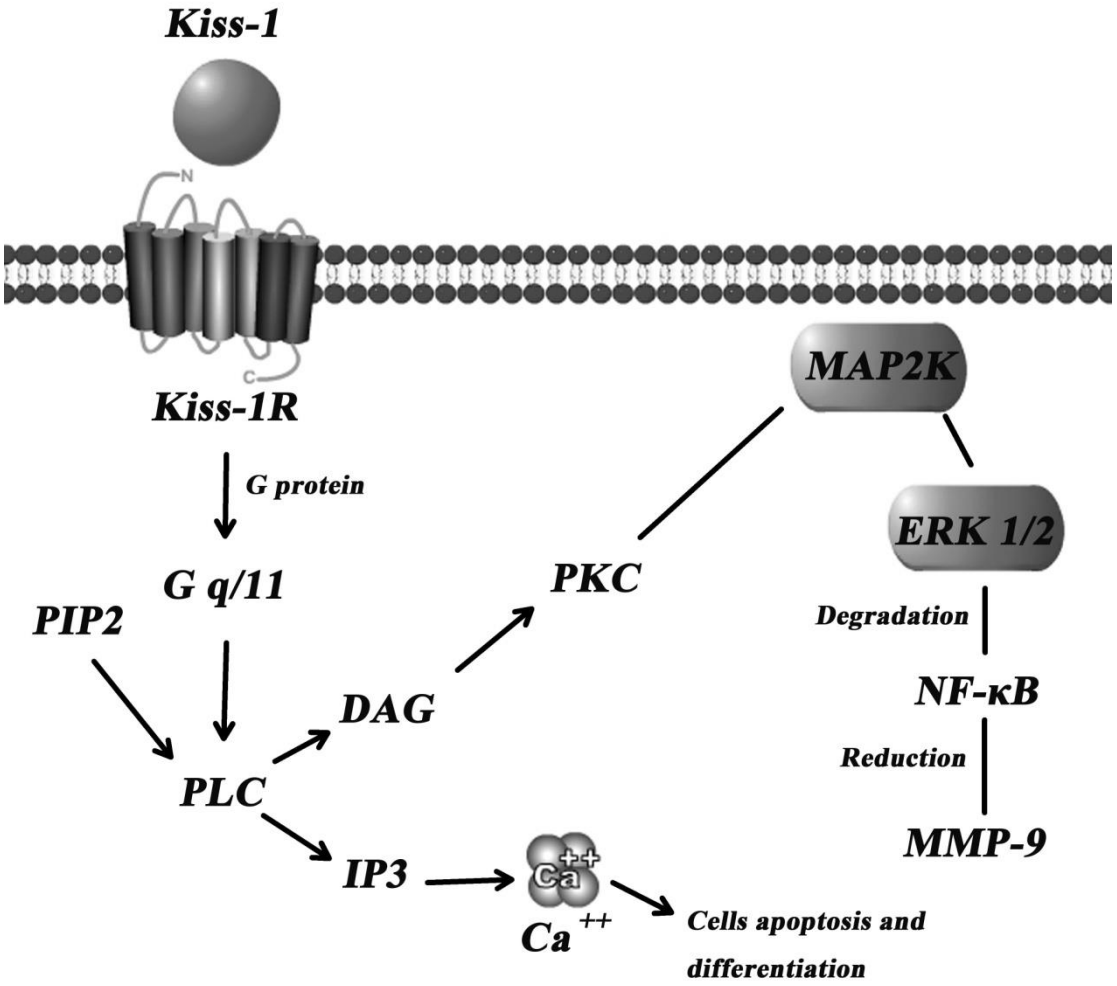

Figure1.6. The suggested mechanisms of neuronal depolarization by Kiss-1 and its receptor (Kiss-1R).Gα q/11 is activated by Kiss-1R and PLC to cleave PIP2 into IP3 and DAG. IP3 promote intracellular Calcium ions release inducing cancer cells to differentiation and apoptosis, while DAG activates a signal cascade by activating PKC. The reduction of MMP-9 caused by the degradation of NF-κB contributes to suppress tumour metastasis through activating MAPK pathway.

1.2.4 Kiss-1 and Kiss-1R in Cancer:

Breast cancer

Lee and Welch (1997) hypothesized that Kiss-1 was possibly suppressed metastasis in other types of tumour, in addition to melanoma from which Kiss1 was discovered. This was on the basis of the map location of Kiss-1gene (chromosome 1 bands q32-41), where its 1q alternations are peculiar in breast tumour carcinomas. To test this hypothesis, the authors firstly transfected full-length Kiss-1 cDNA into a human breast cancer cell line, MDA-MB-435s, and then implanted the cells into athymic nude mice with paired control cells. The results demonstrated that the metastatic probability of transefected cells remarkably increased, although the tumourigenecity was suppressed [71]. To further test the hypothesis, Mitchell and colleagues (2005) discovered by using RT-PCR, that the loss of Kiss-1 gene expression was associated directly with the expression levels of activator protein-2a and specificity protein-1, two known transcription factors expressed in highly metastatic breast cancer cell lines [75]. In addition, Marot and colleagues (2007) found that the low level of Kiss-1 mRNA was expressed in the ERα-negative MDA-MB-231 cells while the ERα-positive MCF7 and T47D cells exhibited higher expression of both Kiss-1 and its receptor. Interestingly, the data from postmenpopausal women with breast cancer showed an opposite relationship [76]. Also, an analysis of Kiss-1 mRNA in paraffin-embedded stage Ⅱ or Ⅲ lymph node positive breast adenocarcinomas demonstrated that the Kiss-1 gene expression was silenced. These observations also

support the anti-metastatic potential of Kiss-1 in certain breast cancers [77]. Likewise, another study investigating the metastasis-suppressor gene profile of breast cancer using frozen tissue samples, analysed Kiss-1 expression at mRNA and protein levels, using RT-PCR and immunohistochemical staining respectively (2005) [78]. The study showed that Kiss-1 mRNA expression was suppressed in brain metastases from breast cancer. In contrast to the studies supporting the anti-metastatic potential of Kiss-1 in breast cancer, Martin *et al*. (2005) found that the expression of Kiss-1 was remarkably increased in primary tumours compared with normal mammary tissues. The increased expression of Kiss-1 in primary tumours was also correlated with the metastasis to lymph nodes. Likewise, the expression of Kiss-1 became higher with tumour grades and increased TMN status. In contrast, its receptor (Kiss-1R) was significantly decreased in patients with poor survival. Moreover, invasiveness of breast cancer cells was impaired by the knockdown of Kiss-1 [79].

Gastric cancer

Dhar *et al*. (2004) found that reduced Kiss-1 expression in gastric cancer was related to increased risk of distant metastases and tumour recurrence. The study analysed the expression of Kiss-1 in frozen tissue samples from 40 gastric adenocarcinomas using RNase protection assays, and had suggested that Kiss-1 was a possible independent predictor of patient survival compared with the conventional routine prognostic predictors of gastric cancer [80]. Likewise, an investigation of two metastasis

suppressor genes, Kiss-1 and KAI-1 in 49 gastric adenocarcinoma tissues together with 20 precancerous tissues showed that Kiss-1 mRNA was remarkably lower in cancer tissues compared with the precancerous tissues. It has again indicated a possible predictive value of Kiss-1 for the prognosis of patients with gastric cancer. Similar results were seen in a study by Yao *et al* (2007) which demonstrated that reduced Kiss-1 expression is seen in moderate-to-severe hyperplasia compared with normal-to-moderate hyperplasia, and also in T3/T4 tumours with lymph node involvement and distant metastases compared with tumours at earlier stages, i.e. T1-2 without any metastasis [81].

Oesophagealcarcinoma

Oesophageal squamous cell carcinoma (ESCC) is one of the malignancies that we have so little effective means to treat. A number of reasons may contribute to the difficulties in treating the tumour, including late diagnosis and advance stages at the time of first visit, commonly seen lymph node metastasis in most patients, the anatomical reasons that the organ is closely surrounded by some key organs and tissues and its rich lymphatic drainage. The latter is of particular interest: even diagnosed at an early stage of ESCC patients would already have lymphatic metastases or develop lymph node metastasis soon after surgery [82]. Therefore, lymph node metastasis is suggested as the most important predictor of prognosis in ESCC. Ikeguchi *et al*. (2004) assessed the expression levels of Kiss-1 and Kiss-1R in

ESCC tumours and noncancerous tissues of oesophagus of 71 patients with oesophageal squamous cell carcinomas. Using real-time PCR, the authors have found that loss of Kiss-1 and its receptor was detected in 86-100% of primary tumours with lymph node metastases, suggesting a relevance to the lymphatic metastasis and unfavorable prognosis, independent of the depth of tumour invasion [83]. Furthermore, loss of Kiss-1 and its receptor was seen in primary tumours with invasion to adventitia compared with the control groups without invasion and was also associated with lymph node metastasis [48]. These findings strongly show that the loss of expression of one or both genes (Kiss-1 and Kiss-1R) is possibly vital in lymph node metastasis, and they can be considered as prognostic factors in ESCC [48].

Hepatocellular carcinoma

A small number of studies on the expression of Kiss-1 are available in the literature regarding tumour thrombus caused by invasion of hepatocellular carcinoma to the portal vein as the most vital prognostic factor of orthotopic liver transplantation for hepatocellular carcinoma (20%-70%) [84]. Hou *et al*. (2007) reported a relationship between the expression of Kiss-1 and MMP-9 in the formation of portal vein tumour thrombus (PVTT) in HCC by analysing 50 specimens of HCC (31 with PVTT and 19 without PVTT). The expression of Kiss-1 was lower in HCC with PVTT than that in HCC without PVTT. It is noteworthy that a contrasting expression pattern of MMP-9

was seen in HCC with and without PVTT. Hou *et al*. thus suggested that Kiss-1 may possibly prevent PVTT by up-regulating MMP-9 expression [85]. Interestingly, and in a clear contrast, higher expression of Kiss-1 and Kiss-1R genes was detected in more advanced tumours by Ikeguchi and co-workers (2003). It indicates that the expression levels of Kiss-1 and its receptor genes may promote tumour progression rather than suppressing the metastasis [86]. Similarly, the strong positive immunoreactivity of Kiss-1 and Kiss-1R was also seen in HCCs which showed higher Kiss-1 expression in the HCC with poor prognosis [87].

Pancreatic cancer

In pancreatic cancer, loss of 6q, 8q, 9q, 17q and 18q has been observed and the loss is associated with lymph node and distant metastases, suggesting that there is a vital suppressor gene existing in these regions for pancreatic cancer [88-89]. Due to the presence of the Kiss1 gene in the region, it was proposed that Kiss-1 expression may be down-regulated in pancreatic cancer. In a subsequent study employing a number of pancreatic cancer cell lines (AsPC-1, BxPC-3, Capan-2, CFPAC-1, PANC-1 and SUIT-2), Masui and co-workers (2004) found that Kiss-1 mRNA was reduced in pancreatic cancer whilst Kiss-1R mRNA expression was higher [90]. In 2007 Liang *et al*. demonstrated once again this view after detecting Kiss-1 expression of pancreatic cancer in the inducted Sprague-Dawley rats using in situ hybridization. Lower levels of Kiss-1 mRNA were observed in the pancreatic cancer tissues compared with

normal pancreatic tissues, suggesting Kiss-1 as a possible inhibitor of pancreatic cancer metastasis[91].

Thyroid cancer

Distant metastasis is also a crucial factor for the shortened survival of patients suffering from thyroid cancer. Patients who develop distant metastases from thyroid cancer have about 50% five year survival rates [92]. Recent studies have demonstrated the importance of certain receptors involved in metastatic capacity of thyroid cancer cells. Through the analysis of 36 thyroid tissue samples (13 papillary carcinomas, 10 follicular carcinomas, 2 benign follicular adenomas and 11 normal) using real-time PCR, Ringel *et al*. reported that higher levels of Kiss-1 and its receptor expression was detected in papillary and follicular cancers compared with normal tissue. The increased expression of both gene products were associated with greater possibility of developing distant metastases [74]. Furthermore, over-expression of Kiss-1R resulted in decreased capabilities of growth and migration of thyroid cancer cells following exposure to Kisspeptin-54 [93]. The authors found that Kisspeptin-54 was able to increase the protein levels of Myocyte-enriched Calcineurin Inter-acting Protein 1 (MCIP1) which is known as a calcineurin inhibitor. MCIP1 has been shown to be increased at the early stage of thyroid tumours and then was reduced or absent from lymph node metastases [93].

Ovarian cancer

Ovarian cancer is one of the leading female cancers globally. Recent data have shown that 24,400 women were newly diagnosed with ovarian cancer and almost 58% of them died from ovarian cancer in the United States in 2003 [94]. Berk and co-workers (2005) measured seven ovarian cancer cell lines using real time quantitative RT-PCR and reported that overexpression of Kiss-1 reduced metastatic colony formation by inhibiting cell migration [95]. Similar data were reported by Gao *et al*., who analysed, using immunohistochemical staining, the expression of Kiss-1 protein in 100 primary ovarian epithelial tumours (10 normal tissues, 20 benign adenomas, 20 borderline tumours and 50 malignant). The study showed that there was a significant increase of Kiss-1 expression levels in cancerous tissues compared with benign and normal ones while the increased Kiss-1 expression in cancer cell lines suppressed the expression of MMP-9 and NF-kB [96]. Furthermore, Hata and colleagues (2007) found that the lower expression of Kisspeptin-54 and Kiss-1R correlated with more deteriorative tumour and worse prognosis in 76 epithelial ovarian cancers [97].

Gestational trophoblast neoplasia (GTN)

All forms of GTN secrete human chorionic gonadotrophin (hCG), which is a helpful marker in the diagnosis, staging and subsequent assessment of the therapeutic response of malignant GTN by monitoring serum levels of hCG. hCG would start to rise and reach a plateaus in those patients who are developing malignant changes. It is

important to detect the serum hCG of the patients with GTN. However, like the problems associated with similar assays, issues exist regarding false positives caused by heterophile antibodies in commercial available tests [98], the research community remains highly interested searching for new biomarker for the tumour type. On the strength of the studies by Horikoshi *et al*. which showed that there was a dramatic increase in the concentration of plasma Kiss-1 receptor (Kisspeptin-54) in pregnancy [99], Dhillo and co-workers assessed the levels of Kisspeptin-54 in GTN by determining plasma Kisspeptin-immunoreactive (Kisspeptin IR) using chromatographic analysis. They found that there was a fluctuation of plasma Kisspeptin-54 following chemotherapy. Moreover, they continued to determine the concentration of plasma kisspeptin IR in female volunteers. Together with hCG, progesterone and estradiol were determined in11 healthy females without pregnancy, 5 healthy females who had previously been pregnant, 13 healthy women in the first trimester of pregnancy, 38 volunteers at 38 weeks of pregnancy and the same females 15 days postpartum, and 11 women diagnosed with invasive GTN using radioimmunoassays and Chemiluminescent Microparticle Immunoassays [100]. The result showed that there was a significant positive correlation between plasma kisspeptin IR and circulating levels of progesterone and estradiol. It suggests that plasma kisspeptin can be considered as a tumour marker in patients with malignant GTN [101].

Bladder cancer

As the fourth most common malignancy among men, bladder cancer can be classified based on the depth of invasion. Non-muscle-invasion (pTis, pTa and pT1) occupied 75% of transitional cell carcinomas (TCCs), muscle infiltration (pT2-pT4) are 20%, and the rest are metastatic at the time of diagnosis [102]. Five year survival rate is more than 90% for patients presenting with localized TCC, whilst it is only 50 and 10% for patients diagnosed with regional and distant metastatic disease spread respectively [102]. Similar to the effect of suppressing cancer metastasis by Kiss-1 observed in other solid tumours, loss of Kiss-1 was seen in the advanced bladder tumours [49]. Moreover, low levels of Kiss-1 expression were associated with increased histopahtological stage, poor tumour cell differentiation and poor survival rate [49, 103].

Prostate cancer

Prostate cancer is the most common malignancy and the second leading cause of cancer mortality among men whose age are older than 40 years. There are no curative therapies for advanced prostate cancer (PCa) [104]. Even if patients have experienced successful surgical resection, recurrence locally or distant metastases which are responsible for majority of PCa-related deaths would has a great opportunity to occur months or years later [105-106]. Because of the lack of timeliness of the analysis of the primary tumour size and histology, the information provided by identification and

characterization of molecular signatures is particularly crucial for the diagnosis of PCa [106]. Down-regulation of Kiss-1 has been shown to be correlated with decreased Kiss-1R expression which is inversely associated with the clinical stage and tumour grade. Forced expression of Kiss-1 increased cell sensitization to anoikis and chemotherapeutic drugs. Kiss-1 suppresses migration and invasion of prostate cancer cells. Kiss-1 has been suggested therefore as a potential factor for risk assessment of PCa progression [50].

Endometrial cancer

Uterine corpus cancer is the main cause of malignant gynaecological disease with more than 42,000 cases diagnosed, which is still stably increasing every year in the United States. Cancer cell invasion followed by metastasis impacts profoundly on patient prognosis and is considered as a vital issue to improve prognosis for females diagnosed with endometrial cancer [107]. Hyun Sook Kang *et al*. assessed Kiss-1 and its receptor expression in 92 adenocarcinomas of endometrial cancer using IHC staining and real time PCR. The result revealed the low expression of Kiss-1 and its receptor was significantly associated with certain wellknown poor prognostic factors of distant metastasis (for example invasion into lymphovascular space and deep myometrium) [107-108]. Furthermore, based on the study of subcutaneous xenograft established by inoculating Ishikawa cells into female nude mice, they reported that the decreased number of lymph node metastases of Kiss-1R + Ishikawa cells was

seen in metastin-10-treated mice, while there was no significant difference in the tumour size between metastin treated and non-treated groups. It indicates that Kiss-1affects metastatic potential of cancer cells rather than directly inhibiting tumour growth [108].

Table 1.9. Table for functions of cancer cells treated with Kisspeptin-10 compared with the control cells

Cell /tumour types	Migration	Invasion	Proliferaiton	Reference
Breast cancer		↓	None	[48, 71]
Pancreatic cancer	↓	None	None	[90]
Ovarian cancer	↓			[95]
Prostate cancer	↓	↓		[50]
Endometrial cancer	↓		None	[108]

Table 1.10. Expression of Kiss-1 and Kiss-1R in cancers compared with the corresponding normal tissues or background tissues

Tumour type	Kiss-1	Kiss-1R	Reference
Breast cancer	↓ / ↑	↓ / ↑	[71, 79]
Gastric cancer	↓		[80-81]
Esophageal carcinoma	↓	↓	[83]
Hepatocellular carcinoma	↑	↑ ↑	[86]
Pancreatic cancer	↓	↑	[90]
Thyroid cancer	↑	↑	[74]
Ovarian cancer	↓	↑	[48]
Gestational trophoblastneoplasia	↓ / ↑	↑ / ↓	[101, 109-110]
Bladder cancer	↓	↑	[49]
Prostate cancer	↓	↓	[50]
Endometrial cancer		↓	[108, 111]

The expression of Kiss-1 and Kiss-1R manifest relative differences compared with normal tissue in a variety of tumours from the data of Table 1.10. As these data were collected from different studies, it is difficult to analyse quantitatively the difference in the expression of Kiss-1 and its receptor among different cancers. However, the expression differences between Kiss-1 and Kiss-1R in comparison with normal tissues can be studied qualitatively in each group of cancers. Up-regulation and down-regulation of Kiss-1 and Kiss-1R expression has been indicated in various malignancies. Reduced expression of both Kiss-1 and Kiss-1R has been detected in gastric cancer (without the data of Kiss-1R), oesophageal carcinoma, prostate cancer and endometrial cancer (without the data of Kiss-1). By contrast, the increased expression of Kiss-1 and its receptor has also been observed in certain solid tumours, including hepatocellular carcinoma, thyroid cancer and gestational trophoblastneoplasia. Interestingly, several data presented contrary expression of Kiss-1 and Kiss-1R even in the same cancer from different studies (e.g. breast cancer and gestational trophoblastneoplasia). Additionally, the opposite expression of Kiss-1 compared with that of Kiss-1R was reported in pancreatic cancer, ovarian cancer and bladder cancer.

1.2.5 Summary

In summary, although it remains controversial, Kiss-1 has been demonstrated as a metastasis suppressor in most cancers, including gastric cancer, oesophageal carcinoma, pancreatic cancer, ovarian cancer, bladder cancer and prostate cancer. Relations between reduced expression of Kiss-1 and poor clinical outcomes have been evident in most malignancies that have been investigated. A possible explanation for the role played by Kiss-1 in cancer biology could be extrapolated from the correlation between Kiss-1 and matrix metalloproteinases (MMPs), especially MMP-9 and MMP-2, whose significance in tumour invasion and metastasis formation is well known [112]. Kiss-1 was reported to regulate MMP-9 expression negatively in ovarian tumour [96]. Takino a *et al*. explained that Kiss-1 protein contributed to form a steady complex with pro-MMP-2 and pro-MMP-9, which possibly have an influence on the proteolytic processing of Kiss-1 rather than the pro-MMP processing [96]. However, there are several reports suggesting contrasting roles may be played by Kiss-1 in certain cancers (e.g. hepatocellular carcinoma and breast cancer) [79, 86]. In these cases it is believed that the relative expression of Kiss-1 and it is receptor may be the determining factor. The reason why the expression of Kiss-1 and its receptor has a contrary effect on progression of hepatocellular carcinoma and breast cancer in comparison with other malignant tumours is still unknown, whereas it is proposed that there is a correlation between Kiss-1 expression and hormonal environment. Gottsch *et al*. reported that role played by the protein product of Kiss-1

and Kiss-1R was a vital part of regulation of GnRH secretion. Neurons expressed Kiss-1 can regulate the release of GnRH via Kiss-1R in either autocrine or paracrine manner, so to regulate the release of LH/FSH by effecting the pituitary, in the meantime, the expression of Kiss-1 would increase through a feedback regulation of high estrogen level [113]. Hence, patients with hepatocellular carcinoma suffering from liver cirrhosis, which leads to a disturbed hormal balance, generally show high estrogen levels, and the hyperestrogenic state would activate the ERα, which binds to the Kiss-1 gene promoter in turn elevating Kiss-1 expression [114]. The possible relationship between Kiss-1 expression and estrogen level may be also appropriate for the situation in breast cancer, since blocking the ER pathway is suggested as one of the most significant systemic therapies in breast cancer [87]. A role played by Kiss-1 and Kiss-1R in other cancers regulated hormone has also been proposed. The elevating expression of Kiss-1 has been detected to suppress metastases in SKOV3 ovarian cancer cells through the reverse effect caused by PKCα [95]. Consistently, it was concordant to the effect found in melanoma cells [115].

1.2.6 Hypothesis and aims of the study

Kiss-1 and Kiss-1R are generally considered as metastasis suppressor, yet the mechanism of Kiss-1 metastasis suppression remains largely unknown.

It was hypothesised that Kiss-1 and its receptor may play a similar metastasis suppressor role in human colorectal cancer by way of aberrant expression and, by molecular and cellular mechansism(s) to be identified, linked to the disease progression of the patients.

Thus the aims of the present study were as follows:

1. To investigate the mRNA expression of Kiss-1 and Kiss-1R in human colorectal cancer cell lines using Q-PCR and RT-PCR;
2. To generate cell models (sublines) from human colorectal cancer cell lines with differential expression of Kiss-1 and Kiss-1R (e.g. Kiss-1 or Kiss-1R knockdown);
3. To investigate the impact of differentially expressed Kiss-1 on the function of colorectal cancer cells (e.g. growth, adhesion, invasion and migration) using in vitro function assays and ECIS assay, subsequently, to deduce the correlatively underlying mechanism(s) on the basis of the results of the function test.
4. To investigate the expression of Kiss-1 and Kiss-1R in human colorectal cancer and deduce the potential clinical and prognostic implications using Q-PCR and IHC.

Chapter 2

Materials and Methods

2.1 General materials

2.1.1. Cell lines:

In this study the following cell lines were used:

HT-115, HRT-18, RKO and Caco-2 cancer cell lines with epithelial morphology were established from highly invasive human colorectal carcinoma, which express high amounts of the tumour marker carcinoembryonic antigen. They were obtained from the European collection of animal cell culture (ECACC), HECV, human endothelial cells were purchased from Interlab, Milan, Italy (Table 2.1).

Table 2.1. Details of cell lines used in this study

	HT-115	**HRT-18**	**RKO**	**Caco-2**
Species	Human	Human	Human	Human
Tissue	Colon	Rectum	Rectum	Rectum
Age	63	67	82	72
Gender	Male	Male	Female	Male
Morphology	Epithelial	Epithelial-like	Epithelial	Epithelial
Growth Mode	Adherent	Adherent	Adherent	Adherent
Karyotype	2n=46	2n=46	2n=46	2n=46
Tumorigenic	specified	Yes	Yes	Yes
Country	UK	UK	UK	UK

Table 2.2. Source of general compounds

Material & Reagent	**Supplier**
10% foetal calf serum (FCS)	PAA Laboratories, Coelbe, Germany
A/G protein agarose beads	Santa-Cruz Biotechnology, Santa-Cruz, CA, USA
Acetic acid	Fisher Scientific, Leicestershire, UK
Acrylamide mix (30%)	Sigma-Aldrich Co, Poole, Dorset, UK
Agarose	Melford Laboratories Ltd, Suffolk, UK
Ammonium persulfate (APS)	Sigma-Aldrich Co, Poole, Dorset, UK
Amphotericin B	Sigma-Aldrich Co, Poole, Dorset, UK
Bio-Rad DC Protein Colourimic Assay	Bio-Rad Laboratories, Hercules, CA, USA
Boric acid	Duchefa Biochemie, Haarlem, Netherlands
Bromophenol Blue	Sigma-Aldrich Co, Poole, Dorset, UK
$CaCl_2$	Sigma-Aldrich Co, Poole, Dorset, UK
Chloroform	Sigma-Aldrich Co, Poole, Dorset, UK
Commasine Blue	Sigma-Aldrich Co, Poole, Dorset, UK
DEPC (Diethylpyrocarbonate)	Sigma-Aldrich Co, Poole, Dorset, UK
Dimethylsulphoxide (DMSO)	Fisons Scientific Equipment, Loughborough, UK
DMEM/Ham's F12 with L-Glutamine medium	PAA Laboratories, Coelbe, Germany
EDTA (Ethylenediaminetetraacetic acid)	Duchefa Biochemie, Haarlem, Netherlands
Ethanol	Fisher Scientific, Leicestershire, UK
Ethidium bromide	Sigma-Aldrich Co, Poole, Dorset, UK
Glycine	Melford Laboratories Ltd, Suffolk, UK
HCL	Sigma-Aldrich Co, Poole, Dorset, UK
Isopropanol	Sigma-Aldrich Co, Poole, Dorset, UK
KCl	Fisons Scientific Equipment, Loughborough, UK
KH_2PO_4	BDH Chemicals Ltd, Poole, England, UK
Mayers Htx	Sigma-Aldrich Co, Poole, Dorset, UK
Methanol	Fisher Scientific, Leicestershire, UK
NaCl	Sigma-Aldrich Co, Poole, Dorset, UK
Na_2HPO_4	BDH Chemicals Ltd., Poole, Dorset, UK
NaN_3	Sigma-Aldrich Co, Poole, Dorset, UK
NaOH	Sigma-Aldrich Co, Poole, Dorset, UK
Nitrocellulose membrane	Ammersham, Cardiff, UK

Penicillin	Sigma-Aldrich Co, Poole, Dorset, UK
Peroxidase conjugated goat anti-rabbit IgG	Sigma-Aldrich Co, Poole, Dorset, UK
Peroxidase conjugated rabbit anti-goat IgG	Sigma-Aldrich Co, Poole, Dorset, UK
Peroxidase conjugated rabbit anti-mouse IgG	Sigma-Aldrich Co, Poole, Dorset, UK
Precision qScriptTM RT PCR kit	Primerdesign LTD, Southampton, UK
REDTaqTM ReadyMix PCR reaction mix	Sigma-Aldrich Co, Poole, Dorset, UK
RNA extraction buffer	Advanced Biotechnologies Ltd, Epsom, Surrey, UK
SDS (Sodium dodecyl sulphate)	Melford Laboratories Ltd, Suffolk, UK
Serum bovine albumin	Sigma-Aldrich Co, Poole, Dorset, UK
Streptomycin	Sigma-Aldrich Co, Poole, Dorset, UK
Sucrose	Fisons Scientific Equipment, Loughborough, UK
SupersignalTM West Dura system	Pierce Biotechnology Inc., Rockford, IL, USA
TBS Automation Wash Buffer	Biocare Medical, Concord, CA, USA
Tetramethylethylenediamine (TEMED)	Sigma-Aldrich Co, Poole, Dorset, UK
TRI Reagent	Sigma-Aldrich Co, Poole, Dorset, UK
Tris-Cl	Melford Laboratories Ltd, Suffolk, UK
TRITC conjugated goat anti-rabbit IgG	Sigma-Aldrich Co, Poole, Dorset, UK
Trion	Sigma-Aldrich Co, Poole, Dorset, UK
Trypsin	Sigma-Aldrich Co, Poole, Dorset, UK
Tween 20	Melford Laboratories Ltd, Suffolk, UK
Vectastain Universal ABC kit	Vector Laboratories Inc, Burlingame, CA, USA
ZnCl	Sigma-Aldrich Co, Poole, Dorset, UK

Table 2.3. Source of general plastic consumables

Hardware/Software	**Supplier**
0.4 μm filtration unit	Sigma-Aldrich Co, Poole, Dorset, UK
16-well chamber slide (for Immunohistochemistry)	Nalge NUNC International,Rochester, NY
$25cm^2$ and $75cm^2$ culture flasks	Cell Star, Germany
Amplifluort detection system	Intergen, England, UK
Cytodex 2 beads	Sigma-Aldrich Co, Poole, Dorset, UK
ECIS (Electrical Cell-Substrate Impedance Sensing), Ztheta	Applied BioPhysics Inc., Troy, New York, USA
ECIS array 96W1E	Applied BioPhysics Inc., Troy, New York, USA
Electroporation cuvette	Euro Gentech, Southampton, UK
iCycler iQ system	Bio Rad, Hercules, CA, USA
Image J	Public Domain
Lecia DM IRB microscope	Lecia GmbH, Bristol, UK
Microscope heated plate	Lecia GmbH, Bristol, UK
Microsoft Excel	Microsoft In., Redmond, WA, USA
Neubauer haemocytometer counting chamber	Reichert, Austria
Nitrocellulose membrane	Hybond C, Ammersham, Cardiff
Partec CyFlow® FloMax software	Partec GmbH, Munster, Germany
Partec CyFlow® SL flow cytometer	Partec GmbH, Munster, Germany
Protein spectrophotometer	BIO-TEK, Wolf Laboratories, York, UK
RNA spectrophotometer	BIO-TEK, Wolf Laboratories, York, UK
Ultra-Turrax T8 Homogenizer	IKA Labortechnik, Staufen, Germany
UV light chamber	Germix
UVI-doc system	UVITech, Inc., Cambridge, England, UK
UVITech imager	UVITech, Inc., Cambridge, England, UK

Table 2.4. Peptide Receptors and inhibitors

Products	**Supplier**	**Catalogue number**
Kisspeptin-10 (human)	Tocris Bioscience, Bristol, UK	No. 2570
Kisspeptin-234	Tocris Bioscience, Bristol, UK	No. 3881
ERK inhibitor Ⅱ, FR180204	Calbiochem, Germany	328007-1MG

Table 2.5. Antibodies

Antibody for	Species	Source	Catalogue number
Kiss-1	Mouse monoclonal IgG	Santa Cruz Biotechnology, Inc. U.S.A.	Sc-101246
GPR54 (Kiss-1R)	Goat polyclonal IgG	Santa Cruz Biotechnology, Inc. U.S.A.	Sc-48220
Anti-Mouse-IgG	Antibody produced in rabbit	Sigma-Aldrich Co, Poole, Dorset, UK	100M4783
Anti-Goat-IgG	Antibody produced in rabbit	Sigma-Aldrich Co, Poole, Dorset, UK	089K4773
p-Tyr (PY20)	Mouse monoclonal IgG_{2b}	Santa Cruz Biotechnology, Inc. U.S.A.	Sc-508
Protein A/G PLUS- Agarose	Immunoprecipitation reagent	Santa Cruz Biotechnology, Inc. U.S.A.	Sc-2003

2.2 Preparation of Reagents, Buffers and Standard solutions

The following solutions were routinely used throughout this study:

2.21 Solutions for use in molecular biology

Tris- Boric acid- EDTA (TBE) Electrophoresis Buffer

The concentration of the stock solution of TBE (1.1M Tris; 900mM Borate; 25mM EDTA; pH 8.3) was prepared at 5 times concentrate. The solution was made by dissolving 540g Tris- Cl (Melford Laboratories Ltd, Suffolk, UK), 275g Boric acid and 46.5g EDTA in 10 litres dH_2O.The pH was adjusted to 8.3 using NaOH and then stored at room temperature. A working solution was prepared by dissolving for 5 times (200ml of stock solution in 800ml of distilled water).

DEPC water

A stock solution was prepared by dissolving 500µl of Diethyl Pyrocarbonate (DEPC) (Sigma-Aldrich, Inc., Poole, Dorset, England, UK) in 9500µl distilled water and autoclaved before use.

Loading buffer

25mg of bromophenol blue (Sigma-Aldrich, Inc., Poole, Dorset, England, UK) and 4g sucrose (Fisons Scientific Equipment, Loughborough, UK) were dissolved in 10ml of distilled water and stored at 4^{o}C (used for DNA electrophoresis).

Preparation of Ethidium Bromide (EtBr) Staining Solution

The working solution was prepared by dissolving 100mg Ethidium Bromide in 10ml of distilled water (strength: 10mg/ml). The solution was mixed well to dissolve the ethidium bromide powder (Sigma-Aldrich, Inc., Poole, Dorset, England, UK) and stored in aluminium foil out of the light.

2.2.2 Solutions for use in cell culture

Preparation of Complete Cell Culture Medium

This solution was prepared by mixing50ml of heat inactive tedfoetal calf serum (FCS) (Sigma-Aldrich Company, LTD Irvine, Ayrshire, UK) in 500ml DMEM/F12 with 2mM L- glutamine (Sigma-Aldrich Company, LTD Irvine, Ayrshire, UK). Five milliliter of antibiotics were added and the medium was then stored for up to a month at 4 ℃.

Balanced Salt Solution (BSS)

A ten litre stock solution of 1 time BSS (137mM NaCl, 2.6mM KCl, 1.7mM Na_2HPO_4 and 8mM KH_2PO_4) was prepared by dissolving 79.5g NaCl, 2.2g KCl, 1.1g Na_2HPO_4 and 2.1g KH_2PO_4 into distilled water. The pH was adjusted to 7.2 with 1M NaOH (Sigma-Aldrich, Inc., Poole, Dorset, England, UK) before use.

Preparation of 0.05M EDTA

A stock solution was prepared by dissolving 40g NaCl, 1g KCl (Fisons Scientific Equipment, Loughborough, UK), 5.72g Na_2HPO_4 (BDH Chemical Ltd., Poole, England, UK), 1g KH_2PO_4 (BDH Chemical Ltd., Poole, England, UK) and 1.4g EDTA (DuchefaBiochemie, Haarlem, The Netherlands) in 5L of dH_2O. The pH was adjusted to 7.4 by adding Sodium Hydroxide (NaOH) and autoclaved before use.

Trypsin (25mg / ml)

A stock solution of trypsin was prepared by dissolving 500mg trypsin in 20ml 0.05 EDTA and then filtered through a 0.2μm mini start filter (Sartorious, Epsom, UK). The preservation condition was -20℃. The working solution was prepared by further dissolving 250μl of trypsin solution in 10ml of 0.05 EDTA and used to detach the cells. The preservation condition was 4℃.

Preparation of100X Antibiotics

Three point three grams of penicillin, 5g streptomycin and 12.5mg Amphotericin B in DMSO were dissolved in 0.5L of BSS and filtered. Five millitre was then added to a 500ml bottle of DMEM Ham's F12media.

2.2.3 Solutions for use in cloning

LB agar

Ten grams tryptone (DuchefaBiochemie, Haarlem, The Netherlands), 5g yeast extract (DuchefaBiochemie, Haarlem, The Netherlands), 15g agar, and 10g NaCl were dissolved in 1L of distilled water. The pH value was adjusted to 7.0 and then the media was autoclaved and stored at room temperature until use. For making a LB agar dish, LB Agar was melted in a microwave. Appropriate antibiotic was added to LB media which was cooled down to about 65^{o}C. The Agar solution was then poured into 10cm^{2} Petri dishes (BibbySterilinLtd., Staffs, UK). The LB Agar dishes were stored at 4^{o}C until hardened.

LB broth

Ten gramstryptone, 10g NaCl and 5g yeast extract was dissolved in 1L of distilled water. After adjusting the pH7.0, the media was autoclaved. Antibiotics were added prior to use.

2.2.4 Solutions for use in protein work

Preparation of Cell Lysis Buffer

The Stock Solution was prepared by dissolving 2mM CaCl2, 0.5% Triton X-100, 1mg/ml aprotinin, 1mg/ml leupeptin and 10mM Sodium Orthovanadate in 50ml distilled water. The solution was prepared as a 2× concentrate and stored at 4 ℃.The working solution was prepared by diluting 10ml of the stock solution in 6.6ml of inhibitor buffer, 200µl of PMSF, 80µL 10mM CaCl, 3ml of 10%Triton X-100 made up to 20ml with distilled water.

Ammonium Persulphate (APS)

The 10% APS solution wasfreshly prepared, prior to use, by dissolving 1g APS in 10ml distilled water and then stored at 4^{o}C.

Tris Buffered Saline (TBS)

A ten time concentration stock solution was prepared by dissolving. 24.228g Tris-Cl and 80.06g NaCl in 1 litre of distilled water. This solution contains 200mM Tris and 1.37M of NaCl. The pH value was adjusted to 7.4 using HCL and then stored at room temperature.

Running buffer (for SDS-PAGE)

The stock solution (10X) was prepared by dissolving 303g of Tris, 100g SDS (MelfordLaboratoriesLtd., Suffolk, UK) and 1.44kg of Glycine (Melford Laboratories Ltd., Suffolk, UK) in 10L distilled water and adjusting the pH value to 8.3 using NaOH. The working solution diluted to 1x running buffer with distilled water before use.

Transfer Buffer (for Western Blot)

A stock solution of total 5 litres was prepared by dissolving 15.15g Tris, 72g Glycine and 1 litre of methanol (Fisher Scientific, Leicestershire, UK) in 4L distilled water.

Preparation of Fluorescamine for protein quantitation

The working Solution was prepared fresh by dissolving 3mg of Fluorescamine in 10ml acetone.

Preparation of Inhibitor Buffer

Two point seventy six grams sodium nitrate, 630g sodium fluoride, 5.58g EDTA, 10g $Na_2H_2PO_4$ and 3×10^5 Units of aprotonin were made up to 1 L distilled water, prepared as a $3\times$ concentrate and stored at 4 ℃.

Preparation of 0.1% Comassie Blue

One gram of Coomassie Blue, 400ml Methanol and 100ml Acetic acid were dissolved in distilled water with making up to 1L. It is then filtered and stored at room temperature.

Preparation of SDS-PAGE Gel

Table 2.6. Solution for preparing resolving gels for Tris-glycine SDS-plolyacrylamide gel electrophoresis

Solution components	**Component volumes [116] per gel mold volume of**
	20ml
8%	
H_2O	9.3
30% acrylamide mix	5.3
1.5 m Tris (pH 8.8)	5
10% SDS	0.2
10% ammonium persulfate	0.2
TEMED	0.012
10%	
H_2O	7.9
30% acrylamide mix	6.7
1.5 m Tris (pH 8.8)	5
10% SDS	0.2
10% ammonium persulfate	0.2
TEMED	0.008
12%	
H_2O	6.6
30% acrylamide mix	8
1.5 m Tris (pH 8.8)	5
10% SDS	0.2
10% ammonium persulfate	0.2
TEMED	0.008

Table 2.7. Solution for preparing 5% stacking gels for Tris-glycine SDS-polyacrylamide gel electrophoresis

Solution components	**Component volumes [116] per gel mold volume of**
	10ml
H_2O	6.8
30% acrylamide mix	1.7
1.5 m Tris (pH 6.8)	1.25
10% SDS	0.1
10% ammonium persulfate	0.1
TEMED	0.01

Table 2.6 and 2.7 are modified from Harlow and Lane (1988); acrylamide mix and TEMED are supplied by Sigma-Aldrich, St. Louis, USA.

2.3 General methods

2.3.1 Cell Culture, maintenance and Storage

Cell lines were cultured in Dulbecco's Modified Eagle's medium (DMEM/ Ham's F-12 with L-Glutamine; Sigma-Aldrich, Inc., Poole, Dorset, England, UK), pH 7.3 containing 2mM L-glutamine and 4.5mM $NaHCO_3$, supplemented with 10% heat inactivated Foetal Bovine Serum (Sigma-Aldrich, Inc., Poole, Dorset, England, UK), and antibiotics. Cells were cultured in either 25cm ²or 75cm ²tissue culture flasks (Greiner Labortechnik, Germany) cultured in depending on the required application. Culture flasks were loosely capped allowing for gaseous exchange and then placed horizontally in a humidified incubator (98% humidification achieved with water tray in the incubator) (Sanyo Electric, Japan) at 37 ℃ with 5% CO_2 (act as a buffer with the $NaHCO_3$) in air.

Cell lines transfected with the pEF6/His plasmid vector were firstly cultured in 5μg/ml blasticidin S (Melford laboratories ltd, Suffolk, UK) selection media. After selection, the cell lines were transferred into 0.5μg/ml blasticidin S maintenance media.

Confluency of cell lines were visually measured using the light microscope. Cells were routinely sub-cultured after reaching 80-90% confluency. All handling of cells were carried out in a Class II Laminar Flow Cabinet with autoclaved and sterile equipment.

2.3.2 Trypsinization and Counting of cell lines

•The tissue culture flask was taken out from incubator. The waste medium was removed by aspiration .Following this, the flasks were rinsed briefly with 5ml of EDTA in Balanced Salt Solution buffer to remove remaining serum which would inhibit the action of trypsin.

•Approximately, 1-2 ml of trypsin / EDTA solution (Trypsin0.01% (w/v) and EDTA 0.05% (w/v) in HBSS buffer) was added to the flasks which were subsequently incubated for 5 minutes at 37 ℃, to allow cell detachment.

•Once detached, 5ml of DMEM was added to each flask to neutralise trypsin. The cell mixture was transferred to a new 30 ml universal container (Greiner Bio-One Ltd, Gloucestershire, UK). The cell pellet was collected from the cell suspension by centrifugation (1,780 rpm for 8 minutes).

•Cell pellets were re-suspended in 5mls of DMEM solution for re-culturing or for immediate experimental work

•Cell counts were performed using a Neubauer haemocytometer counting chamber (Mod-FuchsRosenthal, Hawksley, UK) under an upright microscope (Reichert, Austria) at ×10 objective magnification.

• The haemocytometer calculated the number of cells in a predetermined volume of fluid so to obtain the quantity of cells per millilitre. The haemocytometer chamber was divided into 9 squares with dimensions of 1mm × 1mm ×0.2mm. For ensuring the consistency of cell density and reducing the errors, four corners of 9 squared areas were counted. The number of cells was calculated by using the following equation:

Cell number/ml= (the sum of the number of cells in four corners ÷ 8) x (1×10^4)

2.3.3 Storage of cell lines in liquid nitrogen and cell resuscitation

The cell lines were stored in liquid nitrogen by re-suspending the cell pellet in complete medium (DMEM/HAM's F12) with 10% dimethylsulphoxide (DMSO; Fisons, UK) at a cell density of 1×10^6 cells/ml. One millilitre of cell suspension was transferred into pre-chilled CRYO.S^{TM} tubes (Greiner Bio-One, Germany) and then frozen at -80 ℃ for 1 day before storage in liquid nitrogen (-196 ℃).

To resuscitate the frozen cells, the CRYO.S^{TM} tube was removed from liquid nitrogen and thawed rapidly in a 37 ℃ water bath. The cell suspension was transferred into a

universal container containing 5ml of pre-warmed DMEM/HAM’s F12 and incubated at 37 ℃ for 10 minutes and then centrifuged at 1600 rpm for 5 minutes. The medium was removed by aspiration. 5ml of fresh DMEM/Ham's F12 to added to the pellet to resuspend the cells. The above procedure was repeated twice to remove any possible trace of DMSO. Finally, the cell pellet was re-suspended in 5ml of DMEM/Ham's F12 and transferred to a 25cm ²tissue culture flasks. The cells were incubated at 37 ℃ with 98% humidification and 5% CO_2.

2.4 Methods for RNA detection

2.4.1 Total RNA isolation

Required of reagents:

- RNA isolation reagent
- Chloroform
- Isopropanol
- 75% Ethanol
- DEPC treated water

Ribonucleic acid (RNA) is present within the nucleus, cytoplasm and mitochondria of all living eukaryotic cells. Ribosomal RNA (rRNA), transfer RNA (tRNA) and messenger RNA (mRNA) are the three main subtypes of RNA. mRNA isof particular

importance, as it carries the genetic information for subsequent protein synthesis. The presence of specific mRNA therefore gives a good indication of which proteins are being produced by the cell at the transcript level.

The protocol of RNA isolation was carried out using the Tri Reagent kit (Sigma-Aldrich, Inc., Poole, Dorset, England, UK).

• After the confluency of cells in a monolayer reached approximate 90%, the medium was emptied and replaced with RNA reagent (1ml / 5-10 x 10^5 cells) tolyse the cells. The cell lysate was then transferred into a 1.8 ml eppendorf tube, which was further incubated for 5 minutes at 4^oC

• To the tube, 0.2ml (per 1ml of RNA reagent) chloroform (Sigma-Aldrich, Inc., Poole, Dorset, England, UK) was added. The tube was vigorously mixed for 15 seconds and incubated at 4^oC for 5 a further minute.

• The resulting homogenate was then centrifuged at 12,000rpm for 15 minutes at 4^oC (Boeco, Wolf laboratories, York, UK). The spinning resulted in the separation of the lysate into three phases: a lower pink organic phase containing protein, an inter phase containing DNA, and an upper aqueous phase containing RNA in the acidic environment.

• The aqueous phase containing RNA was carefully transferred into a fresh eppendorf tube before adding an equal volume of isopropanol (Sigma-Aldrich, Inc., Poole, Dorset, England, UK). The homogenate was then incubated for 10 minutes at 4^oC.

After centrifuging the samples at 12,000rpm for 10 minutes at 4^{o}C, it deposited a white pellet (RNA precipitates) on the bottom of the eppendorf tube.

• After carefully removed the supernatant, the RNA precipitate was washed twice with 1ml 75% ethanol in DEPC water. Each wash was carried out by adding 1ml 75% ethanol, vortexing, and centrifuging the samples at 7,500rpm for 5 minutes at 4^{o}C.

• The RNA pellet was briefly dried at 55^{o}C for 5-10 minutes in a Techne, Hybridiser HB-1D drying oven (Wolf laboratories, York, UK), in order to evaporate the remaining ethanol.

• Finally, the RNA pellet was dissolved in 50-100µl of DEPC water (Diethyl pyrocarbonate, Sigma). The impact of DEPC, as a histidine specific alkylating agent, is to inhibit the hydrolysis of RNases on RNA.

2.4.2 RNA Quantification

The concentration and purity of the resulting RNA was determined by measuring its absorbance at wavelength of A260nm/A280nm (WPA UV 1101, Biotech Photometer). A260nm/A280nm ratio gave an estimate of the purity of the RNA, through calculating the difference of absorbance between the RNA sample and DEPC water (as a blank), using a quartz cuvettes (Optiglass limited, Essex, UK).The spectrophotometer detected the concentration of ssRNA (ug/ul) at a wave length of 260nm. The concentration of RNA samples were then standardised using DEPC water and subsequently stored at -80 ℃ for future use.

2.4.3 Reverse Transcription of RNA for production of cDNA

Reverse transcription (RT) leads to synthesis of complementary DNA (cDNA) from RNA. It is followed by polymerase chain reaction (PCR) and the two processes together are known as RT- PCR. RT- PCR is a sensitive technique for the analysis of mRNA as compared with other techniques (e.g. Northern blots, RNA dot blots). Only a small amount of RNA is needed for this technique and it is more sensitive and rapid in detecting genetic sequences compared with other procedures. In this study, RT-PCR was performed using the iScript™ cDNA Synthesis Kit (Bio-Rad Laboratories, California, USA) according to manufacturer's instructions. Each reaction was set up in 200µl PCR tubes (ABgene, Surrey, UK):

Component Volume	Each reaction
5x iScript Reaction Mix	4µl
iScript Reverse Transcriptase	1µl
Nuclease-free water	Xµl
RNA template (0.5µg/µl)	Xµl
Total volume	20µl

The reaction was carried out in a T-Cy Thermocycler (Creacon Technologies Ltd, The Netherlands). The condition of the reaction is shown below:

5 minutes at 25^{o}C

30 minutes at 42^{o}C

5 minutes at 85^{o}C

After the completion of the reaction, the cDNA was diluted with PCR water by a factor of 1:4 and stored at -20^{o}C for further use or used immediately as template for conventional PCR.

2.4.4 Polymerase Chain Reaction (PCR)

Polymerase Chain Reaction is a simple technique to amplifying DNA and produce a desired amount from a single target DNA molecule and was invented by Kary Mullis in 1983[117].

Principle:

• It relies on the principle of a chain reaction in which each target molecule is subject to further amplification.

• Two short DNA sequences (oligonucleotides- Forward and Reverse primers), which bind to the template DNA by base pairing, are required and are complementary to a defined sequence on each of the two strands of the DNA. These primers are aligned with the 3' ends facing each other.

• In this study, the target gene of interest was amplified by PCR using the REDTaq™ Ready Mix PCR Reaction mix (Sigma-Aldrich, Inc., Poole, Dorset, England, UK). A reaction (16µl) was set up in PCR tubes below:

Components	Volume
cDNA template	2µl
Forward primer (working concentration of 1 µM)	1µl
Reverse primer (working concentration of 1 µM)	1µl
2x REDTaq^{TM}ReadyMix	8µl
PCR H_2O	4µl

• The mixture of PCR reaction was placed in a 2720 Thermo cycler (Applied Biosystems).

• A control reaction was included where PCR water was added instead of cDNA template (negative control).

• The conditions of reaction were showed below:

Steps	Temperature	Time	Cycles
Initial denaturation	94^{o}C	5-10 minutes	1
Denaturation	94^{o}C	40 seconds	30-42
Annealing	Primer specific temperature	30-40 seconds	
Extension	72^{o}C	40 seconds	
Final extension	72^{o}C	7-10 minutes	1

2.4.5 Agarose gel electrophoresis and DNA visualisation

Agarose gel electrophoresis is the most common method of DNA separation and analysis. The basis of this technique is to separate the amplified DNA on the basis of charge and size using an electrical current.

Depending on the size of PCR products, an appropriate agarose gel (from 0.8% to 2% agarose powder in TBE buffer) was chosen (Melford Chemicals, Suffolk, UK). Agarose gel was melted by heating (e.g. microwave). After completely melting, the liquid gel solution was poured into electrophoresis cassettes (Scie-Plas Ltd., Cambridge, UK) containing well forming combs. A low percentage agarose gel (0.8%) was used to separate PCR products with a high number of base pairs (>500bp) and 2% agarose gel to separate DNA fragments with low number of base pair (<500bp).
Once the gel had set (30-40 minutes) TBE buffer was poured over the gels to exceed 5mm of the gel surface. 8µl DNA ladder (1kb)(Cat No.M106R; GenScript USA Inc.) or 8-10µl of each sample were loaded into the wells.
The gel was then run at a constant voltage of 100 volts (Gibco BRL Power pack model 250EX, Life Technologies) for 35-55 minutes or until the samples had migrated about two thirds down the agarose gel (depending on the PCR product size). The PCR product was then stained using ethidium bromide solution for around 15 minutes with continuous agitation to ensure uniform staining. Ethidium bromide is a dye, which binds to double stranded DNA between the base pairs and fluoresces when exposed to UV light. This was sometimes followed by destaining in distilled water for

30-60 minutes if it was deemed necessary for removal of strong background staining on the agarose gel from the fluorescent dye.

After staining the PCR products the gels were visualised using an Ultra Violet Transilluminator (UVP, Cambridge, UK) and photographed using the thermal printer or scanned for storing images electronically.

2.4.6 Quantitative RT-PCR (Q-PCR)

PCR has become a crucial technique involved in biomedical research in most laboratories since 1990s. The development of real-time Q-PCR, which added a new dimension to PCR, has significantly improved the quantification of nucleic acid samples. Real-time quantitative polymerase chain reaction (QPCR) was developed in 1992, which allowed quantification of DNA, cDNA, or RNA templates as the products accumulates with each cycle of amplification. It had excellent sensitivity and specificity to detect specific gene sequences in a broad dynamic range. On the basis of the detection of a fluorescent reporter molecule that increases during PCR amplification (the level of fluorescence detected is directly proportional to the PCR product yield). The level of fluorescence was continuously monitored by a sensitive camera attached to a computer and hence the term ‘real-time’.

The current study quantified transcript copy number of the gene transcript of interest using the Ampliflour™ Uniprimer™ system (Intergen company®, New York, USA). The ampliflour probe consisted of a 3’ region specific to the Z-sequence

(ACTGAACCTGACCGTACA) present on the target specific primers, and a 5' hairpin structure labelled with a flurophore (FAM), described by Nazarenko *et al.* in 1997 [118]. The flourophore was linked to an acceptor moiety (DABSYL), which acted to quench the fluorescence emitted by the flourophore, thus preventing any signal from being detected in this hairpin structure.

During PCR, the probe acted as a template for DNA polymerisation in which DNA polymerase uses its 5'-3' exonuclease activity to degrade and unfold the hairpin structure, thereby sufficient fluorescence was allowed to be emitted and detected through by disruption of the energy transfer between flourophore and quencher. The fluorescent signal emitted was directly related to the amount of DNA, which had been amplified during each PCR cycle.

Each amplified reaction was set up below:

Component	**Volume**
Forward primer	0.3µl (10pmol/µl)
Reverse Z primer	0.3µl (1pmol/µl)
Ampliflour probe	0.3µl (10pmol/µl)
2x iQ^{TM}Supermix	5µl
cDNA and PCR H_2O	4µl

Each sample was loaded into a 96-wells plate (Applied biosystems^{TM} Life Technologies LTD, Paisley, UK); Standards were usually arranged in the first row (ranging from copy numbers of 10^1-10^8), covered with optically clear sticky film from ABI. The 96-wells plate was placed in an ABI StepOne Plus thermal cycler (Figure 2.1A) and the reaction was detected by software designed by Applied biosystems (ABI) laboratories, UK, with the conditions shown in the following:

Steps	Temperature	Time	Cycles
Initial denaturation	94^{o}C	5minutes	1
Denaturation	94^{o}C	10 seconds	80-90
Annealing	55^{o}C	35 seconds	
Extension	72^{o}C	20 seconds	

The fluorescent signal was detected at the annealing stage by a camera where its geometric increase directly correlated with the exponential increase of product. This was then used to determine a threshold cycle (TC) for each reaction and the transcript copy number depended on when the fluorescence detection reached this specific threshold.

The degree of fluorescence emitted by a range of standards of a known transcript copy number was then used to compare to the amount emitted by each sample, allowing for the transcript copy number in each sample to be accurately calculated. Furthermore, the transcript copy number of each sample was then normalised against the detection of β-actin or GAPDH copy numbers. The procedure was repeated at least three times. A typical example of the quantitative reaction is shown inFigure2.1.B.

Figure 2.1.A. StepOne Plus instrument used in the present study.

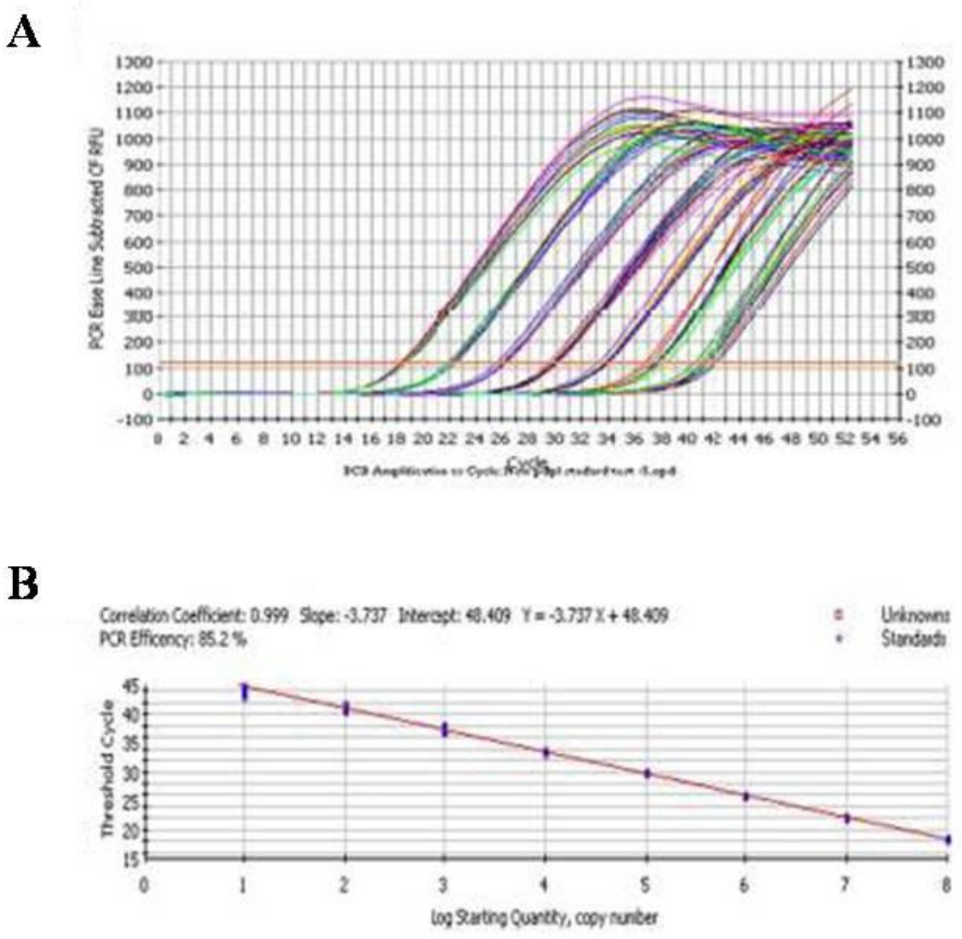

Figure 2.1.B. Qualification of transcript level. A. The levels of transcript from 10^1 to 10^8 copy number of standard samples are detected using ABI's StepOne Plus, from ABI. B. Subsequent generation of a standard curve from these samples.

2.4.7TaqMan® probe based assay

This is an alternative technique to Amplifor. TaqMan® probes were used during the process of PCR amplification so as to detected the presence and quantify the amount of specific target sequences. These Probes were designed as oligonucleotides, which had been tagged with one fluorescent group (6-carboxyfluorescein [6-FAM]) and one fluorescence quenching group (6-carboxy-tetramethyl-rhodamine) at the 5' end and the 3' end respectively. These probes had a higher T_m (Melting Temperature) than the primers, and during the extension phase must be 100% hybridized for success of the assay. The close proximity of the quencher to the reporter fluorochrome prevented its natural fluorescence. However, as the PCR progresses the probe bound to the PCR products and Taq polymerase cleaved the reporter fluorochrome and the quencher from the probe, releasing the sequence specific fluorescent signal (reporter fluorochrome). The amount of fluorescence released during the amplification cycle was proportional to the amount of PCR product generated in each cycle. The operating principle of TaqMan® probes is shown below (Figure 2.2.)

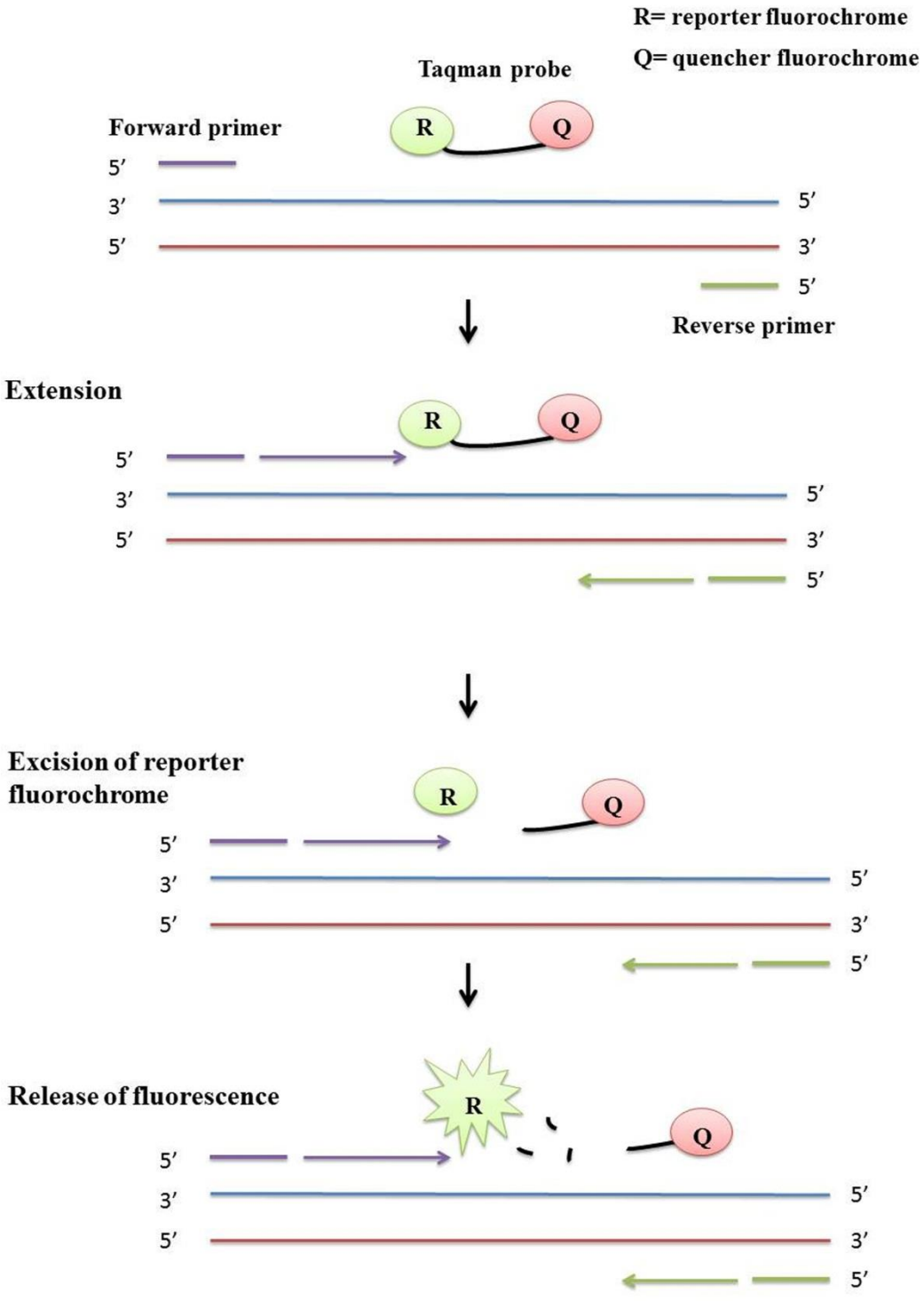

Figure 2.2. The TaqMan® probe based APCR assay

2.5 Methods for protein detection

2.5.1 Protein extraction and preparation of cell lysates

• When cells had reached an adequate confluency, the cell monolayer was first washed with BSS buffer and then scrapped off using a cell scraper. The typical way to quantify the number of cells was to collect the cells second day after the overnight cultivation of the consistent number of each cell line.

•The cell suspension was transferred into a universal tube.

• The supernatant was removed after centrifuging (1,800 rpm) for 8 minutes. The cells were similarly washed in BSS twice.

• The cell pellet was then resuspended in 200-300µl (depending on pellet size) lysis buffer.

• The suspension was then transferred into a 1.8ml eppendorf tube and rotated on a Labinco rotating wheel (Wolf laboratories, York, UK) at room temperature for one hour so as to allow for cell lysis.

• The resulting lysate was centrifuged at 13,000rpm for 15 minutes. The supernatant was transferred to a fresh microfuge tube. The pellet that contained insolubles and any unwanted cell debris was discarded.

• The protein samples were then either quantified for SDS-PAGE as explained below, or stored at -20^{o}C until further use.

2.5.2 Protein quantification and preparation of samples for SDS-PAGE

In order to standardised the protein sample concentration for Western blotting, the amount of protein in each sample was quantified by following the protocol outlined in the Bio-Rad DC Protein Assay kit (Bio-Rad laboratories, Hemel Hampstead, UK). Briefly,

• In a 96 well plate, 50mg/ml of bovine serum albumin (BSA) standard (Sigma, Dorset, UK) was serially diluted in the same lysis buffer, to produce a concentration gradient from 0.78mg/ml to 50mg/ml and used to set up a standard curve of protein concentration.

• Five microlitres of either protein sample or standard was added into fresh wells, before 25µl of 'working reagent A' (prepared by adding 20µl of reagent S per millilitre of reagent A), and then 200µl of reagent B was added to each well.

• After mixing the samples, the plate was left at room temperature for 30-45 minutes in order to allow the colorimetric reaction to take place. Once this was complete, the absorbance of each of the wells was measured at 620nm using the ELx800 plate reading spectrophotometer (Bio-Tek, Wolf laboratories, York, UK).

• Using the absorbance of the standards to set up a standard curve, and by comparing standard to the absorbance of the samples, protein concentration of the test samples was determined. The samples were then diluted in an appropriate amount of lysis buffer in order to normalise them to the required final concentration of 1.0-2.0mg/ml.

• This was then further diluted with 2x Lamelli sample buffer concentrate (Sigma-Aldrich, St Louis, USA) in a ratio of 1:1 before the samples were denatured by boiling at 100^{o}C for 5-10 minutes, and either loaded onto a SDS-PAGE gel or stored at -20^{o}C until further use.

2.5.3 Western blotting: transferring proteins from gel to nitrocellulose membrane

•Once SDS-PAGE was completed, the protein samples were transferred onto a nitrocellulose membrane by Western blotting. The electrophoresis equipment was disassembled and the gel pried out from in between the two glass plates before discarding the stacking gel. The resolving gel was then placed on the bottom graphite base electrode in a SD20 SemiDry Maxi System blotting unit (SemiDRY, Wolf Laboratories, York, UK) on top of 3 pieces of 1x transfer buffer pre-soaked filter paper (Whatman International Ltd., Maidstone, UK), and 1 sheet of Hybond nitrocellulose membrane (Amersham Biosciences UK Ltd., Bucks, UK).

• An additional 3 sheets of pre-soaked filter paper were placed on top of the gel to form a sandwich arrangement of paper: membrane: gel: paper, as shown in figure 2.3.Electroblotting was then carried out at 15v, 500mA, and 8W for around 20 minutes to an hour (depending on protein size).

Once the proteins had been sufficiently transferred, the membranes were placed in the Ponseau S solution, which would temporarily stain the protein band. This would allow visualisation of transferred protein and protein markers.

The membrane was blocked over night at 4^{o}C in 10% skimmed dry milk solution (10% milk powder and 0.1% polyoxyethylene (20) sorbitanmonolaurate (Tween 20) (Sigma-Aldrich, St Louis, USA) in 50ml TBS. This acted to block the proteins onto the membrane for subsequent antibody probing.

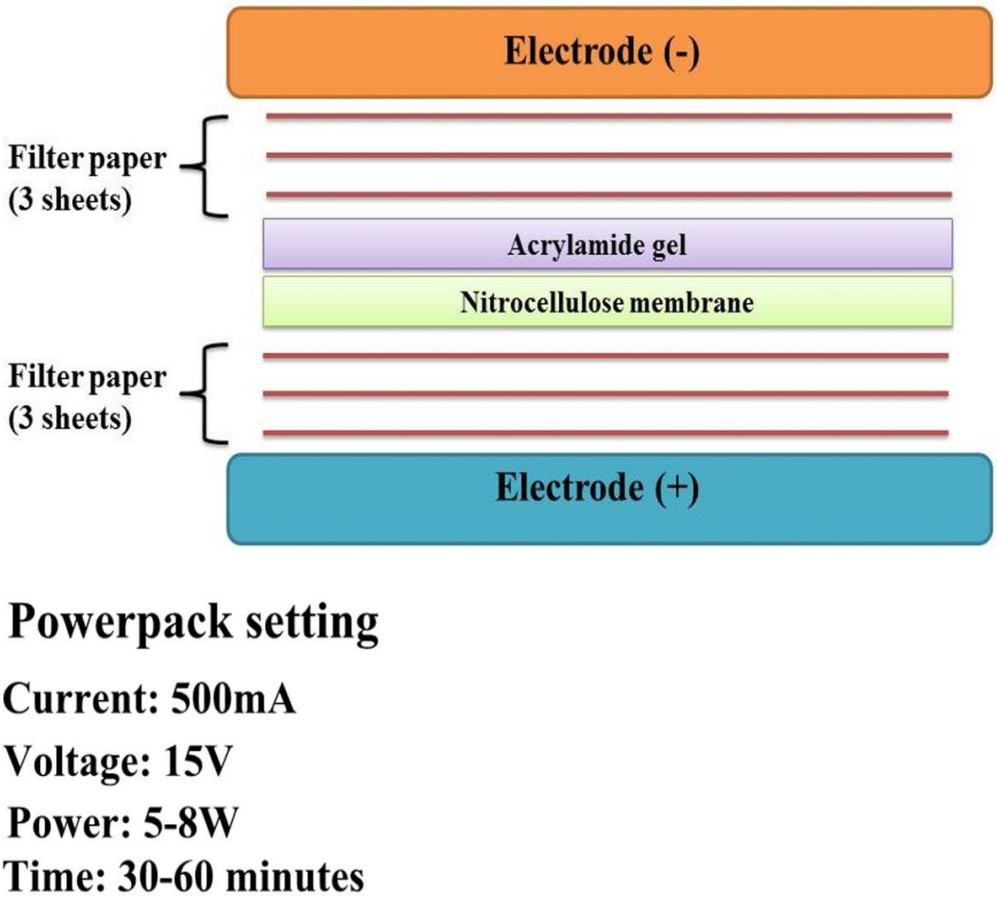

Figure 2.3. Diagrammatic sketch of the electrophoresis equipment transferring proteins from gel to nitrocellulose membrane.

2.5.4 Protein detection using specific Immuno-probing

•The membrane was transferred into 50ml falcon tubes (Nunc, Fisher-Scientific, Leicestershire, UK) ensuring that the membrane surface that had been in contact with the gel was facing upwards. 10% milk blocking solution was added to the membranes and incubated for an hour at room temperature on a roller mixer (Stuart, Wolf-Laboratories, York, UK).

•Once this procedure was complete, the 10% milk solution was poured off and replaced with 10ml of3% milk solution (3% milk powder, 0.1% Tween 20 in TBS) for 15 minutes. This was followed by incubation of the membranes for an hour at room temperature, with primary antibody diluted 1:500 in 5mls of 3% milk solution.

• After pouring off the primary antibody solution, any remaining unbound antibody was washed off twice in 3% milk solution at 15 minute intervals.

• Once washing was completed, the membranes were further incubated with 5ml of 1:1000 HRP (horse raddish peroxidase) conjugated secondary antibody diluted in 3% milk. This was carried out for an hour at room temperature on a roller mixer.

• This was followed by two 15 minute washes in 10ml of 3% milk solution, and two 15 minute washes with Tween TBS (0.2% Tween 20 in TBS), in order to wash off any unbound secondary antibody.

• A final two 15 minute washes with TBS was carried out so as to remove any residual detergent, before placing the membrane in weighing boats containing TBS solution, ready for chemiluminescent detection.

2.5.5 Chemiluminescent protein detection

Chemiluminescent protein detection was carried out using the chemiluminescence detectionkit (Luminata, Millipore), which consisted of a highly sensitive chemiluminescent substrate that detected the horseradish peroxidase (HRP) used during the Western blot procedure. The protocol was carried out as follows:

• One millilitre regent was added into the weighing boat containing the membrane to be analyzed and developed for 5 minutes at room temperature with constant agitation, the membrane was carefully removed from the solution using forceps.

• Any excess solution on the membrane was then drained over a piece of tissue paper and transferred into a fresh weighing boat. The chemiluminescent signal was detected using an UVITEC Imager (UVITEC Inc., Cambridge, UK) which contains both an illuminator and a camera linked to a computer, which then captures and stores the image.

• Each membrane was subjected to varying exposure times until the protein bands were sufficiently visible. These images were then captured and further analyzed with the UVI band software package (UVITEC, Cambridge, UK), which allowed for protein band quantification.

• In this study, GAPDH was used as a housekeeping gene and run alongside any other proteins to be detected, so as to allow for additional normalisation of the samples, and to compensate for any other negligible inaccuracies which might have occurred during the protein quantitation and loading process. The glyceraldehyde 3-phosphate

dehydrogenase (GAPDH) was used due to its highly abundant and conserved nature within eukaryotic cells. It is one of the most widely employed and accepted internal controls in scientific research.

• In order to confirm reliability of the results, each Western blot was carried out three times and the protein bands quantified and standardised against GAPDH, followed by calculation of mean values and graphical presentation of the results.

2.5.6 Preparation of immunoprecipitates

Immunoprecipitation (IP) can be used for analysing intracellular phosphorylation that occurs in downstream signaling cascades. The process involves adding a specific antibody targeted against a protein of interest within a cell lysate. This is then mixed with sepharose or agarose bonded staphylococcal protein A, protein G, or both, in order to collect the ensuing protein-antibody complexes. These complexes are then centrifuged to induce precipitation, run on an SDS-PAGE gel, and evaluated using immunoprobing.

This process was carried out as follows:

• Antibody targeted against a protein of interest was added to the cell lysate samples before being incubated at 4^{o}C for 1 hour on a Labinco rotating wheel.

• Following incubation, 20µl of conjugated A/G protein agarose beads (Santa Cruz Biotechnology, supplied by Insight Biotechnologies Inc, Surrey, England, UK) was

added to each sample and placed back on the wheel for another hour to allow antibody-protein complexes to bind to the beads.

• Centrifuging at 8,000 rpm for 5 minutes to remove any unbound protein or excess antibodies present in the supernatant. The protein pellet was subsequently washed twice with 300µl lysis buffer before being resuspended in 40-60µl of 1x sample buffer, and boiled for 5-10 minutes. The resulting samples were then run on SDS-PAGE, transfered from gel to nitrocellulose membrane, probed by specific antibodies (primary antibody and secondary antibody) and imaged chemiluminescently followed by procedure given in sections 2.6.2- 2.6.5.

2.5.7 Gelatin zymography assay

$1x10^6$ cells were counted and seeded to a tissue culture flask and incubated overnight. After incubation, the cells were washed once with 1x BSS followed by a wash with serum-free DMEM/Ham's F12 and then either incubated in serum-free DMEM control or treated medium for 4 hours. Following a 4 hour treatment, the medium was collected and mixed with a non-reducing sample buffer. Protein samples were separated using SDS-PAGE on gels containing 10% gelatin (Sigma-Aldrich Co, Poole, Dorset, UK).After SDS-PAGE, gels were renatured by washing in renaturing buffer twice (15 minutes for each time) at room temperature, and then soaked in developing buffer at 37^oC for the incubation of 36- 40 hours. Following incubation, the gels were stained with 0.5% Coomassie blue in distilled de-ionized water for 1 hour and washed.

The gel was destained using a destaining buffer for approximate 1 hour based on the staining strength of gel. The gel was generally stained blue. Where there was active MMP-2 and/or MMP-9, the gel stain became bright due to degradation of gelatin by the proteases. Images from the gels were obtained. The density of the protein bands was quantified using a similar method given in early sections.

2.6 Alteration of gene expression

2.6.1 Knocking down gene expression using Ribozyme Transgenes

In order to knockdown the expression of Kiss-1 and its receptor (Kiss-1R), it is targeted at the mRNA level using hammerhead ribozyme transgenes that specifically target and cleave the mRNA transcripts of Kiss-1 and Kiss-1R. The hammerhead ribozyme was first described by Forster and Symons in 1987 as a self-cleaving region in the RNA genome of various plant viroids and virusoids. The hammerhead motif was subsequently integrated into short synthetic oligonucleotides, transforming it into a turnover catalyst capable of cleaving various RNA targets (Uhlenbeck, 1987; Haseloff and Gerlach, 1988).

Hammerhead motifs contain a conserved secondary structure that consists of three helical stems (I, II, and III) enclosing a junction known as the catalytic core, typified by various invariant nucleotides. The best codons demonstrated to be suitable for cleavage are GUC, AUC and UUC (Figure 2.4).

In order to generate a ribozyme transgene specific to Kiss-1 and Kiss-1R, primers were designed using Zuker's RNA mFold programme (Zuker, 2003) according to the secondary structure of the gene transcripts (Figure 2.5 and 2.6). Subsequently, an appropriate GUC ribozyme target site was chosen from within the secondary structure of Kiss-1 or its receptor. The ribozyme was created to specifically bind the sequence adjacent to this GUC codon. This made it possible for the hammerhead catalytic region of the ribozyme to bind to and specifically cleave the GUC sequence within the target mRNA transcript. The transgenes were generated by carrying out touchdown PCR under the following conditions:

Steps	Temperature	Time	Cycles
Initial denaturation	94^{o}C	5 minutes	1
Denaturation	94^{o}C	10 seconds	48
Annealing	70^{o}C 65^{o}C 60^{o}C 57^{o}C 54^{o}C 50^{o}C	15 seconds 15 seconds 15 seconds 15 seconds 15 seconds 15 seconds	
Extension	72^{o}C	20 seconds	
Final extension	72^{o}C	7-10 minutes	1

• Subsequently, the transgenes were run on a 2% agarose gel in order to verify their presence as well as size before being cloned into the pEF6/His plasmid as described in the following section.

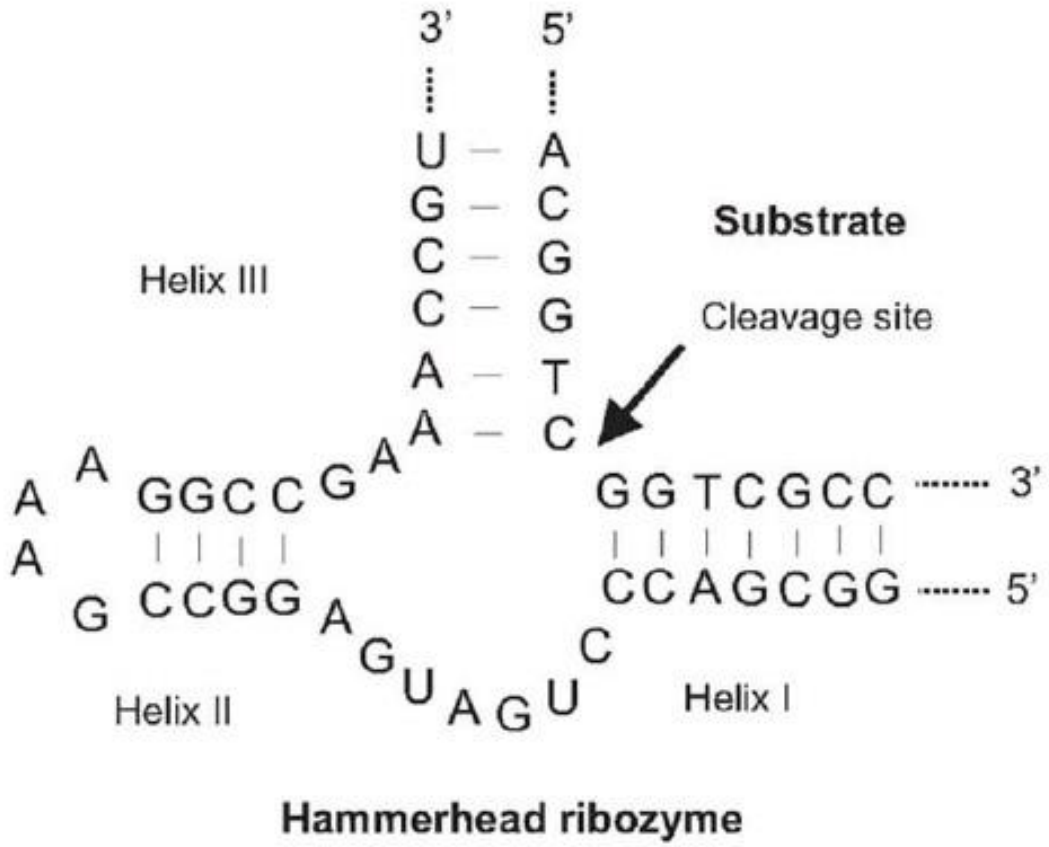

Figure 2.4.Secondary structure of hammerhead ribozyme binding with substrate

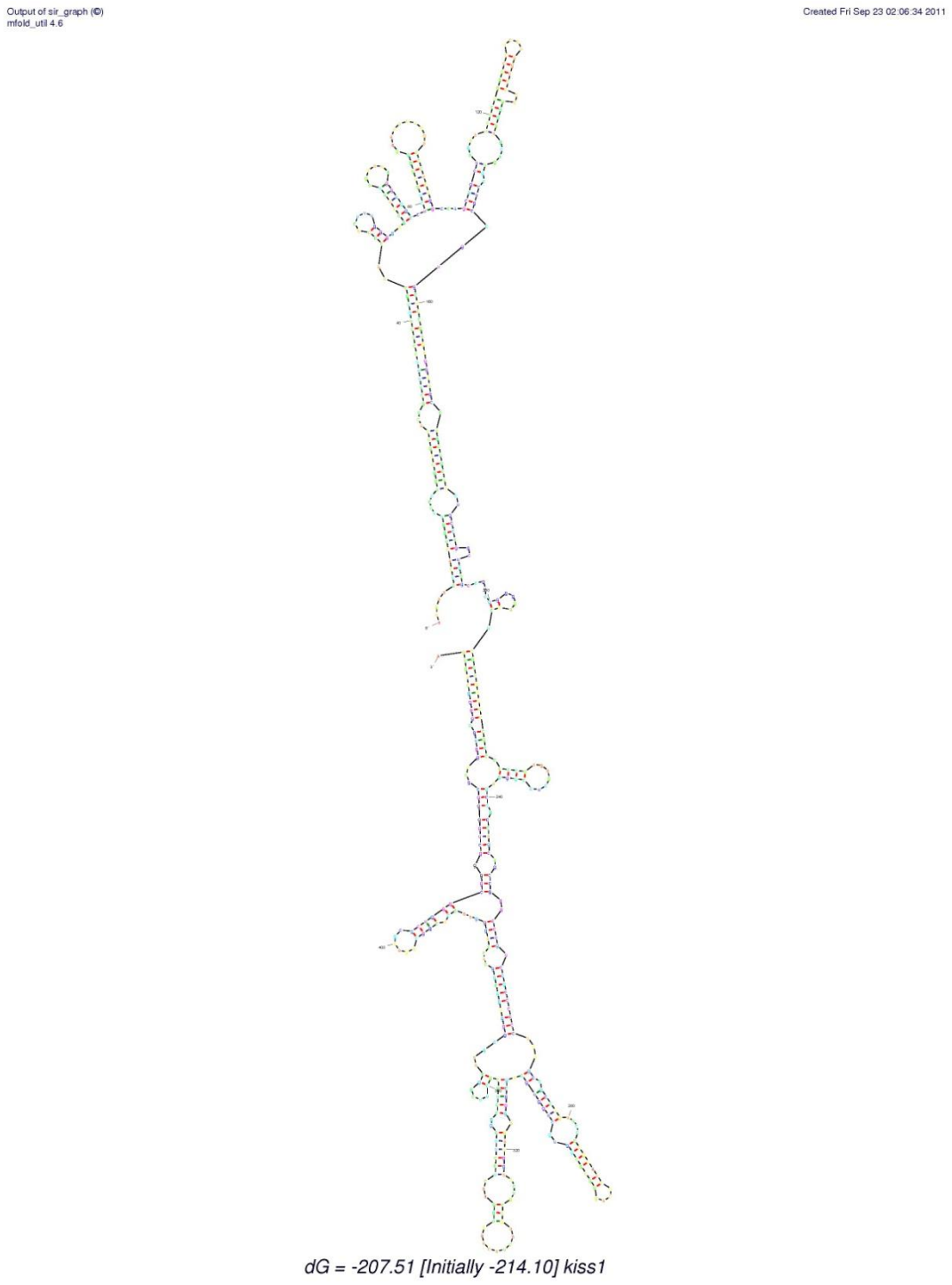

Figure 2.5.Secondary structure of human KiSS-1, generated using the mfold programme (Michael Zucker& Nick Markham, © Rensselaer Polytechnic Institute Hosted by The RNA Institute, 1995-2012, http://mfold.rna.albany.edu/?q=mfold), based on human full length Kiss mRNA

Figure 2.6.Secondary structure of human KiSS-1R/GPF54, generated using the mfold programme (Michael Zucker& Nick Markham, © Rensselaer Polytechnic Institute Hosted by The RNA Institute, 1995- 2012, http://mfold.rna.albany.edu/?q=mfold), based on human full length Kiss mRNA.

2.6.2 TOPO TA gene cloning and generation of stable transfectants

The TOPO TA expression system provided a highly efficient and simple one step cloning approach without the requirement of ligases, specific PCR primers, or any post PCR procedures. The process involved the direct insertion of *Taq*polymerase amplified PCR products (which carried an A-overhang at the 3-end of the product) into a plasmid vector.

This current study used the pEF6/V5-His-TOPO plasmid vector (Invitrogen Inc., Paisley, UK) which was provided linearised with a single 3' Thymidine (T) overhangs for TA cloning, and a covalently bound Topoisomerase. Due to the activity of independent terminal transferase of the template, *Taq*polymerase would catalyse the addition of a single deoxyadenosine (A) to the ends of PCR products. This allowed for efficient ligation of the PCR product into the plasmid vector due its 3' T overhang mentioned above.

2.6.3 TOPO cloning reaction

•The following reagents were placed in a pre-labelled eppendorf tube and mixed gently before being incubated for 5 minutes at room temperature.

4ul of PCR product

1ul salt solution

1ul TOPO vector

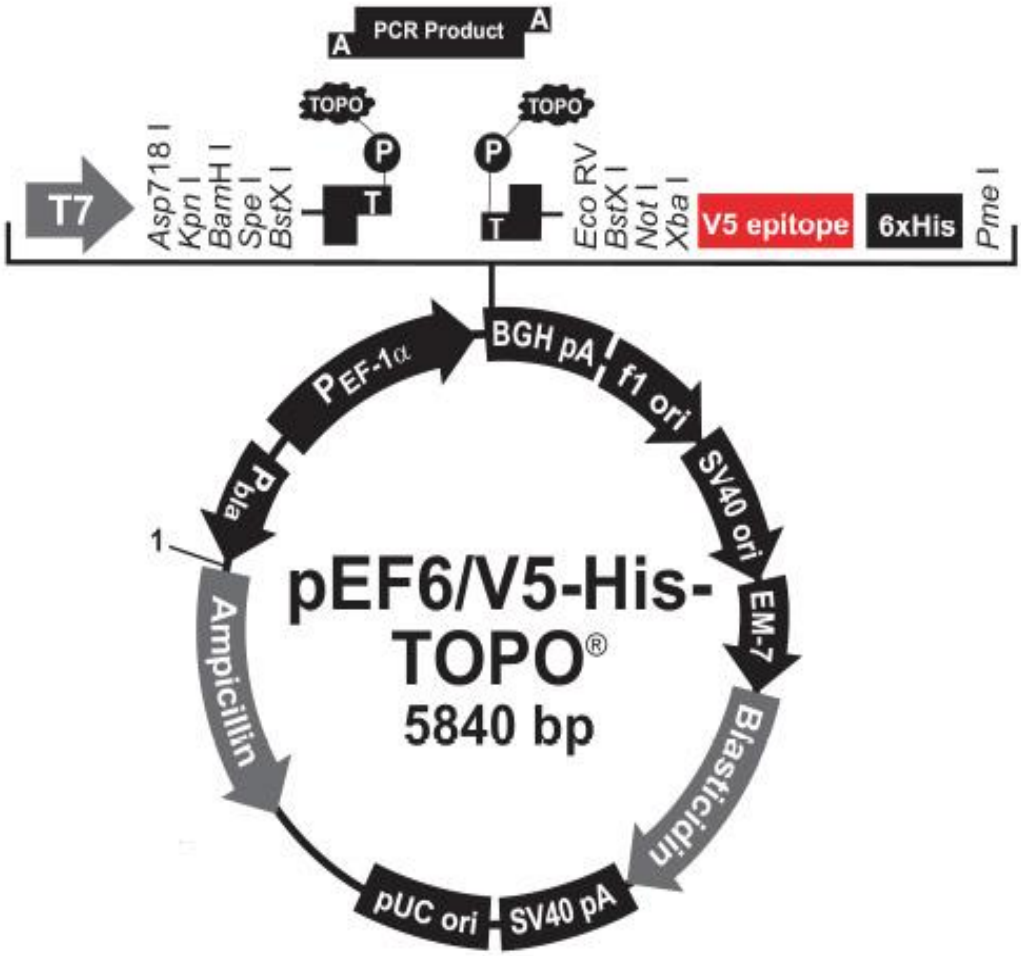

Figure 2.7. Schematic representation of the pEF6 plasmid (From pEF6/V5-His TOPO TA Expression Kit protocol)

2.6.4 Transformation of chemically competent *E. coli*

• Five microlitres of the cloning reaction set up in section 2.7.1 was mixed in a vial with chemically competent One Shot™ TOP10 *E.coli* (In Vitrogen Inc., Paisley, UK) before being incubated on ice for 30 minutes

• This was followed by a heat-shock at 42^{o}C for 30 seconds in a water bath, after which the bacteria was immediate placed on ice for 2 minutes.

• Two hundred and fifty microlitres of SOC medium (warmed to room temperature) was then added to the cell suspension and left to shake horizontally at 200rpm on an orbital shaker (Bibby Stuart Scientific, UK) at 37^{o}C for an hour.

•Following this incubation period, the *E.coli* mixture was spread onto pre-warmed selective LB-agar plates (with 100μg/ml ampicillin) at high and low seeding densities, before being incubated at 37^{o}Cover night.

•As the pEF plasmid carries antibiotic resistance genes to both ampicillin and blasticidin, only the cells that contained the plasmid are capable of growing on the agar. This was a way of selecting only the colonies positive for the plasmid containing your gene of interest. However, to confirm that the gene sequence had been inserted in the correct orientation, the colonies were further tested.

2.6.5 Colony selection and analysis

•In order to confirm that a right product was inserted into the plasmid and that the insert was in the correction orientation, the colonies were subject to more verification.

•This was done by carrying out PCR on around 10 discrete colonies, with three different sets of primers. The first reaction used a forward primer specific for the primer (T7F or BGHR) and a reverse primer specific for the sequence. T7F started around 90bp before the beginning of the insert and so if the insert was ligated in the correct orientation, the resulting product should be around 100bp bigger than the predicted product size. The second reaction contained T7F and a forward primer specific for the sequence. If a product was seen following amplification, then the insert was in the wrong orientation. If a band was seen for both reactions then the colonies contained a mixture of plasmids with both correctly and incorrectly inserted sequences. Finally, in order to verify that the full sequence had been inserted without degradation, a further reaction with T7F and BGHR was carried out on the colonies.

• Individual colonies were examined by lightly touching a labelled colony with a pipette tip, and mixing it into each PCR reaction before specific amplification of the desired sequence. The thermal cycler was set to the following conditions:

Steps	Temperature	Time	Cycles
Initial denaturation	94^{o}C	10 minutes	1
Denaturation	94^{o}C	20 seconds	25
Annealing	55^{o}C	30 seconds	
Extension	72^{o}C	40 seconds	
Final extension	72^{o}C	7 minutes	1

2.6.6 Plasmid purification and amplification

•Following colony analysis, the ones deemed to have the insert in the correct orientation were picked up from the plate and inoculated in 10ml of LB broth with 100μg/ml ampicillin and then being incubated at 37^{o}C over night with constant agitation.

•The amplified *E.coli* were then pelleted by centrifugation at 4^{o}C for 15 minutes at 6,000rpm, and then used for plasmid extraction. This was carried out using the Sigma GenElute Plasmid Mini Prep Kit (Sigma-Aldrich, USA), according to the protocol provided by the manufacture.

•The bacterial pellet was first resuspended in 200μl of resuspension buffer (containing RNase A) before being mixed thoroughly, and transferred into the provided 2ml collection tubes.

•This was followed by the addition of 200μl lysis solution and gently mixing by inverting the tubes 5-6 times. The resulting mixture was left at room temperature for 5 minutes before adding 350μl of neutralisation solution.

•The tubes were inverted several times again, and centrifuged at 12,000rpm for 10 minutes. The resulting supernatant was then transferred into a fresh collection tube containing a Mini Spin Column, which had resin that would bind plasmid DNA after centrifugation at 12,000rpm for 1 minute.

•The flow through was discarded before the column was washed with 700µl of wash solution (containing ethanol) and centrifuging at 12,000rpm for 1 minute. The flow through was discarded once more, before the column was dried by another minute of centrifugation.

•The column was then transferred into a fresh collection tube for elution. This was carried out by adding 100µl of elution solution and centrifuging at 12,000rpm for 1 minute. The resulting flow through containing the purified plasmid was collected, and around 4µl was mixed with a loading dye before running on a 0.8% agarose gel in order to confirm the presence and purification of the plasmid.

2.6.7 Transfection of mammalian cells using electroporation

•Following plasmid extraction, the empty plasmid, and the plasmid containing the ribozyme transgene was used to transfect two colorectal cancer cells (HT-115 and HRT-18)

•The method of transfection used in this study was electroporation using an electroporator (Easyjet, Flowgene, Surrey, UK).

•Once the cells had reached confluency they were detached from their tissue culture flasks, counted, and approximately $1x10^6$ cells were resuspended in 1ml of media.

•300µl of the cell suspension was then added into an electroporation cuvette (Eurgenetech, Southampton, UK), and following the addition of 3-5µl of plasmid, left at room temperature for 5 minutes.

•The cuvette was placed into the electroporator and subjected to an electrical pulse of 290-310V before immediately being transferred into a fresh tissue culture flask containing media.

2.6.8 Establishment of a stable expression mammalian cell line

•Following transfection and in order to obtain a stable cell line expressing the gene of interest, the cultured cells were selected using a specific antibiotics to produce a population of cells that contained the required plasmid, and hence the desired expression of a molecule.

•As mentioned before, the pEF plasmid contained a resistance gene against blasticidin and this was used as a selection marker for mammalian cells. The transfected cells were cultured in selection media containing 5µg/ml blasticidin for around 1-2 weeks. Cells without plasmids will be killed by blasticidin. Only those cells containing the plasmid would survive.

•After selection, the cells were transferred into maintenance media containing 0.5μg/ml blasticidin. In order to verify that the cells were actually expressing the gene of interest, the cells were analyzed by carrying out RT-PCR and Western blotting.

•Once the cells had been verified to stably express the desired molecule ribozyme transgene; they were subjected to various *in vitro* assays in order to test the effect of altering the expression of that molecule on the biological properties of the cells. These assays are outlined in section 2.8.

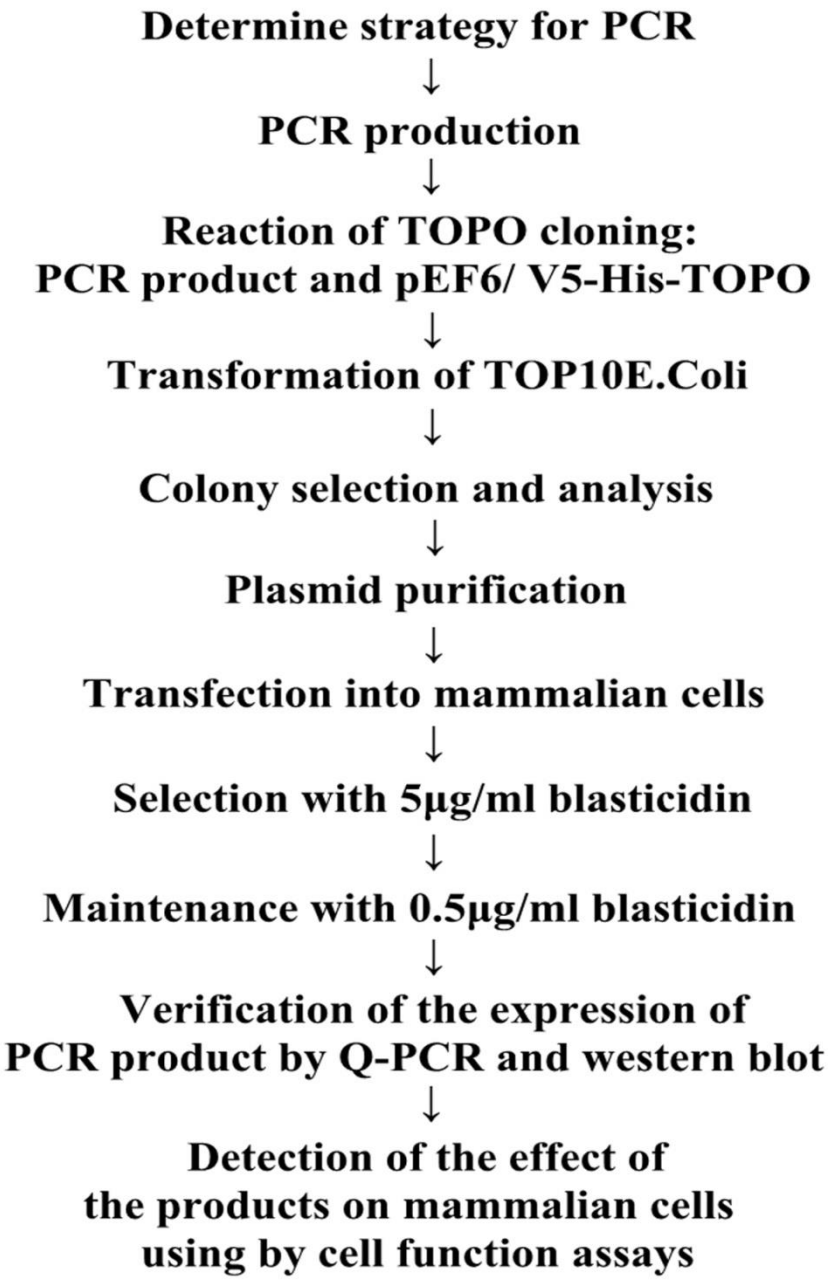

Figure 2.8. Flow diagram presents the general process of cloning and the stable expression of transfected mammalian cell lines

2.7 *In vitro* cell function assays

2.7.1 *In vitro* cell growth assay

•The protocol by Jiang *et al*. was followed (Jiang *et al.*, 1995). 200µl of media containing 3,000 cells was seeded into four 96 well plates. Test agents were added to the wells when appropriate.

•These plates were then incubated at 37^{o}C, with 5% CO_2, for a period of 24, 48, 72 and 120 hours respectively.

•After incubation, the media was discarded, and the cells fixed with 4% formalin for 10-20 minutes, before being subsequently stained with 0.5% crystal violet for 10 minutes. The dye was washed off with water, and the plates left to dry.

•The dye was then solubilised using 200µl acetic acid, and cell growth was assessed by measuring the absorbance at 540nm using a spectrophotometer (BIO-TEK, Elx800, UK). The growth rate was calculated as a percentage, using the absorbance taken at 24 hours as a baseline.

2.7.2 *In vitro* adhesion assay

•Wells in a 96 well plate were coated with 100µl of serum free media with 5µg (stock concentration 0.05µg /µl) Matrigel (BD Matrigel™ Matrix, Magrigel™ Basement Membrane Matrix, Biosciences). The Matrigel was then left to dry for 2 hours at 55^{o}C.

•To rehydrate the Matrigel, 200µl of sterile water was added to each well and left for 45 minutes at room temperature.

•The media was aspirated and 20,000 cells diluted in 200µl media, were seeded into each well and left to adhere at 37^{o}C, with 5% CO_2 for 40 minutes.

• After incubation, the media was discarded, and the wells washed with BSS to remove any unbound cells. The cells that had remained adhered after washing were fixed with 4% formalin for 10-20 minutes, and then stained with 0.5% crystal violet for 10 minutes. The dye was washed off and the plates left to dry before capturing images under the microscope and cell number counted. Due to the fluid dynamics within the small sized wells of a 96 well plate, Matrigel might set unevenly, causing cell aggregation around the edges of the well. Therefore, in order to avoid these areas, only the cells which had adhered to the centre of the well were counted, making sure that the same area of the well was assessed for each sample.

2.7.3 *In vitro* wounding assay

• The protocol by Jiang *et al*. was followed (Jiang *et al.*, 2005). 700µl of media containing 200,000-300,000 cells are seeded into a 24 well plate and cells were treated with a protein of interest in serum free media if required.

•These plates were then left to incubate at 37^{o}C, with 5% CO_2, for a period of 24 hours to allow cells to form a confluent monolayer before the monolayer was

scratch-wounded using a blunted fine needle. Photos were taken using a microscope with camera at 0, 0.25, 1, 2, and 3 hours after wounding.

• Migration distances were measured using Image-J software (National Institutes of Health, USA).

2.7.4 *In vitro* invasion assay

•Trans-well inserts with 8 micrometer pore size (FALCON®, pore size 8.0µm, 24 well format, Greiner Bio one, Germany) were placed into wells of a 24 well plate (NUNC™, Greiner Bio one, Germany), using sterile forceps in order to prevent contamination.

•Each insert was subsequently coated with 100µl serum free media with 50µg Matrigel (stock concentration 0.5µg /µl), and left to dry for 2 hours at 55^{o}C.

•The Matrigel was then rehydrated with 200µl sterile water for an hour at room temperature for 45 minutes.

•The water was carefully discarded, and 20,000 cells in 200µl media were seeded into each insert. 600µl media was then added to the bottom chamber of each well. The cells were incubated for a maximum of 72 hours, with 5% CO_2 at 37^{o}C.

•After 72 hours incubation, the invasive cells invaded through Matrigel, and migrated through the porous membrane to the other side of the insert. The Matrigel layer and the noninvasive cells were then removed from inside of the insert using tissue paper.

This step is essential, as Matrigel would also be stained with crystal violet, making it difficult to distinguish between the background and invading cells.

•The invasive cells were then fixed with 4% formalin for 10-20 minutes, and then stained with 0.5% crystal violet for 10 minutes. Free crystal violet was washed off, the plates left to dry, and the stained cells photographed and counted under a microscope.

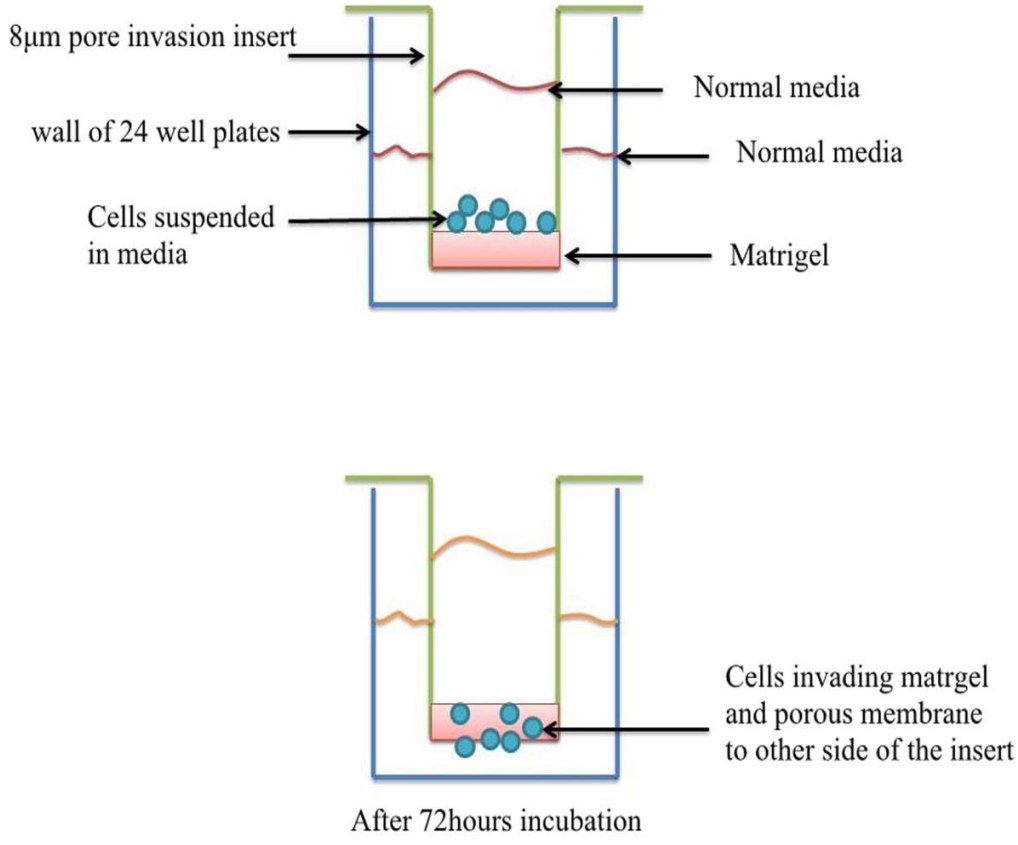

Figure 2.9. Schematic diagrams showing *in vitro* invasion assay

2.8 Electrical cellular impedance sensing (ECIS)

•Electrical Cellular Impedance Sensing (ECIS) is a novel method used as an alternative to the conventional cell function assays mentioned above [119]. Invented by Ivar Givaer, the Noble Prize winner for Physics and Charles Keese, ECIS uses a biophysical method in monitoring cellular behaviour including cell adhesion, cell migration, cell invasion and barrier functions such as tight junctions[119]. It evolved from early simple single unit based analysis to what is now multiple well and automated versatile assays [120].

•The present study used an ECIS Ztheta model. It works on an array of 96 wells, each containing one (96W1E) gold plated electrode or ten (96W10E) gold electrodes. These electrodes measure the electric current and voltage across this electrode, calculating the impedance and resistance. From the impedance changes, effects on cell attachment and motility can be examined [120]. Using 96W1E arrays (ECIS™ cultureware, Applied Biophysics, Inc., NY, USA), each well was stabilised at room temperature for around 20 minutes using 200µl electrode stabilising solution (ECIS™, Applied Biophysics, Inc., NY, USA).

•The solution was then aspirated and replaced with 200µl DMEM/Ham's F12 media containing HEPES buffer (Lonza, Verviers, Belgium) and left until needed.

•The media was aspirated, and 40,000 cells diluted in 200µl DMEM were seeded into each well, and treated with test reagents if required.

•The array was then placed into an ECIS™ CO_2 incubator (RS biotech 9600, R galaxy R+) which was connected to the ECIS™ Ztheta Controller (Applied Biophysics, Inc., NY, USA). The software was set up so that resistance to the current flow was measured at frequencies ranging from 125 to 64,000Hz. Data was normalised using resistance from the first time point.

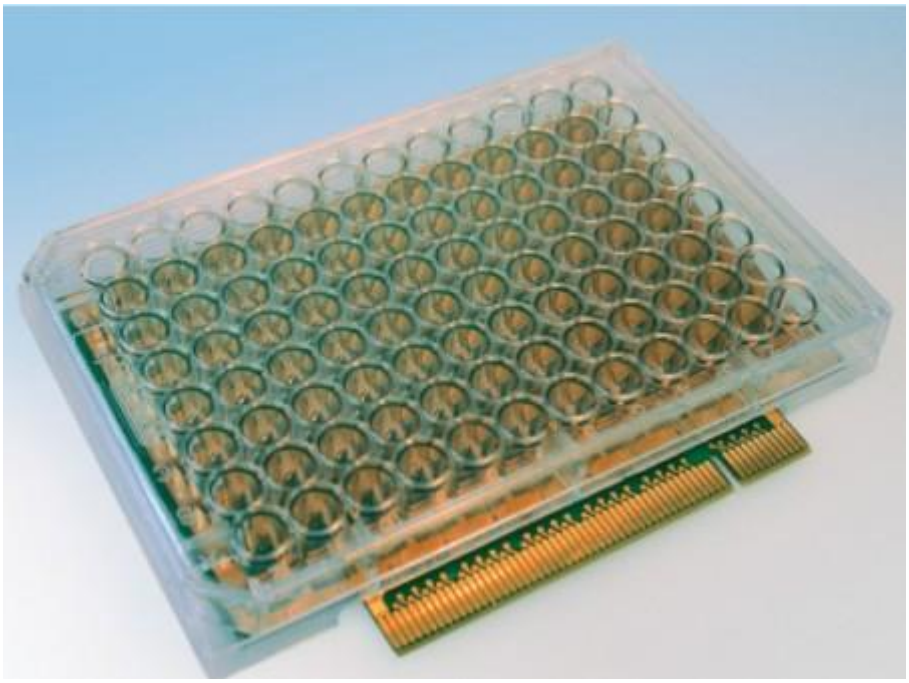

Figure 2.10.A.96W1E arrays (ECIS™ cultureware, Applied Biophysics, Inc., NY, USA)

Figure 2.10.B. The ECIS™ Model Ztheta Controller (Applied Biophysics, Inc., NY, USA)

2.9. *In vivo* tumour model

Athymic nude mice (Strain CD-1) were purchased from Charles River Laboratories (Charles River Laboratories International, Inc., Kent, England, UK). Female 4-6 week old CD-1 mice were used. All the mice were kept in a filter-topped isolation cages and all the procedures were carried out in a class-II cabinet. The study was conducted under the Home Office Project license PPL 30/2591 and personal license number (No. PIL 30/10005).

After the mice were settled for a week in the designated laboratories, HT-115 cells (control or Kiss-1 knockdown cells) were injected subcutaneously at a volume of 100µl which contained Matrigel at final concentration of 2.5ml/ml. The mice were then carefully monitored twice weekly by measuring body weight, tumour size (using a digital caliper), and any size effects, according to the regulations of the Home Office and UKCCCR Guideline for using experimental animals in cancer research. Any severe side effects, significant weight loss (>20% of body weight) and oversized tumours (>1cm in any diameter) would trigger a termination of the study.

The volume of tumours was calculated by using the following formula:

tumour volume (mm^3)= $0.512 \times Width^2 \times length$

2.10. Collection of clinical cohort

This was collected under the Approval by the South East Wales Local Research Ethics Committee (ref 05/WSE03/92) with patient's consent. Fresh tissues were obtained immediately after surgery. Tumour tissues and normal tissues (>10cm away from the tumour margin) were obtained with the pathologist on call and stored immediately in a deep freezer (-80^{o}C) until use.

The frozen tissues were first sectioned using a Leica CM1900 Cryostat (Leica Microsystems Ltd, Bristol, UK) at 8-10 μm thickness. A part of sections (>50) were divided into three portions were pooled and homogenised to extract RNA for molecular bades analysis.

2.11 Data analysis

The statistical comparisons were made using either a non-parametric Mann- Whitney test if the data was not normalized or a Students two tailed t- test if the data was found to be normalized and have equal variances. Graphs were constructed using Microsoft Excel Software Package.

The relationship between the expression of Kiss-1 and Kiss-1R and tumour grade, TNM staging and nodal status was respectively analyzed using Mann-Whitney U and Kruskal-Wallis test. Survival analysis curve were performed using Kaplan-Meier survival analysis. Quantitative data were analyzed using the Student’s t-test, and

chi-squared test, where appropriate. Differences were considered to be statistically significant at $p<0.05$.

For the *in vivo* tumour growth study, both student t test and two way ANOVA tests were employed using the SigmaPlot software.

Chapter 3

The expression of Kiss-1 and Kiss-1R in tissues, cell lines and verification of Kiss-1 and Kiss-1R knockdown

3.1 Introduction

Lee and colleagues (1994) introduced the full length of chromosome 6 into the human metastatic melanoma cell line C8161 using a microcell-mediated transferring technique and then found the introduction of chromosome 6 suppressed metastasis without impacting tumourgenicity and invasion [60]. Two years later, the human Kiss-1 gene was isolated and identified from the melanoma cells by Lee et al [61-62]. Kiss-1 is mapped to chromosome 1q32, which was identified as a human melanoma metastasis suppressor gene through the analysis of subtractive hybridization in highly metastatic cell lines when compared with non-metastatic cell lines [60]. Kiss-1 receptor (Kiss-1R), also known as G-protein coupled receptor 54 (GPR54), HOT7T175, AXOR12 and Metastin receptor, was first discovered and cloned from rat brain by Dennis in 1999 [68]. In humans, it maps to chromosome 19p13.3, contains 5 exons and 4 introns encoding 398 amino acids, resulting in a 75 kDa protein. Kiss-1R shares 81% protein homology with the preceding cloned rat homolog [64, 69]. Tissue distribution of Kiss-1 and its receptor are often concordant, like placenta and the central nervous system in which both genes are highly expressed [48, 61, 69]. High levels of Kiss-1R have been observed in the cerebral vortex, cerebellum, thalamus and pons-medulla [69]. By contrast, Kiss1 is highly expressed in the hypothalamus and pituitary [64]. In addition to the placenta high expression of Kiss-1R is also seen in the pancreas, whilst it has low expression in adipose tissue, lymph nodes, peripheral blood lymphocytes, pituitary gland and spleen [48, 69].

In 1997, Lee and Welch hypothesized that Kiss-1 might suppress metastasis in other tumour types in addition to melanoma. Hence, the human breast cancer cell line MDA-MB-435 transfected with full-length Kiss-1 cDNA was implanted into athymic nude mice with paired control cells. The results demonstrated that the metastatic potential of transfected cells was significantly decreased, but tumourigenicity was not inhibited [71]. In light of these observations, Kiss-1 and its receptor were suggested as a pair of metastasis suppressors in several cancers. However, it remains largely unknown what effect Kiss-1 and Kiss-1R may have in malignancies and the molecular mechanisms or pathways underlying their influence on tumour suppression. The expression of Kiss-1 and Kiss-1R genes are mainly found in the placenta, but Kiss-1 was also detected in colon, pancreas and intestinal tissue [121]. No previous studies have specially shown a possible role of Kiss-1 and its receptor in colorectal cancer. However, Chen *et al.*, (2012) reported that Kiss-1 expression increased in the colorectal cancer cell line SW480 irradiated with 6-MV X-rays for 48 hours, which resulted in a decrease in proliferation and an increase in apoptosis [122]. Their investigation provides some indication that Kiss-1 may have an inhibitive effect on colorectal cancer cells. The present study aimed to establish the role played by Kiss-1 and Kiss-1R has in colorectal cancer cells. Initially, the mRNA expression of Kiss-1 and Kiss-1R were screened in four human colorectal cancer cell lines, subsequently to knock down the expression level of Kiss-1 and Kiss-1R in those cells, which have relatively high expression of Kiss-1 and Kiss-1R.

3.2 Materials and methods

3.2.1 Materials

Primers

All the primers used were synthesized and provided by Invitrogen (Paisley, UK).

Primer sequences are shown in Table 3.1

Table 3.1. The sequences of the primers Kiss-1/Kiss-1R, Kiss-1/Kiss-1R ribozymes and GAPDH.

Gene	Sense primer	Antisense primer
Kiss-1	5’-TGAACTCACTGGTTTCTTGG-3’	5’-CGAAGGAGTTCCAGTTGTAG-3’
Kiss-1R	5’-CTTCATGTGCAAGTTCGTC-3’	5’-CACCAGGAACAGCTGGAT-3’
Kiss-1 rib	5’-CTGCAGCTCTCGGGGGGGCGGGGACAGCGAGGTCCCCCCTGATGAGTCCGTGAGGA-3’	5’-ACTAGTGCCAGCTGCTACTGCCA-3’
Kiss-1R rib	5’-CTGCAGTTCCGCATCGGCTTGTGGCGGCACTGATGAGTCCGTGAGGA-3’	5’-ACTAGTGCCCCGCCTGGCGCTGGCTGTTTCGTCCTCACGGACT-3’
GAPDH	5’-GGCTGCTTTTAACTCTGGTA-3’	5’-GACTGTGGTCATGAGTCCTT-3’

The details of the touchdown PCR reaction and colony analysis using PCR have been described in Chapter 2.

Antibodies

Polyclonal anti-Kiss-1 antibody (sc-101246, mouse polyclonal IgG_{2a}) and polyclonal anti Kiss-1R antibody (sc-48220, goat polyclonal IgG) were obtained from Santa Cruz Biotechnology (Santa Cruz, California, USA).

3.2.2 Generation of Kiss-1 and Kiss-1R ribozyme transgenes

Hammerhead ribozymes targeting Kiss-1 and Kiss-1R were designed using Zuker's mRNA Fold programme (Zuker, 2003) based on the secondary structure of both Kiss-1 and Kiss-1R mRNA. The transgenes were synthesised using touchdown PCR with the reaction conditions described in Chapter 2. The products were then run on a 2% agarose gel to verify their presence as well as size, before being cloned into the pEF6/His plasmid vector.

3.2.3 TOPO TA cloning and generation of stable transfectants

The ribozymes obtained from the above procedure were subsequently cloned into the pEF6/V5-His-TOPO vector. One microlitre of the vector, 1 µl salt solution, 1 µl of the ribozyme products and 3 µl H_2O were gently mixed and allowed to react at room temperature for 5 minutes. This was followed by transferring the reaction mixture to the TOP10 *E.Coli*, a chemically competent *E.Coli* strain. After 30 minutes on ice, the bacteria were subject to heat shock at 42^{o}C for 3 seconds, before being placed on ice for 2 minutes. The bacterial mixture was added to SOC media and placed on an

orbital shaker for 1 hour, at a speed of 200rpm. The bacterial solution was plated on liquid broth (LB)-ampicillin agar plates and allowed to grow overnight. Only the cells containing the plasmid were able to grow on the agar, as the pEF plasmid has antibiotic resistance genes to ampicillin and blasticidin (figure 3.1). Colonies of transformed *E.Coli*,transgenes of Kiss-1 and Kiss-1R cloned into pEF6/V5-His-TOPO plasmids (Invitrogen Inc., Paisley, UK) were analyzed RT-PCR, using the T7F primer coupled either with RbBMR and RbTPF primers. After amplifying the correct colonies the plasmids were extracted using the Sigma GenElute Plasmid MiniPrep Kit (Sigma-Aldrich, USA).

Control plasmid and the plasmid containing theribozyme transgene was used to transfect both the HT115 and HRT18 cell lines respectively. The transfected cells were cultured in selection media containing 5μg/ml blasticidin for around 1-2 weeks so that only those cells containing the plasmid would survive. Following selection, the cells were transferred into maintenance media containing 0.5μg/ml blasticidin, to verify the knockdown of Kiss-1 and Kiss-1R by carrying out RT-PCR, Q-PCR and Western blot. $HT115^{wt}$, $HT115^{pEF}$, $HT115^{Kiss\text{-}1\ kd}$ and $HT115^{Kiss\text{-}1R\ kd}$ represent for HT115 wild type, HT115 pEF, HT115 Kiss-1 knockdown and HT115 Kiss-1R knockdown cells respectively; $HRT18^{wt}$, $HRT18^{pEF}$, $HRT18^{Kiss\text{-}1\ kd}$ and $HRT18^{Kiss\text{-}1R\ kd}$ represent for HRT18 wild type, HRT18 pEF, HRT18 Kiss-1 knockdown and HRT18 Kiss-1R knockdown cells respectively.

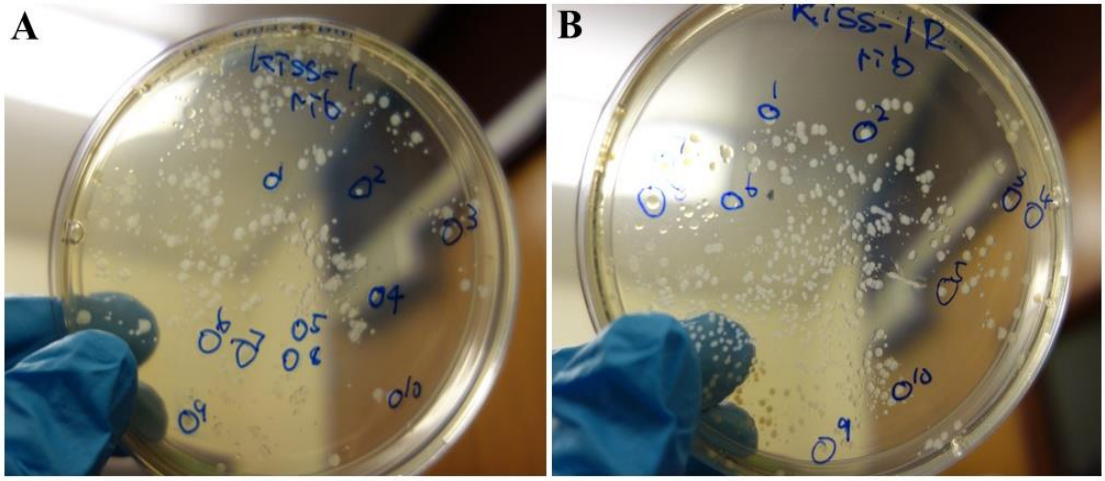

Figure 3.1. Gel image for the plasmid of Kiss-1 and Kiss-1R. A. After incubation at 37^{o}C overnight, the Kiss-1 ribozyme colonies positive for the plasmid containing the gene of interest were grown on the agar. Ten independent colonies were selected and numbered for analyzing the gene sequence ligated into the vector in the correct orientation. B. The Kiss-1R ribozyme colonies positive for the plasmid were grown on the agar. Ten independent colonies were numbered and then selected to verify the gene sequence inserted in the correct orientation by PCR reaction.

3.2.4 RNA isolation, cDNA synthesis, RT-PCR and Q-PCR

RNA isolation was carried out using the Tri Reagent kit (Sigma-Aldrich, Inc., Poole, Dorset, England, UK), and then converted into cDNA by reverse transcription using the iScript™ cDNA Synthesis Kit (Bio-Rad Laboratories, California, USA). cDNA as the template was detected by RT-PCR and Q-PCR. The reaction conditions of RT-PCR and Q-PCR were described in Chapter 2. The products were run on an agarose gel (the concentration depends on the size of product) and stained using ethidium bromide solution for visualizing using an Ultra Violet Transilluminator (UVP, Cambridge, UK).

3.2.5 Protein extraction, SDS-PAGE and Western blot analysis

Protein was extracted from cells and quantified using the DC Protein Assay kit (BIO-RAD, USA). Proteins were separated according to charge using SDS-PAGE and blotted onto nitrocellulose sheets. Specific primary (anti-Kiss-1 and Kiss-1R 1:500) and HRP-conjugated secondary antibodies (1:1000) were used to probe proteins, and bands stained by the chemiluminescence detection kit (Luminata, Millipore) were visualized using the Supersignal^{TM} West Dura system (Pierce Biotechnology, USA).

3.3 Results

3.3.1 Colorectal cancer cell lines screening for the expression of Kiss-1 and Kiss-1R

The expression of Kiss-1 and Kiss-1R were examined in four colorectal cancer cell lines of human origin including HT115, HRT18, RKO and Caco-2. They were from highly invasive human colorectal carcinoma. Figure 3.2 showed the expression of Kiss-1 and Kiss-1R in the cell lines. On the whole, both Kiss-1 and Kiss-1R were generally expressed in all the four colorectal cancer cells, while the expression levels displayed differences in different cell line. Although the mRNA expression of both Kiss-1 and Kiss-1R were detected in four colorectal cancer cells, higher levels were seen in HT115 and HRT18 cells compared with RKO and Caco-2 cells. From these analysis, HT115 and HRT18 cells were chosen for Kiss-1 and Kiss-1R knock down.

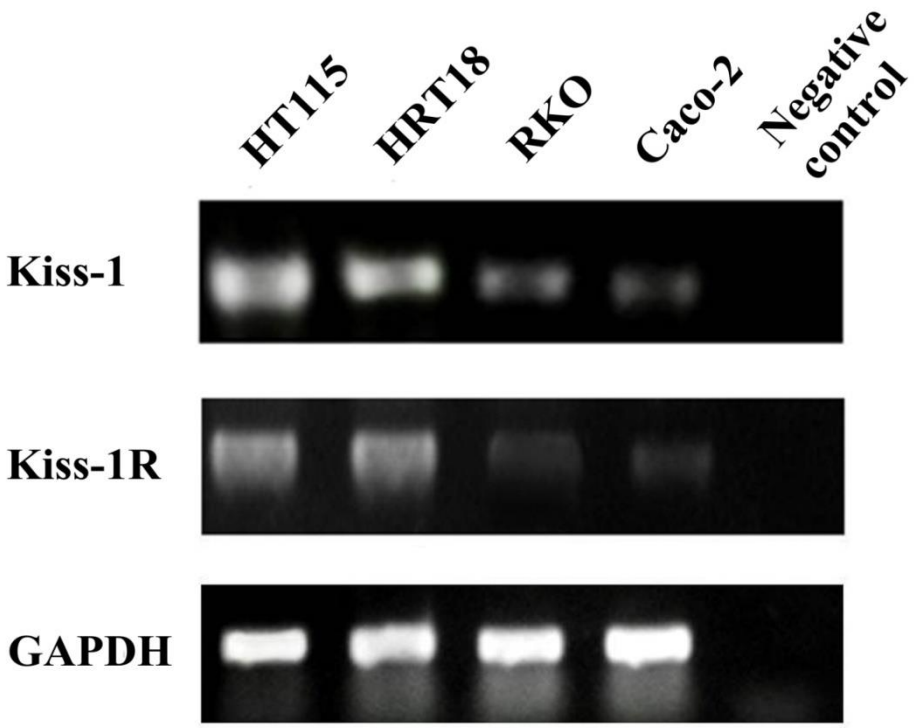

Figure 3.2. Colorectal cancer cells screening for the expression of Kiss-1 and Kiss-1R. mRNA expression of Kiss-1 and Kiss-1R was screened in four colorectal cancer cells (HT115, HRT18, RKO and Caco-2) using conventional PCR techniques.

3.3.2 Generation of Kiss-1 and Kiss-1R ribozyme transgenes

For the purpose of silencing both Kiss-1 and Kiss-1R expression in colorectal cancer cells, anti-Kiss-1 and anti-Kiss-1R ribozyme transgenes were generated and cloned into pEF6/His plasmids respectively, allowing for mammalian cell transfection. In order to verify correct orientation of the ribozyme transgenes, two primers (RbTPF and RbBMR) were paired with BGHR respectively. If the transgene is correctly orientated, the bands of PCR product would be determined from RbTPF+ BGHR reaction. In contrast, a wrong sized product would arise for the RbBMR+ BGHR reaction.

From Figure 3.3.B, it is demonstrated that colony 18-1 (Kiss-1) and 19-7 (Kiss-1R) had the highest levels of correctly orientated ribozyme transgenes, in the meantime, the bands of wrongly orientated ribozyme transgenes were weakest. Colonies 18-1 and 19-7 were subsequently collected and amplified. The plasmids were extracted from the correct colonies and were verified with DNA electrophoresis. Based on the difference of migrating speed and the amount of negative charge, open circular DNA, linear DNA and covalently closed circular DNA presented three bands respectively after electrophoresis from the top down in Figure 3.3.C. As the surface of covalently closed circular DNA, which had the strongest band, carried the least negative charge, it had the fastest speed from a negative pole to a positive pole. There were no white bands observed in the sample holes, it illustrated the high purity of plasmids was without proteins.

A

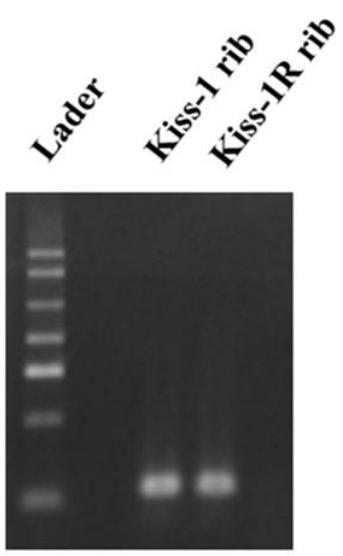
Lader
Kiss-1 rib
Kiss-1R rib

B

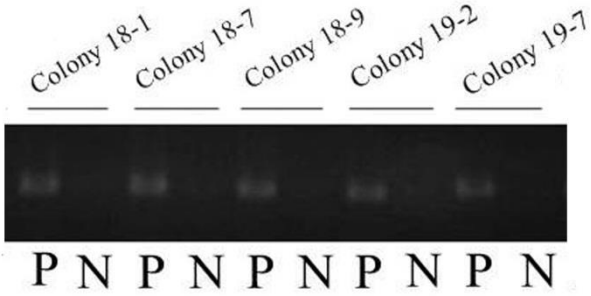
Colony 18-1
Colony 18-7
Colony 18-9
Colony 19-2
Colony 19-7
P N P N P N P N P N

(**Figure 3.3**)

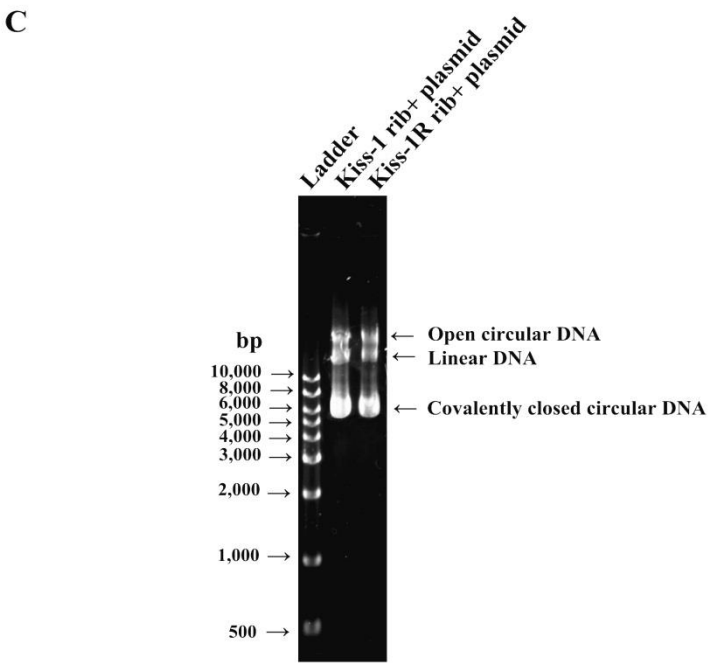

Figure 3.3. Ribozyme transgene synthesis.A.The ribozymes generated using touchdown PCR, run on an agarose gel. B. The colonies were analysed using PCR after transformation into *E.coli* cells, to verify correct orientation of the transgene. P represented correct orientation (140bp ribozyme sequence plus 173bp sequence downstream of the insert site), which used a ribozyme specific primer (RbTPF) and a plasmid specific primer (BGHR) in a PCR reaction; N stood for incorrect orientation (140bp ribozyme sequence plus 173bp sequence downstream of the insert site), where a ribozyme primer (RbBMR) was coupled with a plasmid specific primer (BGHR), in a PCR reaction. C. The plasmids of Kiss-1 and Kiss-1R extracted from the correct colonies were verified with DNA electrophoresis. Three bands appeared after electrophoresis because of the difference of their migrating speed in the process of gel electrophoresis, the order from the top – down is: open circular DNA, linear DNA and covalently closed circular DNA.

3.3.3 Verification of Kiss-1 knockdown in HT115 and HRT18 cells

To ensure the knockdown of Kiss-1 was successful, we used Q-PCR and Western blots to verify the message and protein in the transfected cells. Figure 3.4 and 3.5 showed that the expression of Kiss-1mRNA was significantly reduced in the ribozyme transgene transfected cells ($HT115^{Kiss\text{-}1\ kd}$ and $HRT18^{Kiss\text{-}1\ kd}$) compared with the levels of expression seen in wild type cells ($HT115^{wt}$ and $HRT18^{wt}$) and control transfection with empty plasmid ($HT115^{pEF}$ and $HRT18^{pEF}$). The levels of Kiss-1mRNA from three repeats, which was normalized against corresponding internal control (GAPDH) using Quantitative real time PCR are described at Figure 3.4.B and 3.5.B. The expression of Kiss-1 was decreased in $HT115^{Kiss\text{-}1\ kd}$ cells as compared with both$HT115^{wt}$ and $HT115^{pEF}$ cells ($p< 0.05$). Figure 3.6 and 3.7 showed the expression of Kiss-1 knock down at the protein level in both HT115 and HRT18 cells using Western blots. The volume of the Kiss-1 protein bands with three repeats normalized against corresponding internal control (GAPDH) is demonstrated at figure 3.6.B and 3.7.B. Similarly, the expression of Kiss-1 was decreased in both $HT115^{Kiss\text{-}1\ kd}$and $HRT18^{Kiss\text{-}1\ kd}$ cells compared with the respective controls ($p< 0.05$).

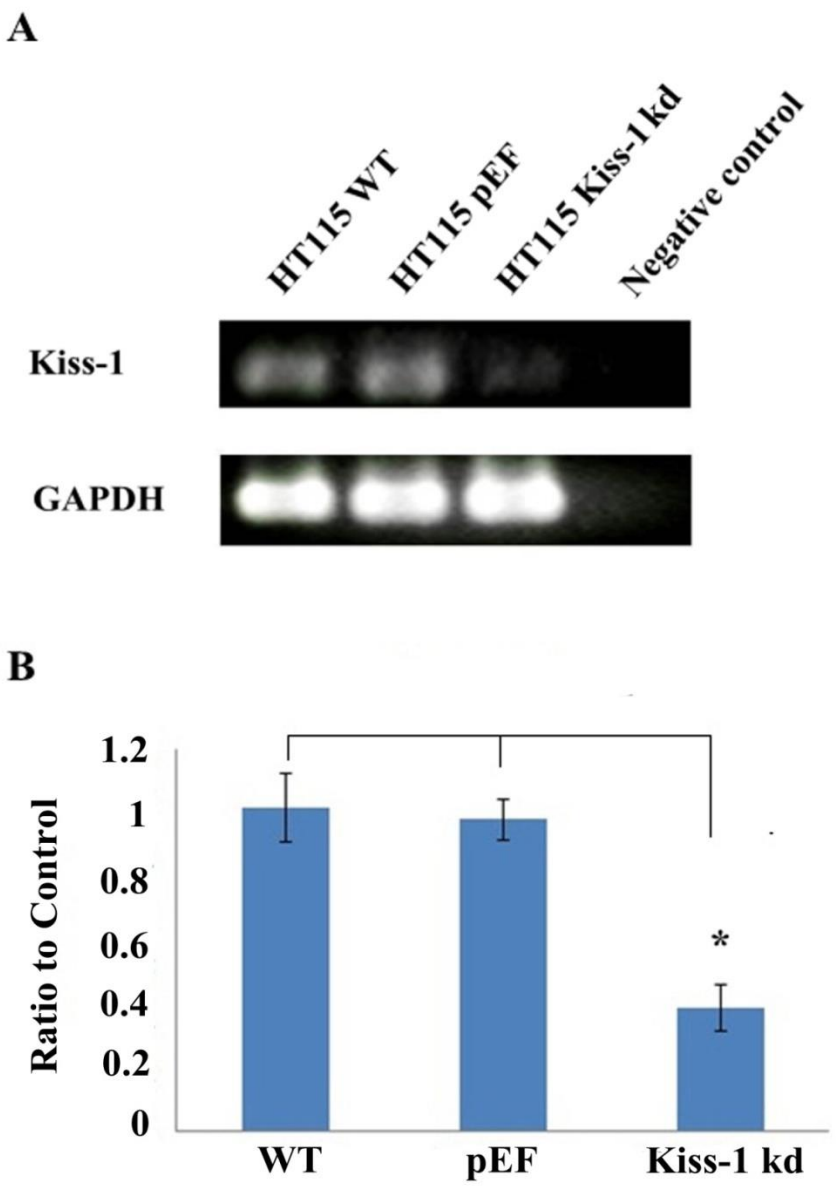

Figure 3.4. Verification of knockdown of Kiss-1 in HT115 cells. A. RT-PCR displayed reduced level of Kiss-1 in mRNA in $HT115^{Kiss\text{-}1\ kd}$cells compared with control cells ($HT115^{wt}$ and $HT115^{pEF}$ cells). B. Quantitative real time PCR showed Kiss-1 mRNA volume of three repeats which was normalised against corresponding internal control (GAPDH). The expression of Kiss-1decreased significantly in $HT115^{Kiss\text{-}1\ kd}$ cells compared with $HT115^{wt}$ (p= 0.0083) and $HT115^{pEF}$ cells (p= 0.0033). Asterisk represented p< 0.005. Original data is shown in Table 1 of Appendices.

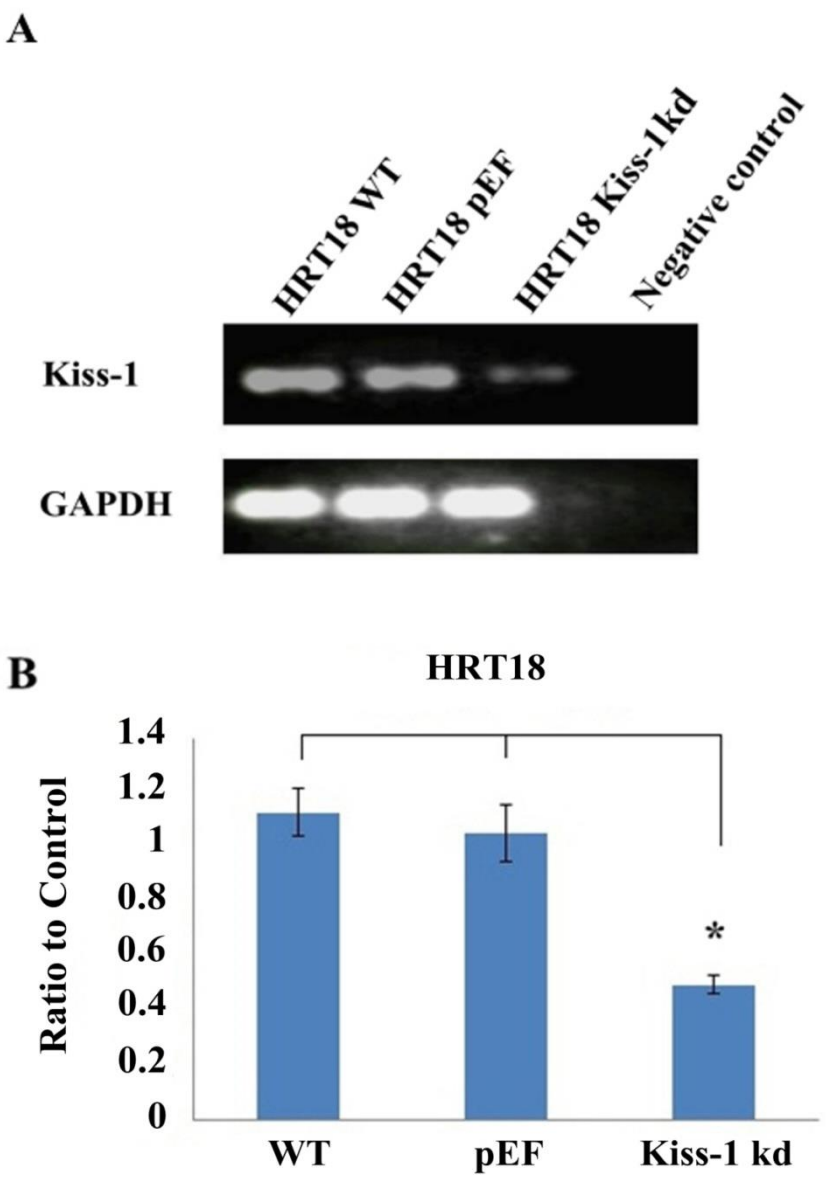

Figure 3.5. Verification of knockdown of Kiss-1 in HRT18 cells. A. RT-PCR displayed a reduced mRNA expression level of Kiss-1 in HRT18$^{\text{Kiss-1 kd}}$ cells compared with control cells (HRT18$^{\text{wt}}$ and HRT18$^{\text{pEF}}$ cells). B. Quantitative real time PCR showed Kiss-1 mRNA volume of three repeats which was normalized against corresponding internal control (GAPDH). The expression of Kiss-1 decreased significantly in HRT18$^{\text{Kiss-1 kd}}$ cells compared with HRT18$^{\text{wt}}$ (p= 0.000031) and HRT18$^{\text{pEF}}$ cells (p= 0.0008) respectively. Asterisk represented p< 0.005. Original data is shown in Table 2 of Appendices.

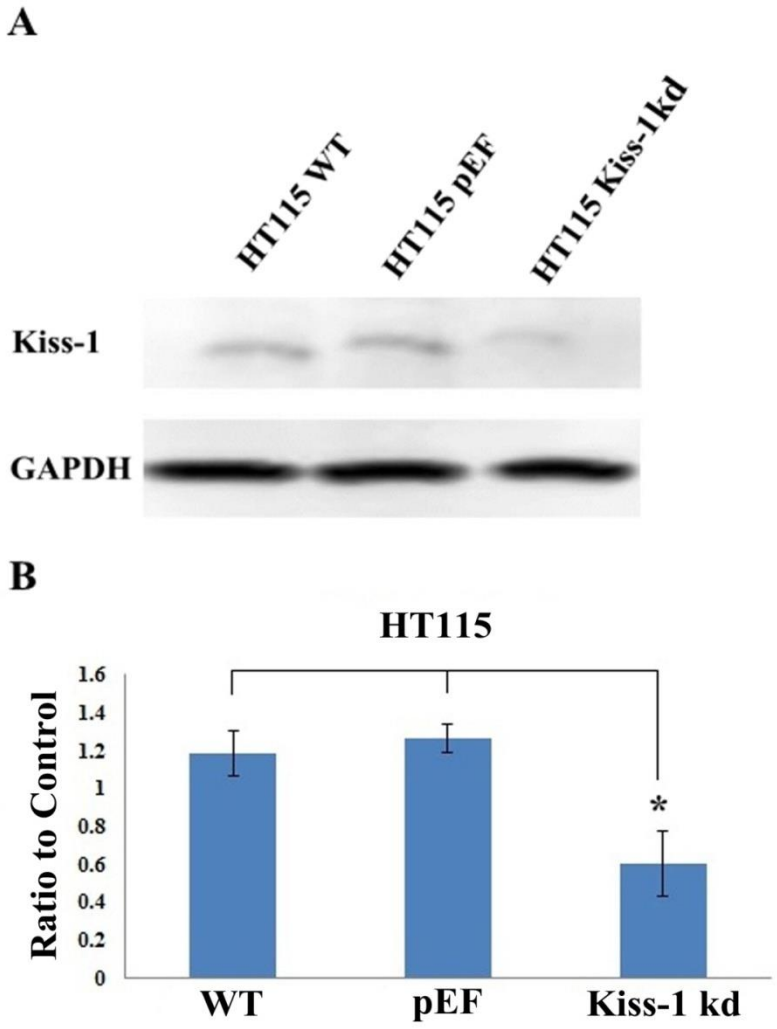

Figure 3.6. Confirmation of Kiss-1 knockdown in HT115 cells. A. Kiss-1 protein bands volume of three repeats which was normalized against corresponding internal control (GAPDH). B. The expression of Kiss-1 showed a significant decrease in $HT115^{Kiss\text{-}1\ kd}$ cells compared with both that in $HT115^{wt}$ (p= 0.0083) and $HT115^{pEF}$ (p= 0.0035) cells. Asterisk stood for p< 0.05. Original data is shown in Table 3 of Appendices.

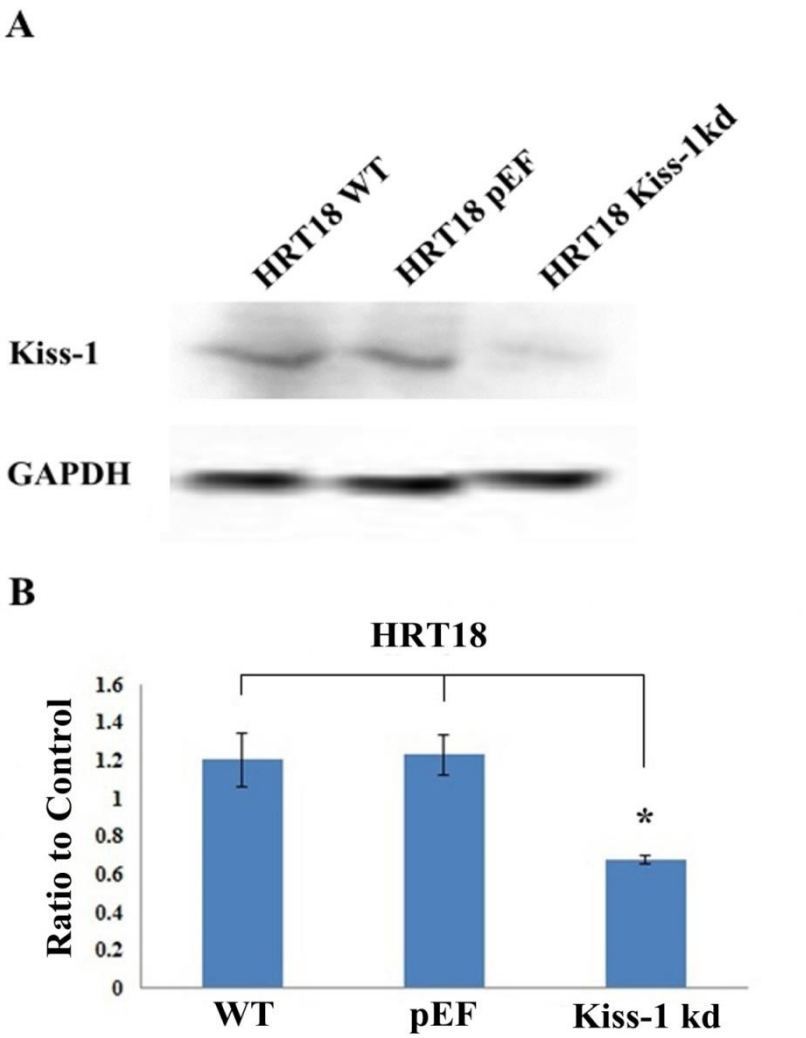

Figure 3.7. Confirmation of Kiss-1 knockdown in HRT18 cells. A. Kiss-1 protein bands volume of three repeats which was normalized against corresponding internal control (GAPDH). B. The expression of Kiss-1 showed a significant decrease in $HRT18^{Kiss\text{-}1\ kd}$ cells compared with both that in $HRT18^{wt}$ (p= 0.0031) and $HRT18^{pEF}$ (p= 0.00081) cells. Asterisk stood for p< 0.05. Original data is shown in Table 4 of Appendices.

3.3.4 Verification of Kiss-1R knockdown in HT115 and HRT18 cells

We further detected the expression of Kiss-1R knockdown compared with control groups (wild type and pEF) in both HT115 and HRT18 cells at both mRNA and protein levels using Q-PCR and western blots. Figure 3.8 and 3.9 display the decreased expression of Kiss-1R mRNA in the ribozyme transgene transfected cells ($HT115^{Kiss\text{-}1R\ kd}$ and $HRT18^{Kiss\text{-}1R\ kd}$) compared with the levels of expression seen in wild type ($HT115^{wt}$and $HRT18^{wt}$) cells and empty plasmid ($HT115^{wt}$and $HRT18^{pEF}$) cells. The levels of Kiss-1R mRNA from three repeats, normalized against corresponding internal control (GAPDH) using Quantitative real time PCR is demonstrated at figure 3.8.B and 3.9.B. An obviously significantly decreased expression of Kiss-1R in $HT115^{Kiss\text{-}1R\ kd}$ and $HRT18^{Kiss\text{-}1R\ kd}$ cells was seen when compared with $HRT18^{wt}$ and $HRT18^{pEF}$ cells ($p< 0.05$). Figure 3.10 and 3.11illustrate the expression of Kiss-1R knockdown at protein level using western blots. The levels of Kiss-1R from three repeats normalized against corresponding internal control (GAPDH),is shown at Figures 3.10.B and 3.11.B. Similarly, the expression of Kiss-1R was decreased in $HT115^{Kiss\text{-}1R\ kd}$ and $HRT18^{Kiss\text{-}1R\ kd}$ cells compared with control groups respectively ($p< 0.05$).

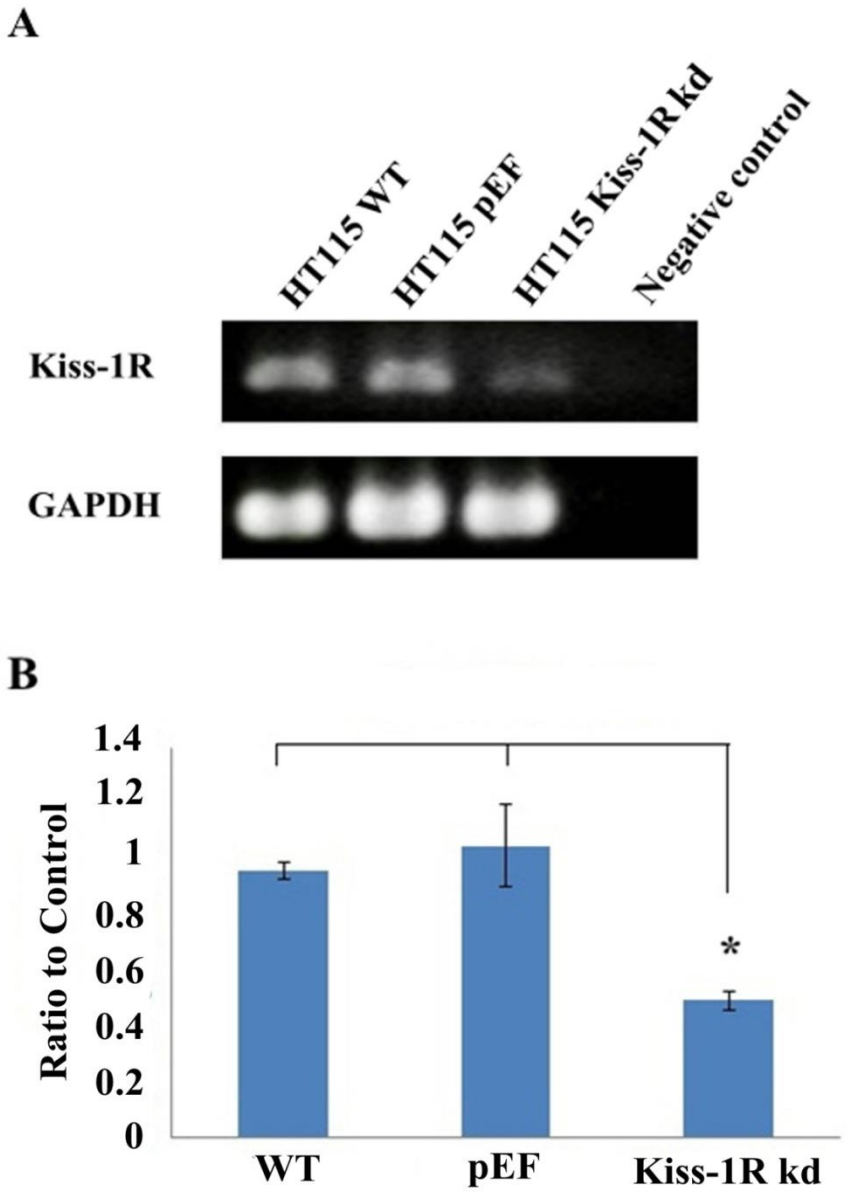

Figure 3.8. Confirmation of knockdown of Kiss-1R in HT115 cells. A. RT-PCR displayed reduced mRNA expression level of Kiss-1R in $HT115^{Kiss\text{-}1R\ kd}$ cell compared with control cells ($HT115^{wt}$ and $HT115^{pEF}$ cells). B. Quantitative real time PCR showed Kiss-1 mRNA volume of three repeats which was normalised against corresponding internal control (GAPDH). The expression of Kiss-1R decreased significantly in $HT115^{Kiss\text{-}1R\ kd}$ cells compared with $HT115^{wt}$ (p= 0.00017) and $HT115^{pEF}$ cells (p= 0.000044) respectively. Asterisk represented p< 0.005. Original data is shown in Table 5 of Appendices.

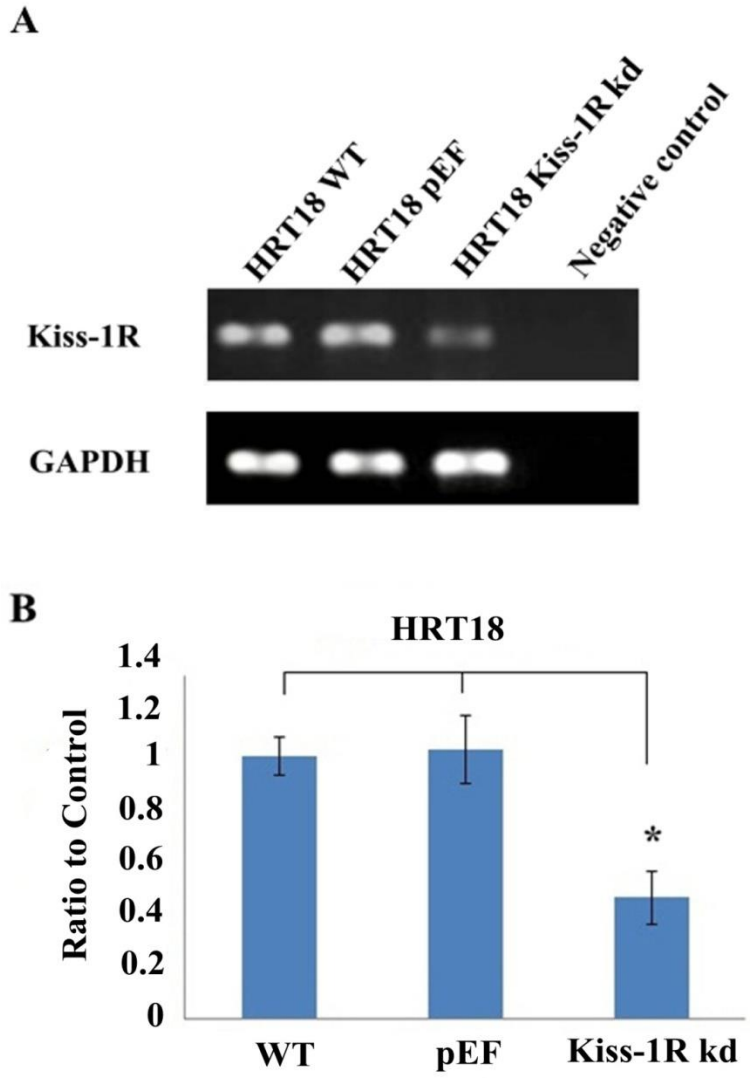

Figure 3.9. Confirmation of knockdown of Kiss-1R in HRT18 cells. A. RT-PCR displayed reduced mRNA expression level of Kiss-1R in HRT18$^{\text{Kiss-1R kd}}$ cells compared with control cells (HRT18^{wt} and HRT18^{pEF} cells). B. Quantitative real time PCR showed Kiss-1R mRNA volume of three repeats which was normalized against corresponding internal control (GAPDH). The expression of Kiss-1R decreased significantly in HRT18$^{\text{Kiss-1R kd}}$ cells compared with HRT18^{wt} (p= 0.0016) and HRT18^{pEF} cells (p= 0.0038) respectively. Asterisk represented p< 0.005. Original data is shown in Table 6 of Appendices.

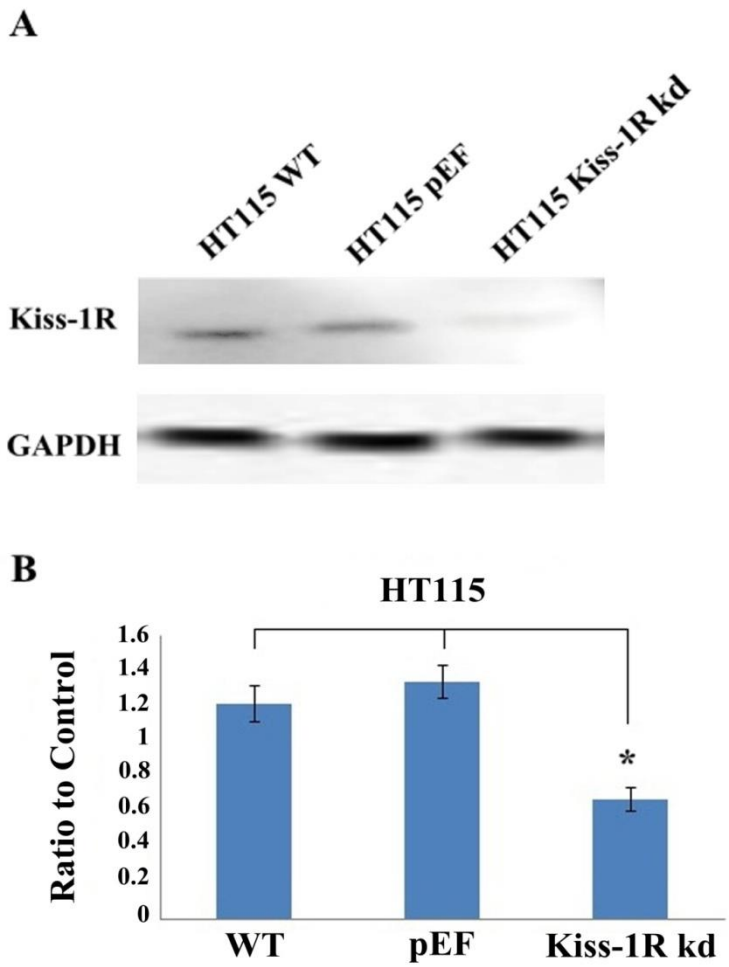

Figure 3.10. Confirmation of Kiss-1R knockdown in HT115 cells. A. Kiss-1R protein bands volume of three repeats which were normalized against corresponding internal control (GAPDH). B. The expression of Kiss-1R showed a significant decrease in $HRT18^{Kiss\text{-}1R\ kd}$ compared with that in $HT115^{wt}$ (p= 0.0013) and $HRT18^{pEF}$ (p= 0.0056) cells. Asterisk stood for $p< 0.05$. Original data is shown in Table 10 of Appendices.

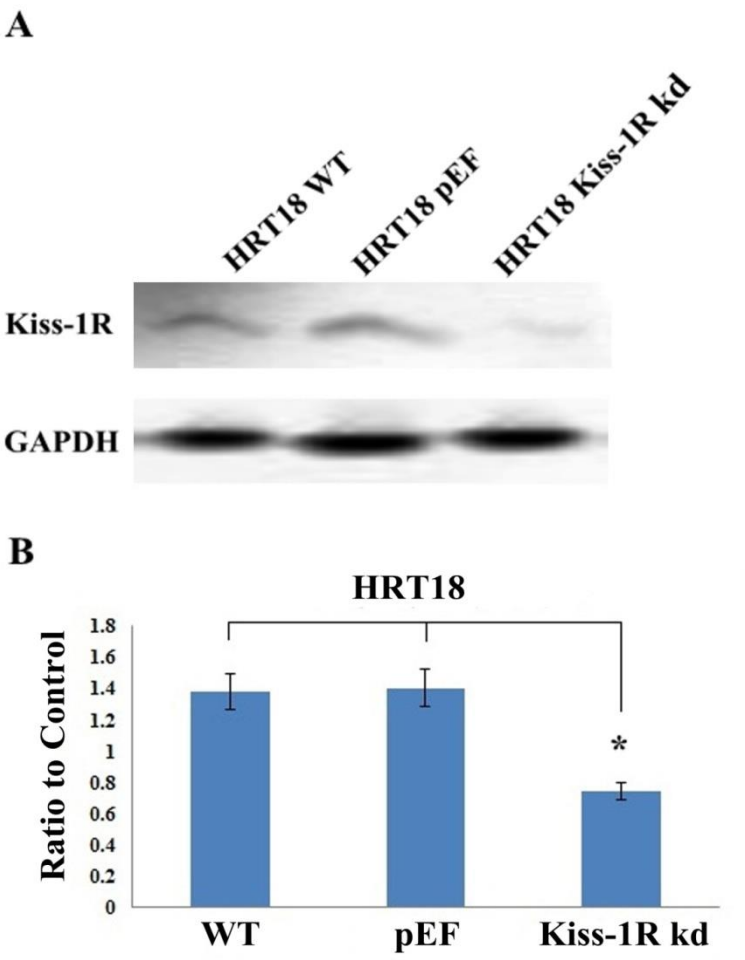

Figure 3.11. Confirmation of Kiss-1R knockdown in HRT18 cells. A. Kiss-1R protein bands volume {normalized against corresponding internal control (GAPDH)}. B. The expression of Kiss-1R showed a significant decrease in $HRT18^{Kiss\text{-}1R\ kd}$ cells compared with that in $HRT18^{wt}$ (p= 0.0011) and $HRT18^{pEF}$ (p= 0.001) cells. Asterisk stood for p< 0.05. Original data is shown in Table 8 of Appendices.

3.4 Discussion

Kiss-1 has been known as a novel metastasis suppressor due to its inhibitory role in lung metastases without affecting tumorigenicity [61]. Tissue distribution of Kiss-1 and its receptor are often concordant, like placenta, where both of their transcripts are high [48, 61, 69]. In further studies on the biological function of Kiss1 in metastasis, Ohtaki*et al* (2001) transferred Kiss-1R into Chinese hamster ovary (CHO) cells and then implanted the melanoma cells (B16-BL6) transfected with Kiss-1R into the nude mice in order to observe their lung metastases. The results revealed that Kiss-1 inhibited the migration and invasion of CHO cells and also reduced the ratio of lung metastases [48]. There have been a growing number of reports pointing to a metastasis suppressor role for Kiss-1 in solid cancers, such as breast cancer, gastric cancer, oesophageal carcinoma, pancreatic cancer, ovarian cancer, bladder cancer and prostate cancer. A relationship between reduced expression of Kiss-1 and poor clinical outcomes has been evident in most malignancies that have so far been investigated. However, few studies attempted to define the potential function of Kiss-1 and Kiss-1R involved in colorectal cancer and cancer metastasis. In the current study, four colorectal cancer cells (HT115, HRT18, RKO and Caco-2) were screened for the mRNA expression of Kiss-1 and Kiss-1R and were found positive, particularly in HT115 and HRT18 cells. We transfected anti-human Kiss-1 and Kiss-1R hammerhead ribozymes into two colorectal tumour cell lines (HT115 and HRT18), which had high expression of both Kiss-1 and Kiss-1R, so to create cell models with differential

expression of Kiss-1 and Kiss-1R, for further investigation of the biological impact of both molecules on colorectal cancer cells. HT115 and HRT18 cell lines with epithelial morphology have been established from highly invasive human colorectal carcinomas, which express high amounts of the tumor marker carcino-embryonic antigen (CEA). The sources of HT115 and HRT18 cells were from colon and rectum tissues respectively.

The expression of Kiss-1 and Kiss-1R knockdown verified at both mRNA and protein levels were successful. There were significant difference between the knockdown groups and the control groups (wild type and pEF) ($p< 0.05$). In addition, $HT115^{pEF}$ and $HRT18^{pEF}$ revealed similar expression of Kiss-1 and Kiss-1R with HT115 WT and HRT18 WT respectively at both transcript and protein levels ($p> 0.05$). For improving the efficiency of research and cutting cost, we decided to choose HT115 pEF and HRT18 pEF as the controls in the subsequent experiments. pEF control transfected cells should be a more convincing cell subline than wild type cells as controls once the similar expression levels between pEF cells and wild type cells have been verified. Subsequently, we used these stabilized transfected cell lines to deduce the role played by Kiss-1 and Kiss-1R on how they influence the function of colorectal cancer cells through *in vitro* function assays. These data are shown in the next chapter.

Chapter 4

Influence of targeting Kiss-1 and Kiss-1R on the proliferation, adhesion, invasion and migration of colorectal cancer cells

4.1 Introduction

Tumour metastasis remains the leading cause of cancer related mortality and morbidity, although diagnostic and therapeutic modalities in the treatment of cancer patients have been significantly developed. Tumour metastasis depends on the characteristics of cancer cells, which make themselves more effective in adapting the *in vivo* environments and in competing for resources with normal cells. These characteristics include proliferation, adhesion, invasion and migration. The liver is the most frequently visited organ by colorectal cancer cells. Many studies have reported that tropism of cancer cells to specific organs is regulated by the complexity of genetic alterations, likewise, the maintenance of cell stability lies in the activity of tumour suppressor genes, which can inhibit the proliferation of cells. Kiss-1 has been suggested to have an inhibitory effect on the migration of pancreatic cancer, ovarian cancer and prostate cancer cells and the invasion of breast cancer and prostate cancer cells [48, 50, 71, 95]. Kiss-1 has been reported to negatively regulate MMP-9 expression in ovarian tumour [96]. MMP-9 is known as one of the most important proteases related to tumour metastasis and is capable of degrading the primary structure of extracellular matrix and basement membrane (collagen, laminin, fibronectin). However, the influence of Kiss-1 and Kiss-1R on the function of colorectal cancer cells remains unknown. The expression of Kiss-1 and Kiss-1R knockdown in the colorectal cancer cell lines (HT115 and HRT18) was described in Chapter 3. The stably transfected cells were used in *in vitro* cell function assays,

which included growth, adhesion, invasion and migration assays in order to investigate if there were any changes in the function of these transfected cell lines through the effect of Kiss-1 and Kiss-1R knock down.

4.2 Materials and methods

4.2.1 Cell lines

In this study, HT115 and HRT18 colorectal cancer cells transfected with empty plasmid and the plasmids of Kiss-1 and Kiss-1R knockdown were used. The cells were maintained in DMEM media with 10% FBS, antibiotics and 0.5µg/ml blasticidin.

4.2.2 *In vitro* cell growth assay

Cells were seeded into 96-well plates at 2, 500 cells/well, which were cultured using normal media (10% foetal calf serum, 0.1% antibiotics). The cells were cultured in triplicate for 1, 3 and 5 days. After incubation the cells were fixed in 4% formalin and stained by 0.5% crystal violet (w/v). The crystal violet stain was then extracted using 10% (v/v) acetic acid, and the absorbance was determined using a spectrophotometer (Bio-Tek, ELx800) at a wavelength of 540nm.

4.2.3 *In vitro* cell adhesion assay

A 96-well plate was precoated with5µg Matrigel (Collaborative Research Products, Bedford, Massachusetts, USA) and allowed to air dry. Following rehydration using serum free media, 40,000 cells were seeded into each well. After 40 minutes of incubation, non-adherent cells were washed off using BSS. The adherent cells were then fixed with 4% formalin and stained using 0.5% crystal violet. The number of adherent cells was counted under a microscope.

4.2.4 *In vitro* invasion assay

Transwell inserts (with 8µm pore) were precoated with 50µg Matrigel and air dried. Following rehydration, 40,000 cells were seeded into each insert. After incubation for three days, cells which had invaded through the matrix and adhered to the other side of the insert were fixed in 4% formalin, and stained with 0.5% (weight/volume) crystal violet. The number of invaded cells was then counted under a microscope.

4.2.5 *In vitro* Wounding assay

Cells were seeded into a 24-well plate at a density of 200,000 per well and allowed to form a monolayer of cells. The monolayer of cells was then scratched to create a wound. Migration of the cells at wounding edges was monitored over a period up to 18 hours. Optimas 6.0 motion analysis (Meyer Instruments, Houston, Texas) was used to track the leading edge of the cells to measure the distance of the migration.

4.2.6 Electric cell-substrate impedance sensing (ECIS)

The ECIS system (Ztheta, Applied Biophysics Inc., USA) was used to quantify cell migration as previously reported (Jiang *et al.,* 2008) and 96W1E arrays were used in this study. Cells (HT115 pEF, HT115 Kiss-1 knockdown and HT115 Kiss-1R knockdown) were prepared for six groups and seeded at 40,000 cells per well in 200µl of DMEM medium alone or medium supplemented with 200nM ERK (FR180204) small inhibitor (MERCK, Germany), Kisspeptin-10 (Tocris Bioscience, Bristol, UK) and Kisspeptin-234 (Tocris Bioscience, Bristol, UK), which is a Kisspeptin-10/Kiss-1R antagonist, which belongs to Kisspeptin-10 analog (Tocris Bioscience, Bristol, UK). The details of treatment for each group are as follows: group 1 was treated with serum free; group 2 was treated with Kisspeptin-10; group 3 was treated with Kisspeptin-234; group 4 was treated with ERK inhibitor; group 5 was treated with ERK inhibitor+ Kisspeptin-10; group 6 was treated with ERK inhibitor+ Kisspeptin-234. The resistance was recorded for 8 hours after wounding and the data was analyzed using an ECIS-9600 software package.

4.2.7 *In vivo* tumour model

Female CD-1 mice aged 4-6 weeks old were used for this study. All the mice were kept in filter-topped isolation cages and all the procedures were carried out in a class-II cabinet. After mice were settled for a week in the designated laboratories, HT115 cells (control or Kiss-1 knockdown cells) were injected subcutaneously at a

volume of 100µl which contained Matrigel at final concentration of 2.5mg/ml The mice were then carefully monitored twice weekly by measuring body weight and tumour size (using a digital caliper), and looking for any side effects.

The volume of tumours was calculated by using the following formula:

$$\text{tumour volume } (mm^3) = 0.512 \times (\text{Width} \times 2) \times \text{length}$$

4.3 Results

4.3.1 Effect of Kiss-1 and Kiss-1R knockdown on HT115 cancer cell growth

There was a steady increase in cell growth of both Kiss-1 and Kiss-1R knockdown HT115 cells compared with HT115 pEF cell line (Figure 4.1 A). In particular, the growth rate of the Kiss-1 knockdown cells (1223.32 ± 356.59) and Kiss-1R knockdown cells (1138.22 ± 213.46) increased gradually in comparison with the control group (HT115 pEF 829.611 ± 265.92) at the fifth day, however the value did not reached the level of statistical significance ($p > 0.05$).

4.3.2 Effect of Kiss-1 and Kiss-1R knockdown on HRT18 cancer cell growth

Similarly to that seen with HT115 cell lines, both Kiss-1 and Kiss-1R knockdown showed a relatively gentle increase in growth compared with the control group in the HRT18 cell lines (Figure 4.1 B). The cell growth was moderately increased in $HRT18^{Kiss1kd}$ (728.58 ± 159.50) and $HRT18^{Kiss1rkd}$ (678.99 ± 124.27) in comparison

with the control group (HRT18 pEF: 570.13 ± 47.40), while the value did not show a statistically significant ($p > 0.05$).

4.3.3 Effect of Kiss-1 and Kiss-1R knockdown on HT115 cancer cell adhesion

HT115 cells were further investigated for their adhesive properties in an *in vitro* Matrigel adhesion assay. Compared with the control group (HT115 pEF35 ±7.80), both Kiss-1 and Kiss-1R knockdown cells did not demonstrate a significant change (32 ±9.02 and 41.5 ±12.66 respectively) (Figure 4.2).

4.3.4 Effect of Kiss-1 and Kiss-1R knockdown on HRT18 cancer cell adhesion

Likewise, HRT18 cells were investigated for their adhesive properties in an *in vitro* Matrigel adhesion assay. Similarly, there was mild fluctuation between the cells with Kiss-1 knockdown (28.67 ±10.91) and Kiss-1R knockdown (43.5 ±13.58) and the HRT18 pEF cells (26 ±7.89) (Figure 4.3).

4.3.5 Influence of Kiss-1 and Kiss-1R knockdown on HT115 cell invasion

Figure 4.4 showed that the cells with Kiss-1 knockdown (55.91 ±2.75) significantly increased in invasiveness compared with HT115 pEF cells (27 ± 3.16) ($p = 0.015$). While HT115 Kiss-1R knock down cells did not demonstrate a significant difference with the control (Figure 4.4).

4.3.6 Influence of Kiss-1 and Kiss-1R knockdown on HRT18 cell invasion

Similarly, there was an increase of invasion in the Kiss-1 knockdown HRT18 cells (59.13 ± 6.34) compared with HRT18 pEF cells (39.75 ± 6.90) from Figure 4.5 ($p = 0.0077$). There was no statistical significance between the HRT18 Kiss-1R knockdown and HRT18 pEF cells ($p < 0.05$).

4.3.7 Effect of Kiss-1 and Kiss-1R knockdown on the motility of HT115 cells

To analyse the motility of HT115 cells, a scratch wounding assay was employed. After 2 hours the cells with Kiss-1 knockdown showed a significant increase in the pace of migration compared with the control group with the difference appearing to reach maximum (59.16 ± 6.52) at the fifth hour (Figure 4.6) ($p = 0.0094$). However the difference of the migration of HT115 Kiss-1 knockdown and HT115 pEF cells did not show a statistical significance ($p > 0.05$).

4.3.8 Effect of Kiss-1 and Kiss-1R knockdown on the motility of HRT18 cells

A similar influence of Kiss-1 knockdown on HRT18 cells was seen which revealed significant increase in motility compared with the control group, consistently from 3^{td} hour to 5^{th} hour. At the end of the test, the cells with kiss-1 knockdown and pEF reached 59.18 ± 6.25 and 40.62 ± 7.59 respectively. There was a significant difference between HRT18 Kiss-1 knockdown and HRT18 pEF cells ($p = 0.001289$), while

HRT18 Kiss-1R rib (43.95 ±6.44) did not show a significant difference with HRT18 pEF (Figure 4.7).

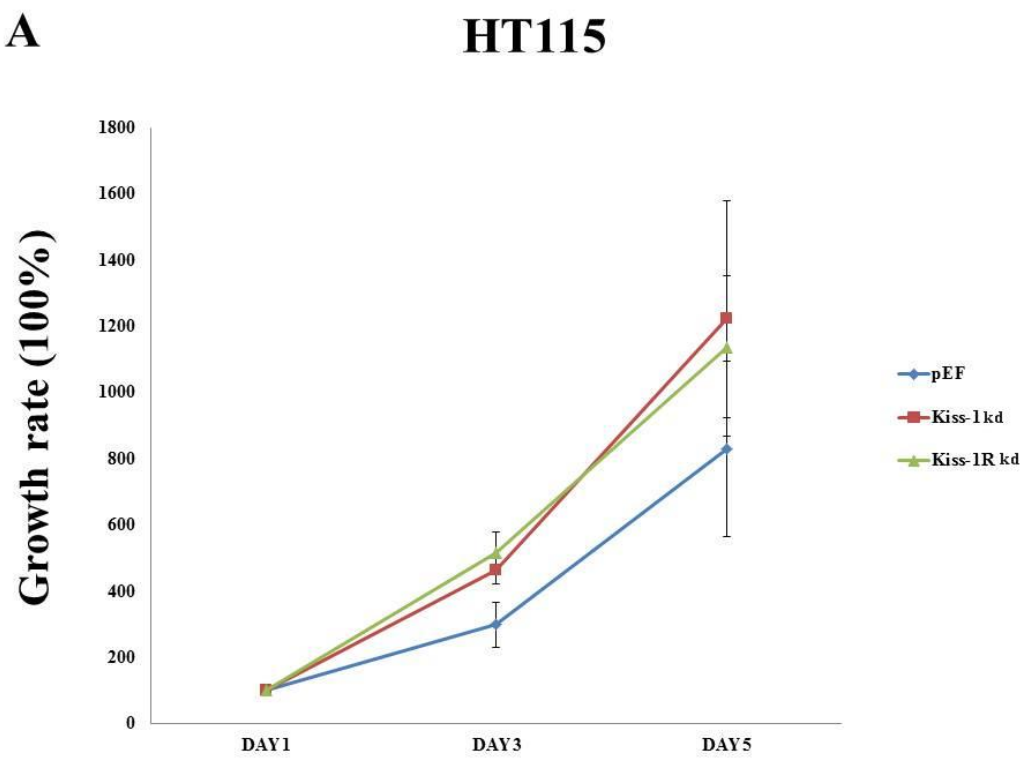

HT115 pEF (mean ± SD) N=6	HT115 Kiss-1 kd (mean ± SD) N=6	HT115 Kiss-1R kd (mean ± SD) N=6
829.611 ± 265.92	1223.32 ± 356.59	1138.22 ± 213.46

Figure 4.1.A.HT115 cells with knockdown of Kiss-1 and Kiss-1Rconsistently increased growth compared with HT115 pEF. After 5 days incubation there was a slight increase in the $HT115^{kiss\text{-}1kd}$ cells (1223.32 ± 356.59) and $HT115^{kiss\text{-}1rkd}$ cells (1138.22 ± 213.46) compared with the control $HT115^{pEF}$ (829.611 ± 265.92). Data shown is representative of 3 repeats of experiment. Each experiment has 6 independent repeats. Error bars represent standard deviation. The absorbance of Day 1 was used as a baseline to normalise the data. Original data is shown in Table 9 of Appendices.

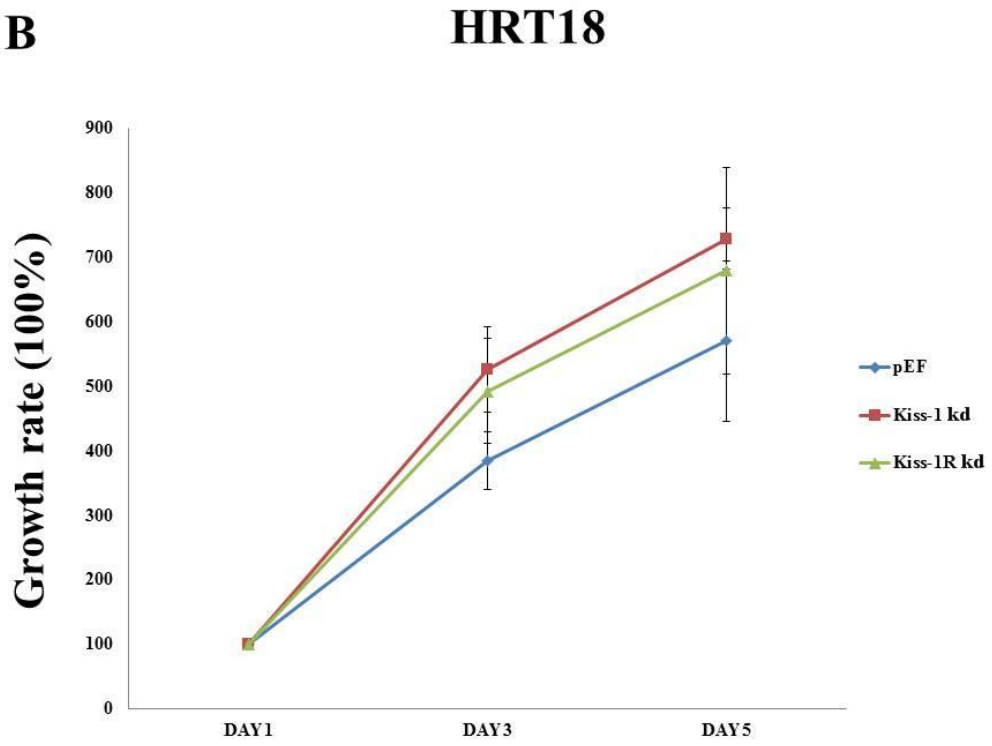

HRT18 pEF (mean ± SD) N=6	HRT18 Kiss-1 kd (mean ± SD) N=6	HRT18 Kiss-1R kd (mean ± SD) N=6
570.13 ± 47.40	728.58 ± 159.50	678.99 ± 124.27

Figure 4.1.B. HRT18 cells with Knockdown of Kiss-1 and Kiss-1R increased growth compared with HRT18pEF. After 5 days incubation there was a slight increase in the HRT18$^{kiss\text{-}1kd}$cells and HRT18$^{kiss\text{-}1rkd}$ cells compared with the control HRT18^{pEF}. Data shown is representative of 3 repeats of experiment. Each experiment has 6 independent repeats. Error bars represent standard deviation. The absorbance of Day 1 was used as a baseline to normalise the data. Original data is shown in Table 10 of Appendices.

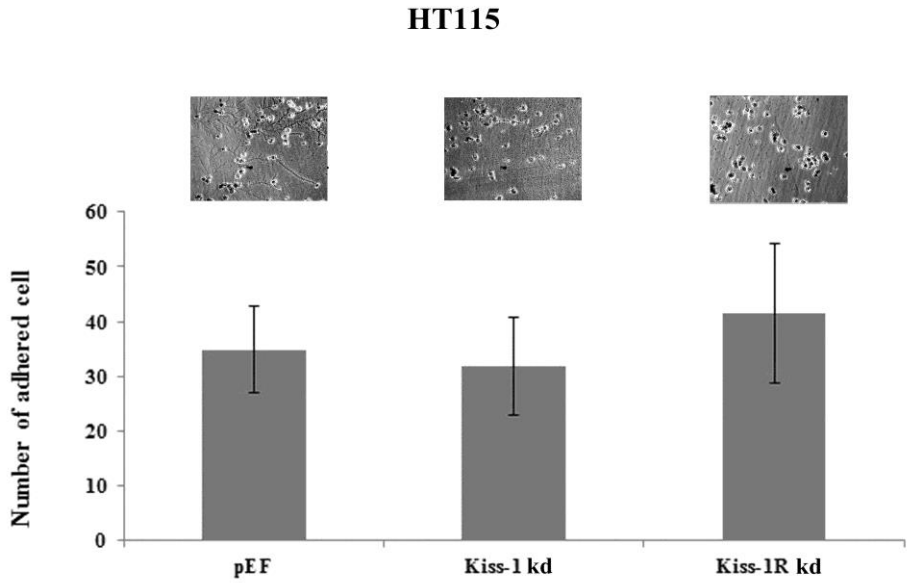

HT115 pEF (mean ± SD) N=6	HT115 Kiss-1 kd (mean ± SD) N=6	HT115 Kiss-1R kd (mean ± SD) N=6
35 ±7.80	32 ±9.02	41.5 ±12.66

Figure 4.2. Knockdown of Kiss-1 and Kiss-1R in HT115 cells did not display significantly different adhesive ability compared with the control group. Three Representative images of cells following staining are displayed in the top. The cells on an artificial Matrigel basement membrane, showed a slight decrease in $HT115^{kiss\text{-}1kd}$ cells compared with the control $HT115^{pEF}$ after 40 minutes incubation. While there was a gentle increase in $HT115^{kiss\text{-}1rkd}$ cells compared with the control $HT115^{pEF}$ cells. Data shown is representative of 3 repeats of experiment. Each experiment has 6 independent repeats. Error bars represent standard deviation. Original data is shown in Table 11 of Appendices.

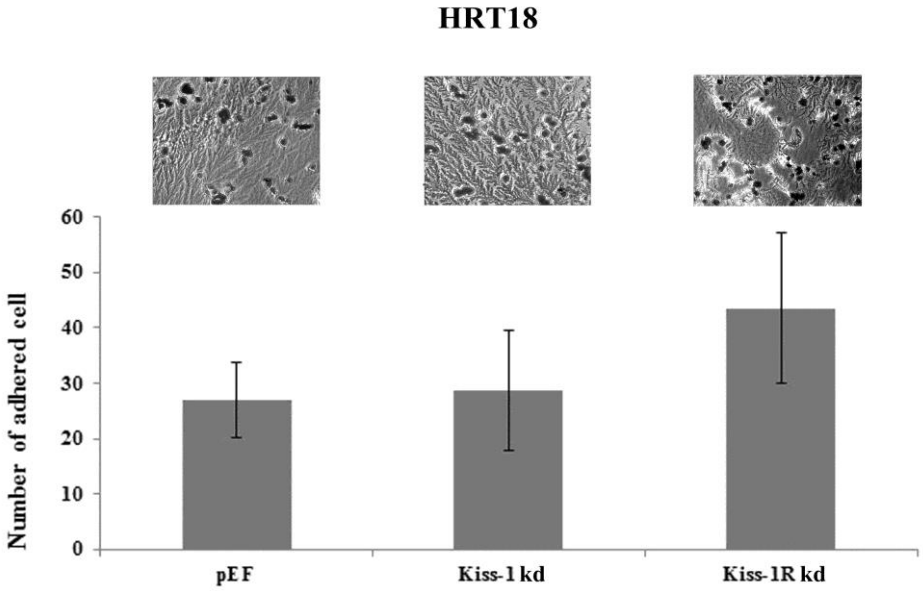

HRT18 pEF (mean ± SD) N=6	HRT18 Kiss-1 kd (mean ± SD) N=6	HRT18 Kiss-1R kd (mean ± SD) N=6
26 ±7.89	28.67 ±10.91	43.5 ±13.58

Figure 4.3. Knockdown of Kiss-1 and Kiss-1R in HRT18 cells did not display significantly different adhesive ability compared with the control group. Three representative images of cells following staining are displayed in the top. The cells on an artificial Matrigel basement membrane, showed a gentle increase in $HRT18^{kiss\text{-}1kd}$ and $HRT18^{kiss\text{-}1rkd}$ cells compared with the control $HRT18^{pEF}$ after 40 minutes incubation. Data shown is representative of 3 repeats of experiment. Each experiment has 6 independent repeats. Error bars represent standard deviation. Original data is shown in Table 12 of Appendices.

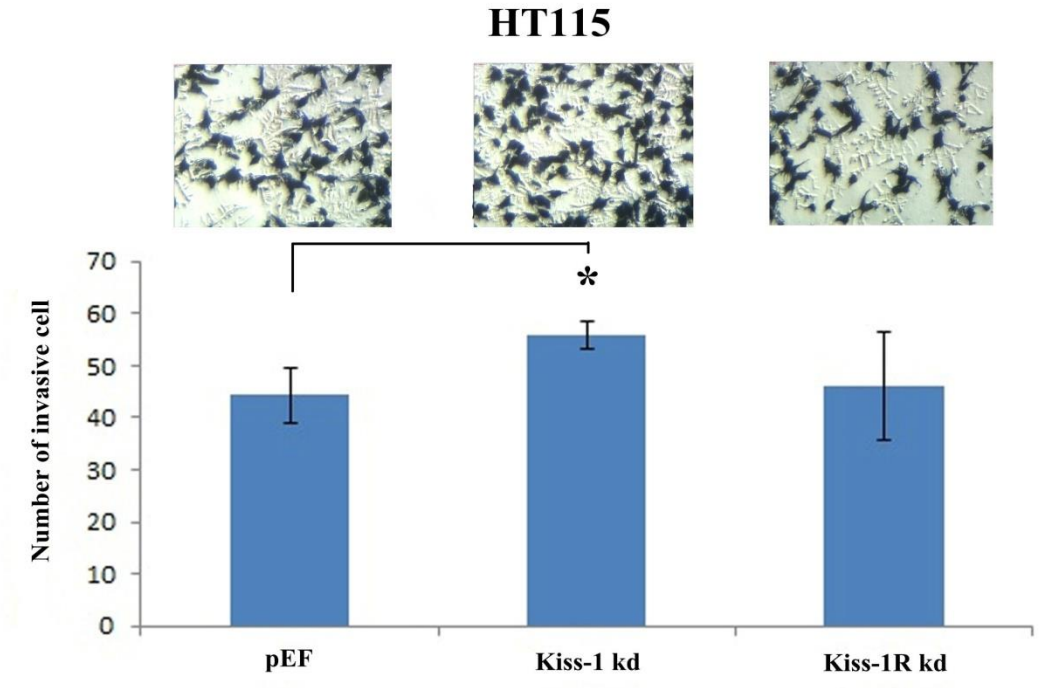

HT115 pEF (mean ± SD) N=4	HT115 Kiss-1 kd (mean ± SD) N=4	HT115 Kiss-1R kd (mean ± SD) N=4
44.25±5.38	55.91±2.75	46±10.36

Figure 4.4. The influence of Kiss-1 and Kiss-1R knockdown on the invasive capability of HT115 cells. Three representative images of cells following staining are displayed in the top. There was a marked increase of cell invasion in $HT115^{Kiss\text{-}1kd}$ compared with that of the control ($HT115^{pEF}$) after 3 day incubation of the cells on an artificial Matrigel basement membrane. Data shown is representative of 3 repeats of experiment. Each experiment has 4 independent repeats. Error bars represent standard deviation.*represents $p< 0.05$ analyzed by T-test ($HT115^{Kiss\text{-}1kd}$ vs $HT115^{pEF}$: $p= 0.015$). Original data is shown in Table 13 of Appendices.

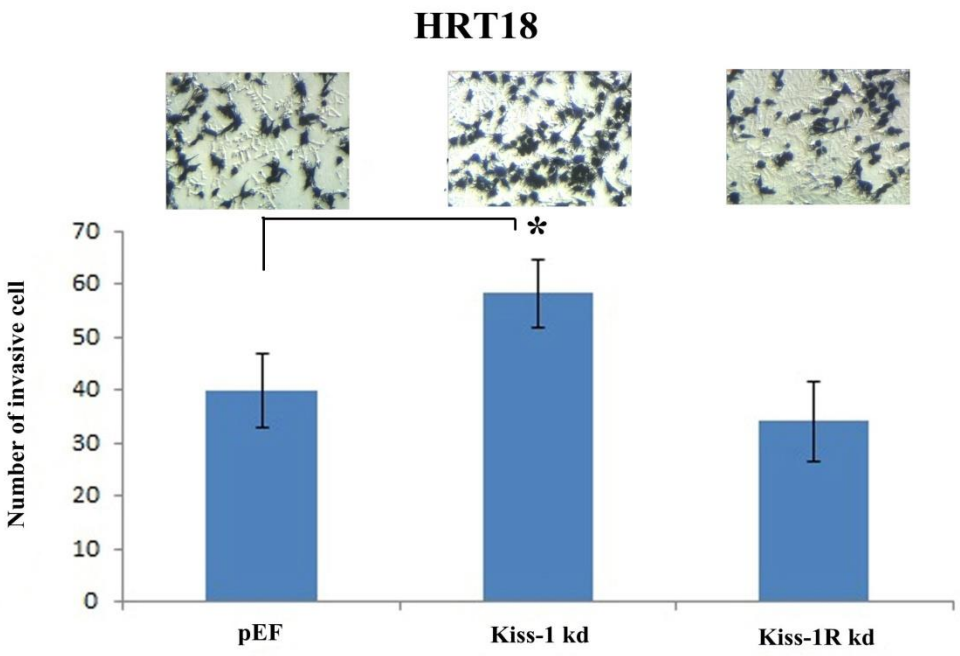

HRT18 pEF (mean ± SD) N=4	HRT18 Kiss-1 kd (mean ± SD) N=4	HRT18 Kiss-1R kd (mean ± SD) N=4
39.75 ±6.90	59.13 ± 6.34	34 ±7.03

Figure 4.5. The effects of Kiss-1 and Kiss-1R knockdown on the invasive capability of HRT18 cells. Three representative images of cells following staining are shown in the top. There was a significant increase of cell invasion in $HRT18^{Kiss\text{-}1kd}$cells compared with the control $HRT18^{pEF}$ after 3 day incubation of the cells on an artificial Matrigel basement membrane. Data shown is representative of 3 repeats of experiment. Each experiment has 4 independent repeats. Error bars represent standard deviation.*stands for $p< 0.05$, analysed by T-test ($HRT18^{Kiss\text{-}1kd}$ vs $HTRT18^{pEF}$: $p= 0.0077$). Original data is shown in Table 14 of Appendices.

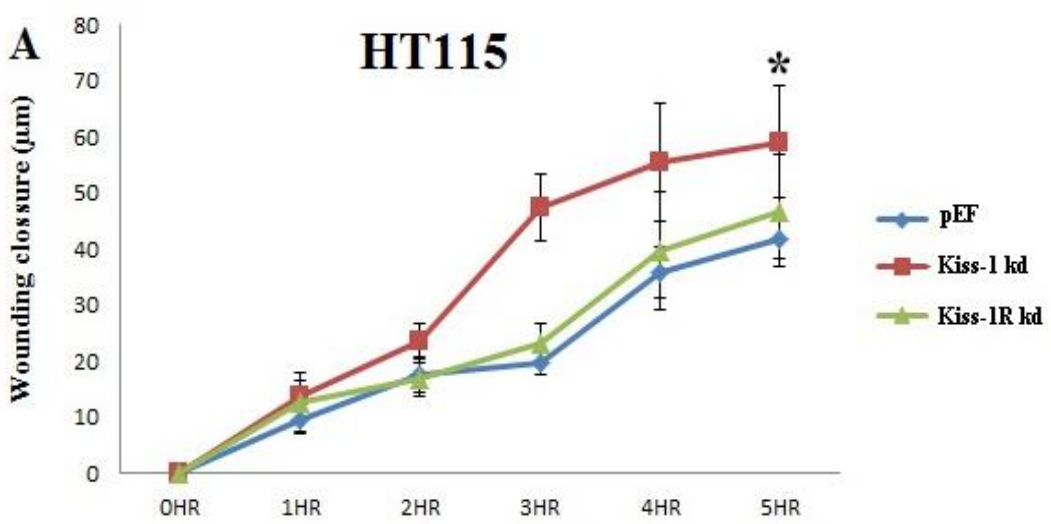

HT115 pEF (mean ±SD)	HT115Kiss-1 kd (mean ± SD)	HT115 Kiss-1R kd (mean ± SD)
41.70 ± 3.98	59.16 ± 10.54	46.87 ±9.89

Figure 4.6. Knockdown of Kiss-1 had a discernible effect on the migration of HT115 cells. After 2 hours the significant difference in cell motility of $HT115^{kiss\text{-}1kd}$ was visualized compared with the control $HT115^{pEF}$. Data shown is representative of 3 repeats of experiment. Error bars represent standard deviation.*represents $p< 0.05$, analyzed by T-test ($HT115^{Kiss\text{-}1kd}$ vs $HT115^{pEF}$: $p= 0.0094$). Original data is shown in Table 15 of Appendices.

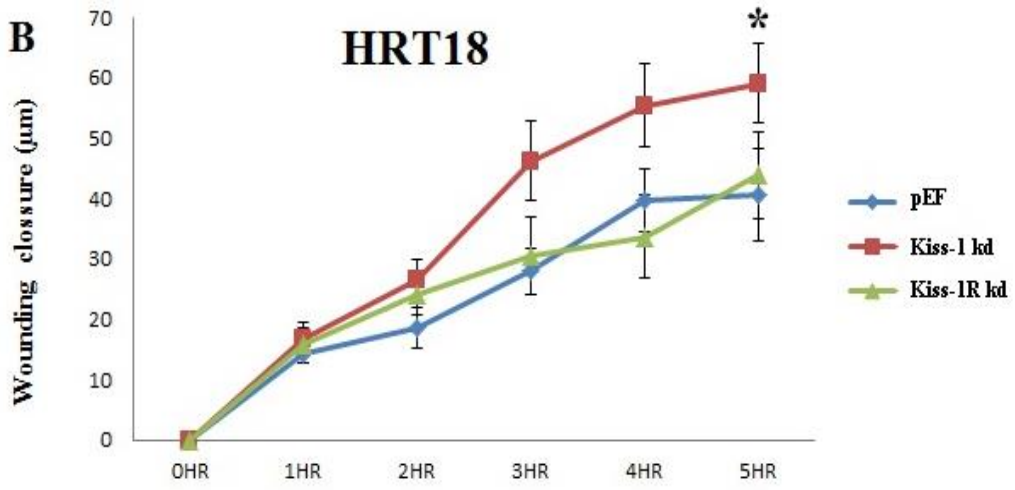

HRT18 pEF (mean ± SD) N=6	HRT18 Kiss-1 kd (mean ± SD) N=6	HRT18 Kiss-1R kd (mean ± SD) N=6
40.62 ±7.59	59.18 ±6.52	43.95 ±6.44

Figure 4.7. Knockdown of Kiss-1 had a marked effect on the migration of HRT18 cells. There was a consistent difference in cell motility of $HRT18^{kiss\text{-}1kd}$ cells compared with the control$HRT18^{pEF}$ from 3rd hour to 5th hour. Data shown is representative of 3 repeats of experiment. Error bars represent standard deviation.* stands for $p< 0.05$, ***$p< 0.001$ analyzed by T-test ($HRT18^{Kiss\text{-}1kd}$ vs $HRT18^{pEF}$ $p=$ 0.001289). Original data is shown in Table 16 of Appendices.

4.3.9 Effect of Kiss-1 and Kiss-1R knockdown on the motility of cancer cells, ECIS based analysis

Figure 4.8 demonstrates that HT115 Kiss-1 knockdown cells treated with Kisspeptin-10 had a significant decrease in motility compared with the control (no treatment) (p= 0.0205), while there was no significant difference between control and the Kiss-1R knockdown cells. In contrast, neither Kiss-1 knockdown or Kiss-1R knockdown cells treated with Kisspeptin-234 showed a difference in comparison with the control groups (no treatment) (p> 0.05) (Figure 4.9). From Figure 4.10, it can be easily seen that the adherence of Kiss-1 knockdown cells treated with ERK inhibitor significantly decreased compared with that of the control group (no treatment) after wounding (p= 0.0397). There was a slight decrease in the Kiss-1R knockdown cells treated with ERK inhibitor compared with the untreated cells, but the difference did not reach the significant level (p> 0.05). A similar situation was also observed in the comparison between the control group (no treatment) and the cells treated with ERK inhibitor+ Kisspeptin-234 (Figure 4.12). What is more, by contrast to the groups treated with ERK inhibitor and ERK inhibitor+ Kisspeptin-234, there were more striking links between the Kiss-1 knockdown cells treated with ERK inhibitor+ Kisspeptin-10 and its control (no treatment) (p= 0.0164) (Figure 4.11).

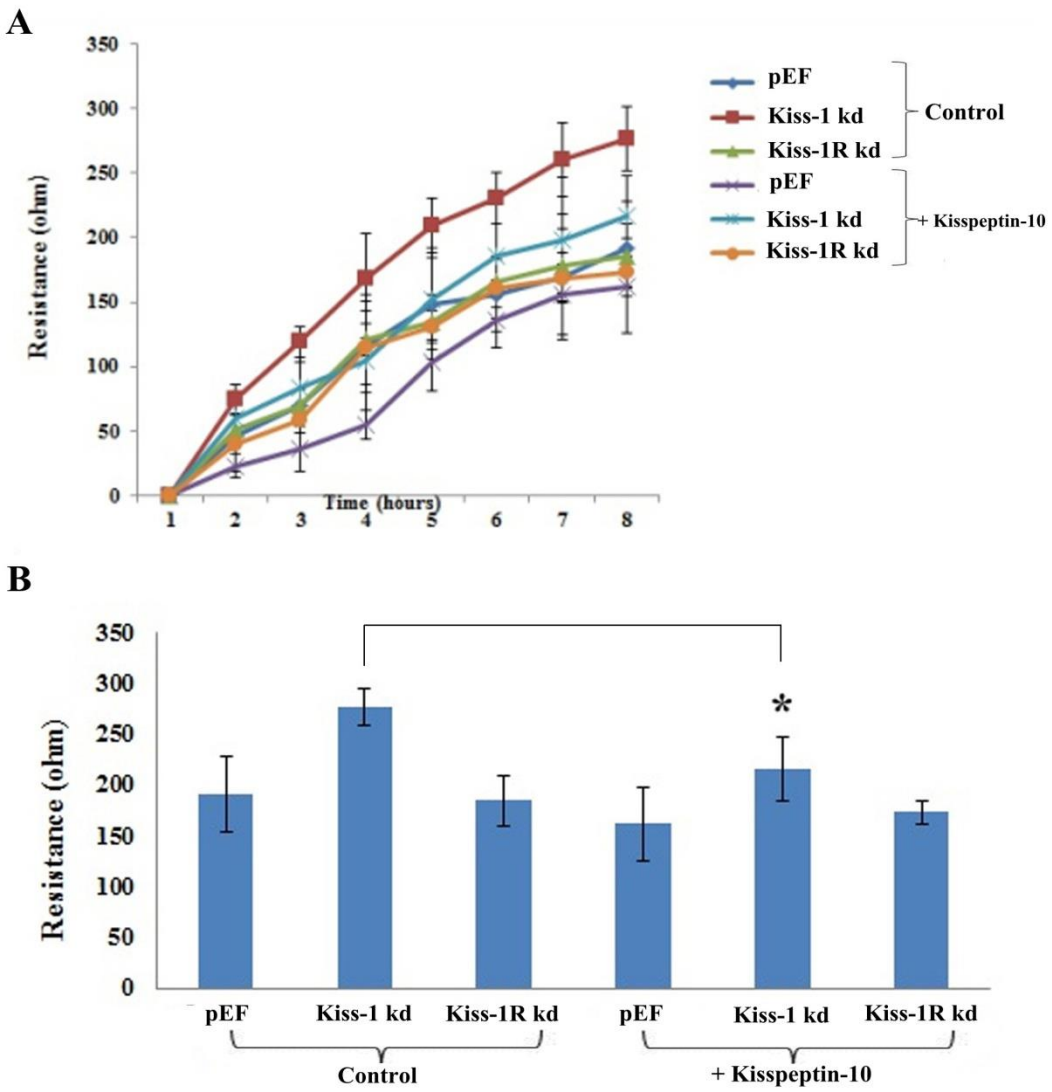

Figure 4.8.A and B. The effect of Kiss-1 and Kiss-1R knockdown on the migration ability of HT115 cells treated with Kisspeptin-10 compared with control group (serum no treatment). A. ECIS traces (mean of 4 sets) of cell migration of cells in two groups of experiments, namely, serum free and Kisspeptin-10, during an 8 hour experiment, following electric wounding. B. Overall changes of resistance on the eighth hour *p< 0.05vs the respective control group at the specific time point. Original data is shown in Table 17 of Appendices.

C

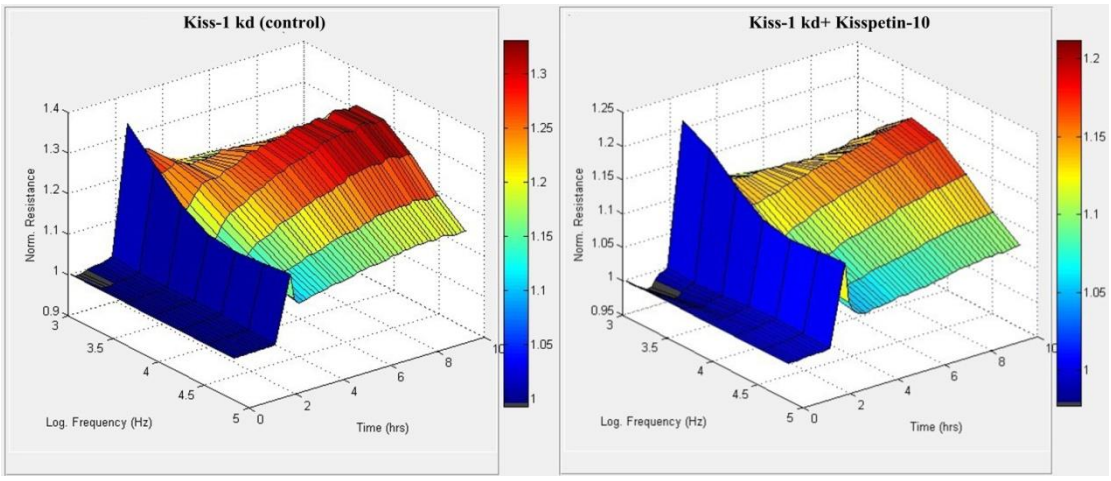

Figure 4.8.C. The effect of Kiss-1 knockdown on the migration ability of HT115 cells treated with Kisspeptin-10 compared with control group (no treatment). Left: HT115 kiss-1 knockdown cells control; right: the same cells treated with kisspeptin-10. The decreased migration of cells treated with Kisspeptin-10 compared with the control (no treatment) using ECIS was shown as 3D model. Shown are changes of normalized resistance measured at different frequencies over a period up to 8 hours.

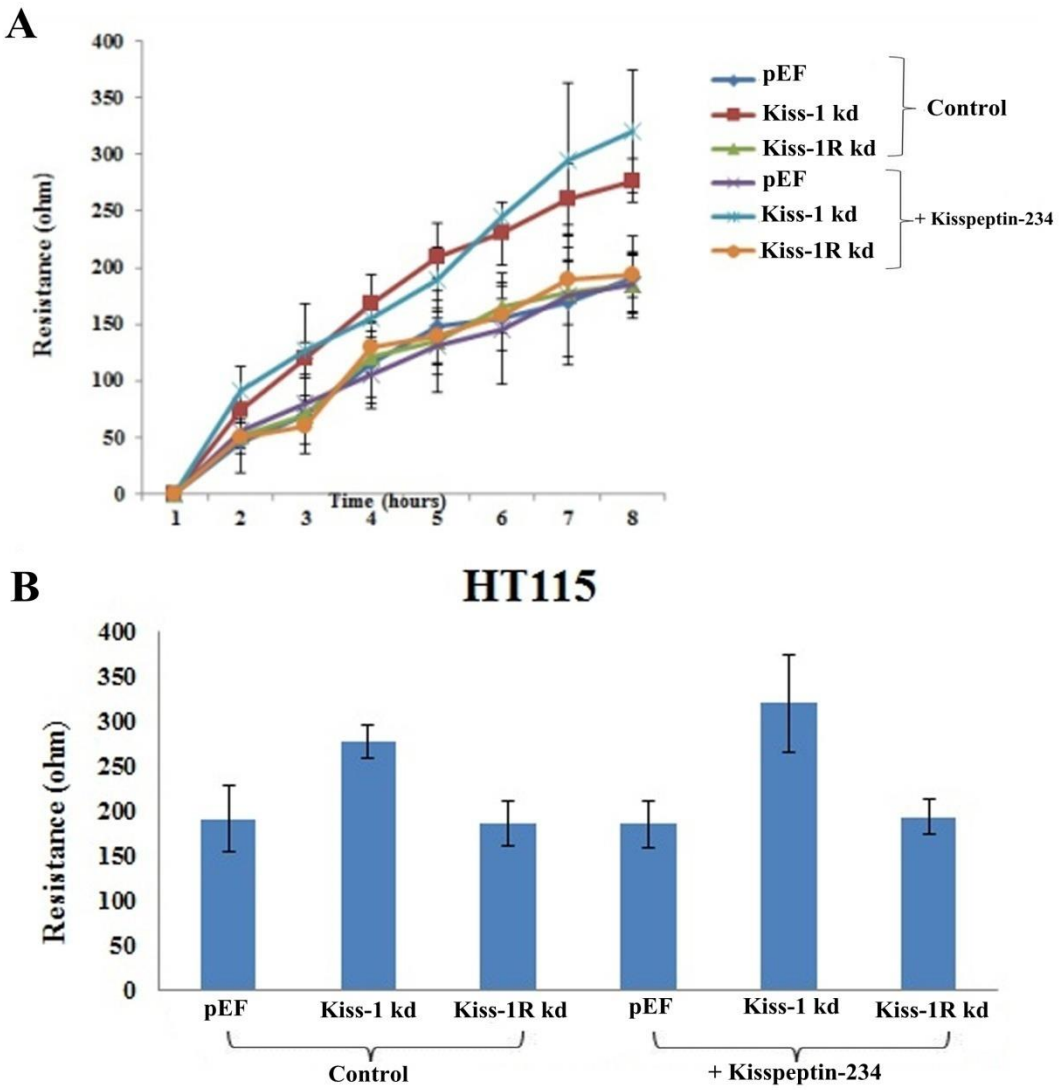

Figure 4.9. The effect of Kiss-1 and Kiss-1R knockdown on the migration ability of HT115 cells treated with Kisspeptin-234 compared with control group (no treatment). A. Cells in two different experimental settings (no treatment and Kisspeptin-234) during 8 hours after wounding. B. Overall changes of resistance on the eighth hour. Original data is shown in Table 18 of Appendices.

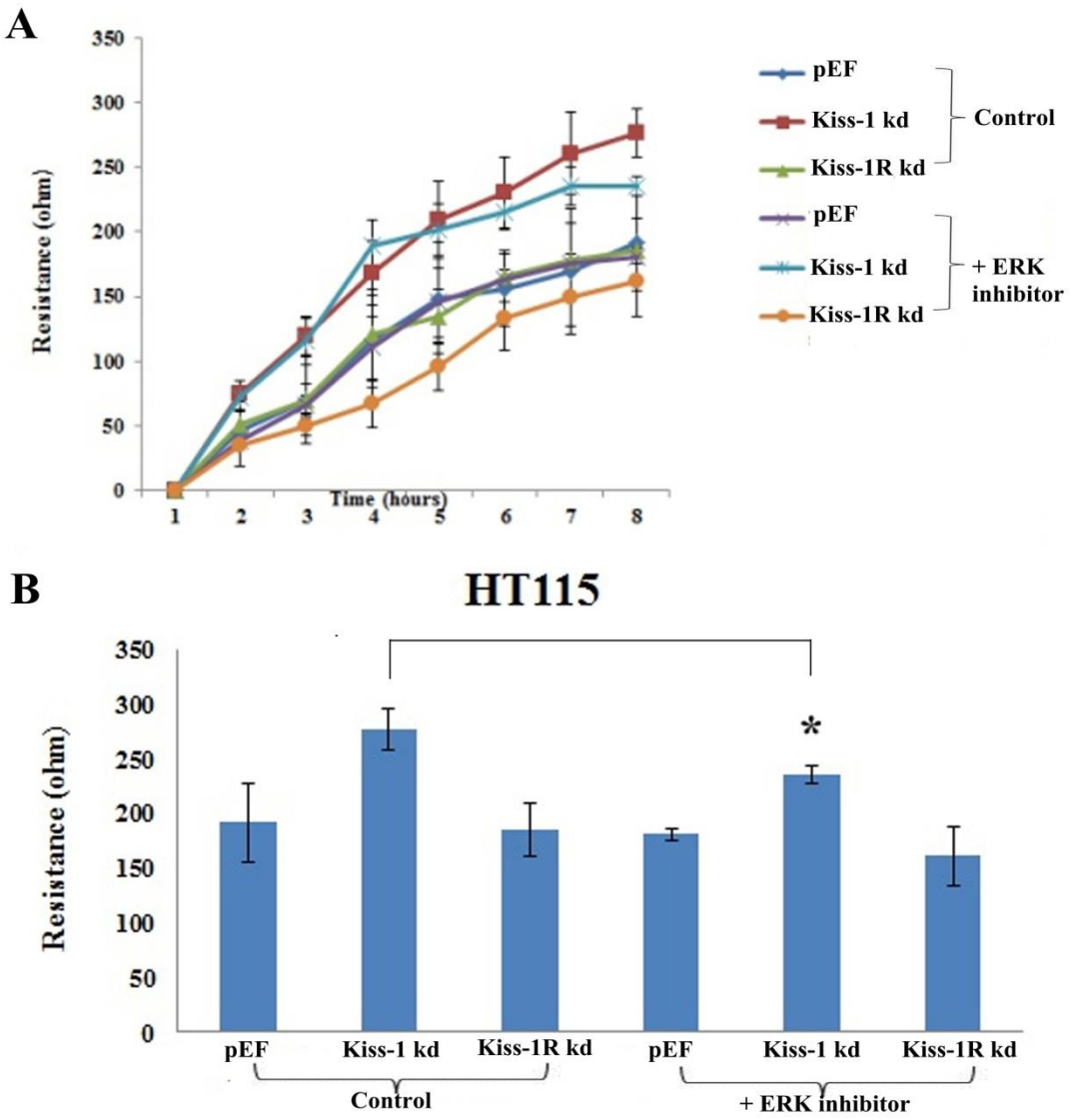

Figure 4.10.A and B. The effect of Kiss-1 and Kiss-1R knockdown on the migration ability of HT115 cells treated with ERK inhibitor compared with control group (no treatment). A. The mean trace of the cells in two groups of experiments (no treatment and ERK inhibitor) during 8 hours after wounding. B. Overall changes of resistance on the eighth hour. *p< 0.05 vs the respective control group at the specific time point. Original data is shown in Table 19 of Appendices.

C

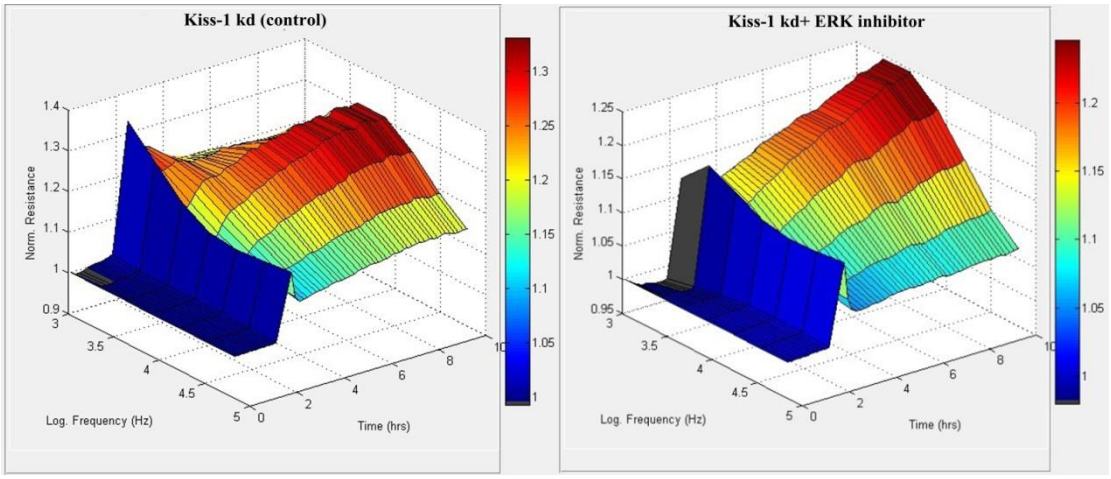

Figure 4.10.C. The effect of Kiss-1 knockdown on the migration ability of HT115 cells treated with ERK inhibitor compared with control group (no treatment), shown in 3D. Shown are changes of normalized resistance measured at different frequencies over a period up to 8 hours.

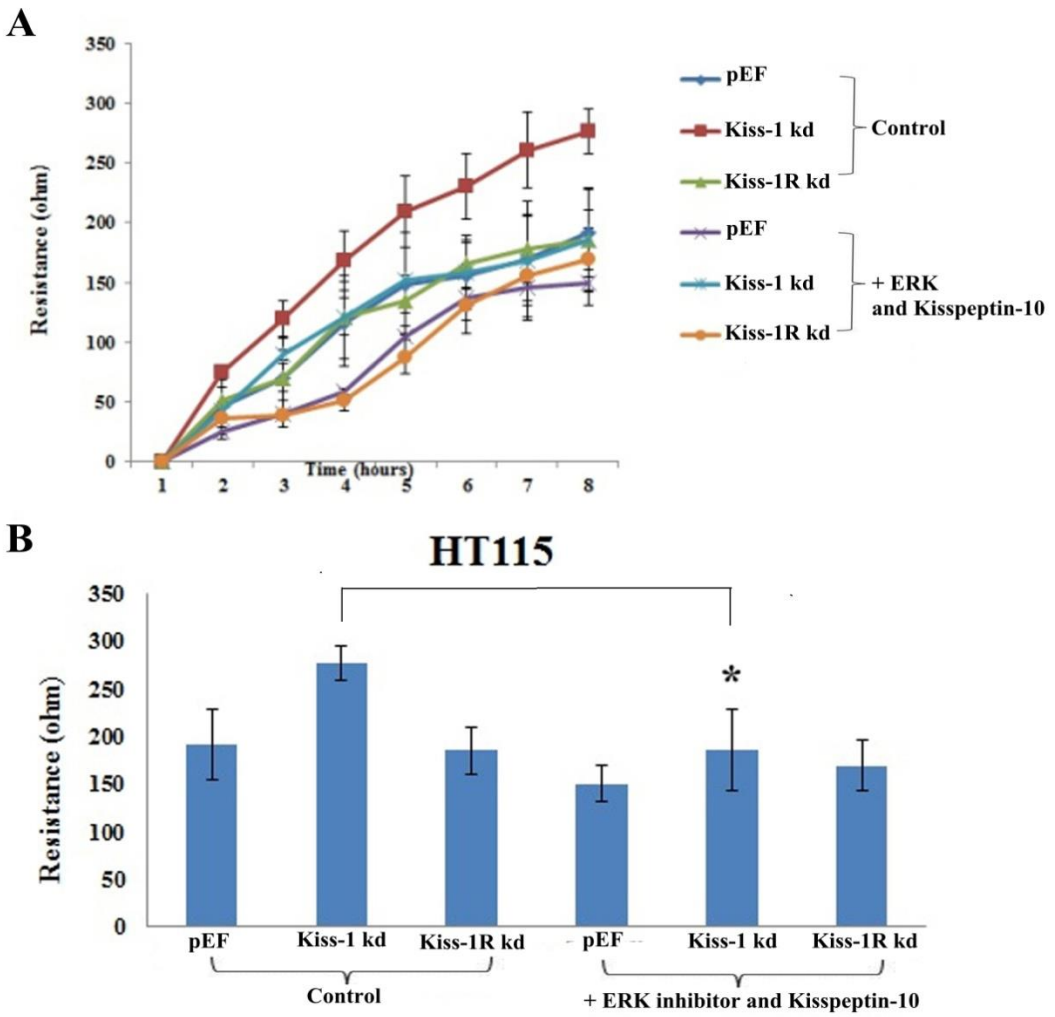

Figure 4.11.A and B. The effect of Kiss-1 and Kiss-1R knockdown on the migration ability of HT115 cells treated with ERK inhibitor and Kisspeptin-10 compared with control group (no treatment). A. Cell responses after wounding (no treatment and ERK inhibitor+ Kisspeptin-10) during 8 hours after wounding. B. Overall changes of resistance on the eighth hour *p< 0.05 vs the respective control group at the specific time point. Original data is shown in Table 20 of Appendices.

C

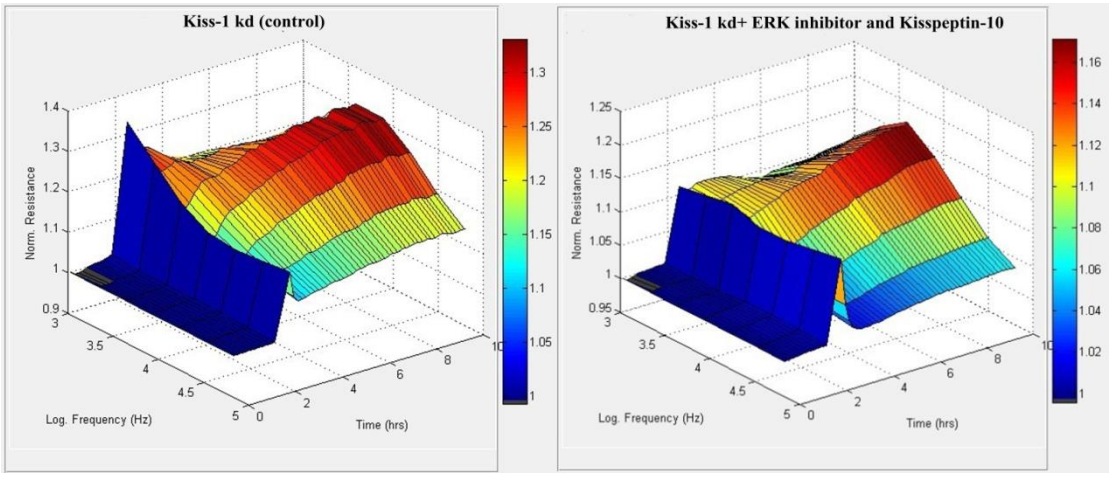

Figure 4.11.C. The effect of Kiss-1 knockdown on the migration ability of HT115 cells treated with ERK inhibitor+ Kisspeptin-10 compared with control group (no treatment), shown in 3D. Shown are changes of normalized resistance measured at different frequencies over a period up to 8 hours.

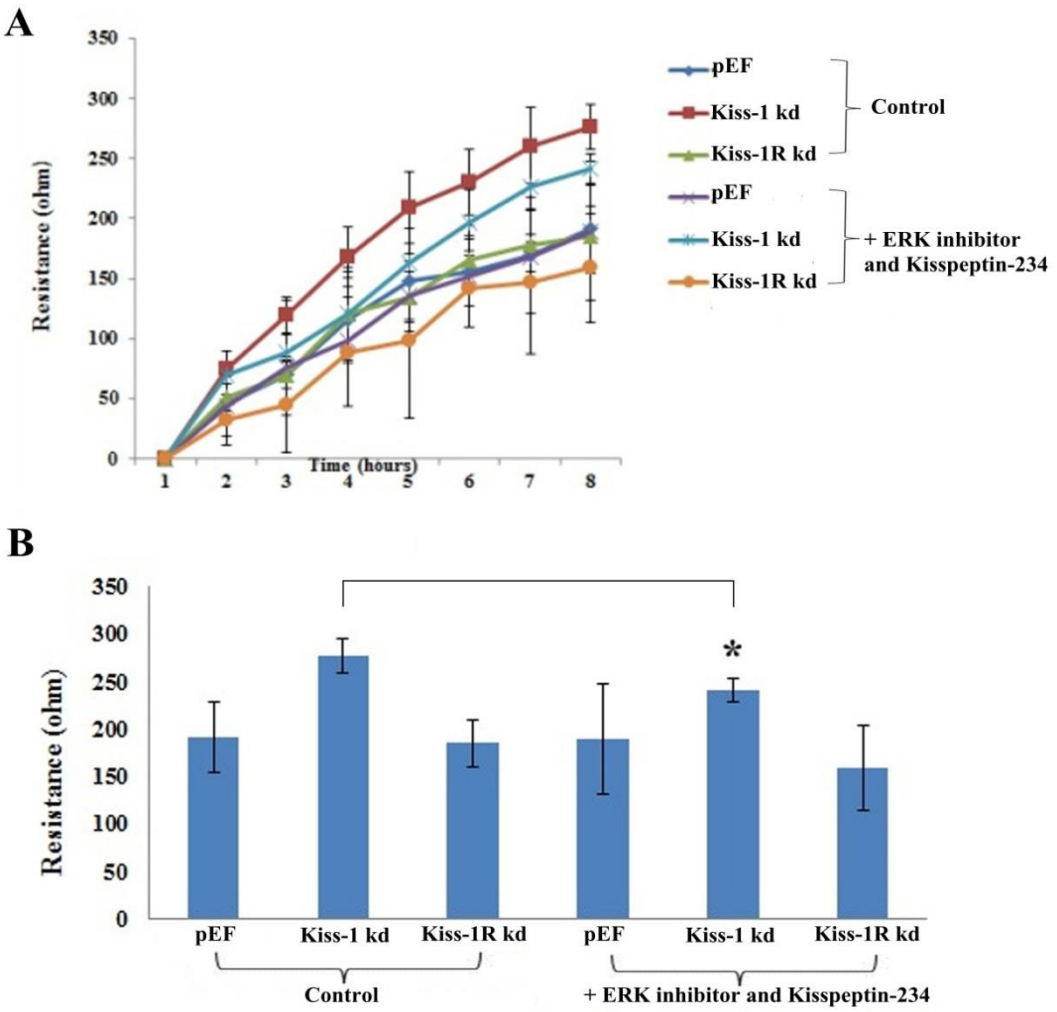

Figure 4.12.A and B. The effect of Kiss-1 and Kiss-1R knockdown on the migration ability of HT115 cells treated with ERK inhibitor+ Kisspeptin-234 compared with control group (no treatment). A. Cells responses in different experimental settings, namely serum free and ERK inhibitor+ Kisspeptin-234, over an 8 hours period after wounding. B. Overall changes of resistance on the eighth hour *p< 0.05 vs the respective control group at the specific time point. Original data is shown in Table 21 of Appendices.

C

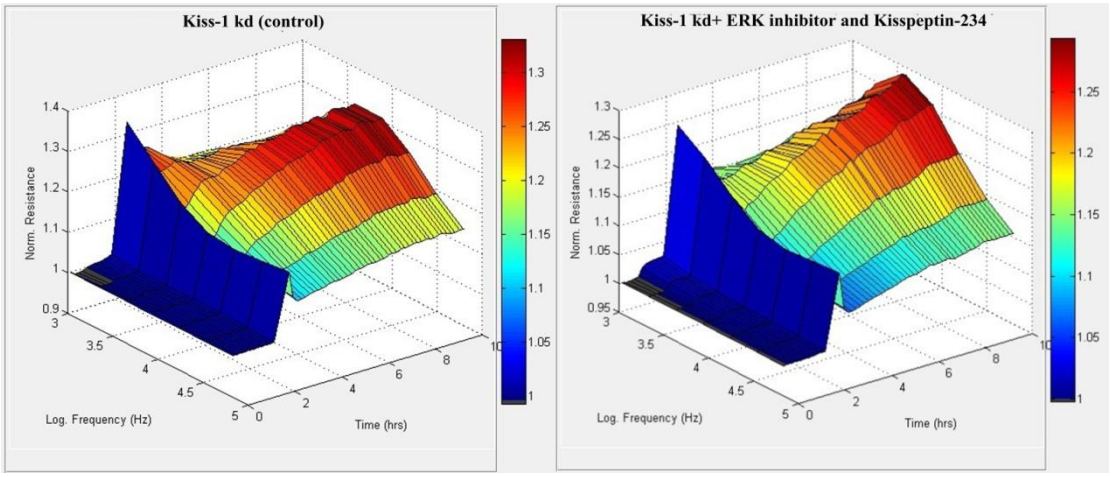

Figure 4.12.C. The effect of Kiss-1 knockdown on the migration ability of HT115 cells treated with ERK inhibitor+ Kisspeptin-234 compared with control group (no treatment), as shown in a 3D model. Shown are changes of normalized resistance measured at different frequencies over a period up to 8 hours.

4.3.10 Knockdown of Kiss-1 reduced tumour growth *in vivo*

From Figure 4.13, it is observed that the tumour growth of the group of Kiss-1 knockdown increased significantly compared with the control group during the 7 week period. On the eighth day, both the Kiss-1 knockdown group and the control group have measurable tumours with no statistical difference between the two groups ($p > 0.05$) after that the tumour size of both groups gradually decreased. The possible reason was that the Matrigel, which was used to suspend the cells, formed nodules at the initial stage after injection and also insufficient number of tumour cells injected. However, significant differences were observed between the Kiss-1 knockdown group and the control group at 22^{nd} ($p = 0.034882$), 29^{th} ($p=0.009967$) and 36^{th} ($p = 0.039235$) days respectively. Using Two-was ANOVA analysis (Tukey corrections) with time and group as variables, there is a significant different between the control and Kiss-1 knockdown groups ($P=0.002$) (Figure4.13).

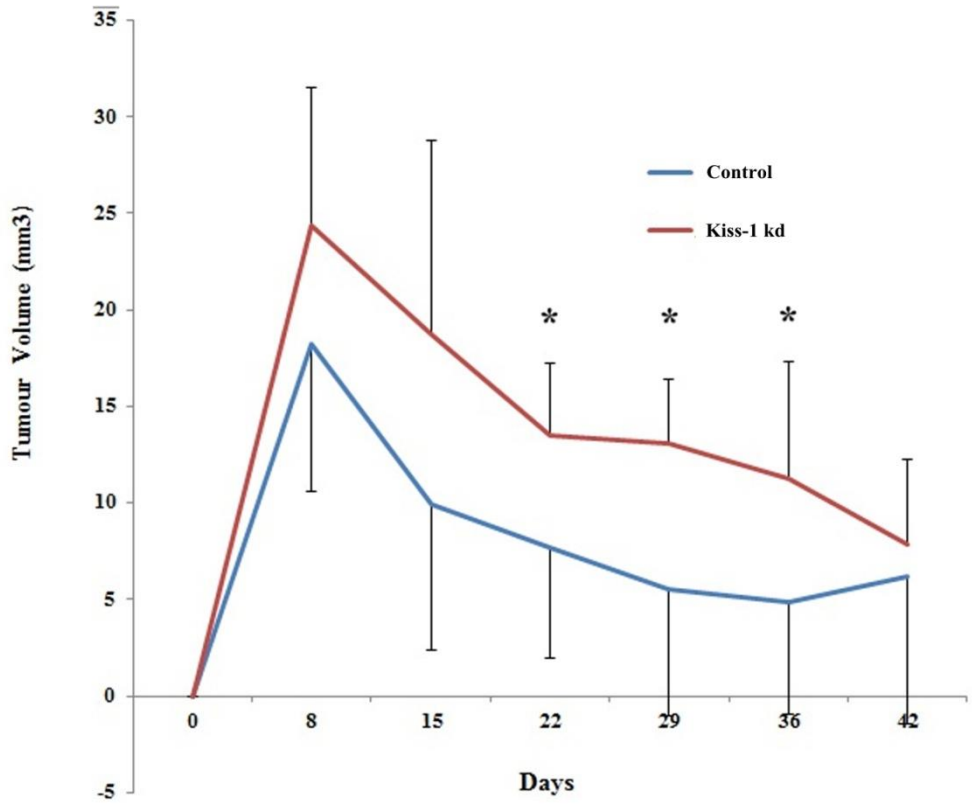

Figure 4.13.*In vivo* tumour growth of HT115 cells in CD-1 athymic nude mice. * $p<0.05$ vs the respective control group at the specific time point. The two groups had a significant difference over the 7 weeks period by using two-way ANOVA (Tukey model) test ($p=0.002$)

4.4 Discussion

For the last two decades, more than 30 putative metastasis suppressors have been recognized [123]. These molecules inhibit widely multiple steps of the metastatic cascade, which include adhesion, invasion, angiogenesis and colonization of ectopic tissues. Most of the molecules do not significantly affect the growth of cancer cells, thus marking them different from the classical oncogenes. The *kiss-1* gene was first suggested as a metastasis suppressor in human melanoma [61]. Nash *et al.* reported that Kiss-1 re-expression inhibit multiple organ metastasis combined with Kiss-1 receptor (Kiss-1R) [124]. Studies with human melanomas, breast cancer and pancreatic cancer xenografts demonstrated that Kiss-1 reduced proliferation of orthotopic tumours to other organs in all of the tested models [61, 71, 124-125]. Kiss-1 kept disseminated tumour cells in a dormant state so as to block the development of macroscopic metastases [71, 124-126]. Once the dissemination of cancer cells, which occurs before macroscopic detection clinically, is intervened, its value will contribute to the cancer therapy. However, the function of Kiss-1 as a metastasis suppressor in some cancers, including colorectal cancer is not clear. For this purpose, we used transfected HT115 and HRT18 cells with Kiss-1 and Kiss-1R knockdown and empty plasmid (pEF) to deduce the influence of Kiss-1 and its receptor on the function of colorectal cancer cells. Through the comparison between the control group and the knockdown groups, we wanted to verify if Kiss-1 and Kiss-1R may transform the function of colorectal cancer cells. The *in vitro* function

assays included growth, adhesion, invasion and migration assays, we repeated each assays more than three times to avoid artificial errors and ensure stability and accuracy of the results. The general trend of all repeats manifested consistency. There was no statistically significant effect of Kiss-1 and Kiss-1R knockdown on the growth of both HT115 and HRT18 cells (p>0.05), even if the growth of cells with Kiss-1 and Kiss-1R knockdown increased compared with both HT115 and HRT18 pEF cells (Kiss-1 kd in HT115: p= 0.0609; Kiss-1R kd in HT115: p= 0.057; Kiss-1 kd in HRT18: p= 0.059; Kiss-1R kd in HRT18: p= 0.089). Similarly, the effect of Kiss-1 and its receptor on the adhesion of HT115 and HRT18 cells did not show a significant difference compared with controls (p> 0.05). However the contrast observations were made with invasion assays, namely there were significant links between Kiss-1 knockdown cells and the controls in both HT115 and HRT18 cell lines but not with Kiss-1R knockdown cells.

With regard to the influence of Kiss-1on the motility of colorectal cancer cells, migration assays have shown that Kiss-1 negatively regulated the motility of both HT115 and HRT18 cells. The inhibitory influence of Kiss-1 was more significant on HRT18 cells than on HT115 cells at the 5^{th} hour. There was no obvious difference between the knockdown groups and the control group during the first 2 hours. After that the cells with Kiss-1 knockdown revealed a visible increase compared with the pEF cells. *P* value in figure 4.5 (p= 0.0077) and 4.6 (p= 0.0094) demonstrated the links between knockdown groups and the control at 5^{th} hour, while there was no

significant difference between the Kiss-1R knockdown cells and the controls (HT115 pEF and HRT18 pEF).

Through the analysis of ECIS assays, we focused on the investigation of the involvement of the ERK pathway and Kisspeptin-10 in Kiss-1 and Kiss-1R on cell migration. As shown in figure 4.8 and 4.10, the Kiss-1 knockdown cells treated with Kisspeptin-10 and ERK inhibitor respectively showed a significant decrease of migration ability compared with the control groups. It validated again the previous conclusion of the inhibitory effect of Kiss-1 on the migration ability of colorectal cancer cells using wounding assays through the treatment of Kisspeptin-10. What is more, it pointed out the inhibitory influence of Kiss-1 on cell migration via the ERK pathway. Furthermore, Figure 4.11 illustrated that the combined action of ERK inhibitor and Kisspeptin-10 caused more significant decrease of adhered cells in the Kiss-1 knockdown cells compared with the control through two tracks: the inhibition of the ERK signaling pathway and the increased activity of Kiss-1.

The study has further demonstrated, using an *in vivo* tumour model, that knocking down Kiss-1 from HT115 cells resulted in a marked increase in tumour growth as shown in figure 4.13. The present study was limited due to various restraints including the experimental conditions and number of cells injected, as there was little information in the literature on using this cell line in animal studies. This resulted in the steady decline of tumour size in both control and Kiss-1 knockdown groups. Future studies would need to re-explore the optimal conditions for using this cell line

with the particular experimental settings. The cell number of MDA-MB-435s transfected by full-length Kiss-1 cDNA used in the *in vivo* study at 1997 by D.R. Welsh should be a great reference for our future studies. In addition, Kisspeptin-10 should be suggested as a treatment to determine if it would have a negative effect on the tumour growth of the *in vivo* tumour model. However, the significant difference between the two groups is nonetheless highly supportive of the potential tumour suppressor role of Kiss-1.

Overall, it is easily seen that Kiss-1 had a significant inhibition on the migration and invasion of HT115 and HRT18 cells, while it did not show a strong inhibitory effect on the growth and adhesion in colorectal cancer cells. It prompted the conclusion that Kiss-1 may have a negative regulatory effect on the motility of colorectal cancer cells, while Kiss-1R did not seemingly exhibit as strong an inhibition on the migration and invasion of colorectal cancer cells as Kiss-1 ($p< 0.05$). In the following chapter, we will further analyze how Kiss-1 affects the colorectal cancer cells in the signaling pathway. Kiss-1 has been reported to activate a variety of signals (e.g. phospholipase C, protein kinase C, ERK1/2, intracellular Ca^{2+} mobilization) through Kiss-1R [126]. On the basis of the study of *in vitro* function assays, which displayed the significant inhibitory effect on the motility and invasion of colorectal cancer cells, the interaction between Kiss-1 and MMPs were considered in the MAPK signaling pathway, especially MMP-9 and MMP-2. MMPs, as the most important proteases related with tumour metastasis, can degrade extracellular matrix and basement membrane. Yan et

al, [127] proved that there was a marked reduction of *in vitro* invasion through Matrigel®-coated porous filters by HT-1080 cells which had reduced transcription and activity of MMP-9 following the over-expression of Kiss-1 [73]. This report provides grounds of argument to support the next study of the influence of Kiss-1 on MMPs through MAPK signal pathway in colorectal cancer cells.

Chapter 5

The influence of Kiss-1 on the enzyme activities of MMP-9 and MMP-2

5.1 Introduction

Metastasis is the most life-threatening complication of solid tumours [128]. Surgical intervention would be easy to get rogue lesions and micro-metastases in distant sites if it did not achieve complete resection of the primary neoplasm. This is particularly apparent in melanoma, in which 90% of the patients who died of melanoma were found to have lung metastasis at the time of autopsies [129]. What is more, the incidence rate of melanoma has increased 15 fold during the last 50 years, which has made its contribution to morbidity and mortality a public health concern. Therefore, a clear understanding of tumour metastasis and the role played by metastasis suppressor genes in regulating this cascade are important[129]. Kiss-1 was suggested as a novel tumour suppressor genes and provides us with a vital target for investigation in melanoma [61]. This has been further demonstrated by data presented in Chapter-5 of this thesis, in which Kiss-1 demonstrated a tumour suppressive role in colorectal cancer. However, the mechanism of the metastasis suppressor function of Kiss-1 remains poorly understood. Yan *et al*. reported that Kiss-1 can diminish P65 and P50 NF-KB proteins which can combine with the promoter of MMPs, so as to reduce the synthesis of MMPs and inhibit the effects on the mobility and invasion of cancer cells [48, 70, 73]. Another study demonstrated that the activation of Kiss-1R by Kisspeptin-10 can abolish the activation of protein kinase B [116] by the tyrosine kinase receptors for epidermal growth and lymphoid cell lines. Furthermore, the signaling of Kiss-1R was found to be the main trigger of apoptosis in epithelial and

lymphoid cell lines [130]. Interestingly, this phenomenon depended on the activation of the ERK pathway rather than the inhibition of Akt [130]. This data may establish the novel experimental basis for a paracrine mode of action by which Kisspeptins inhibit the metastatic potential of cancer cells.

The previous chapter showed a significant effect of Kiss-1 and its receptor knockdown on the motility of colorectal cancer cells. Here, in light of previous study, we investigated if Kiss-1R was phosphorylated at the phospho-tyrosine phosphorylation site when combined with Kisspeptin-10 in colorectal cancer cells in the light of previous studies and if Kiss-1 inhibits MMP-9 and MMP-2 through ERK signaling pathway as a potential mechanism of action to account for the suppression of colorectal cancer cells motility.

5.2 Materials and methods

5.2.1 Cell lines

HT115 and HRT18 cell lines were routinely cultured in DMEM-F12 medium as described in Chapter 2.

5.2.2 Generation of Kiss-1 and Kiss-1R ribozyme transgenes

Hammerhead ribozymes targeting Kiss-1 and Kiss-1R were designed based on the secondary structure of Kiss-1 and Kiss-1R mRNA respectively and synthesized following the method described in Chapter 2.

5.2.3 Generation of Kiss-1 and Kiss-1R knockdown in colorectal cancer cell lines

The plasmids were transfected into colorectal cells through by the electroporation at 310V. Subsequently, the cells were placed into 5 μg/ml blasticidin selection for a sufficient period to kill cells which did not contain the plasmid. Empty plasmid vectors were used to transfect the cells as control. The verification of Kiss-1 and Kiss-1R knockdown in the transfected cells was done using RT-PCR, Q-PCR and Western blotting as described in Chapter 3.

5.2.4 Immunoprecipitation

In our study, immunoprecipitation (IP) was used for testing if Kiss-1R can be phosphorylated at the tyrosine phosphorylation site in colorectal cancer cells. The process involves adding a specific antibody (Kiss-1R in this case) recognising a protein of interest within a cell lysate. This is then mixed with sepharose or agarose bonded staphylococcal protein A, protein G, or both, in order to collect the ensuing protein-antibody complexes. These complexes are then centrifuged to induce precipitation, run on an SDS-PAGE gel, and evaluated using immune probing. The details of the process have been outlined in Chapter 2.

5.2.5 Gelatin zymography assay

$1x10^6$ cells were counted and seeded to a tissue culture flask and incubated overnight. After incubation, the samples were washed once with 1x BSS followed by a wash with serum-free DMEM and then either incubated in serum-free DMEM control or treated medium for 4 hours. Following the 4 hours treatment, the samples were prepared in non-reducing sample buffer and the medium was collected. Protein samples were separated using SDS-PAGE on gels containing 10% gelatin (Sigma-Aldrich Inc, USA).After SDS-PAGE, gels were renatured by washing with buffer twice (15 minutes for each wash) at room temperature, and then soaked in developing buffer at 37^oC for 36- 40 hours incubation. Following incubation, the gels were stained with 0.5 % Coomassie blue in distilled de-ionized water for 1 hour and washed in destain buffer for approximate 1 hour based on the staining strength of gel. The presence of clear bands where MMP2 and MMP9 were located and gelatin was degraded, indicated proteins activity.

5.3 Results

5.3.1 Tyrosine phosphorylation were increased by Kiss-1R knockdown

To investigate the influence and functional status of Kiss-1R and the effects of Kisspeptin-10, a Kiss-1 receptor agonist, on colorectal cancer cells on tyrosine phosphorylation, Immunoprecipitation (IP) was carried out to examine tyrosine phosphorylation level of Kiss-1R in HT115 pEF cells treated with Kisspeptin-10 (Figure 5.1.A). The cells were divided into four groups, which respectively accepted different treatment: no treatment (control), Kisspeptin-10, Kisspeptin-234 and positive control (sodium orthovanadate and hydrogen peroxide). Kisspeptin-234 is Kisspeptin-10/Kiss-1R antagonist, which belongs to Kisspeptin-10 analogue. Results demonstrated that the tyrosine phosphorylation of Kiss-1R in the cells treated with Kisspeptin-10 was strongly activated compared with both the cells without treatment and the cells treated with Kisspeptin-234 ($p< 0.001$), in the meantime, there was no significant difference between those cells treated with Kisspeptin-234 and control cells ($p= 0.4035$). The detailed data is showed in Table 5.1. For obtaining actual and reliable research results, the experiment was repeated three times and mean value taken.

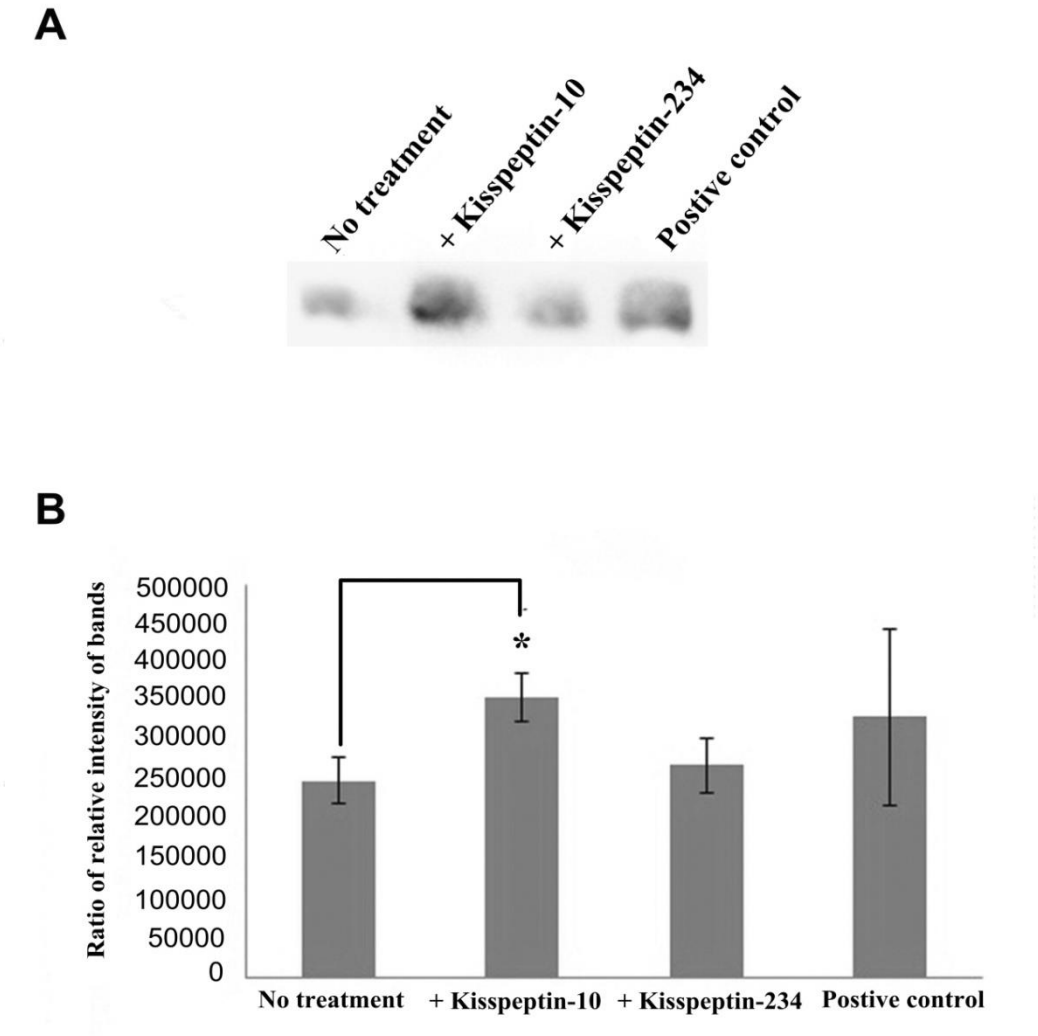

Figure 5.1. Effect on tyrosine phosphorylation of Kiss-1R in HT115 pEF.
A. Immunoprecipitation and Western blot displayed bands in HT115 pEF cells, which were treated with no treatment (control), Kisspeptin-10, Kisspeptin-234 and positive control for each group. Anti-Kiss-1R was used for the immunoprecipitation and primary antibody in the Western blot and probing was PY20.
B. The comparison among four different treatments, showed the representative histogram of the difference in intensity of bands in HT115 pEF. The intensity of band of cell treated with Kispeptin-10 was significantly increased compared with the control. Experiment was repeated three times and mean value taken. Error bars represent SD. Asterisk represents $p< 0.05$. Relative intensity of bands was analyzed using by Image-J software. Original data is shown in Table 22 of Appendices.

Table 5.1. The intensity of bands in HT115 pEF

Control **Mean+SD** **N=3**	**+Kisspeptin-10** **Mean+SD** **N=3**	**+Kisspeptin-234** **Mean+SD** **N=3**	**Positive control** **Mean+SD** **N=3**
250356.3+ **30308.83**	**356095+** **31705.2**	**269073+** **34635.64**	**331635.7+** **112206.7**

Control vs + Kisspeptin-10, *P*= 0.01396; + Kisspeptin-234 vs + Kisspeptin-10, *P* = 0.03259

5. 3.2 ERK inhibition impact on MMP-9 activity in Kiss-1 knockdown and control cells following treated with Kisspeptin-10 and Kisspeptin-234.

In chapter 4, we established that Kiss-1 inhibited the migration and invasion of colorectal cancer cells (HT115 and HRT18). A previous study has reported that the overexpression of Kiss-1 could reduce transcription and activity of MMP-9 and in doing so suppress the invasion of HT-1080 cells [73]. In addition, thyroid cancer cells transfected with Kiss-1R showed a strong and sustained phosphorylation of ERK1/2 after treatment with Kiss-1 [74]. Here, we further explored the influence of Kiss-1 knockdown together with treatment with Kisspeptin-10 and 234 on MMP-9 and MMP-2 activity, together with the inhibition of ERK pathway in the HT115 cell line. The cells were divided into three treatment groups namely no treatment (control group), Kisspeptin-10 and Kisspeptin-234 respectively. For each group, two pairs of HT115 pEF and HT115 Kiss-1 knockdown cells were treated without or with ERK

inhibitor, namely control and + ERK inhibitor respectively. Figure 5.2 displays the results from zymography experiments and shows that expression of Kiss-1 and treatment of the cells with the inhibitors had a greater impact on the enzyme activity of MMP-9 than on that of MMP-2. Hence, the difference in MMP-9 expression in HT115 cells was chosen to analyse further. The results showed that the intensity of MMP-9 bands in the cells treated with the ERK inhibitor was decreased compared with the control in all three groups (no treatment, Kisspeptin-10 and Kisspeptin-234) (figure 5.3 and 5.4). Figure 5.3 showed that the difference of the enzyme activity of MMP-9 in HT115 pEF cells of all three groups. The enzyme activity of MMP-9 in HT115 pEF cells treated with ERK inhibitor was significantly inhibited compared with that of controls in all three groups (cells+ ERK inhibitor vs control in the group of no treatment: p= 0.006577; cells+ ERK inhibitor vs control in the group of Kisspeptin-10: p= 0.001839; cells+ ERK inhibitor vs control in the group of Kisspeptin-234: p= 0.005935). Figure 5.4 demonstrated that that the difference of the enzyme activity of MMP-9 in HT115 Kiss-1 knockdown cells of all three groups. Similarly with HT115 pEF cells, the enzyme activity of MMP-9 in HT115 Kiss-1 knockdown cells treated with ERK inhibitor brought about a strong inhibition in comparison with the controls in the groups of no treatment (p= 0.00017) and Kisspetin-10 (0.001544). Furthermore, the results pointed out that both HT115 pEF and HT115 Kiss-1 knockdown cells treated with Kisspeptin-10 showed a decreased expression of MMP-9 in comparison with the cells treated with serum free and

Kisspeptin-234 from Figure 5.3 and 5.4. The experiments were repeated three times and mean value taken.

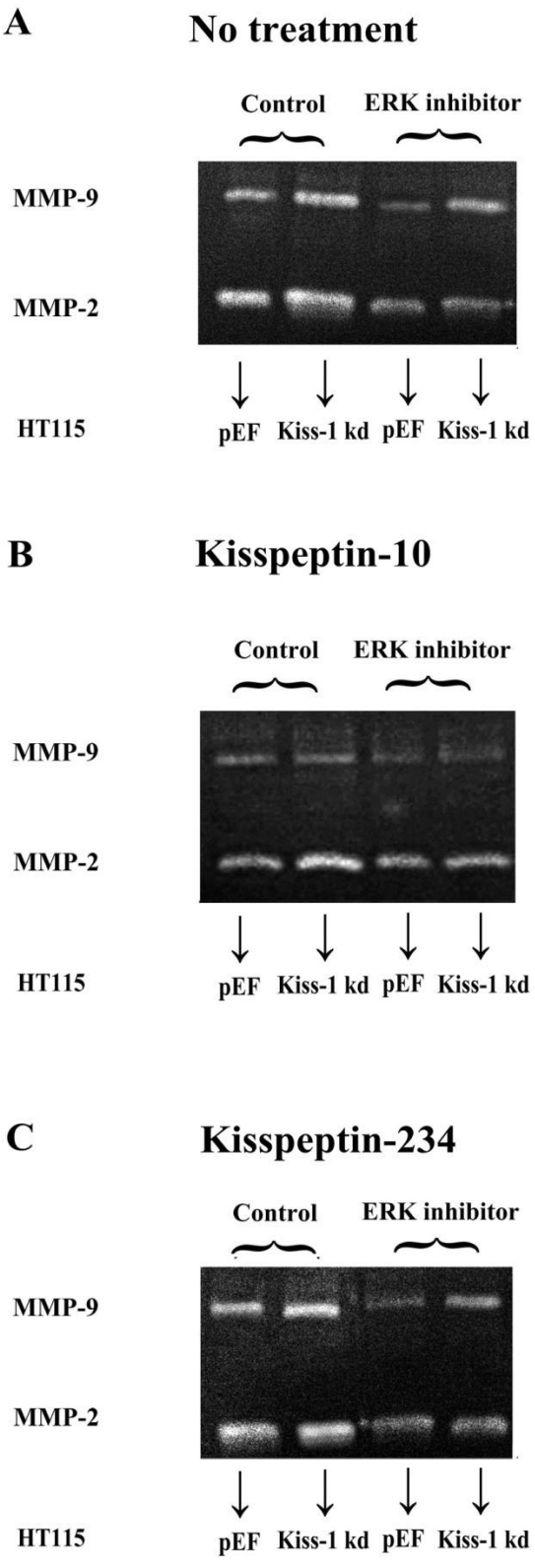

(Figure 5.2, Legend please see next page)

Figure 5.2. The enzyme activity of MMP-9 and MMP-2 in HT115 pEF and HT115 Kiss-1 knockdown (kd) cells, following treatment (no treatment, Kisspeptin-10 and Kisspeptin-234). A. The enzyme activity of MMP-9 and MMP-2 in the control group and the group treated with ERK inhibitor. B. The expression of MMP-9 and MMP-2 in HT115 pEF and HT115 Kiss-1 knockdown (kd) cells, which were treated with Kisspeptin 10, in the presence of ERK inhibitor. C. The enzyme activity of MMP-9 and MMP-2 in the group treated with Kisspeptin-234, in the presence ERK inhibitor.

Table 5.2. The intensity of MMP-9 bands in HT115 pEF and HT115 Kiss-1 knockdown (kd) cells with no treatment

Treatment	**Control**		**ERK inhibitor**	
Cell lines	**HT115 pEF**	**HT115 Kiss-1 kd**	**HT115 pEF**	**HT115 Kiss-1 kd**
Intensity of bands (mean+ SD, n= 3)	5058.33±143.16	5516.33±82.25	4597±47.16	4790±42.52

Table 5.3. The intensity of MMP-9 bands in HT115 pEF and HT115 Kiss-1 knockdown (kd) cells treated with Kisspeptin-10

Treatment	**Control**		**ERK inhibitor**	
Cell lines	**HT115 pEF**	**HT115 Kiss-1 kd**	**HT115 pEF**	**HT115 Kiss-1 kd**
Intensity of bands (mean+SD, n= 3)	4935± 58.65	4944± 63.07	4570± 60.01	4632± 30.99

Table 5.4. The intensity of MMP-9 bands in HT115 pEF and HT115 Kiss-1 knockdown (kd) cells treated with Kisspeptin-234

Treatment	**Control**		**ERK inhibitor**	
Cell lines	**HT115 pEF**	**HT115 Kiss-1 kd**	**HT115 pEF**	**HT115 Kiss-1 kd**
Intensity of bands (mean+ SD, n= 3)	5181± 120.75	5361.33± 237.769	4701±108.04	5027± 116.66

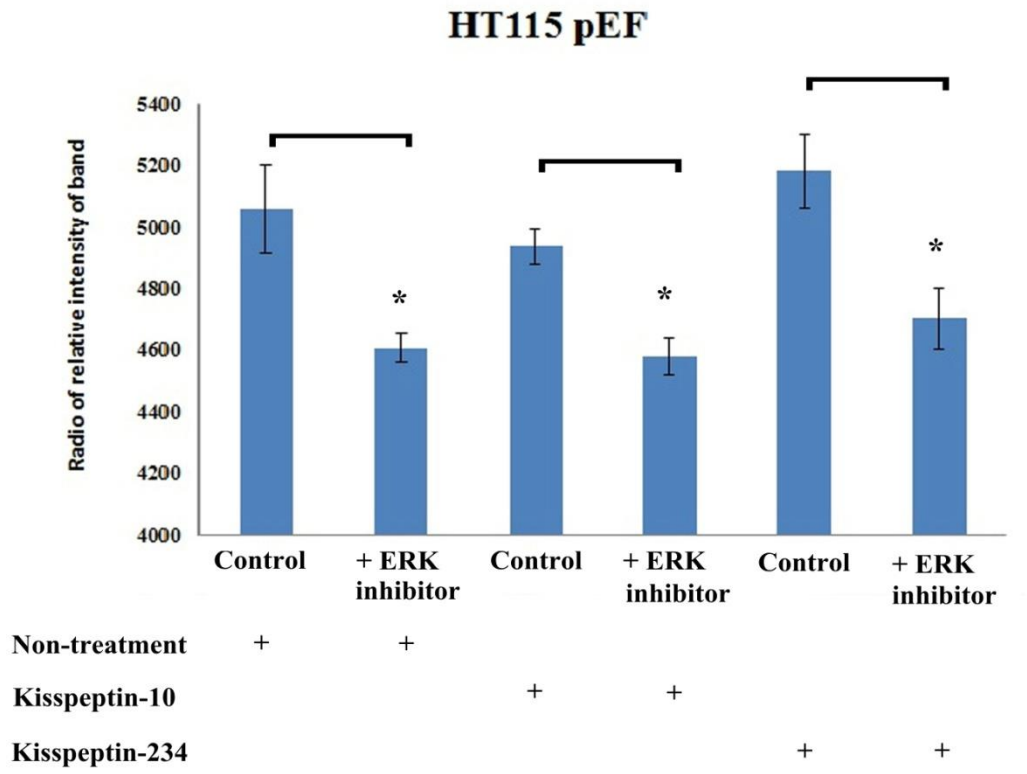

Figure 5.3. Effects of Kiss-1 and ERK inhibitor on MMP activities. The histograms demonstrated that the difference of MMP-9 enzyme activity in three groups of HT115 pEF cells (no treatment, Kisspeptin-10 and Kisspeptin-234).Plus sign (+) represents for corresponding treatment. For each group, the enzyme activity of MMP-9 in pEF cell treated with ERK inhibitor all showed the significant decrease compared with the control. Asterisks stand for $p< 0.05$. Experiment was repeated three times and mean value taken. Relative intensity of bands was analyzed using by Image-J software. Original data is shown in Table 23 of Appendices.

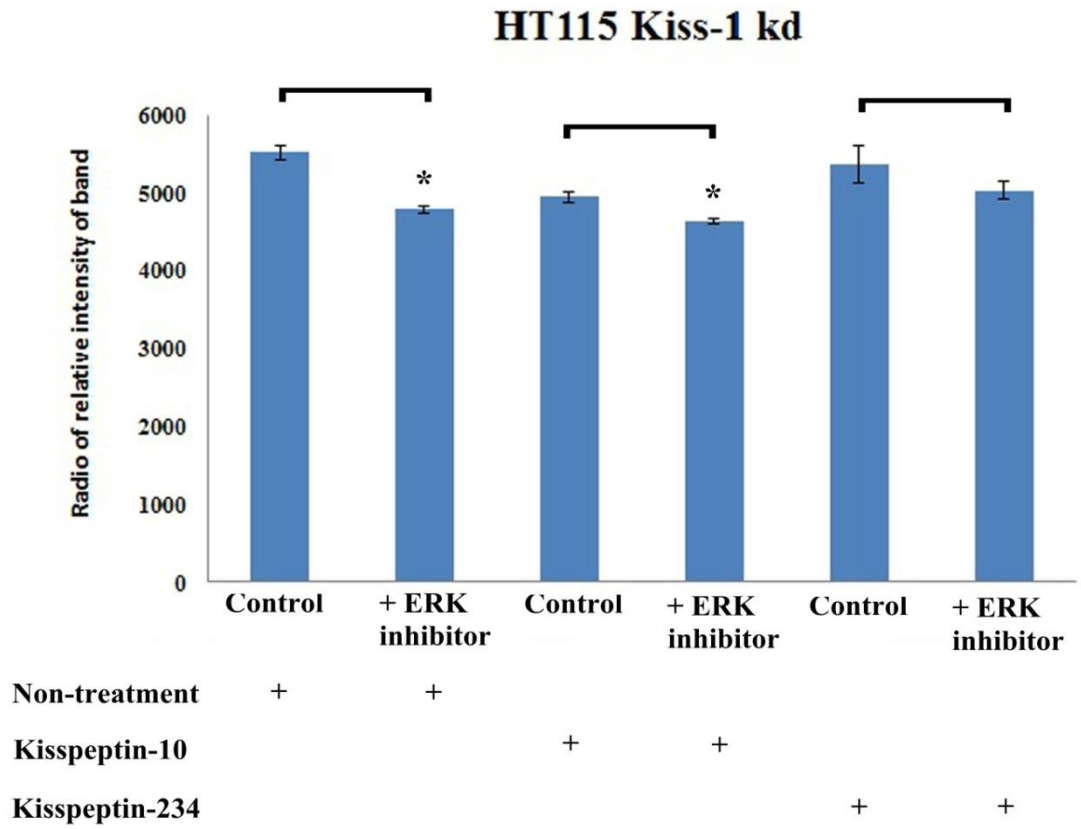

Figure 5.4. The bar graphs show the difference of MMP-9 enzyme activity in HT115 Kiss-1 knockdown cells. The cells were separated into three groups on the basis of three different treatments (no treatment, Kisspeptin-10 andKisspeptin-234). Plus sign (+) represents for corresponding treatment. The significant decrease of the enzyme activity of MMP-9 in Cells treated with ERK inhibitor compared with the controls was observed in both no treatment and Kisspeptin-10 groups. Asterisks stand for $p<$ 0.05. Experiment was repeated three times and mean value taken. Relative intensity of bands was analyzed using by Image-J software. Original data is shown in Table 23 of Appendices.

5.4 Discussion

Previous studies have reported the inhibitory impact of Kiss-1 on MMP-9 and the increased ERK phosphorylation caused by ARO cells treated with Kiss-1 [73-74]. Masato and colleagues reported that Kiss-1R bound with Kisspeptin derived from the product of Kiss-1 stimulated PIP_2 hydrolysis, Ca^{2+} mobilization, arachidonic acid rease and ERK1/2 tyrosine phosphorylation in Chinese hamster ovary K1 cells [64]. Our current study aimed to test if treatment of HT115 cells with Kisspeptin-10 may cause phosphorylation of the Kiss-1 receptor. It was also aimed to examine the impact of Kisspeptin-10 on the on MMP-9 and MMP-2 in the context of Kiss-1 knockdown. The third aim was to test if ERK signal pathway plays a role in Kiss-1 mediated effect on MMP-9 and MMP-2. Knocking down Kiss-1 in HT115 cells (Figure-5.2) resulted in an increase in MMP-9 activities. This change of MMP-9 activities was significantly blocked when ERK pathway was blocked by an ERK inhibitor. Furthermore, It can be seen that the activated Kiss-1 receptor from cells treated with Kisspeptin-10 was significantly stronger than that for the cells treated with serum free and Kispeptin-234 ($p< 0.001$) through the analysis of Immunoprecipitation in HT115 cells. This suggests that Kisspeptin-10, a Kiss-1 agonist is able to activate the Kiss-1 receptor in HT115 cells. As expected, Kisspeptin-234, a Kisspeptin-10/Kiss-1R antagonist has no significant effect on the receptor activation ($p> 0.05$).

The present study indicates that Kiss-1 may suppress motility of colorectal cancer cells through inhibiting the expression of MMP-9 and that this effect is likely to be via the ERK signaling pathway.

Chapter 6

Expression of Kiss-1 and Kiss-1R in Human colorectal cancer tissues and the association with clinicopathological characteristics

6.1 Introduction

Colorectal cancer as the second most common diagnosed cancer, it is believed to occur globally at a rate of approximate 1,200,000 new cases every year, accounting for approximately 10% of all incident cancers, with mortality rates due to colorectal cancer estimated at about 609,000 [3]. Local recurrence and metastases occur in about 50% of colorectal cancer patients after radical operation. For the purpose of predicting the prognosis of patients with colorectal cancer and recording the anatomic extent of colorectal cancer, several classification system have been established and modified (e.g. Dukes classification, TNM classification and T staging classification). The discovery of suitable biomarkers, which have correlation with tumour stage, invasion or recurrence, to aid in identifying colorectal cancer with high metastatic potential is key and would allow patients with colorectal cancer to receive effective chemo-radiotherapy soon after surgery.

The Kiss-1 gene has been reported to be a novel metastasis suppressor gene in human melanoma and breast cancer cells [61, 71]. Kiss-1 encodes a 54-amino acid peptide, which is the endogenous ligand of an orphan G-protein-coupled receptor (Kiss-1R). After binding with Kiss-1R, Kiss-1 gene product acted with a metastasis suppressor function, activity to inhibit chemotaxis, invasion and metastasis of cells [48]. The influence of Kiss-1 and Kiss-1R on the function of colorectal cancer cells through the analysis of *in vitro* function assays has been introduced in Chapter 4. However, the clinical importance of the expression of Kiss-1 and its receptor remains unknown in

colorectal cancer. There is no available data about the association of Kiss-1 and Kiss-1R with tumour or patients clinicopathological characteristics in human colorectal cancer. In the present study, we analyzed the quantitative expression levels of Kiss-1 and Kiss-1R mRNAs and protein in colorectal cancer tissues and para-tumorous tissues in relation to tumour histopathological grade, stage and nodal status using the real-time Q -PCR. We also correlate the level of expression with the prognosis and clinical outcome of the patients. On the basis of the analysis above, we evaluated the efficiency of Kiss-1 and Kiss-1R as biological markers for the malignant potential of colorectal cancer.

6.2 Materials and methods

Colorectal tissues

Colorectal cancer tissues (n=94) and normal background tissues (n=80) were collected immediately after surgery and stored in a deep freeze (-80℃) until use. Patients were routinely followed after surgery and the median follow up period was 120 months for this study. The histopathological details, tumour grading (modified Bloom and Richardson's grading system), Duke staging, tumour staging (TNM) and the prognostic index for the patients is shown in table 6.1.

Real-time quantitative polymerase chain reaction (Q-PCR)

Real-time quantitative PCR, using the Amplifluor™ technique, was used for verifying the level of mRNA expression of Kiss-1 from the prepared cDNA samples mentioned above. All colorectal cDNA samples were simultaneously examined for Kiss-1 expression along with an applicable set of plasmid standards. Q-PCR primers for Kiss-1and Kiss-1R were designed using Beacon Design software (PREMIER Biosoft, Palo Alto, CA). Sequences of primers used in the current study are provided in Chapter 2. Real-time PCR conditions were given in Chapter-2.

Data analysis

The relationship between Kiss-1 and Kiss-1R expression and tumour grade, TNM staging and nodal status was analyzed using Mann-Whitney U and Kruskal-Wallis tests. Survival analysis curve were performed using Kaplan-Meier survival analysis. Differences were considered to be statistically significant at $p<0.05$.

6.3 Results

Detailed patient information is outlined in table 6.1.The clinical cohort of Kiss-1 and Kiss-1R has been shown in Table 6.2 (A and B) below.

Table 6.1. Detailed information of patients with colorectal cancer

Category		No.
T/N		
	Normal	80
	Tumour	94
PairedT/N		
	Paired normal	68
	Paired tumour	68
Location		
	Left colon	22
	Right colon	28
	Transcolon	2
	Rectum	22
Dukes classification		
	A	7
	B	33
	C	32
	B&C	65
Tumour stage		
	T1	2
	T2	10
	T3	40
	T4	18
	T2&3	50
	T3&4	58
Lymph node involvement		
	Node 0	39
	Node 1	16
	Node 2	15
	Node1&2	31
TNM staging		
	I	9
	II	30
	III	26
	IIIA	2
	IIIB	12
	IIIC	12
	IV	6
	II &III	56
	III&IV	32
	II &III&IV	62
Clinical outcome		
	No invasive	50
	Invasive	26
	Dis free	35
	Incidence	23
	No recurrence	58
	Local reurrence	7
	No metastasis	50
	Metastasis	19
	Alive	36
	Death	22
	Non treat	42
	Chemradio	5

Table 6.2.A. The correlation of the expression of Kiss-1 and clinical parameters. Red colouration is used to indicate statistical significance (*p* value< 0.05). The *p* value [131] in the statistical difference between tumour stage 2 and tumour stage 3 and 3&4

Category		Median	IQR	*p*-Value	*p*-Value (2)
T/N					
	Normal	97	6-2345		
	Tumour	35	1-2108	0.3775	
PairedT/N					
	Paired normal	82	6-2344		
	Paired tumour	8	0-1855	0.1672	
Location					
	Left colon	624	173-1968		
	Right colon	719	44-2000	0.899	
	Transcolon	154	N/A	0.958	
	Rectum	673	175-2522	0.907	
Dukes classification					
	A	5539	848-24856		
	B	780	104-2272	0.043	
	C	611	190-1221	0.015	
	B&C	643	163-1468	0.018	
Tumour stage					
	T1	8000	N/A		
	T2	1721	789-10369	1	
	T3	639	71-1332	0.226	0.0381
	T4	592	215-1600	0.186	
	T2&3	684	127-2150	0.393	
	T3&4	635	126-1419	0.195	0.0285
Lymph node involvement					
	Node 0	872	213-2874		
	Node 1	715	67-1428	0.326	
	Node 2	609	200-643	0.045	
	Node1&2	609	187-1008	0.063	
TNM staging					
	I	2081	814-20038		
	II	756	122-2473	0.06	
	III	611	84-1079	0.009	
	IIIA	1178	N/A	0.556	
	IIIB	738	N/A	0.095	
	IIIC	463	113-635	0.003	
	IV	610	249-2489	0.112	
	II &III	639	98-1471	0.016	
	III&IV	611	190-1221	0.009	
	II &III&IV	639	175-1466	0.015	
Clinical outcome					
	No invasive	835	127-2372		
	Invasive	579	161-948	0.1907	
	Dis free	759	84-2081		
	Incidence	635	217-2187	0.8115	
	No recurrence	735	89-2373		
	Local reurrence	643	269-3718	0.604	
	No metastasis	735	84-2522		
	Metastasis	634.3	213-1463	0.92	
	Alive	661	86-1876		
	Death	572	195-1644	0.923	

Table 6.2.B. The correlation of the expression of Kiss-1R and clinical parameters. Red colouration is used to indicate statistical significance (*p* value< 0.05). The *p* value [131] stands for the statistical difference between tumour stage 2 and tumour stage 3, 4 and 3&4.

Category		Median	IQR	*p*-Value	*p*-Value (2)
T/N					
	Normal	30	1-2406		
	Tumour	<0.000001	<0.000001-<0.000001	<0.0001	
PairedT/N					
	Paired normal	23	0-522		
	Paired tumour	<0.000001	0-0.02	<0.0001	
Location					
	Left colon	<0.000001	<0.000001-0.01		
	Right colon	<0.000001	<0.000001-0.009	0.8791	
	Transcolon	0.00452	N/A		
	Rectum	<0.000001	<0.000001-0.13	0.447	
Dukes classification					
	A	0.00015	<0.000001-0.00103		
	B	0.0004	<0.000001-0.0091	0.6616	
	C	<0.000001	<0.000001-0.09	0.1431	
	B&C	<0.000001	<0.000001-0.02	0.221	
Tumour stage					
	T1	1.06E-05	N/A		
	T2	0.00005	<0.000001-0.00171		
	T3	<0.000001	<0.000001-0.03		0.0972
	T4	<0.000001	<0.000001-0.02		0.2268
	T2&3	<0.000001	<0.000001-0.02		
	T3&4	<0.000001	<0.000001-0.03		0.1077
Lymph node involvement					
	Node 0	0.0003	<0.000001-0.0071		
	Node 1	<0.000001	<0.000001-0.02	0.3236	
	Node 2	0.01	<0.000001-1.76	0.335	
	Node1&2	<0.000001	<0.000001-0.04	0.2095	
TNM staging					
	Ⅰ	0.00003	<0.000001-0.00033		
	Ⅱ	0.0005	<0.000001-0.0105	0.1939	
	Ⅲ	<0.000001	<0.000001-0.03	0.0817	
	ⅢA	0.00807	N/A		
	ⅢB	<0.000001	<0.000001-0.01	0.0523	
	ⅢC	0.01	<0.000001-6.35	0.1864	
	Ⅳ	<0.000001	<0.000001-47.0	0.1967	
	Ⅱ&Ⅲ	0.001	<0.000001-0.017	0.1119	
	Ⅲ&Ⅳ	<0.000001	<0.000001-0.09	0.051	
	Ⅱ&Ⅲ&Ⅳ	<0.000001	<0.000001-0.03	0.0513	
Clinical outcome					
	No invasive	<0.000001	<0.000001-0.008		
	Invasive	<0.000001	<0.000001-0.05	0.1907	
	Dis free	0.00019	<0.000001-0.00523		
	Incidence	0.01	<0.000001-0.12	0.0207	
	No recurrence	<0.000001	<0.000001-0.013		
	Local reurrence	0.00653	<0.000001-0.02245	0.6923	
	No metastasis	<0.000001	<0.000001-0.009		
	Metastasis	<0.000001	<0.000001-0.13	0.0765	
	Alive	0.00028	<0.000001-0.00724		
	Death	<0.000001	<0.000001-0.13	0.0158	
	Non treat	0.0002	<0.000001-0.006		
	Chemradio	0.0796	0.012-0.1607	0.0115	

6.3.1 Expression of Kiss-1 in colorectal cancer tissues and normal background tissues

We analysed the expression of Kiss-1 in both colorectal cancer tissues and adjacent tissues using real time quantitative RT-PCR (expressed as median Kiss-1 transcript levels/50 ng mRNA). As shown in Table6.2.A tumour tissues had lower level of Kiss-1 compared with normal tissues, however the difference was not statistically significant.

6.3.2 Expression of Kiss-1 and its relation to Dukes classification

Duke B, C and B&C carcinoma had decreased level of Kiss-1 expression compared with Duke A carcinoma. This difference was found to be statistically significance (Figure 6.1).

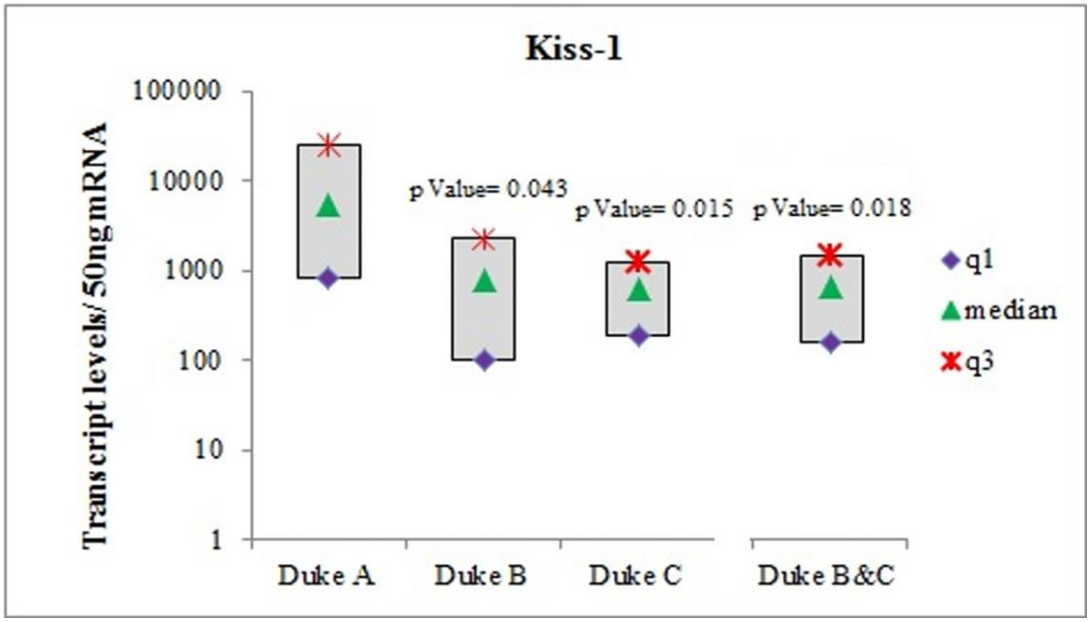

Statistic	Duke A	Duke B	Duke C	Duke B&C
q1	848	104	190	163
min	90	<0.00001	<0.00001	<0.00001
median	5539	780	611	643
max	31329	27762	24974	27762
q3	24856	2272	1221	1468

Figure 6.1. The relationship between Kiss-1 transcript levels and Dukes staging. The expression of Kiss-1 in duke B, C and B&C all showed a significant decrease compared with that in duke A

6.3.3 Expression of Kiss-1 and its correlation with Tumour stage

As shown in Figure 6.3, a gradual reduction of the level of kiss-1 was displayed from Tumour stage Ⅱ to Ⅳ and also Tumour stage Ⅲ&Ⅳ, however, none of these differences was found to be statistically significant. Interestingly, there was statistical significance between Kiss-1 level in Tumour stage Ⅱ and stage Ⅳ and Ⅲ&Ⅳ (Figure 6.2).

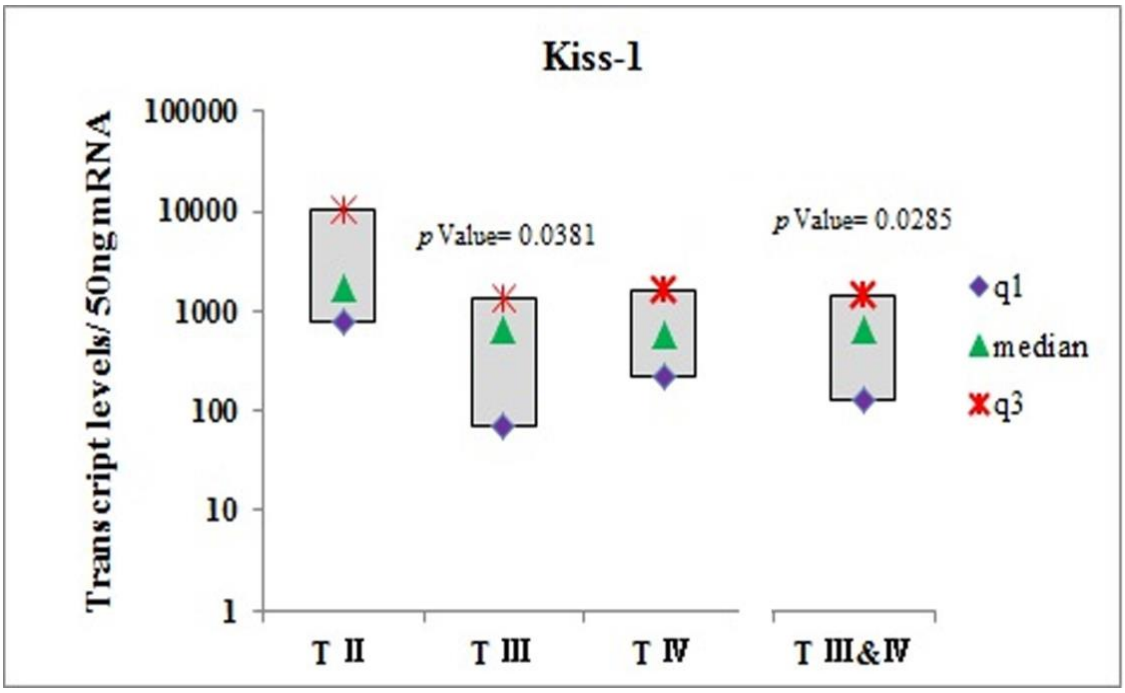

Statistic	T Ⅱ	T Ⅲ	T Ⅳ	T Ⅲ&Ⅳ
q1	789	71	215	126
min	90	<0.00001	<0.00001	<0.00001
median	1721	639	592	635
max	31329	27762	5242	27762
q3	10369	1332	1600	1419

Figure 6.2. The relationship between Kiss-1 transcript level and Tumour staging. There were significant links between tumour stage Ⅱ and stage Ⅲ and Ⅲ&Ⅳ respectively.

6.3.4 Expression of Kiss-1 and its relationship to Lymph node involvement

Kiss-1 expression was found to be reduced with the deepening of lymph node involvement (from Node 0 to Node 2). Statistically reduced levels of Kiss-1 were observed in Node 2 compared with Node 0 (Figure 6.3). Node 0 stands for no node involvement; Node 1 stands for 1 to 3 lymph nodes close to the bowel found to contain cancer cells; Node 3 stands for more than 3 lymph nodes found to contain cancer cells and further than 3cm away from the main tumour in the bowel or the presence of cancer cells in lymph nodes connected to the main blood vessels around the bowel.

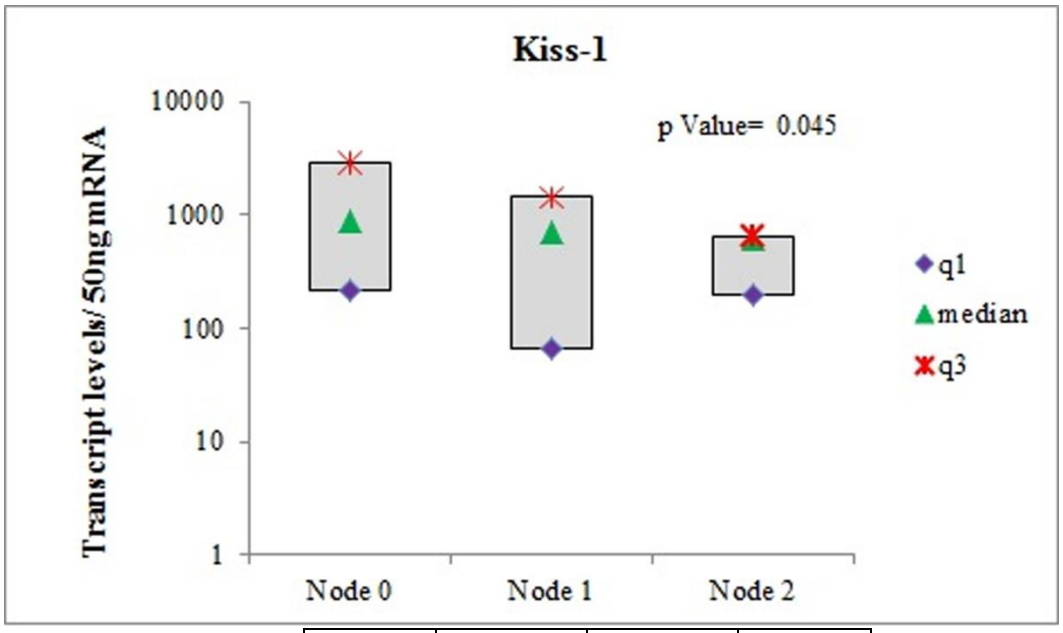

Statistic	Node 0	Node 1	Node 2
q1	213	67	200
min	<0.00001	<0.00001	43
median	872	715	609
max	31329	24974	1463
q3	2874	1428	643

Figure 6.3. The correlation of Kiss-1 levels in Lymph node involvement node 0 and node 2.

6.3.5 Expression of Kiss-1 and its correlation with TNM staging

The expression level of Kiss-1 decreased as TNM stage progressed, and statistical analysis revealed significant links between TNM stage Ⅰ and stage Ⅲ, ⅢC, Ⅱ&Ⅲ, Ⅲ&Ⅳ and Ⅱ&Ⅲ&Ⅳ, which is outlined in Figure 6.4.

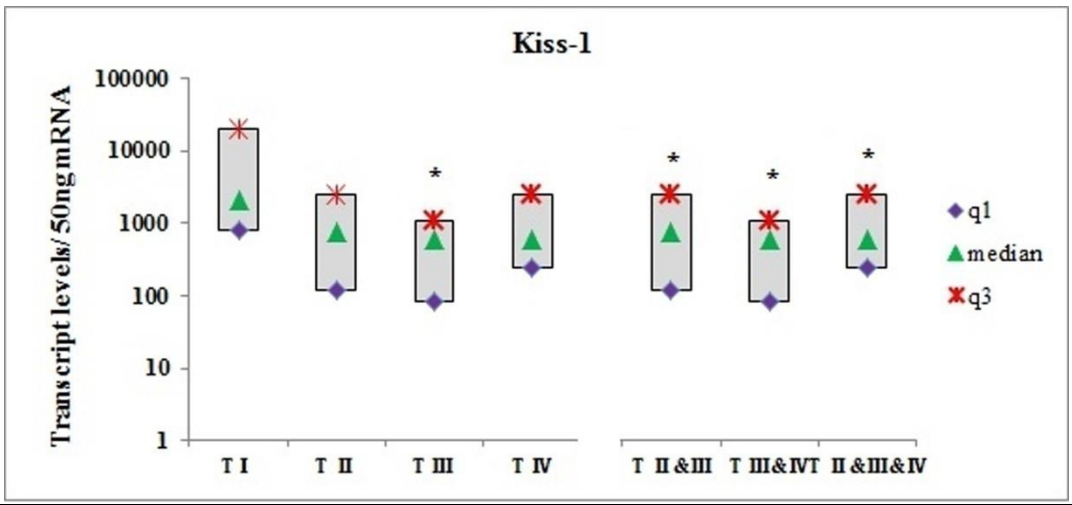

Statistic	T Ⅰ	T Ⅱ	T Ⅲ	T Ⅳ	T Ⅱ&Ⅲ	T Ⅲ&Ⅳ	T Ⅱ&Ⅲ&Ⅳ
q1	814	122	84	249	122	84	249
min	90	<0.00001	<0.00001	187	<0.00001	<0.00001	<0.00001
median	2081	756	611	610	756	611	610
max	31329	27762	24974	5746	27762	24974	27762
q3	20038	2473	1079	2489	2473	1079	2489

Statistic	T Ⅰ	T ⅢA	T ⅢB	T ⅢC
q1	814	N/A	N/A	113
min	90	882	<0.00001	43
median	2081	1178	738	463
max	31329	1473	24974	1463
q3	20038	N/A	N/A	635

Figure 6.4. The correlation between Kiss-1 transcript levels and TNM stage. The expression of Kiss-1 in TNM stage Ⅲ (p= 0.009), stage ⅢC (p= 0.003), stage Ⅱ&Ⅲ (p= 0.000.016), stage Ⅲ&Ⅳ (p= 0.009) and stage Ⅱ&Ⅲ&Ⅳ (p= 0.015) all showed the significant decreases in comparison with that in stage Ⅰ. Colorectal cancer TNM stage Ⅲ has been divided into ⅢA (T1 –T2, N1/N1c, M0 or T1, N2a, M0), ⅢB (T3-T4a, N1/N1c, M0 or T2-T3, N2a, M0 or T1-T2, N2b, M0) and ⅢC (T4a, N2a, Mo or T3-T4a, N2b, M0 or T4b, N1-N2, M0) by AJCC in 2010. Asterisks represented for p< 0.05

6.3.6 The expression of Kiss-1R in tumour tissues and normal background tissues

The expression of Kiss-1R transcript was examined in the specimens of 81 colorectal adenocarcinoma patients using by real-time quantitative PCR (expressed as median Kiss-1R transcript levels/50 ng mRNA and all the data has been normalized by GAPDH). A significantly decreased mRNA expression level of Kiss-1R was observed in tumour tissues compared with the normal background tissues (Table 6.3) and in paired tumour and normal background tissues (Table 6.4).

Table 6.3. The correlation of Kiss-1R expression in tumour tissues compared with normal background tissues; transcript normalized by GAPDH (shown as Kiss-1R: GAPDH ratio). *P*< 0.0001.

Statistic	Normal	Tumour
q1	1	<0.000001
min	90	<0.000001
median	30	<0.000001
max	1704709	447209
q3	2406	<0.000001

Table 6.4. The relationship of Kiss-1R expression in paired tumour tissues and in paired normal background tissues; transcript normalized by GAPDH (shown as Kiss-1R: GAPDH ratio). *P*< 0.0001.

Statistic	Paired normal	Paired tumour
q1	<0.000001	<0.000001
min	<0.000001	<0.000001
median	23	<0.000001
max	809996	133.36
q3	522	0.02

6.3.7 The correlation of Kiss-1R expression with clinical outcome

Compared with levels in disease free patients, an enhanced expression of Kiss-1R was associated with patient morbidity over the follow up period (Figure 6.5). A significant difference was observed in the expression levels between alive patients and those who had died (Table 6.5). Interestingly, Kiss-1R expression in those patients undergoing chemo-radio therapy was conspicuously high in comparison with that in patients without therapy (Table 6.6).

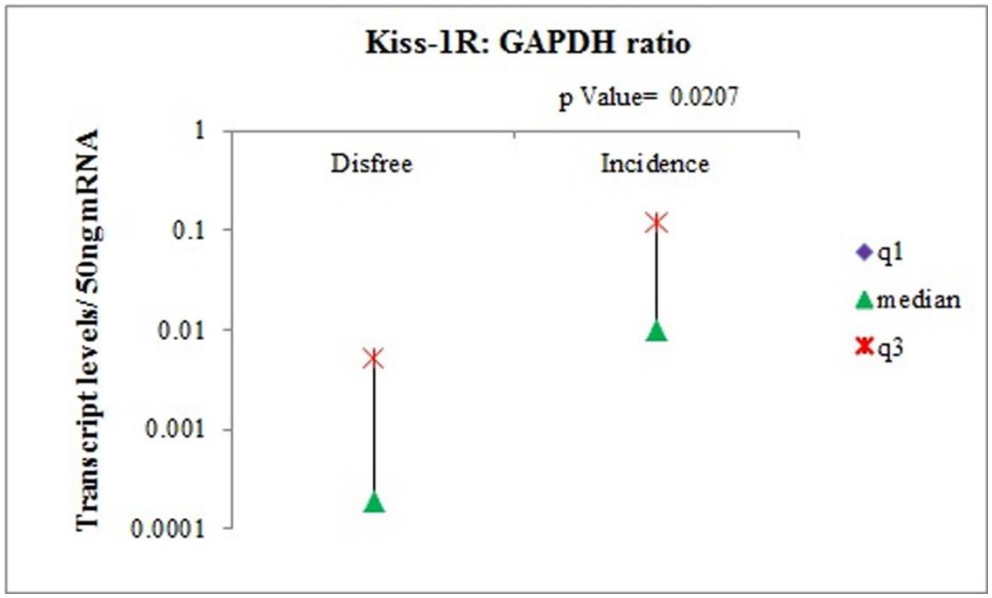

Statistic	Disfree	Incidence
q1	<0.000001	<0.000001
min	<0.000001	<0.000001
median	0.00019	0.01
max	0.22669	41.73
q3	0.00523	0.12

Figure 6.5. The correlation of Kiss-1R expression in new morbidity crowd compared with the patients who remained disease free; transcript normalized by GAPDH (shown as Kiss-1R: GAPDH ratio).

Table 6.5. The correlation of Kiss-1R expression in the alive patients and those who died; transcript normalized by GAPDH (shown as Kiss-1R: GAPDH ratio). *P*=0.0158

Statistic	Alive	Dead
q1	<0.000001	<0.000001
min	<0.000001	<0.000001
median	0.00028	<0.000001
max	0.22669	41.73
q3	0.00724	0.13

Table 6.6. The correlation of Kiss-1R expression in the patients without therapy and the patients with chem-radio therapy; transcript normalized by GAPDH (shown as Kiss-1R: GAPDH ratio). *P*= 0.0115

Statistic	Nontreat	Chemo-radio
q1	<0.000001	0.012
min	<0.000001	<0.000001
median	0.0002	0.0796
max	0.1719	6.354
q3	0.006	0.1607

6.3.8 Correlation between Kiss-1 expression and prognosis

Patients were divided into groups using Dukes classification as a general guide. If the levels of Kiss-1 and Kiss-1R transcripts in tumour samples are higher than the tumour samples with Duke B, the samples will be considered as having a high level described as Figure 6.6.A and B and Figure 6.7.A and B. Kaplan-Meier survival analysis demonstrated that patients with a low expression level of Kiss-1 had lower overall survival, being 120.340 months (95%C.I. 97.287- 143.392 months), compared with 136.275 months (95%C.I. 111.031- 161.520 months) of patients with high expression of Kiss-1 (Figure 6.6.A). In regards to disease free survival, a poor survival rate was observed in the group with low expression levels of Kiss-1 in comparison with the high expression levels (Figure 6.6.B). However, all of the data above did not demonstrated statistical significance ($p > 0.05$).

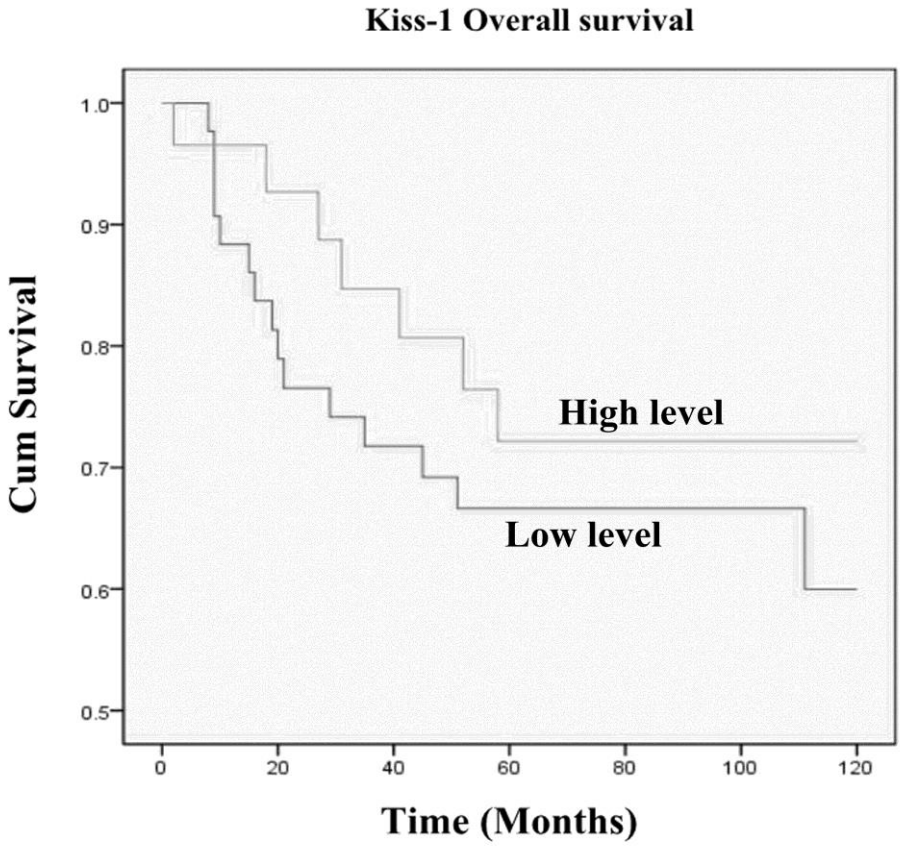

Figure 6.6.A. The Kaplan-Meier survival model of correlation between Kiss-1 transcript levels and overall survival. Patients with low levels of Kiss-1 had a relatively poor disease free survival (median=120.340 months, 95% C.I. 97.287-143.392 months) compared with those with higher levels (median= 136.275 months, 95%C.I. 111.031- 161.520 months) (p> 0.05).

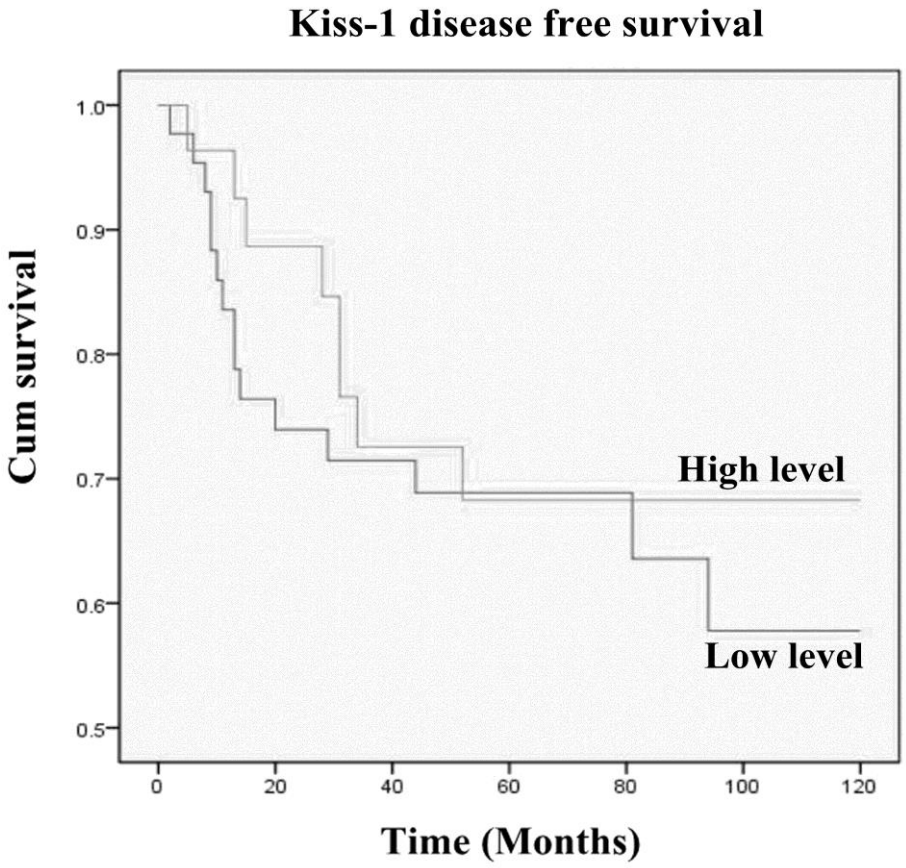

Figure 6.6.B. The Kaplan-Meier survival model of correlation between Kiss-1 transcript levels and the disease free survival.

6.3.9 Increased Kiss-1R is correlated with poor prognosis

By contrast to Kiss-1, the expression pattern of Kiss-1R revealed the opposed relationship with prognosis in both overall survival and disease free survival. Patients with high levels of Kiss-1R {median: 85.798 (95%C.I. 49.989- 121.606)} had a significantly shorter overall survival in comparison with those with low levels {median: 142.987 (95%C.I. 124.261- 161.712)} (p= 0.011) (Figure 6.7.A). Figure 6.7.B showed the high expression of Kiss-1R transcripts was also associated with poor prognosis in disease free survival. The patients with lower expression of Kiss-1R had longer disease free survival {median: 133.176 (95%C.I. 111.675- 154.676)} compared with those with high expression levels in {median: 88.347 (95%C.I. 50.108- 126.587)} (p= 0.033).

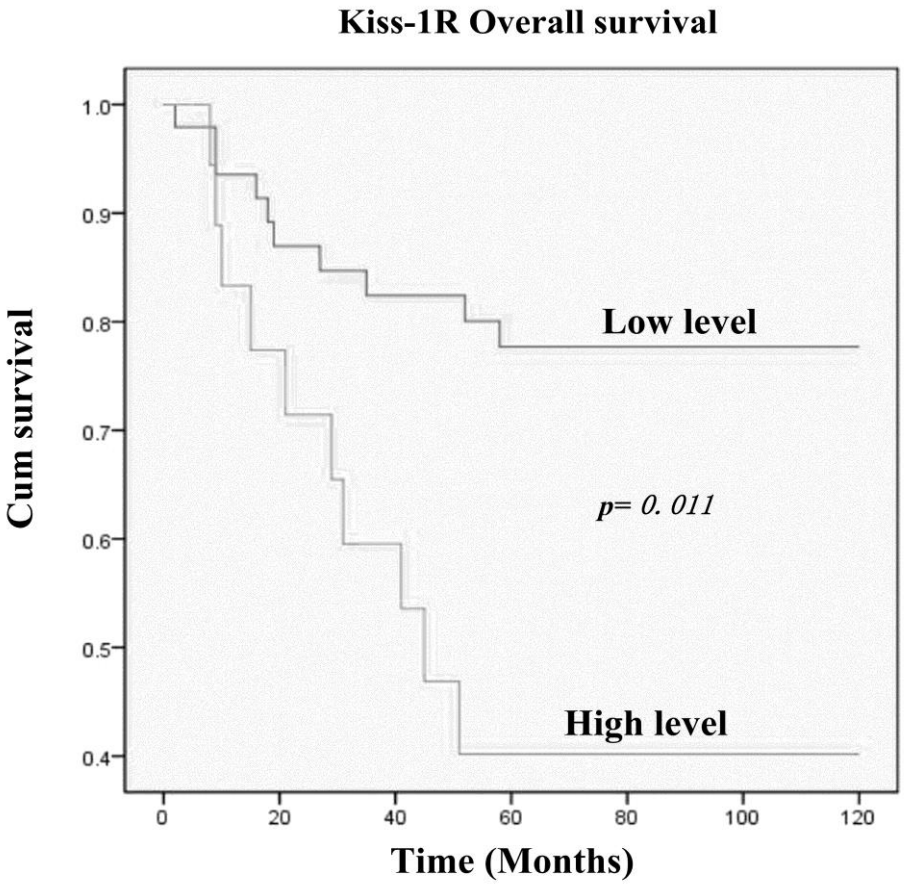

Figure 6.7.A. Kaplan- Meier survival analysis displaying relationship between the transcript levels of Kiss-1R and overall survival. Patients with high levels of Kiss-1R had a remarkably shorter overall survival (median= 85.798 months, 95%C.I. 49.989-121.606) compared with those with lower levels (median= 142.987 months, 95% C.I. 124.261- 161.712) (p= 0.011).

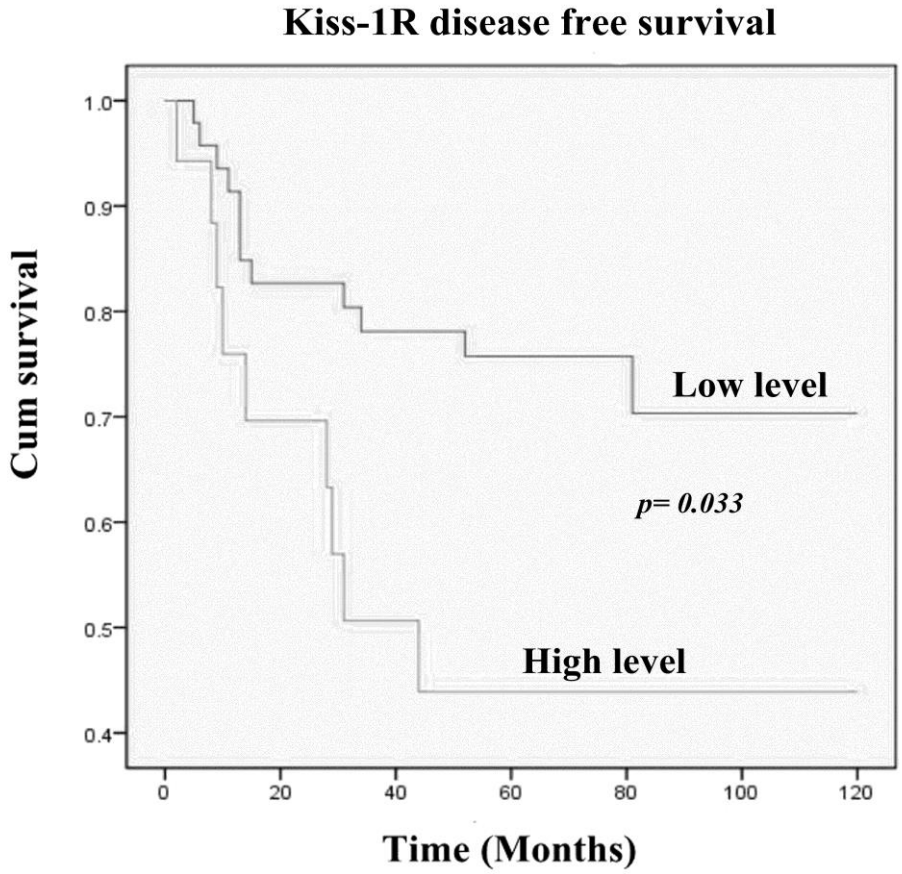

Figure 6.7.B. Kaplan- Meier survival analysis displaying the relationship between the transcript levels of Kiss-1R and overall survival. Patients with high levels of Kiss-1R had a remarkably shorter overall survival (median= 88.347 months, 95%C.I. 50.108-126.587) compared with those with lower levels (median= 133.176 months, 95%C.I. 111.675- 154.676) (*p*= 0.033).

6.3.10 Multivariate analysis of Kiss-1 and Kiss-1R as prognostic factors.

Through multivariate analysis, we attempted to find out if Kiss-1 and Kiss-1Rare independent prognostic factors. Table 6.7 showed the correlation of colorectal related death and T staging and Kiss-1R respectively had statistical significance. TNM staging and Kiss-1R are also independent factors for colorectal cancer related incidence (table 6.8).

Table 6.7. Multifactors against colorectal cancer related death

Dependent variables	Type III Sum of square	df	Mean Square	F	Sig.
Invasion	.547	2	.273	1.155	.322
Location	.485	2	.243	.187	.830
Dukes	.604	2	.302	.687	.507
Tstage	3.377	2	1.688	3.938	.025
TNM	16.216	2	8.108	1.990	.146
Node	2.004	2	1.002	1.507	.230
Differentiation	.222	2	.111	.514	.601
Kiss-1	.422	2	.211	.844	.435
Kiss-1R	2.142	2	1.071	6.302	.003

Table 6.8. Multifactors against colorectal cancer incidence (death, recurrence and metastasis)

Dependent variables	Type III Sum of square	df	Mean Square	F	Sig.
Invasion	.731	3	.244	1.010	.396
Location	3.249	3	1.083	.856	.470
Dukes	1.829	3	.610	1.415	.249
Tstage	3.102	3	1.034	2.258	.092
TNM	36.942	3	12.314	3.216	.030
Node	5.074	3	1.691	2.669	.057
Differentiation	.768	3	.256	1.181	.326
Kiss-1	.523	3	.174	.683	.566
Kiss-1R	2.126	3	.709	4.003	.012

6.4 Discussion

Since being suggested as a novel metastasis suppressor in human melanoma and breast cancer cells [61, 71], Kiss-1 has been detected in various cancers through the analysis of real-time Quantitative PCR . Reduced expression of Kiss-1 was observed in gastric cancer, oesophageal carcinoma, pancreatic cancer, ovarian cancer, bladder cancer and prostate cancer [80, 83, 90]. These studies suggest that the Kiss-1 gene may act as a metastasis suppressor in those cancers. What is more, it also has been reported that Kiss-1 expression correlated with several clinical and histopathological parameters. For example, Kiss-1 was suggested as an independent predictor of patient survival in comparison with the traditional prognostic predictors of gastric cancer, as its expression had a relationship with frequent metastases and tumour recurrence [80]. Schmid and colleagues, on the other hand, have also reported that Kiss-1 may be a prognosis factor in hepatocellular carcinoma (HCCs), as its increased expression was related to poor prognosis [87].

However, the expression of Kiss-1 and its receptor (Kiss-1R) and their correlation to the clinical outcome in colorectal cancer remains unknown. For this purpose, we investigated Kiss-1 and Kiss-1R expression in 171 (normal background= 80; tumour= 94) samples of which 136 were paired samples (n=68 pairs) of patients with colorectal adenocarcinoma using real-time PCR. There was no significant links between the expression of Kiss-1 in normal background tissues compared with tumour tissues, while its expression was correlated significantly with Dukes and TNM

staging, tumour stage and lymph node involvement. Kiss-1 expression was down-regulated in all the advanced stages mentioned. The relatively small sample size likely accounted for the lack of statistical significance between Kiss-1 in adjacent tissues and tumour tissues. In contrast to Kiss-1, there was statistical significance between Kiss-1R expression in normal background and tumour tissues, in which Kiss-1R expression was significantly decreased in tumour tissues compared with adjacent normal tissues ($p< 0.0001$). By compared with Kiss-1, Kiss-1R did not show any correlation with clinical classification of colorectal cancer ($p> 0.05$), while loss of Kiss-1R expression was significantly associated with death and no chemo-radio therapy) ($p< 0.05$). By contrast, the increased expression of Kiss-1R had positive correlation with colorectal incidence ($p= 0.0207$). These results suggested that Kiss-1R may be a poor prognostic factor. Using multivariate analysis, we discovered that Kiss-1R had strong correlation with any colorectal death and poor clinical outcome. These prompted that Kiss-1R, T staging and TNM staging could be independent prognostic factors. Kiss-1R was found to be more sensitive than other dependent variables. These results indicate that Kiss-1 and Kiss-1R may play the role as a tumour suppressor in colorectal cancer. In the meantime, the decreased expression of Kiss-1 was relevant to Duke staging, TNM staging and possibly acts as a poor prognosis factor.

Chapter 7

General discussion

Metastasis, as a complex multistep process, includes impairment of cell-cell adhesion in neoplastic epithelium, invasion of adjacent tissues and dissemination of cancer cells through the manner of lymphatic and haematogenous metastasis [132-133]. To block the metastatic process at an early stage has become a hot subject in cancer research [134]. Hence, we are interested in identifying metastasis suppressor genes, which may have the potential to control the dissemination of cancer cells. Kiss-1 gene, initially described as a metastasis suppressor in melanoma cancer [61], encodes a number of peptides (e.g. Kisspeptin-10, Kisspeptin-13, Kisspeptin-14 and Kisspeptin-54). These peptides are endogenous ligands of Kiss-R, which is a G protein-coupled receptor, referred as hOT7T175, AXOR12 or GPR54. The Kiss-1 gene has been suggested as a suppressor of metastasis in a variety of cancers through the regulation of cellular migration and invasion [48].

Influence of Kiss-1 and Kiss-1R on the functions (proliferation, adhesion, invasion and migration) of colorectal cancer cells

The data obtained from the present study suggests that Kiss-1 significantly inhibits the motility and invasion of HT115 and HRT18 colorectal cancer cells, but has no effects on the proliferation and adhesion of HT115 and HRT18 cells. These results are consistent with the previous studies in breast cancer, ovarian cancer and prostate cancer [50, 71, 95]. Interestingly, the similar increase of cell migration in Kiss-1R knockdown cells compared with the controls was not observed in both HT115 and

HRT18 cells. From this one hypothesis suggested that the inhibitory effect of Kiss-1 on colorectal cancer cells may not completely combine with Kiss-1R but other unkown receptors. The motility of Kiss-1R knockdown cells would increase as same as the Kiss-1 knockdown cells, if Kiss-1 indeed had the inhibitory influence on cell migration through the combination with Kiss-1R, as Kiss-1 would not regulate the cell migration in Kiss-1R knockdown cells. While the result that slight difference of cell migration between the Kiss-1R knockdown cells and the control cells supported this hypothesis.

The inhibition of cell migration via treating with Kisspeptin-10 and ERK inhibitor

Several studies have suggested that the mechanism by which Kiss-1 inhibits metastasis may involve the extracellular-regulated kinase 1/2 (ERK1/2) phosphorylation and decreased matrix metalloproteinase-2 (MMP-2) expression [74, 90, 135]. In addition, Yan and *et al.* reported that Kisspeptin-10/Kiss-1R activation can dephosphorylate nuclear factor kappa B (NF-Kappa B), so that cause it to dissociate from MMP-9 promoter. This process ultimately results in a decrease of MMP-9 expression in the placenta [73]. However, relevant research was needed to delineate the signaling pathways in the colorectal cancer cells. As a contribution to this endeavour, we have examined the effects of Kisspeptin-10 and ERK inhibitor on the migration ability of HT115 pEF, HT115 Kiss-1 knockdown and HT115 Kiss-1R

knockdown cells using ECIS assays (The details have been described in Chapter 4).Kisspeptin-10, a short peptide of 10 amino acids, is proteolytically processed from Kiss-1. Kisspeptin-10 is ten times as active as Kiss-1 [136]. The results demonstrate the migration ability of HT115 pEF and Kiss-1 knockdown cells treated with Kisspeptin-10 decreased strongly compared with the control groups ($p< 0.05$). This result is consistent with the previous *in vitro* function assays and provides further evidence that Kiss-1 indeed inhibits the migration of colorectal cancer cells. The decreased migration of cells treated with ERK inhibitor compared with the controls pointed out that the regulation of Kiss-1/Kiss-1R system on colorectal cancer cells may be via ERK signalling pathway.

The inhibitory effect of Kiss-1 on tumour growth in *in vivo* animal model

We detected the influence of Kiss-1 knockdown on tumour growth in an *in vivo* tumour model. It was observed the tumour growth of Kiss-1 knockdown cells increased remarkably in comparison with the control group during the 7 week period, especially at 22^{th} ($p= 0.034882$), 29^{th} ($p= 0.009967$) and 36^{th} ($p= 0.039235$) days. This result indicates a potential therapeutic value of Kiss-1 and its analogue (Kisspeptin-10). However, the present *in vivo* model and *in vivo* results are far from satisfactory. Firstly, the size of the tumours seen in the present study were rather small and secondly, tumours in both control and Kiss-1 knockdown groups tend to get smaller after two weeks of implantation. The main reason for these results is that

HT115 has been rarely used in *in vivo* studies and we have not been able to find literature support for the experimental conditions. At the time of these experiments, the available cells were rather limited, due to time constrains. In future studies, it will be necessary to conduct an experiment by using a much larger cell number for injection.

Kiss-1/Kiss-1R negatively regulated cell invasion/motility by inhibiting MMP-9 via the ERK signaling pathway.

Kiss-1 significantly inhibits the motility and invasion of HT115 cells. It is clear that this action is at least partly mediated by regulating the activity of MMP9. The study further indicates that this effect on MMP-9 is via the ERK pathway rather than the JNK pathway. In summary, it is suggested that Kiss-1 inhibits ERK activation via Kiss-1R and consequently reduces the enzymatic activity of MMP-9 caused by the degradation of NF-κB, which contributes to the suppression of tumour metastasis (Figure 7.1).

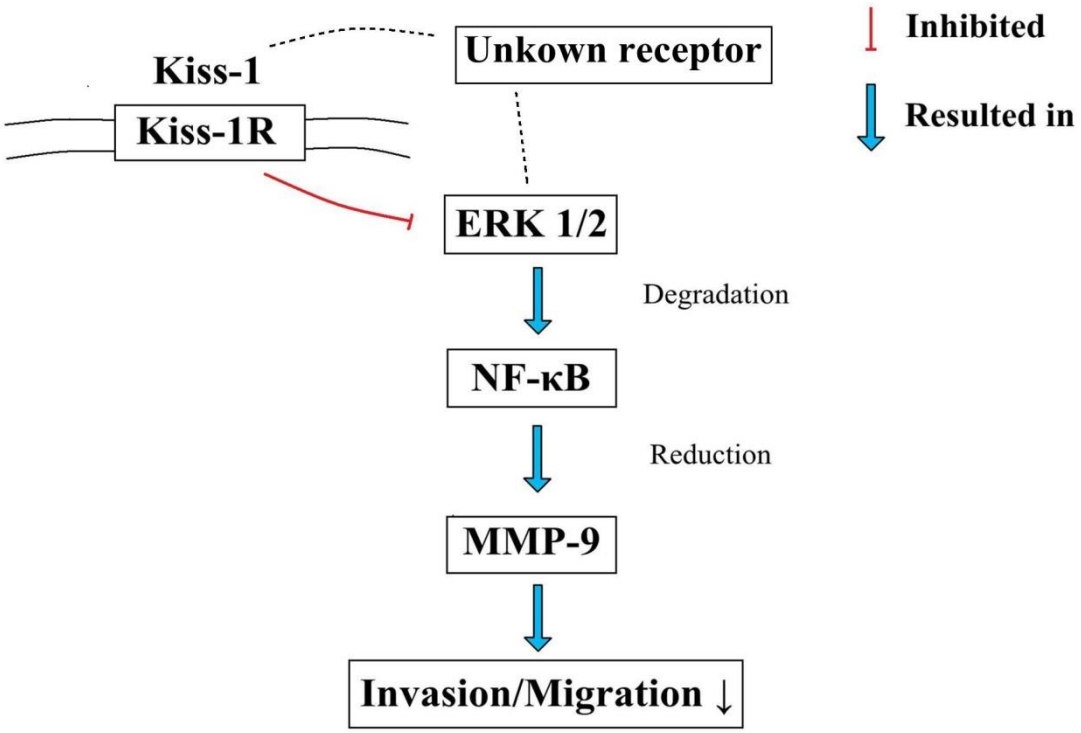

Figure 7.1. Potential interacting pathways and molecules involved in the functions of Kiss-1 and Kiss-1R in colorectal cancer cells.

Aberrant expression of Kiss-1/Kiss-1R in colorectal cancer

Next, our study focused on analyzing the quantitative expression levels of Kiss-1 and Kiss-1R mRNAs and protein using real-time Q-PCR. The expression of Kiss-1 was correlated significantly with Dukes classification, TNM staging, tumour stage and lymph node involvement. Interestingly, these stages are classified by the level of tumour invasion and metastasis. Hence, the conclusion from clinical cohort was consistent with the previous study: Kiss-1 has a significant and negative correlation with tumour metastasis and invasion. Loss of Kiss-1R expression was significantly associated with disease free compared with the incidence group, while the increased expression of Kiss-1R may have positive correlation with alive compared with the

death groups (0.0158). Moreover, high expression of Kiss-1R transcripts was associated with poor prognosis in both overall survival (p= 0.011) and disease free survival (p=0.033) compared with low expression of Kiss-1R clinically. Aberrant expression of Kiss-1 and Kiss-1R expression is definitely a point for consideration. One hypothesis is that there may be another unknown receptor involved in Kiss-1 regulation of colorectal cancer cells or there may be another ligand with Kiss-1R. Navenot *et al.* reported that the Kiss-1/Kiss-1R also influenced signaling events by interacting with the chemokine receptor (CXCR4) and the gonadotrophin-releasing hormone receptor [137].

Perhaps the most intriguing property of Kiss-1 is how it could be exploited clinically. In the future we are interested in investigating the influence of Kisspeptin-10 on tumour growth and metastasis based on our previous studies in an *in vivo* tumour model. What is more, Ziegler *et al.* reported that anti-proliferative function of Kisspeptin-10 was regulated by the expression levels of Kiss-1R [138]. There was no effect on proliferation observed in the breast cancer cells expressing Kiss-1R endogenously, while Kisspeptin-10 had a significant inhibition on proliferation of transfected neuronal cells over-expressing Kiss-1R [138]. Hence, to detect the influence of Kisspeptin-10 on colorectal cancer through changing Kiss-1R's expression levels will be the subjects of follow-up studies.

In conclusion, the present thesis has presented evidence that Kiss-1 is a putative tumour suppressor molecule in human colorectal cancer. This is seen by its inhibitory effect on the migration and invasion of the cells, on actions achieved by downregulating the activities of MMP9, via a ERK dependent pathway. The preliminary data from in vivo tumour model and studies on a clinical cohort of colorectal cancer patients supports this argument.

Future directions:

The present study has further demonstrated the pivotal role of Kiss-1 and Kiss-1 receptor in human colorectal cancer. However, the study has also raised more questions and points to new directions for future research.

1. Future research need to base upon more large clinical samples, so that to investigate the expression of Kiss-1 and Kiss-1R in tumour tissue compared with normal tissue at the protein level using IHC.
2. The role of Kiss-1 the downstream of Kiss-1 receptor. Although the present study has shown that Kiss-1 regulates the MMP-9, the exact mechanism by which Kiss-1 leads to this regulation is not clear. It will be useful in the future to investigate transcriptional regulation and possible post-translational regulation for MMP-9 in this context.

3. Other potential receptors for Kiss-1 and the contribution of these potential receptors to the tumour suppressive role of Kiss-1. The complex nature of cell response to Kiss-1 has indicated that there may be more receptors for Kiss-1 involved. This has been demonstrated in some recent studies. To clarify this aspect is highly useful in determining the role of the molecule in the regulation in colorectal cancer and other tumour types.

4. The potential therapeutic implications of the Kiss-1 agonists in cancer. In most cancer types, Kiss-1 has been shown to act as a tumour suppressor. It will be highly useful to investigate if specific activation of Kiss-1 may have therapeutic implications. Although the present study was aimed at this aspect, the time restraint and availability of Kiss-1 and Kiss-1 agonist made this evaluation impossible. It will be a highly practical study to pursue.

5. Investigation of the mutation of Kiss-1 receptor mutation in human cancers. This would allow an understanding into the genetic and biological impact of the receptor complex in a clinical context, either for therapeutic or prognostic considerations.

Chapter 8

References

References

1. Roy, P. and R. Last, *Colorectal cancer.* Clin Evid, 2005(14): p. 551-6.
2. Parkin, D.M., et al., *Global cancer statistics, 2002.* CA Cancer J Clin, 2005. **55**(2): p. 74-108.
3. Jemal, A., et al., *Cancer statistics, 2010.* CA Cancer J Clin, 2010. **60**(5): p. 277-300.
4. Koh, E., V. Do, and M. Barton, *Frontiers of cancer care in Asia-Pacific region: cancer care in Australia.* Biomed Imaging Interv J, 2008. **4**(3): p. e30.
5. Genega, E.M., et al., *Impact of the 1998 World Health Organization/International Society of Urological Pathology classification system for urothelial neoplasms of the kidney.* Mod Pathol, 2005. **18**(1): p. 11-8.
6. CR-UK, *Statistics.* http://www.cancerresearchuk.org/cancer-info/cancerstats/types/bowel/incidence/uk-bowel-cancer-incidence-statistics, 2012.
7. Jemal, A., et al., *Global patterns of cancer incidence and mortality rates and trends.* Cancer Epidemiol Biomarkers Prev, 2010. **19**(8): p. 1893-907.
8. Lieberman, D.A., et al., *Patterns of endoscopy use in the United States.* Gastroenterology, 2000. **118**(3): p. 619-24.
9. Parkin, D.M., P. Pisani, and J. Ferlay, *Global cancer statistics.* CA Cancer J Clin, 1999. **49**(1): p. 33-64, 1.
10. Brown, M.O., A.P. Lanier, and T.M. Becker, *Colorectal cancer incidence and survival among Alaska Natives, 1969-1993.* Int J Epidemiol, 1998. **27**(3): p. 388-96.
11. Nelson, R.L., V. Persky, and M. Turyk, *Determination of factors responsible for the declining incidence of colorectal cancer.* Dis Colon Rectum, 1999. **42**(6): p. 741-52.
12. Chung, D.C. and A.K. Rustgi, *The hereditary nonpolyposis colorectal cancer syndrome: genetics and clinical implications.* Ann Intern Med, 2003. **138**(7): p. 560-70.
13. Marra, G. and C.R. Boland, *Hereditary nonpolyposis colorectal cancer: the syndrome, the genes, and historical perspectives.* J Natl Cancer Inst, 1995. **87**(15): p. 1114-25.
14. Powell, S.M., et al., *Molecular diagnosis of familial adenomatous polyposis.* N Engl J Med, 1993. **329**(27): p. 1982-7.
15. Chen, Y., et al., *Structural studies of initial lymphatics adjacent to gastric and colonic malignant neoplasms.* Lymphology, 1999. **32**(2): p. 70-4.
16. Colquhoun, P.H. and S.D. Wexner, *Surgical management of colon cancer.* Curr Gastroenterol Rep, 2002. **4**(5): p. 414-9.
17. Shatari, T., et al., *Vascular anatomy for right colon lymphadenectomy.* Surg Radiol Anat, 2003. **25**(2): p. 86-8.
18. Edge, S.B. and C.C. Compton, *The American Joint Committee on Cancer: the 7th edition of the AJCC cancer staging manual and the future of TNM.* Ann Surg Oncol, 2010. **17**(6): p. 1471-4.
19. Stein, W., et al., *Characteristics of colon cancer at time of presentation.* Fam Pract Res J, 1993. **13**(4): p. 355-63.
20. Majumdar, S.R., R.H. Fletcher, and A.T. Evans, *How does colorectal cancer present? Symptoms, duration, and clues to location.* Am J Gastroenterol, 1999. **94**(10): p. 3039-45.

21. Stotland, B.R., et al., *Preoperative and postoperative imaging for colorectal cancer.* Hematol Oncol Clin North Am, 1997. **11**(4): p. 635-54.

22. Rocklin, M.S., A.J. Senagore, and T.M. Talbott, *Role of carcinoembryonic antigen and liver function tests in the detection of recurrent colorectal carcinoma.* Dis Colon Rectum, 1991. **34**(9): p. 794-7.

23. Nollau, P., et al., *Enrichment of mutant alleles by chromatographic removal of wild type alleles: a new principle for the detection of alleles with unknown point mutations at excess of wild type alleles.* Clin Chem Lab Med, 1999. **37**(9): p. 877-81.

24. Beck, D.E., *Laparoscopy and endoscopy.* Clin Colon Rectal Surg, 2010. **23**(1): p. 3.

25. Soreide, K., et al., *Endoscopy, morphology, morphometry and molecular markers: predicting cancer risk in colorectal adenoma.* Expert Rev Mol Diagn, 2009. **9**(2): p. 125-37.

26. Roy, H.K., et al., *Colonoscopy and optical biopsy: bridging technological advances to clinical practice.* Gastroenterology, 2011. **140**(7): p. 1863-7.

27. Moss, A.A., et al., *A uniform, CT-based staging system for malignant neoplasms of the alimentary tube.* AJR Am J Roentgenol, 1981. **136**(6): p. 1251-2.

28. Fenlon, H.M., et al., *A comparison of virtual and conventional colonoscopy for the detection of colorectal polyps.* N Engl J Med, 1999. **341**(20): p. 1496-503.

29. Sonnenberg, A., F. Delco, and P. Bauerfeind, *Is virtual colonoscopy a cost-effective option to screen for colorectal cancer?* Am J Gastroenterol, 1999. **94**(8): p. 2268-74.

30. Morrin, M.M. and J.T. LaMont, *Screening virtual colonoscopy--ready for prime time?* N Engl J Med, 2003. **349**(23): p. 2261-4.

31. Pickhardt, P.J., et al., *Computed tomographic virtual colonoscopy to screen for colorectal neoplasia in asymptomatic adults.* N Engl J Med, 2003. **349**(23): p. 2191-200.

32. Willett, C.G., B.G. Czito, and D.S. Tyler, *Intraoperative radiation therapy.* J Clin Oncol, 2007. **25**(8): p. 971-7.

33. Kleihues, P. and L.H. Sobin, *World Health Organization classification of tumors.* Cancer, 2000. **88**(12): p. 2887.

34. Jessup, J.M., et al., *The National Cancer Data Base. Report on colon cancer.* Cancer, 1996. **78**(4): p. 918-26.

35. Moertel, C.G., et al., *Levamisole and fluorouracil for adjuvant therapy of resected colon carcinoma.* N Engl J Med, 1990. **322**(6): p. 352-8.

36. Carraro, P.G., et al., *Obstructing colonic cancer: failure and survival patterns over a ten-year follow-up after one-stage curative surgery.* Dis Colon Rectum, 2001. **44**(2): p. 243-50.

37. Andre, T., et al., *Oxaliplatin, fluorouracil, and leucovorin as adjuvant treatment for colon cancer.* N Engl J Med, 2004. **350**(23): p. 2343-51.

38. Kohnoe, S., Y. Kakeji, and Y. Maehara, *[Progress in adjuvant therapy for colorectal cancer].* Gan To Kagaku Ryoho, 2002. **29**(13): p. 2488-97.

39. Dorudi, S., R.J. Steele, and C.S. McArdle, *Surgery for colorectal cancer.* Br Med Bull, 2002. **64**: p. 101-18.

40. Shimada, Y., et al., *[Radiation-induced colorectal cancer: second primary cancer after radiotherapy].* Nihon Rinsho, 2011. **69 Suppl 3**: p. 126-32.

41. Kerr, D.J., et al., *Intrahepatic arterial versus intravenous fluorouracil and folinic acid for colorectal cancer liver metastases: a multicentre randomised trial.* Lancet, 2003. **361**(9355): p. 368-73.

42. Hecht, J.R., et al., *Lack of correlation between epidermal growth factor receptor status and response to Panitumumab monotherapy in metastatic colorectal cancer.* Clin Cancer Res, 2010. **16**(7): p. 2205-13.

43. Leichman, C.G., et al., *Quantitation of intratumoral thymidylate synthase expression predicts for disseminated colorectal cancer response and resistance to protracted-infusion fluorouracil and weekly leucovorin.* J Clin Oncol, 1997. **15**(10): p. 3223-9.

44. Metzger, R., et al., *High basal level gene expression of thymidine phosphorylase (platelet-derived endothelial cell growth factor) in colorectal tumors is associated with nonresponse to 5-fluorouracil.* Clin Cancer Res, 1998. **4**(10): p. 2371-6.

45. Salonga, D., et al., *Colorectal tumors responding to 5-fluorouracil have low gene expression levels of dihydropyrimidine dehydrogenase, thymidylate synthase, and thymidine phosphorylase.* Clin Cancer Res, 2000. **6**(4): p. 1322-7.

46. Iqbal, S. and H.J. Lenz, *Targeted therapy and pharmacogenomic programs.* Cancer, 2003. **97**(8 Suppl): p. 2076-82.

47. McLeod, H.L., *Individualized cancer therapy: molecular approaches to the prediction of tumor response.* Expert Rev Anticancer Ther, 2002. **2**(1): p. 113-9.

48. Ohtaki, T., et al., *Metastasis suppressor gene KiSS-1 encodes peptide ligand of a G-protein-coupled receptor.* Nature, 2001. **411**(6837): p. 613-7.

49. Sanchez-Carbayo, M., et al., *Tumor suppressor role for myopodin in bladder cancer: loss of nuclear expression of myopodin is cell-cycle dependent and predicts clinical outcome.* Oncogene, 2003. **22**(34): p. 5298-305.

50. Wang, H., et al., *Clinical and biological significance of KISS1 expression in prostate cancer.* Am J Pathol, 2012. **180**(3): p. 1170-8.

51. Cutait, R., et al., *[The value of colonoscopy in low digestive hemorrhages of unexplained cause: analysis of 132 patients].* Rev Paul Med, 1980. **96**(3-4): p. 66-8.

52. Clevers, H., *Wnt/beta-catenin signaling in development and disease.* Cell, 2006. **127**(3): p. 469-80.

53. Lee, E., et al., *The roles of APC and Axin derived from experimental and theoretical analysis of the Wnt pathway.* PLoS Biol, 2003. **1**(1): p. E10.

54. Sparks, A.B., et al., *Mutational analysis of the APC/beta-catenin/Tcf pathway in colorectal cancer.* Cancer Res, 1998. **58**(6): p. 1130-4.

55. Morin, P.J., et al., *Activation of beta-catenin-Tcf signaling in colon cancer by mutations in beta-catenin or APC.* Science, 1997. **275**(5307): p. 1787-90.

56. Romagnolo, B., et al., *Intestinal dysplasia and adenoma in transgenic mice after overexpression of an activated beta-catenin.* Cancer Res, 1999. **59**(16): p. 3875-9.

57. Messerini, L., A. Palomba, and G. Zampi, *Primary signet-ring cell carcinoma of the colon and rectum.* Dis Colon Rectum, 1995. **38**(11): p. 1189-92.

58. Yerushalmi, H.F., et al., *Role of polyamines in arginine-dependent colon carcinogenesis in Apc(Min) (/+) mice.* Mol Carcinog, 2006. **45**(10): p. 764-73.

59. Mehlen, P., et al., *The DCC gene product induces apoptosis by a mechanism requiring receptor proteolysis.* Nature, 1998. **395**(6704): p. 801-4.

60. Welch, D.R., et al., *Microcell-mediated transfer of chromosome 6 into metastatic human C8161 melanoma cells suppresses metastasis but does not inhibit tumorigenicity.* Oncogene, 1994. **9**(1): p. 255-62.

61. Lee, J.H., et al., *KiSS-1, a novel human malignant melanoma metastasis-suppressor gene.* J Natl Cancer Inst, 1996. **88**(23): p. 1731-7.

62. Lee, J.H. and D.R. Welch, *Identification of highly expressed genes in metastasis-suppressed chromosome 6/human malignant melanoma hybrid cells using subtractive hybridization and differential display.* Int J Cancer, 1997. **71**(6): p. 1035-44.

63. Bilban, M., et al., *Kisspeptin-10, a KiSS-1/metastin-derived decapeptide, is a physiological invasion inhibitor of primary human trophoblasts.* J Cell Sci, 2004. **117**(Pt 8): p. 1319-28.

64. Kotani, M., et al., *The metastasis suppressor gene KiSS-1 encodes kisspeptins, the natural ligands of the orphan G protein-coupled receptor GPR54.* J Biol Chem, 2001. **276**(37): p. 34631-6.

65. Miele, M.E., et al., *A human melanoma metastasis-suppressor locus maps to 6q16.3-q23.* Int J Cancer, 2000. **86**(4): p. 524-8.

66. Shirasaki, F., et al., *Loss of expression of the metastasis suppressor gene KiSS1 during melanoma progression and its association with LOH of chromosome 6q16.3-q23.* Cancer Res, 2001. **61**(20): p. 7422-5.

67. Goldberg, S.F., et al., *Melanoma metastasis suppression by chromosome 6: evidence for a pathway regulated by CRSP3 and TXNIP.* Cancer Res, 2003. **63**(2): p. 432-40.

68. Lee, D.K., et al., *Discovery of a receptor related to the galanin receptors.* FEBS Lett, 1999. **446**(1): p. 103-7.

69. Muir, A.I., et al., *AXOR12, a novel human G protein-coupled receptor, activated by the peptide KiSS-1.* J Biol Chem, 2001. **276**(31): p. 28969-75.

70. Hori, A., et al., *Metastin suppresses the motility and growth of CHO cells transfected with its receptor.* Biochem Biophys Res Commun, 2001. **286**(5): p. 958-63.

71. Lee, J.H. and D.R. Welch, *Suppression of metastasis in human breast carcinoma MDA-MB-435 cells after transfection with the metastasis suppressor gene, KiSS-1.* Cancer Res, 1997. **57**(12): p. 2384-7.

72. Lee, K.H. and J.R. Kim, *Kiss-1 suppresses MMP-9 expression by activating p38 MAP kinase in human stomach cancer.* Oncol Res, 2009. **18**(2-3): p. 107-16.

73. Yan, C., H. Wang, and D.D. Boyd, *KiSS-1 represses 92-kDa type IV collagenase expression by down-regulating NF-kappa B binding to the promoter as a consequence of Ikappa Balpha -induced block of p65/p50 nuclear translocation.* J Biol Chem, 2001. **276**(2): p. 1164-72.

74. Ringel, M.D., et al., *Metastin receptor is overexpressed in papillary thyroid cancer and activates MAP kinase in thyroid cancer cells.* J Clin Endocrinol Metab, 2002. **87**(5): p. 2399.

75. Mitchell, D.C., et al., *Transcriptional regulation of KiSS-1 gene expression in metastatic melanoma by specificity protein-1 and its coactivator DRIP-130.* Oncogene, 2007. **26**(12): p. 1739-47.

76. Marot, D., et al., *High tumoral levels of Kiss1 and G-protein-coupled receptor 54 expression are correlated with poor prognosis of estrogen receptor-positive breast tumors.* Endocr Relat Cancer, 2007. **14**(3): p. 691-702.

77. Kostadima, L., G. Pentheroudakis, and N. Pavlidis, *The missing kiss of life: transcriptional activity of the metastasis suppressor gene KiSS1 in early breast cancer.* Anticancer Res, 2007. **27**(4B): p. 2499-504.

78. Stark, A.M., et al., *Reduced metastasis-suppressor gene mRNA-expression in breast cancer brain metastases.* J Cancer Res Clin Oncol, 2005. **131**(3): p. 191-8.

79. Martin, T.A., G. Watkins, and W.G. Jiang, *KiSS-1 expression in human breast cancer.* Clin Exp Metastasis, 2005. **22**(6): p. 503-11.

80. Dhar, D.K., et al., *Downregulation of KiSS-1 expression is responsible for tumor invasion and worse prognosis in gastric carcinoma.* Int J Cancer, 2004. **111**(6): p. 868-72.

81. Yao, H.L., et al., *[In situ hybridization study on the expression of Kiss-1 and KAI-1 metastasis suppressor genes in gastric cancer].* Zhonghua Wei Chang Wai Ke Za Zhi, 2007. **10**(3): p. 274-7.

82. Tachibana, M., et al., *Prognostic factors in T1 and T2 squamous cell carcinoma of the thoracic esophagus.* Arch Surg, 1999. **134**(1): p. 50-4.

83. Ikeguchi, M., K. Yamaguchi, and N. Kaibara, *Clinical significance of the loss of KiSS-1 and orphan G-protein-coupled receptor (hOT7T175) gene expression in esophageal squamous cell carcinoma.* Clin Cancer Res, 2004. **10**(4): p. 1379-83.

84. Cedrone, A., et al., *Portal vein thrombosis complicating hepatocellular carcinoma. Value of ultrasound-guided fine-needle biopsy of the thrombus in the therapeutic management.* Liver, 1996. **16**(2): p. 94-8.

85. Hou, Y.K., et al., *[Expression of tumor metastasis-suppressor gene KiSS-1 and matrix metalloproteinase-9 in portal vein tumor thrombus of hepatocellular carcinoma].* Ai Zheng, 2007. **26**(6): p. 591-5.

86. Ikeguchi, M., Y. Hirooka, and N. Kaibara, *Quantitative reverse transcriptase polymerase chain reaction analysis for KiSS-1 and orphan G-protein-coupled receptor (hOT7T175) gene expression in hepatocellular carcinoma.* J Cancer Res Clin Oncol, 2003. **129**(9): p. 531-5.

87. Schmid, K., et al., *KiSS-1 overexpression as an independent prognostic marker in hepatocellular carcinoma: an immunohistochemical study.* Virchows Arch, 2007. **450**(2): p. 143-9.

88. Rigaud, G., et al., *Allelotype of pancreatic acinar cell carcinoma.* Int J Cancer, 2000. **88**(5): p. 772-7.

89. Yatsuoka, T., et al., *Association of poor prognosis with loss of 12q, 17p, and 18q, and concordant loss of 6q/17p and 12q/18q in human pancreatic ductal adenocarcinoma.* Am J Gastroenterol, 2000. **95**(8): p. 2080-5.

90. Masui, T., et al., *Metastin and its variant forms suppress migration of pancreatic cancer cells.* Biochem Biophys Res Commun, 2004. **315**(1): p. 85-92.

91. Liang, S. and Z.L. Yang, *[Expression of KiSS-1mRNA in pancreatic ductal adenocarcinoma and non-cancerous pancreatic tissues in SD rats].* Zhong Nan Da Xue Xue Bao Yi Xue Ban, 2007. **32**(1): p. 109-13.

92. Singer, P.A., et al., *Treatment guidelines for patients with thyroid nodules and well-differentiated thyroid cancer. American Thyroid Association.* Arch Intern Med, 1996. **156**(19): p. 2165-72.

93. Stathatos, N., et al., *KiSS-1/G protein-coupled receptor 54 metastasis suppressor pathway increases myocyte-enriched calcineurin interacting protein 1 expression and chronically inhibits calcineurin activity.* J Clin Endocrinol Metab, 2005. **90**(9): p. 5432-40.

94. Jemal, A., et al., *Cancer statistics, 2003.* CA Cancer J Clin, 2003. **53**(1): p. 5-26.

95. Jiang, Y., et al., *KiSS1 suppresses metastasis in human ovarian cancer via inhibition of protein kinase C alpha.* Clin Exp Metastasis, 2005. **22**(5): p. 369-76.

96. Gao, G.L., et al., *[Expression of KiSS-1, matrix metalloproteinase-9, nuclear factor-kappaBp65 in ovarian tumour].* Zhonghua Fu Chan Ke Za Zhi, 2007. **42**(1): p. 34-8.

97. Hata, K., et al., *Expression of metastin and a G-protein-coupled receptor (AXOR12) in epithelial ovarian cancer.* Eur J Cancer, 2007. **43**(9): p. 1452-9.

98. Cole, L.A., *Phantom hCG and phantom choriocarcinoma.* Gynecol Oncol, 1998. **71**(2): p. 325-9.

99. Horikoshi, Y., et al., *Dramatic elevation of plasma metastin concentrations in human pregnancy: metastin as a novel placenta-derived hormone in humans.* J Clin Endocrinol Metab, 2003. **88**(2): p. 914-9.

100. Cole, L.A. and J.M. Sutton, *Selecting an appropriate hCG test for managing gestational trophoblastic disease and cancer.* J Reprod Med, 2004. **49**(7): p. 545-53.

101. Dhillo, W.S., et al., *Plasma kisspeptin is raised in patients with gestational trophoblastic neoplasia and falls during treatment.* Am J Physiol Endocrinol Metab, 2006. **291**(5): p. E878-84.

102. Jemal, A., et al., *Cancer statistics, 2008.* CA Cancer J Clin, 2008. **58**(2): p. 71-96.

103. Nicolle, G., et al., *Metastin (KISS-1) and metastin-coupled receptor (GPR54) expression in transitional cell carcinoma of the bladder.* Ann Oncol, 2007. **18**(3): p. 605-7.

104. Buchan, N.C. and S.L. Goldenberg, *Intermittent androgen suppression for prostate cancer.* Nat Rev Urol, 2010. **7**(10): p. 552-60.

105. Ramiah, V., D.J. George, and A.J. Armstrong, *Clinical endpoints for drug development in prostate cancer.* Curr Opin Urol, 2008. **18**(3): p. 303-8.

106. Plantade, A., et al., *[Locally advanced prostate cancer: definition, prognosis and treatment].* Bull Cancer, 2007. **94**(7 Suppl): p. F50-61.

107. Creasman, W.T., et al., *Carcinoma of the corpus uteri. FIGO 26th Annual Report on the Results of Treatment in Gynecological Cancer.* Int J Gynaecol Obstet, 2006. **95 Suppl 1**: p. S105-43.

108. Kang, H.S., et al., *GPR54 is a target for suppression of metastasis in endometrial cancer.* Mol Cancer Ther, 2011. **10**(4): p. 580-90.

109. Ohta, S., et al., *Downregulation of metastasis suppressor genes in malignant pheochromocytoma.* Int J Cancer, 2005. **114**(1): p. 139-43.

110. Janneau, J.L., et al., *Transcriptional expression of genes involved in cell invasion and migration by normal and tumoral trophoblast cells.* J Clin Endocrinol Metab, 2002. **87**(11): p. 5336-9.

111. Jiang, T., et al., *[Expression and clinical significance of KISS-1 and GPR54 mRNA in endometrial carcinoma].* Zhonghua Zhong Liu Za Zhi, 2005. **27**(4): p. 229-31.

112. Nomura, H., et al., *Expression of membrane-type matrix metalloproteinase in human gastric carcinomas.* Cancer Res, 1995. **55**(15): p. 3263-6.

113. Gottsch, M.L., D.K. Clifton, and R.A. Steiner, *Kisspepeptin-GPR54 signaling in the neuroendocrine reproductive axis.* Mol Cell Endocrinol, 2006. **254-255**: p. 91-6.

114. Li, D., et al., *Estrogen regulates KiSS1 gene expression through estrogen receptor alpha and SP protein complexes.* Endocrinology, 2007. **148**(10): p. 4821-8.

115. Dissanayake, S.K., et al., *The Wnt5A/protein kinase C pathway mediates motility in melanoma cells via the inhibition of metastasis suppressors and initiation of an epithelial to mesenchymal transition.* J Biol Chem, 2007. **282**(23): p. 17259-71.

116. Christie, M., et al., *Different APC genotypes in proximal and distal sporadic colorectal cancers suggest distinct WNT/beta-catenin signalling thresholds for tumourigenesis.* Oncogene, 2012.

117. Mullis, R.L. and R.A. Hanson, *Perspective-taking among offender and nonoffender youth.* Adolescence, 1983. **18**(72): p. 831-6.

118. Nazarenko, I.A., S.K. Bhatnagar, and R.J. Hohman, *A closed tube format for amplification and detection of DNA based on energy transfer.* Nucleic Acids Res, 1997. **25**(12): p. 2516-21.

119. Campbell, C.E., et al., *Monitoring viral-induced cell death using electric cell-substrate impedance sensing.* Biosens Bioelectron, 2007. **23**(4): p. 536-42.

120. Keese, C.R., et al., *Electrical wound-healing assay for cells in vitro.* Proc Natl Acad Sci U S A, 2004. **101**(6): p. 1554-9.

121. Makri, A., et al., *The kisspeptin (KiSS-1)/GPR54 system in cancer biology.* Cancer Treat Rev, 2008. **34**(8): p. 682-92.

122. Chen, S.Q., et al., *[Kiss-1 gene expression after radiation and its association with proliferation and apoptosis in colorectal cancer cells].* Zhonghua Wei Chang Wai Ke Za Zhi, 2012. **15**(5): p. 508-11.

123. Stafford, L.J., K.S. Vaidya, and D.R. Welch, *Metastasis suppressors genes in cancer.* Int J Biochem Cell Biol, 2008. **40**(5): p. 874-91.

124. Nash, K.T., et al., *Requirement of KISS1 secretion for multiple organ metastasis suppression and maintenance of tumor dormancy.* J Natl Cancer Inst, 2007. **99**(4): p. 309-21.

125. McNally, L.R., et al., *KISS1 over-expression suppresses metastasis of pancreatic adenocarcinoma in a xenograft mouse model.* Clin Exp Metastasis, 2010. **27**(8): p. 591-600.

126. Beck, B.H. and D.R. Welch, *The KISS1 metastasis suppressor: a good night kiss for disseminated cancer cells.* Eur J Cancer, 2010. **46**(7): p. 1283-9.

127. Nakamura, T., et al., *Axin, an inhibitor of the Wnt signalling pathway, interacts with beta-catenin, GSK-3beta and APC and reduces the beta-catenin level.* Genes Cells, 1998. **3**(6): p. 395-403.

128. Harms, J.F., D.R. Welch, and M.E. Miele, *KISS1 metastasis suppression and emergent pathways.* Clin Exp Metastasis, 2003. **20**(1): p. 11-8.

129. Bailly, M., N. Zebda, and J.F. Dore, *Human melanoma metastasis related to specific adhesion with lung cells rather than direct growth stimulation.* Anticancer Res, 1994. **14**(5A): p. 1791-9.

130. Navenot, J.M., N. Fujii, and S.C. Peiper, *KiSS1 metastasis suppressor gene product induces suppression of tyrosine kinase receptor signaling to Akt, tumor necrosis factor family ligand expression, and apoptosis.* Mol Pharmacol, 2009. **75**(5): p. 1074-83.

131. Harris, D.L., et al., *Dietary fat-influenced development of colon neoplasia in Apc Min mice exposed to benzo(a)pyrene.* Toxicol Pathol, 2009. **37**(7): p. 938-46.

132. Sourla, A., et al., *Plasminogen activator inhibitor 1 messenger RNA expression and molecular evidence for del(7)(q22) in uterine leiomyomas.* Cancer Res, 1996. **56**(13): p. 3123-8.

133. Koutsilieris, M., et al., *The assessment of disease aggressivity in stage D2 prostate cancer patients (review).* Anticancer Res, 1990. **10**(2A): p. 333-6.

134. Bogdanos, J., et al., *Endocrine/paracrine/autocrine survival factor activity of bone microenvironment participates in the development of androgen ablation and chemotherapy refractoriness of prostate cancer metastasis in skeleton.* Endocr Relat Cancer, 2003. **10**(2): p. 279-89.

135. Yoshioka, K., et al., *Effects of a KiSS-1 peptide, a metastasis suppressor gene, on the invasive ability of renal cell carcinoma cells through a modulation of a matrix metalloproteinase 2 expression.* Life Sci, 2008. **83**(9-10): p. 332-8.

136. Olbrich, T., et al., *Kisspeptin-10 inhibits bone-directed migration of GPR54-positive breast cancer cells: Evidence for a dose-window effect.* Gynecol Oncol, 2010. **119**(3): p. 571-8.

137. Navenot, J.M., et al., *Kisspeptin-10-induced signaling of GPR54 negatively regulates chemotactic responses mediated by CXCR4: a potential mechanism for the metastasis suppressor activity of kisspeptins.* Cancer Res, 2005. **65**(22): p. 10450-6.

138. Ziegler, E., et al., *Antiproliferative effects of kisspeptin10 depend on artificial GPR54 (KISS1R) expression levels.* Oncol Rep, 2013. **29**(2): p. 549-54.

Appendices

Table 1.

	1(normalized by GAPDH)	2(normalized by GAPDH)	3(normalized by GAPDH)	Average (normalized by pEF)	SD
HT115 WT	0.95654	0.98432	1.1876	0.976179481	0.12615
HT115 pEF	1.0655	0.9961	1.1432	1	0.073589
HT115 Kiss-1 kd	0.4033	0.5697	0.4508	0.444271093	0.085715

Table 2.

	1(normalized by GAPDH)	2(normalized by GAPDH)	3(normalized by GAPDH)	Average (normalized by pEF)	SD
HRT18WT	1.46432	1.47564	1.29425	1.048954566	0.101616
HRT18 pEF	1.4327	1.3981	1.2058	1	0.122243
HRT18 Kiss-1 kd	0.5094	0.5812	0.5709	0.41160878	0.038823

Table 3.

	1(normalized by GAPDH	2(normalized by GAPDH)	3(normalized by GAPDH)	Average	SD
HT115 WT	1.204	1.295	1.054	1.184333	0.121698
HT115 pEF	1.254	1.343	1.19873	1.265243	0.072789
HT115 Kiss-1 kd	0.7945	0.52423	0.4832	0.600643	0.169134

Table 4.

	1(normalized by GAPDH	2(normalized by GAPDH)	3(normalized by GAPDH)	Average	SD
HRT18 WT	1.1342	1.36432	1.1042	1.200907	0.142313
HRT18 pEF	1.142342	1.34242	1.194325	1.226362	0.103815
HRT18 Kiss-1 kd	0.665747	0.65453	0.694645	0.671641	0.020697

Table 5.

	1(normalized by GAPDH)	2(normalized by GAPDH)	3(normalized by GAPDH)	Average (normalized by pEF)	SD
HT115 WT	1.089534	1.0342	1.09534	0.861498153	0.033748
HT115 pEF	1.3432	1.1954	1.198	1	0.169184
Ht115 Kiss-1R kd	0.4965	0.50543	0.5643	0.419159129	0.036838

Table 6.

	1(normalized by GAPDH)	2(normalized by GAPDH)	3(normalized by GAPDH)	Average (normalized by pEF)	SD
HRT18 WT	1.66345	1.49534	1.454	0.977824649	0.110935
HRT18 pEF	1.7833	1.5351	1.399	1	0.194856
HRT18 Kiss-1R kd	0.531	0.7915	0.8012	0.450184424	0.153277

Table 7.

	1(normalized by GAPDH)	2(normalized by GAPDH)	3(normalized by GAPDH)	Average	SD
HT115 WT	1.2942	1.2542	1.10432	1.217573	0.100099
HT115 pEF	1.43534	1.343245	1.24356	1.340715	0.095915
HT115 Kiss-1R kd	0.605345	0.7023	0.72455	0.677398	0.063384

Table 8.

	1(normalized by GAPDH)	2(normalized by GAPDH)	3(normalized by GAPDH)	Average	SD
HRT18 WT	1.51423	1.334325	1.294325	1.38096	0.117135
HRT18 pEF	1.3425	1.543563	1.32423	1.403431	0.121701
hRT18 Kiss-1R kd	0.68543	0.742342	0.799433	0.742402	0.057001

Table 9.

		1	**2**	**3**	**4**	**5**	**6**	**Average**	**SD**
pEF	DAY1	100	100	100	100	100	100	100	0
	DAY3	190.5353	297.5346	306.6544	401.5325	299.6646	295.64564	298.5944991	66.856449
	DAY5	400.253	890.34265	865.5453	820.5364	1230.453	770.5353	829.610887	265.9226
Kiss-1 kd	DAY1	100	100	100	100	100	100	100	0
	DAY3	440.4254	423.543543	483.5145	505.4552	510.545	419.534	463.836291	41.07393
	DAY5	700.5435	1656.43242	1350.565	1500.345	1193.545	938.5451	1223.329419	356.5948
Kiss-1 R kd	DAY1	100	100	100	100	100	100	100	0
	DAY3	546.1423	502.543254	489.4325	546.6555	410.5435	597.54325	515.4767227	64.03742
	DAY5	1101.432	849.42534	1193.543	1437.314	1282.145	965.4536	1138.218986	213.4649

Table 10.

		1	2	3	4	5	6	Average	SD
pEF	DAY1	100	100	100	100	100	100	100	0
	DAY3	472.4234	349.54534	466.2343	337.5346	328.4325	350.54254	384.118793	66.5348
	DAY5	515.4252	626.54363	573.4352	595.4235	510.5454	599.42454	570.1329342	47.40103
Kiss-1 kd	DAY1	100	100	100	100	100	100	100	0
	DAY3	449.5345	575.54353	519.4535	536.5345	648.4253	427.45254	526.1573213	81.43068
	DAY5	504.313	728.42342	818.3452	955.4235	601.4234	763.5345	728.5771809	159.5005
Kiss-1R kd	DAY1	100	100	100	100	100	100	100	0
	DAY3	485.4325	463	504.534	454.5345	468.5345	576.545	492.1688417	44.98514
	DAY5	805.5353	718.25245	593.5345	504.5235	819.5435	632.5363	678.987605	124.2656

Table 11.

							Average	STDEV
pEF	43	39	24	38	26	39	34.83333	7.833688
Kiss-1 kd	29	18	38	26	41	39	31.83333	9.020347
Kiss-1R kd	40	20	39	49	43	58	41.5	12.66096

Table 12.

							Average	STDEV
pEF	35	23	21	19	33	31	27	6.811754546
Kiss-1 kd	34	20	19	18	39	42	28.66667	10.91176735
Kiss-1R kd	39	41	20	50	58	53	43.5	13.57571361

Table 13.

HT115	FIELD 1	FIELD 2	FIELD 3	FIELD 4	AVERAGE	SD
pEF	41	46	39	51	44.25	5.377422
Kiss-1 kd	57	53	54	59	55.91	2.753785
Kiss-1R kd	47	36	41	60	46	10.36018

Table 14.

HRT18	FIELD 1	FIELD 2	FIELD 3	FIELD 4	AVERAGE	SD
pEF	47	38	31	43	39.75	6.898067
Kiss-1 kd	51	66	60	56	59.13	6.344289
Kiss-1R kd	35	33	43	25	34	7.033691

Table 15.

		1	2	3	4	5	6	Average	SD
pEF	0HR	0	0	0	0	0	0	0	0
	1HR	8.53453	10.54353	9.76577	9.45353	8.53532	10.53655	9.5615 3677	2.396 813
	2HR	16.44534	17.56456	15.64564	19.53453	19.5345	17.56437	17.714 8232	3.140 3727
	3HR	17.54353	18.6363	20.5435	19.53453	18.0908	20.53463	19.813 8817	2.167 9479
	4HR	39.53453	35.43534	40.53453	37.53453	33.0808	36.5336	35.775 5557	4.605 8485
	5HR	43.43253	39.54365	38.5363	41.53636	42.53453	42.64574	41.704 8535	3.982 1873
Kiss-1 kd	0HR	0	0	0	0	0	0	0	0
	1HR	9.532453	13.42534	13.63564	7.764744	12.08758	9.645645	13.848 57	5.633 8058
	2HR	23.53534	26.42453	21.53453	24.53453	22.54353	23.64576	23.703 04	3.190 8387
	3HR	43.53454	49.53645	45.42344	52.53453	47.43535	48.43543	47.483 29	5.959 071
	4HR	45.53453	66.42343	57.53454	53.54353	54.53453	57.53453	55.684 19	10.54 7208
	5HR	56.43423	57.54353	56.54353	70.54353	54.44233	61.43243	59.156 6	10.54 691
Kiss-1R kd	0HR	0	0	0	0	0	0	0	0
	1HR	8.432432	11.43254	14.4232	13.53454	9.432423	13.5453	12.63 341	5.219 7437
	2HR	18.31435	15.54356	14.53454	17.43254	15.54353	16.45435	16.80 381	2.965 1286
	3HR	21.53454	25.54354	22.54353	27.53635	22.63464	23.54354	23.22 269	3.532 9808
	4HR	42.43254	33.52525	34.54325	40.45325	45.53453	47.54544	39.67 238	10.60 9333
	5HR	45.54353	43.54353	46.53636	53.54354	39.53465	49.53453	46.87 269	9.893 303

Table 16.

		1	2	3	4	5	6	Average	SD
pEF	0HR	0	0	0	0	0	0	0	0
	1HR	5.4324	9.543544	6.564577	8.543535	7.564565	6.947657	14.43271	1.4626762
	2HR	20.54325	15.64577	16.64577	14.54357	21.56465	22.64565	18.59811	3.4039321
	3HR	25.43436	20.56456	23.43254	26.54353	31.43254	28.55365	27.99353	3.8153532
	4HR	40.56544	42.64577	32.64766	47.65477	37.45365	43.7689	39.78936	5.2330136
	5HR	35.63463	39.53654	45.75677	35.43253	48.75676	49.64575	40.62716	7.5952498
Kiss-1 kd	0HR	0	0	0	0	0	0	0	0
	1HR	12.64565	18.56646	13.64646	16.6478	15.65646	13.64574	16.80143	2.76607
	2HR	29.64577	24.64577	20.67578	26.67568	25.76586	28.65465	26.67725	3.4286749
	3HR	48.56465	40.76586	50.65766	47.67587	47.76987	44.64749	46.3469	6.5246739
	4HR	55.56488	55.5645	57.75859	49.65756	59.75688	56.87098	55.5289	6.957276
	5HR	54.45647	57.56457	54.76577	62.08679	57.53656	61.65465	59.17747	6.5176819
Kiss-1R kd	0HR	0	0	0	0	0	0	0	0
	1HR	12.645647	16.65765	13.56456	17.64575	15.65458	15.45254	15.77012	2.8147381
	2HR	21.43535	28.34654	24.64674	27.6457647	29.64575	22.46356	24.30759	3.5907615
	3HR	33.75786	27.53646	35.76757	32.67677	29.67659	30.56476	30.49667	6.4458184
	4HR	29.56475	27.45437	37.56475	39.56458	31.76757	33.65757	33.76226	6.9797378
	5HR	43.64565	47.64575	44.53646	50.45435	41.64565	46.75675	43.94743	6.4384178

Table 17.

	pEF		Kiss-1 kd		Kiss-1R kd	
Time(hrs)	Average	SD	Average	SD	Average	SD
1	0	0	0	0	0	0
2	18.49	8.07129482	75.25	37.69569888	43.14285714	26.85776468
3	42.6765	6.6935524	119.0375	46.23869553	70	33.62662635
4	53.01375	10.627645	168.6125	57.49803568	102.1	35.62293269
5	87.653	7.88537439	209.675	73.03380333	130.3857143	42.9903256
6	91.6485	15.7367823	230.15	81.38290449	149.2142857	48.12419449
7	104.66075	7.89553551	260.5125	89.98014761	154.2857143	48.22182869
8	110.9575	13.6390298	276.4	89.80784248	159.9142857	36.60266059
	pEF		Kiss-1 kd		Kiss-1R kd	
Time(hrs)	Average	SD	Average	SD	Average	SD
1	0	0	0	0	0	0
2	2.3	2.924608236	48.93333333	30.91429012	22.425	20.47655163
3	13.95	6.733250825	85.7	45.20387152	40.7	34.09574754
4	33.05	18.27283959	128.1	56.31894294	65.025	42.81435702
5	43.2	18.89144427	167.7333333	70.2156915	86.65	51.06469753
6	54.525	25.09028697	183.9333333	56.75000734	93.025	50.1428875
7	59.075	21.79837532	203.8	60.61330987	98.225	57.14690864
8	63.55	27.00253075	208.4666667	77.33319684	105.95	55.10919464

Table 18.

	pEF		Kiss-1 kd		Kiss-1R kd	
Time(hrs)	Average	SD	Average	SD	Average	SD
1	0	0	0	0	0	0
2	18.49	8.07129482	75.25	37.69569888	43.14285714	26.85776468
3	42.6765	6.6935524	119.0375	46.23869553	70	33.62662635
4	53.01375	10.627645	168.6125	57.49803568	102.1	35.62293269
5	87.653	7.88537439	209.675	73.03380333	130.3857143	42.9903256
6	91.6485	15.7367823	230.15	81.38290449	149.2142857	48.12419449
7	104.66075	7.89553551	260.5125	89.98014761	154.2857143	48.22182869
8	110.9575	13.6390298	276.4	89.80784248	159.9142857	36.60266059
	pEF		Kiss-1 kd		Kiss-1R kd	
Time(hrs)	Average	SD	Average	SD	Averag e	SD
1	0	0	0	0	0	0
2	19.79646	2.117614242	91.7	18.55927441	36.225	17.63091508
3	43.7117825	9.864968611	127.8	29.51078899	54.625	13.56376914
4	48.924075	6.755564468	155.55	45.21950169	81.875	26.22370111
5	80.29365	12.1117425	200.88	8.059156283	111.04765	30.19606735
6	86.1195	7.128527009	253.8485	30.771077	125.7507	26.4968366
7	94.09805	11.61444408	268.4725	39.08461622	131.0257875	25.66771927
8	101.7600075	11.86046328	300.575	43.20288378	145.52415	44.24373398

Table 19.

	pEF		Kiss-1 kd		Kiss-1R kd	
Time(hrs)	Average	SD	Average	SD	Average	SD
1	0	0	0	0	0	0
2	18.49	8.07129482	75.25	37.69569888	43.14285714	26.85776468
3	42.6765	6.6935524	119.0375	46.23869553	70	33.62662635
4	53.01375	10.627645	168.6125	57.49803568	102.1	35.62293269
5	87.653	7.88537439	209.675	73.03380333	130.3857143	42.9903256
6	91.6485	15.7367823	230.15	81.38290449	149.2142857	48.12419449
7	104.66075	7.89553551	260.5125	89.98014761	154.2857143	48.22182869
8	110.9575	13.6390298	276.4	89.80784248	159.9142857	36.60266059
	pEF		Kiss-1 kd		Kiss-1R kd	
Time(hrs)	Average	SD	Average	SD	Average	SD
1	0	0	0	0	0	0
2	18.795	2.195093012	59.93333333	18.7526887	50.2	36.26219335
3	38.856325	18.82532999	105.3	34.14659573	50.925	36.98345351
4	56.64	13.24466119	152.4666667	48.01635138	71.525	34.04539861
5	70.644175	14.71468974	202.6333333	79.07251946	91.025	37.66079969
6	83.118375	9.957250352	216.0333333	95.0757768	105.225	37.73162908
7	94.0191925	12.7960285	247.4666667	104.2611625	113.925	43.57624544
8	98.68246325	9.059680542	256.2666667	112.5380973	111.15	40.62745377

Table 20.

	pEF		Kiss-1 kd		Kiss-1R kd	
Time(hrs)	Average	SD	Average	SD	Average	SD
1	0	0	0	0	0	0
2	18.49	8.07129482	75.25	37.69569888	43.14285714	26.85776468
3	42.6765	6.6935524	119.0375	46.23869553	70	33.66262635
4	53.01375	10.627645	168.6125	57.49803568	102.1	35.62293269
5	87.653	7.88537439	209.675	73.03380333	130.3857143	42.9903256
6	91.6485	15.736782 3	230.15	81.38290449	149.2142857	48.12419449
7	104.66075	7.89553551	260.5125	89.98014761	154.2857143	48.22182869
8	110.9575	13.639029 8	276.4	89.80784248	159.9142857	36.60266059
	pEF		Kiss-1 kd		Kiss-1R kd	
Time(hrs)	Average	SD	Averag e	SD	Averag e	SD
1	0	0	0	0	0	0
2	5.153333333	5.143254482	45.25	9.509819487	25.606875	17.2022543
3	8.282066667	7.100744365	86.65	15.22289942	55.1125	34.89002976
4	36.98533333	24.16145094	130.1	28.21004549	96.008	41.20953922
5	44.29166667	26.67528485	174.15	70.75349226	106.03925	43.47115072
6	46.996632 5	7.283100038	208.725	109.4107056	134.06625	23.26621311
7	57.75225	7.27725875	214.8744	37.53052356	140.7275	23.42352432
8	64.968	5.47881155	220.4775	30.60479087	146.2835	24.17114436

Table 21.

	pEF		Kiss-1 kd		Kiss-1R kd	
Time(hrs)	Average	SD	Average	SD	Average	SD
1	0	0	0	0	0	0
2	18.49	8.07129482	75.25	37.69569888	43.14285714	26.85776468
3	42.6765	6.6935524	119.0375	46.23869553	70	33.62662635
4	53.01375	10.627645	168.6125	57.49803568	102.1	35.62293269
5	87.653	7.88537439	209.675	73.03380333	130.3857143	42.9903256
6	91.6485	15.7367823	230.15	81.38290449	149.2142857	48.12419449
7	104.66075	7.89553551	260.5125	89.98014761	154.2857143	48.22182869
8	110.9575	13.6390298	276.4	89.80784248	159.9142857	36.60266059
	pEF		Kiss-1 kd		Kiss-1R kd	
Time(hrs)	Average	SD	Average	SD	Average	SD
1	0	0	0	0	0	0
2	8.525	10.6828133	72.45	14.32119641	37.43625	9.169237859
3	24.9	22.94704048	119.225	25.53081471	64.839	13.72197695
4	41.6	30.50497227	163.525	30.25396668	91.5687	32.52052788
5	61.2	40.9341748	197.725	56.83655595	106.4957075	36.30109155
6	71.4	48.51315973	226.875	41.96954253	118.7645	44.15770038
7	81.55	62.13520205	228.5575	39.83797884	121.82125	24.34660085
8	83.77	26.19229516	243.39	40.89756064	135.77425	63.56995972

Table 22.

	1	**2**	**3**	**Average**	**SD**
No treatment	253617	218549	278903	250356.3	30308.83
Kisspeptin-10	390971	348299	329015	356095	31705.2
Kisspeptin-234	230861	277956	298402	269073	34635.64
postive control	354362	209805	430739	331635.3	112206.7

Table 23.

No treatment

		1	2	3	Average	SD
Control	**pEF**	5125	4894	5156	5058.333	143.1584
	Kiss-1 kd	5509	5438	5602	5516.333	82.24557
ERK inhibitor	**pEF**	4659	4595	4567	4607	47.1593
	Kiss-1 kd	4807	4742	4822	4790.333	42.5245

Kisspeptin-10

		1	2	3	Average	SD
Control	**pEF**	5003	4904	4899	4935.333	58.65435
	Kiss-1 kd	4941	4883	5009	4944.333	63.0661
ERK inhibitor	**pEF**	4620	4609	4511	4580	60.00833
	Kiss-1 kd	4599	4660	4639	4632.667	30.98925

Kisspeptin-234

		1	2	3	Average	SD
Control	**pEF**	5172	5065	5306	5181	120.7518
	Kiss-1 kd	5489	5508	5087	5361.333	237.7695
ERK inhibitor	**pEF**	4602	4705	4798	4701.667	98.04251
	Kiss-1 kd	5098	4893	5092	5027.667	116.6633

Table 24.

Kiss-1

	1	2	3	4	5	6	7	Average	SD
Normal	76740	80231	81566	80395	77138	73134	78200.67	3136.773	76740
Tumour	11048	10485	11879	12789	10528	13976	11784.17	1387.843	11048

Kiss-1R

	1	2	3	4	5	6	7	Average	SD
Normal	37626	45891	38141	32789	39742	36791	38496.67	4303.448	37626
Tumour	1903	5901	4031	5697	3956	4391	4313.167	1446.261	1903